Sustainable Aviation:

A techno-economic “Well-to-wake” evaluation of the aviation fuels LH_2, LCH_4 and Jet A-1

A thesis accepted by the Faculty of Energy-, Process- and Bio-Engineering of the University of Stuttgart to fulfil the requirements for the degree of Doctor of Engineering Sciences (Dr.-Ing.)

by

Moritz Ludwig Raab

born in Gräfelfing

Main examiner:	Prof. Dr. rer. nat. habil. André Thess
Co examiner:	Univ.-Prof. Dr. rer. nat. Johannes Reichmuth

Date of oral exam: 2nd December 2025

Institute for Building Energetics, Thermotechnology and Energy Storage (IGTE) at the University of Stuttgart

2026

Declaration

I hereby certify that this dissertation entitled with: “A techno-economic “Well-to-wake” evaluation of the aviation fuels LH_2, LCH_4 and Jet A-1” is entirely my own work except where otherwise indicated. Passages and ideas from other sources have been clearly indicated.

München, _____ _____

Moritz Ludwig Raab

Acknowledgement

This thesis was developed during my time as research associate at the German Aerospace Center (DLR) in Stuttgart. I am very grateful to have had the opportunity to work in this inspiring research environment and would like to thank the following people, who encouraged and supported me in the past years.

I would like to thank Prof. André Thess, for the opportunity to be considered as PhD candidate, his encouragement to pursue new ideas and valuable feedback in the seminars. I also want to thank Prof. Johannes Reichmuth for accepting to co-referee this thesis.

Also, I want to thank Dr. Ralph-Uwe Dietrich, for giving me the opportunity to work at the DLR, his supervision and the possibility to benefit from his experience, for numerous discussions about the thesis and its results and possible implications for further research topics.

I would like to thank my colleagues that made these years an unforgettable part of my life, which I will always remember with pleasure. I also would like to thank my students and co-authors of my papers.

Further, I am also very thankful for the support I have received from my friends and family.

Table of contents

Abstract

This thesis presents a comprehensive techno-economic assessment of the implications if the aviation industry shifts from fossil-based kerosene towards the utilisation of electricity-based fuels, with liquid hydrogen, liquid methane and renewable kerosene as the only fuel options. The entire pathway from the provision of renewable electricity, the fuel synthesis, logistics, changes at the airport infrastructure up to the utilization in different aircraft categories is considered. The pathway selected for analysis is based on the assumption that renewable electricity will be supplied at *El Ouatia* in Morocco, with the airports of Frankfurt and Munich in Germany acting as the fuel supply points for three different aircraft categories, each with a capacity of 100, 180 and 425 passengers, respectively. For these aircraft, up to 10 different destinations are considered, depending on the flight range of the evaluated aircraft. The different fuels are compared by determining the specific costs of air travel in $€_{2020}$ per passenger per 100 km.

It is shown that a shift towards electricity-based fuels significantly increases the costs of air travel compared to utilizing fossil kerosene with CO_2 abatement costs exceeding 1300 $€_{2020}$ per t $_{CO_2}$. The results for an aircraft with a capacity of 180 passengers are 3.08, 4.57 and 5.11 $€_{2020}$ per passenger per 100 km for liquid hydrogen, liquid methane and kerosene, respectively. It is shown that the supply of renewable electricity and the fuel synthesis itself dominate the overall costs. If the highest possible flight range for an aircraft with a capacity of 180 passengers is considered, they make up almost 80 % in the case of liquid hydrogen, 88 % in the case of liquid methane and more than 92 % in the case of kerosene. Thus, the investment of new airport infrastructure and the development of new aircraft have a less significant role. The results enable stakeholders from the aviation industry, policy makers and research institutes to focus on those aspects that will achieve the overarching “net zero” target of the aviation industry in the most economically way.

Kurzzusammenfassung

In dieser Arbeit sind in einer umfassenden technisch-ökonomischen Analyse die Auswirkungen dargestellt, welche sich ergeben, falls die Luftfahrtindustrie von der Nutzung fossilen Kerosins auf strombasierte Kraftstoffe übergeht. Als potenzielle Kraftstoffe sind flüssiger Wasserstoff, flüssiges Methan und erneuerbares Kerosin berücksichtigt. Der gesamte Pfad von der Bereitstellung des erneuerbaren Stroms, der Kraftstoffsynthese, der Logistik, den Änderungen an der Flughafeninfrastruktur bis hin zur Nutzung in verschiedenen Flugzeugkategorien wird dabei betrachtet und in die jeweiligen Teilschritte zerlegt. Für die Analyse wird davon ausgegangen, dass erneuerbarer Strom in *El Ouatia*, Marokko bereitgestellt wird. Die Flughäfen in Frankfurt und München in Deutschland werden als die zu versorgenden Flughäfen betrachtet. Die Nutzung der verschiedenen Treibstoffe wird in drei verschiedenen Flugzeugkategorien mit einer Kapazität von jeweils 100, 180 bzw. 425 Passagieren evaluiert. Dabei werden abhängig von der Reichweite der untersuchten Flugzeuge bis zu 10 verschiedene Zielorte berücksichtigt. Der Vergleich der betrachteten Kraftstoffe erfolgt dabei, indem die spezifischen Flugkosten in $€_{2020}$ pro Passagier und 100 km ermittelt werden.

Es wird gezeigt, dass eine Umstellung auf strombasierte Kraftstoffe die Kosten des Flugverkehrs im Vergleich zur Verwendung von fossilem Kerosin deutlich erhöht. Die Ergebnisse für ein Flugzeug mit einer Kapazität von 180 Passagieren belaufen sich auf 3.08 $€_{2020}$ pro Passagier und 100 km bei der Verwendung von flüssigem Wasserstoff, 4.57 $€_{2020}$ pro Passagier und 100 km bei flüssigem Methan und 5.11 $€_{2020}$ pro Passagier und 100 km bei Kerosin. Die CO_2-Vermeidungskosten übersteigen dabei 1300 $€_{2020}$ pro t_{CO_2}. Die Gesamtkosten werden von 2 Teilschritten dominiert, der Bereitstellung des erneuerbaren Stroms und der Kraftstoffsynthese. Unter Berücksichtigung der maximalen Reichweite des Flugzeuges mit einer Kapazität von 180 Passagieren, fallen auf diese beiden Teilschritte bei Verwendung von flüssigem Wasserstoff fast 80 %, im Falle von flüssigem Methan 88 % und im Falle von Kerosin mehr als 92 % der Gesamtkosten. Die Investitionen in die neue Flughafeninfrastruktur sowie die Entwicklung neuer Flugzeuge haben eine weniger bedeutende Rolle. Die Ergebnisse ermöglichen es den Akteuren der Luftfahrtindustrie, den politischen Entscheidungsträgern sowie Forschungsinstituten, sich auf die Aspekte zu konzentrieren, mit denen das übergeordnete „Netto-Null“-Ziel der Luftfahrtindustrie auf die ökonomischste Weise erreicht werden kann.

Nomenclature

Abbreviations:

AEA	All-electric aircraft
AEM	Anion exchange membrane
ASF	Anderson-Schulz-Flory
ASTM	American Society for Testing and Materials
ATJ	Alcohol-to-jet
CHJ	Catalytic hydrothermolysis jet fuel
DAC	Direct air capture
FT	Fischer Tropsch
HEFA	Hydroprocessed esters and fatty acids
IATA	International Air Transport Association
ICCT	International Council on Clean Transportation
LCH_4	Liquid methane
LH_2	Liquid Hydrogen
LHV	Lower heating value
LNG	Liquefied natural gas
MTPA	Million tons per annum
PAX	Passenger
PBtX	Power-and-biomass-to-X
PEM	Proton exchange membrane
PtX	Power-to-X
PV	Photovoltaics (referring to solar energy)
RE	Renewable energy
rWGS	Reverse water gas shift
SAF	Sustainable aviation fuel
SEC	Specific energy consumption
SOEC	Solid oxide electrolyzer cell
SPK	Synthetic paraffin kerosene

Variables and constants (Greek letters):

α	Chain growth probability in the FT process
x	Mole fraction
ΔH^0	Standard enthalpy of reaction

Variables and constants (Latin letters):

C	CO_2 abatement costs

1 Introduction

On October 4th, 2021, the member airlines of the International Air Transport Association (IATA) passed a resolution committing themselves to achieve “net zero” by the year 2050 (1). The motivation behind this resolution is to decrease the CO_2 emissions of the aviation industry caused by burning fossil kerosene, thereby supporting the goals of the so-called “Paris Agreement” (2). The resolution and its specifics, including the definition of “net zero” are not further discussed; however, it addresses the challenge faced by the aviation industry: How can the CO_2 emissions be reduced while the demand for air travel is predicted to grow in the coming decades? (3, 4)

The aviation industry addressed this question by introducing so-called sustainable aviation fuels (SAF) that can substitute for fossil kerosene, though their market penetration has been limited so far. A detailed introduction to SAFs is provided in subchapter 1.2.1. The European legislator is emphasising the substitution of kerosene with SAF through the “ReFuelEU Aviation” initiative (5). This regulation mandates a minimum SAF share of 2 % for flights departing in the EU from 2025 onwards, increasing to 70 % by 2050. This initiative only accounts for departures within the EU, other areas of the world like the USA or China have not introduced similar initiatives (yet). Thus, it is questionable whether this regulation can reduce the emissions at a sufficient rate.

Another approach that is currently followed by the aviation industry is the introduction of LH_2 as aviation fuel. This approach represents a radical technological change that requires adaptations from every party involved in the value chain. It strongly depends on political regulations and the willingness of clients, manufacturers etc. to adapt if concepts like these stand a chance to eventuate in the future. Since there are several approaches to decarbonize the aviation industry an unbiased comparison based on a techno-economic evaluation is necessary.

This thesis compares the different options and determines the corresponding costs per distance covered per person, whereby the challenge arises that existing technologies are compared with non-existing technologies. It is therefore necessary to be transparent and discuss the leverage of individual input parameters, especially if it considers the uncertainty regarding non-existing technologies. In this chapter, first the CO_2 emissions of the aviation industry are analysed in further detail. Non-CO_2 emissions like water vapor, NO_x, etc. are neglected, as this would be part of an in-depth life cycle assessment of future aviation that might follow in studies based on this thesis.

Then, in subchapter 1.2, the options to decarbonize the industry are discussed and background information is given for the corresponding options (a thorough literature review is given in chapter 2). The research question of this thesis is introduced in subchapter 1.3.

1.1 CO_2 emissions of the aviation industry

This subchapter discusses only direct CO_2 emissions from the aviation industry. It is noted that it is challenging to state absolute values since, in most studies, only the emissions from commercial passenger aviation are stated. They accounted for 71 % of the emissions from the aviation industry in 2018, according to Gössling and Humpe (3). Data from military aviation and private aircraft are usually not published; however, they have a less dominant role as shown in Gössling and Humpe.

The forecast of the annual CO_2 emissions from commercial aviation industry is depicted in Figure 1. Due to the aforementioned aspects, the values from Figure 1 should be taken as an order of magnitude and it is noted, that effects from the COVID pandemic are not shown in the graphs since the figure was created before 2020. But the issue behind the introductory question mentioned above is depicted. With the predicted demand growth of 4 % per year, the emissions in the year 2030 will roughly double compared to the 2005 level. In the further outlook, the annual CO_2 emissions could rise to more than 3 Gt until the year 2050. While efficiency improvements lead to a certain reduction of the emissions, the overall emissions are still rising (6).

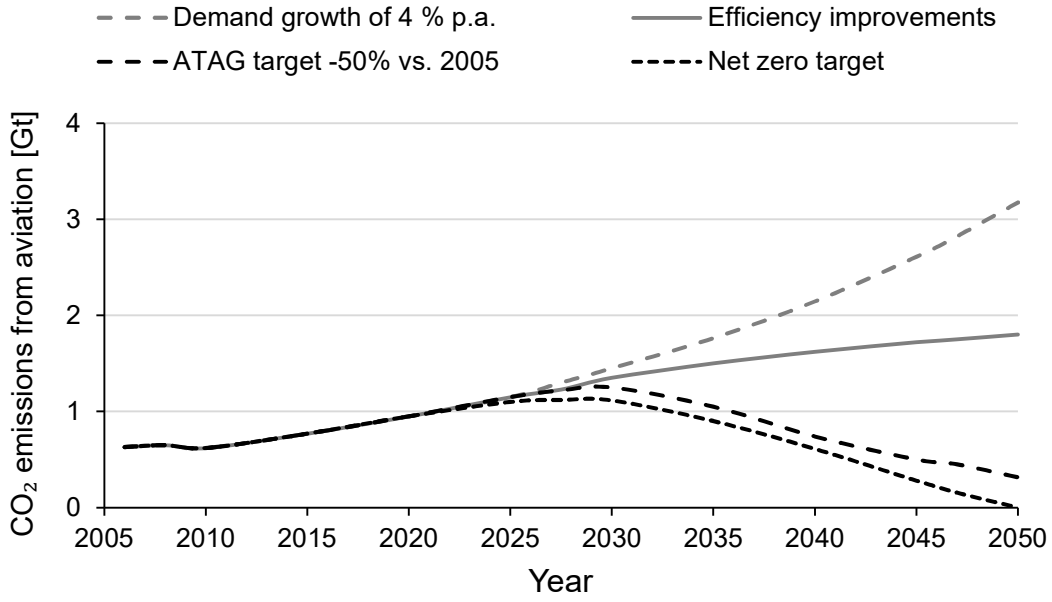

Figure 1: CO_2 emissions from aviation - Historic and projections from 2020 (pre Covid) | adapted from (7)

Before discussing the options to reduce the emissions, it is essential to understand the relationship between emissions, aircraft size, and distance flown. This is shown in Figure 2 for the year 2018, where the total emissions of commercial passenger aviation amounted to 766 Mt of CO_2 (1).

Legend for CO_2 emission:

negligible	0 - 2 %	2 - 5 %	5 - 10 %	10 - 15 %

	Range up to [in 1000 km]									Share of total	
Plane size (PAX capacity)	0.5	1.0	2.0	3.0	4.5	7.0	8.0	10	> 10	CO_2 emissions	Global fleet
Commuter < 19										< 1%	4%
Regional 20 - 80										3%	13%
Short-range 81 - 165										24%	53%
Medium-range 166 - 250										43%	18%
Long-range > 250										30%	12%
Total share of CO_2 emissions	4%	13%	25%	14%	11%	12%	7%	7%	7%		

Figure 2: CO_2 emissions of civil aviation per segment and range for the year 2018 | PAX = passenger (4)

Several aspects can be concluded from this data, in particular:

- Shorter flights with a flight distance of up to 1,000 km, emitted less than 20 % of the total CO_2
- Planes with a capacity higher than 165 passenger caused more than 70 % of the total CO_2 emissions
- A quarter of the total emissions resulted from flights with a distance between 1,000 and 2,000 km
- Flights with a distance of more than 4,500 km caused 44 % of the emissions

These conclusions are relevant because some of the options introduced in subchapter 1.2 are only applicable for flights up to a certain distance and/or capacity. And thus, even though every option to decrease the CO_2 emissions from aviation should somehow be considered, the efforts to introduce a certain technology should comply with the respective reduction potential.

1.2 Options to decarbonize the civil aviation industry

The demand for civil aviation stems from the demand of people to travel i.e., to have a certain kind of mobility. Even though this mobility demand can be met by alternatives like high-speed trains or any other sort of vehicle, at least to a certain extent, only aviation is considered in this thesis. Furthermore, renewable carbon-based fuels also emit CO_2 when burned. But CO_2, or other forms of carbon, e.g. biomass, is used as reactant in the production process of these fuels. Therefore, no fossil CO_2 is emitted (neglecting the carbon footprint of the electricity and/or carbon supply).

The most "straightforward" approach to reduce the CO_2 emissions is the usage of so-called renewable kerosene. The annotation "straightforward" is used because from the point of view of the airline operators almost no changes have to be made and the same infrastructure at the airports and the same aircraft can be used. **SAF**, for "sustainable aviation fuel", is used in this thesis as abbreviation to refer to every renewable produced kerosene-type jet fuel. Every other approach to decarbonize the aviation industry apart from SAF is summarized by the expression "new technologies" or "radical technology changes" (1, 8). According to IATA, they include the usage of liquid hydrogen (**LH_2**), fully electric aircraft and new structural plane designs (9). In a recent paper published by Eurocontrol, liquid methane (**LCH_4**) and ammonia were further referred to as fuel alternatives for long-haul aviation (10). In this paragraph, different options are briefly discussed to provide an overview and lead to the research question of this thesis. Research activities that align with the research question of this thesis are thoroughly discussed in chapter 2.1. The following options are discussed:

- Substitution of fossil kerosene with SAF
- The introduction of the "all-electric aircraft"
- Using LH_2 in aviation
- Using LCH_4 in aviation

Apart from SAF, every option requires tremendous changes in the aviation industry, e.g. new aircraft, new airport infrastructure, new logistics etc. To better address the respective aspects of the considered fuels in the further course, the relevant properties are listed in Table 1 without further discussion at this point.

Table 1: Properties of evaluated aviation fuels

	Unit	**LH_2**	**LCH_4**	**Jet A-1 / SAF**
Density (liq. / @ 1 bar)	kg/m^3	70.8	422.6	810*
Boiling point @ 1 bar	°C	-252	-161	> 150
Volumetric energy density	MJ_{LHV}/m^3	8.50	21.13	34.83

Gravimetric energy density	MJ_{LHV}/kg	120	50	43*
Relative energy density – volumetric	-	0.24	0.61	1
Relative energy content – by mass	-	2.79	1.16	1
Water emissions from combustion	mol $_{H_2O}$ / MJ_{LHV}	4.13	2.49	1.82**
CO_2 emissions from combustion	mol $_{CO_2}$ / GJ_{LHV}	0	1.25	1.63**
Flammability limit in air	volumetric	4 – 74 %	4.4 – 16.5 %	0.7 – 5 %

* Since Jet A-1 is a mixture, average values are used | ** for $C_{12}H_{26}$ as exemplary molecule

1.2.1 Renewable kerosene-type jet fuel

Kerosene-type jet fuels are a mixture of hydrocarbons that so far, are mostly based on crude-oil distillation. Thus, it is not a defined chemical substance like hydrogen or methane but a mixture of hydrocarbons having a carbon number usually between 8 and 16 (11). The aviation industry relies on different fuel specifications to guarantee certain fuel characteristics, e.g. Jet A, Jet A-1 or JP-5 that differ by their flash points, freeze points etc. Nevertheless, the expressions “kerosene” and “aviation fuel” are used in this thesis as generic terms for every kerosene-type jet fuel.

There are several production routes for alternative kerosene (i.e., not based on crude-oil distillation) that have already been certified for usage in commercial aviation (12). Currently, these fuels can be used in a mixture with fossil kerosene with a blending limit of up to 50 % (13). Though in 2017, the share of alternative kerosene accounted for only 0.004 % of the total kerosene demand (14). But it is aimed to further increase the blending limit and first experiments with 100 % share of alternative kerosene have already been conducted in March 2023 (15). The production processes of alternative kerosene and their feedstocks are listed in Table 2 which is based on the standard “ASTM D7566-22a | Standard Specification for Aviation Turbine Fuel Containing Synthesized Hydrocarbons” (12).

Table 2: Certified production processes for renewable kerosene – taken from (12, 13)

Technology	**Feedstock**
Fischer Tropsch (FT) - synthesized isoparaffinic kerosene (SPK) → (FT-SPK)	Wastes (municipal solid wastes, etc.), coal, gas, sawdust
Hydroprocessed fatty acid esters and fatty acids (HEFA)	Vegetable oils: palm, camelina, jatropha, Animal fats, waste greases and used cooking oil

Hydroprocessed hydrocarbons (HH-SPK) or HC-HEFA	Oils produced from (*botryococcus braunii*) algae
Synthesized Iso-paraffin	Sugarcane, sugar beet
Alcohol-to-jet (ATJ) (via Isobutanol and Ethanol)	Sugarcane, sugar beet, sawdust, lignocellulosic feeds
Catalytic hydrothermolysis jet fuel (CHJ)	Waste oils or energy oils

With the production processes listed in Table 2 it might be assumed that the production capacity of these processes just has to be increased, together with the blending limit allowance, and the aviation industry is independent from crude-oil based fuels. But there are technical, economic and regulatory hurdles that need to be addressed and that limit the production, at least of some of the listed pathways.

One aspect is that “alternative kerosene” does not necessarily mean “sustainable kerosene”. While the expression “sustainable” is not defined in this thesis and no life cycle assessment will be conducted, it seems evident that the shift from crude-oil based to coal-based kerosene is not viable a solution. In general, the availability and usability of the feedstock is challenging and plays a crucial role. Especially, if the produced fuel should be accounted for in the SAF-quota given in the “ReFuelEU Aviation” initiative. Also, a “food vs. fuel” debate could arise when biogenic feedstocks are used. This topic has been discussed thoroughly in literature and is rather a socio-economic and ethical topic (16, 17) and is not part of this thesis.

The first question that arises, is, if there is enough feedstock for the processes listed in Table 2 to decarbonize the aviation industry. In 2021, the “International Council on Clean Transportation” (ICCT) published a working-paper where the potential of waste fats, used cooking oils, cover crops, agricultural and forestry residues are evaluated (18). They concluded, that in the year 2030 up to 5.5 % of the jet fuel demand in the EU can be supplied via SAF produced in the EU, most of which is based on agricultural residues. But if higher shares are aspired the second question arises: Where could the remaining SAF be coming from, especially if biogenic feedstocks might be limited? One option is the electricity-based production route. There, electricity is used to produce hydrogen, which then reacts with CO or CO_2 to produce kerosene. This pathway is one example of the so-called “**Power-to-X**” (PtX) processes. The technical aspects of this production pathway are discussed in detail in subchapter 1.3.1. Considering the electricity used in this process it is noted that it should have a low carbon footprint (i.e., based on PV, Wind, hydropower, nuclear). Otherwise, the overall

CO_2 emissions might be higher compared to simply burning crude-oil-based kerosene. A special case is the “Power-and-biomass-to-X” (PBtX) process where biomass is used as carbon source and hydrogen based on electricity is used (19). But this route is not considered in this thesis. Compared to sole biomass or waste-based processes, the PtX pathway offers a route without practical production capacity limitations. Though currently the supply of electricity is one of the limiting factors of this technology. If the regulatory framework is given, production capacity of renewable electricity and consequently of PtX-based SAF is increased worldwide, a global market could develop where countries with suitable conditions could supply the remaining countries in the world. Similar to the global crude-oil market, where, as a comparison, more than 90 % of the EU-wide crude-oil demand is covered by imports (20).

The most relevant hurdle has not been discussed yet and is most likely valid for every process. SAF is more expensive than their fossil counterpart. Depending on the production process, the costs increase at least by a factor of two (21). From the point of view of an airline operator the question arises, why SAF should be used. Therefore, initiatives like “ReFuelEU Aviation” are required where mandatory quotas are set so that the share of fossil kerosene will be reduced over time.

1.2.2 All-electric aircraft

One approach to avoid any kind of direct emissions is the all-electric aircraft (AEA). There, all the required energy is supplied from batteries. Smaller AEA are under development by companies like “lilium” (22), but their focus lies in the use-case of so called “air-taxis”. Regarding these types of aircraft, the reference is made to Figure 2. Small aircraft with a capacity of less than 19 people play a minor role in the total emissions of the aviation industry.

According to the review paper by Ghassemi et al., the performance of several electric components has to be increased by numerous factors, that a single-aisle aircraft like the Boeing 737 can be powered all-electric and reach 5,000 km (23). According to their study, this includes:

- 3-fold increase in the power density of power electronic converters
- 3-5-fold increase in the power density of the electric motors
- 4-fold increase in the specific energy density of Li-ion batteries

Other authors like Schäfer et al. are less optimistic and doubt, that AEA will be capable of operating over distances above 1,500 nautical miles (2,222 km) (24). They state that for these distances, the specific energy density of the battery system would need to be 1,600 Wh/kg, compared to the current value of about 250 Wh/kg (which is more than a 6-fold increase).

The development of the electric components cannot be predicted and the influence of commuter-sized aircraft like they are developed by “lilium” only play a minor role in the emissions from the aviation industry. Therefore, all-electric aircraft are not considered to have a significant contribution on the decarbonization of the aviation industry.

1.2.3 Liquid hydrogen - LH_2

The utilization of liquid hydrogen (**LH_2**) as aviation fuel was first demonstrated with a B-57 in the year 1956 by NASA and was repeated in 1988 in the former USSR with a Tu-155 (25). In both planes, one of the engines was powered with hydrogen as jet fuel. Since these first experiments, numerous studies focused on the implementation of LH_2 in commercial aviation. In 2020, Airbus introduced the ZEROe program with the goal to develop the first zero emission commercial aircraft until the year 2035 (26). Also several research projects and start-up companies focus on the introduction of LH_2 in aviation (27-29). Details of the current research activities are given in subchapter 2.1.2. In this subchapter, general advantages and disadvantages of utilizing LH_2 as aviation fuel are discussed as well as aspects of the supply chain.

One of the most relevant positive aspect is that no direct CO_2 emissions result from the utilization of hydrogen. Furthermore, hydrogen can be used in combustion engines as well as in fuel-cells and thus, is suitable for hybrid-electric aircraft. These are aircraft that run on electricity that is provided from batteries as well as hydrogen fuel-cells (Compared to AEA, not all the energy has to be stored in the battery). Regarding the production route, hydrogen can be derived from reforming processes (requires usually a fossil feedstock and is thus neglected) as well as via water electrolysis. Water electrolysis is the process step that every PtX process (except power-to-heat) has in common. Details of the PtX processes are discussed in subchapter 1.3.1, the advantage of LH_2 as aviation fuel is the fact, that instead of subsequent chemical conversion processes only a liquefaction step is required.

Disadvantageous aspects of LH_2 are linked to the general properties of hydrogen. One aspect is referring to the energy density which is listed in Table 1. While the gravimetric energy density of LH_2 is relatively high and almost three times higher than that of kerosene, the volumetric energy density is quite low and only 24 % as high compared to kerosene. Thus, an imaginary LH_2-A380 that remains unchanged compared to its conventional version apart from the fuel in its tanks would only have a range of 3,000 km instead of 12,400 km (30). But LH_2 cannot be stored in the wings in the same way as kerosene due the cryogenic properties. Since this “wet-wing” fuel storage is not feasible the aspect of the lower volumetric energy density becomes even a larger challenge that needs to be addressed.

These cryogenic properties are also challenging in the overall supply chain. Liquid hydrogen has a temperature of -252 °C at ambient pressure. Therefore, LH_2 must be kept

cool and isolated during the whole supply chain to avoid losses. Furthermore, due to unavoidable heat input from the environment, the evaporating share of LH_2 must be dealt with either by venting, reliquefication or any other sort of utilization. Since hydrogen-air mixtures form explosive atmospheres in the range from 4 – 74 vol-$\%_{H_2}$ and the minimum ignition energy of hydrogen in air can be as low as 19 µJ for ideal mixtures, safety issues are a major concern when hydrogen has to be vented. Also, people handling the liquid must pay attention not to get in contact with cold surfaces, though since LNG is already a global commodity, this issue is manageable.

Despite the challenges that arise from the low gravimetric energy density, LH_2 might be a suitable fuel for the decarbonization of the aviation industry. The fact that no CO_2 is produced from its utilization is very promising. Also, the aspect that it can be used in fuel-cells as well as in combustion engines could further be beneficial. But a completely new infrastructure would be required. Safety is a major concern, if LH_2 is introduced globally the ground staff handling the liquid must be trained and become aware of the dangers coming from LH_2. Also, new aircraft designs are necessary to overcome the issues with onboard hydrogen storages.

1.2.4 Liquid methane - LCH_4

Another cryogenic liquid that has been considered as aviation fuel is liquid methane (**LCH_4**). First studies considering methane as a fuel for commercial aviation were conducted by NASA in 1980 (31). In the aforementioned Tu-155 in addition to tests with LH_2, experiments were also carried out with LNG (the fossil variant of LCH_4) to evaluate its potential as jet fuel (32). Details of the current research activities are given in section 2.1.3. In this subchapter, general advantages and disadvantages of utilizing LCH_4 as aviation fuel are discussed as well as aspects of the supply chain.

One major advantage compared to LH_2 is the fact, that LNG as fossil counterpart to LCH_4 is already a widely available commodity with an established global supply chain (33). Therefore, compared to LH_2, the “chicken-and-egg” problem regarding transport facilities is less of an issue. LNG could be used right away, with fossil LNG phased out gradually over the years. The advantage of utilizing LNG instead of kerosene is the fact, that the CO_2 emissions per energy unit provided are reduced by 25 %, as shown in Table 1.

However, disadvantageous aspects of LCH_4 are similar to the aspects stated for LH_2. The volumetric energy density of LCH_4 is also lower than for Jet A-1, though with a ratio of 0.61 compared to Jet A-1 it is not as low as hydrogen with 0.24. Due to its cryogenic properties the conventional “wet-wing” fuel storage is also not feasible and different aircraft concepts are required. Another issue is the potency of methane as greenhouse gas. Over the span of 100 years it has a greenhouse gas potential of 30, meaning 1 kg of methane released to the atmosphere has the same effect as 30 kg of CO_2 (34).

Although a life cycle assessment is not conducted in this thesis, it is noted that leakages in the supply chain and during utilization (methane slip) must be avoided so that LCH_4 usage can be beneficial compared to the usage of fossil fuels.

As with kerosene type jet fuel, there are various methods how methane can be produced alternatively. The main distinction is between the biogenic and the catalytic pathway. The biogenic production pathway relies on the anaerobic metabolic conversion of CO_2, methanol or acetic acid into CH_4 and can only be performed by Archaea (35). However, this pathway is not further considered. The chemical-catalytic pathway, known as "Sabatier-reaction", was first described by Paul Sabatier in 1897. The chemical equation is given in subchapter 1.3.1, but it is one of the least complex PtX synthesis processes after the basic hydrogen production. As with hydrogen, a liquefaction step is required to increase the volumetric energy density, cooling methane is to -161 °C. Though compared to hydrogen the required temperature is not as low. Furthermore, the amount of electric energy that is required to retrieve "one unit of cryogenic fuel" is lower for methane than for hydrogen. This aspect is shown with the values given in Table 3.

Table 3: Comparison of the electric energy demand to retrieve liquid H_2 and CH_4

	SEC $\left[\frac{kWh_{El}}{kg}\right]$	**LHV** $\left[\frac{kWh_{th}}{kg}\right]$	**SEC/LHV** $\left[\frac{kWh_{El}}{kWh_{th}}\right]$
Methane	0.4*	13.9	0.028
Hydrogen	6.0	33.3	0.180

SEC = "specific energy consumption" to liquefy one kg of the corresponding fuel
*Value varies slightly for LNG due to varying feed composition

While the values for SEC given in Table 3 are rather generic (and optimistic for hydrogen) since they strongly depend on the refrigerants, feed pressure, feed temperature and, if natural gas is considered, on the gas composition, the general message is still valid and given by the right column. The amount of electric energy that is required to liquefy a certain energetic content is several times higher for hydrogen than for methane. This difference affects liquefaction after the initial synthesis step as well as for the boil-off management during the whole supply chain.

In summary, one could argue that LCH_4 combines the negative aspects of LH_2 with being a cryogenic fuel and the negative aspect of SAF that it still emits CO_2 during utilization (and therefore requires a carbon source in the production process). But regarding its properties it is not "as cryogenic" as LH_2, the specific energy demand to liquefy the molecule is lower than for LH_2, the volumetric energy density of LCH_4 is significantly higher than for LH_2 and the synthesis via the PtX route is less complex than for

SAF (details in subchapter 1.3.1). Therefore, LCH_4 is seen as a viable, and in the opinion of the author, currently underestimated alternative to decarbonize the aviation industry.

1.3 Chemical background and research question

1.3.1 Introduction to "power-to-x" processes

The expression "Power-to-X" is an umbrella term for the approach to synthesize chemicals based on electric energy. The concept originated from the conversion of electric energy into a chemical energy carrier and thus, to store energy. The chemical energy carrier can be used as fuel (so-called "e-Fuels") or, if chemicals like ammonia are produced, they can also substitute their fossil counterparts. In most cases only the water electrolysis acts as interface between the electricity (thus "Power") and the downstream processes where the desired product is synthesized, though there are research activities that focus on other electrochemical conversion steps, e.g. the reduction of CO_2 to CO. The remaining process steps also require electric energy, e.g. compression of gases, but they do not incorporate an electrochemical conversion step.

This thesis considers LH_2, LCH_4 and SAF, which are all produced via the PtX pathway. The source of the required electricity is discussed in subchapter 1.3.2. The chemical reactions involved are given in the following sections. Hydrogen is produced in a water electrolyzer according to the reaction given with Equation 1.

Equation 1: Splitting of water in hydrogen and oxygen

$$H_2O_{(l)} \rightleftharpoons H_2 + \frac{1}{2}\,O_2 \qquad \Delta H^0 = 298\,\frac{\mathrm{kJ}}{\mathrm{mol}}$$

There are several electrolyzer technologies available, namely proton exchange membrane (PEM) electrolyzer, alkaline electrolyzer, anion exchange membrane (AEM) electrolyzer and solid-oxide (SOEC) electrolyzer. An overview over the different technologies is given by Kumar and Lim (36). Every type of electrolyzer has its own advantages and disadvantages regarding the costs, flexibility to react to electric load changes, technical maturity or degradation behaviour which is not further discussed. The electric energy demand to produce hydrogen via liquid water electrolysis is in the range of 50 - 55 kWh/kg (36). After the electrolyzer unit and depending on the process, hydrogen is either:

- fed to a liquefaction unit (LH_2),
- fed to a methane synthesis (LCH_4) or
- fed to a Fischer-Tropsch process (SAF).

Aspects of the liquefaction units will be discussed in subchapter 2.1.2. The hydrogen liquefaction unit has an additional electric energy demand of at least 6 kWh/kg $_{H_2}$.

The methanation reaction i.e., the aforementioned “Sabatier-reaction” is given in Equation 2.

Equation 2: Methane synthesis based on H_2 and CO_2

$$4\,H_2 + CO_2 \rightleftharpoons 2\,H_2O_{(g)} + CH_4 \qquad \Delta H^0 = -164\frac{\text{kJ}}{\text{mol}}$$

The CO_2 source is not further discussed at this point. The exothermic nature is a positive aspect on the one hand since no external energy is required and heat released can be utilized elsewhere. On the other hand, this translates to energetic losses. One methane molecule contains 83 % of the chemical energy that is stored in four molecules of hydrogen, resulting in a 17 % chemical energy loss, without even considering the additional energy demand of the CO_2 supply. After the methanation unit, the gas is purified and then fed to a methane liquefaction unit.

Regarding the Fischer-Tropsch process, there are two main reactions involved (only the low-temperature process with Cobalt catalysts is considered). The first is the reverse water-gas-shift (rWGS) reaction to produce CO, the second is the “actual” Fischer-Tropsch reaction where a mixture of hydrocarbons is formed. The need for an upstream reaction step is a significant issue and has thoroughly been discussed in a thesis by Adelung (37) . The rWGS reaction is shown in Equation 3, the Fischer-Tropsch reaction in Equation 4.

Equation 3: Reverse water-gas-shift reaction

$$H_2 + CO_2 \rightleftharpoons H_2O_{(g)} + CO \qquad \Delta H^0 = 41\frac{\text{kJ}}{\text{mol}}$$

Equation 4: Hydrocarbon synthesis via Fischer-Tropsch reaction

$$2\,H_2 + CO \rightleftharpoons H_2O + -CH_2- \qquad \Delta H^0 = -152\frac{\text{kJ}}{\text{mol}}$$

The Fischer-Tropsch process does not produce a defined chemical compound but a mixture of hydrocarbons. Therefore, only the formation of a single hydrocarbon snippet is indicated in Equation 4. The distribution of products synthesised in this reaction can be described with the “Anderson–Schulz–Flory” (ASF) distribution (38). In the process hydrocarbons are produced by combining carbon atoms that are adsorbed to the catalyst. The probability, that a carbon atom is attached to another carbon atom is described with factor α, which is the “chain growth probability”. The mathematic formula of the ASF distribution is described with Equation 5 (39).

Equation 5: Anderson–Schulz–Flory distribution for hydrocarbons produced in a FT process

$$x_n = (1-\alpha)\cdot\alpha^{n-1}$$

The equation estimates the mole fraction of a hydrocarbon with the chain length “n” (for methane n = 1, for ethane n = 2, etc.). The value of α is influenced by several factors like

temperature, pressure, catalyst etc. This equation is not valid for the whole range of hydrocarbons, especially for light hydrocarbons like methane a correction term is required. The produced mixture of hydrocarbons has to undergo further steps like distillation or isomerisation that it complies with jet fuel specifications. Hydrocarbons that have not the required chain length can either be utilized elsewhere as side products or undergo further cracking or alkylation steps to increase the SAF yield of the process (39).

As for the methanation process, the overall chemical reaction is exothermic and thus, associated with energetic losses. For the formation of $C_{12}H_{26}$ as exemplary fuel molecule Equation 3 and Equation 4 can be combined to Equation 6. The amount of chemical energy stored in $C_{12}H_{26}$ is 84 % compared to the energy that is stored in 37 molecules of hydrogen. Though, the synthesis is not as selective compared to the methanation process.

Equation 6: Synthesis of dodecane as exemplary molecule for kerosene type jet fuel

$$37\ H_2 + 12\ CO_2 \rightleftharpoons 24\ H_2O + \ C_{12}H_{26} \qquad \Delta H^0 = -1331 \frac{\mathrm{kJ}}{\mathrm{mol}_{C_{12}H_{26}}}$$

1.3.2 Research question - Well to wake evaluation

As a summary of this chapter the following statements can be made.

- The most straightforward approach to reduce the CO_2 emissions of the aviation industry is the substitution of fossil kerosene with renewable kerosene. But the availability of biogenic feedstocks or organic waste streams pose a challenge towards its broader implementation.
- While all-electric aircraft offer an alternative for short-distance air travel with air-taxis, chemical energy carriers will be required for larger aircraft.
- Even in a scenario with no changes of the fuel type, PtX processes will be required to reduce the CO_2 emissions from the aviation industry substantially.
- Every PtX process considered in this thesis has hydrogen in its production chain. While the downstream processes are all subject to energetic losses, the direct utilization of hydrogen poses other difficulties resulting from its physical properties like the low volumetric energy density.
- The PtX based synthesis of LCH_4 is less complex than the PtX based synthesis of SAF

Based on these statements the following question arises:

- What is the “best” option to decarbonize the aviation industry? -

In this thesis, “best” is defined as most economic option. It could also be defined as fastest to implement, best for the environment, most socially accepted, most likely etc.

While these definitions are also relevant to give an overall picture, they cannot be evaluated with the evaluations performed in this thesis.

The options to decarbonize the aviation industry are indicated in Figure 3.

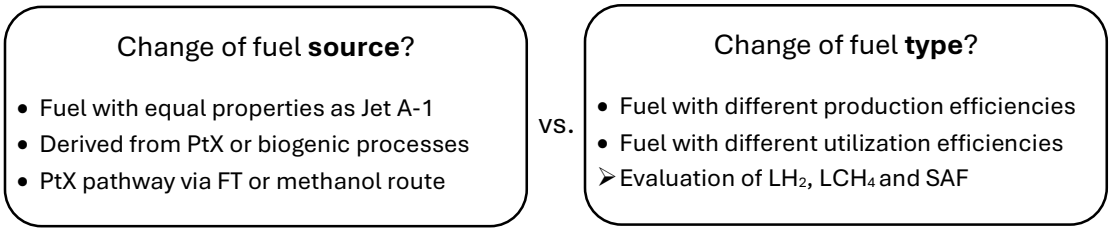

Figure 3: Approaches to decarbonize the aviation industry

The pathway and methodology to answer this aspect from a techno-economic perspective is the research question of this thesis. The focus on the production of the different fuel types is not sufficient, at least when cryogenic fuels are included. There, the implications of how the different fuel properties influence the aircraft design is not considered. Thus, an indicator is required to compare the different fuels when the utilization is included.

The indicator used in this thesis is $\frac{€}{PAX\ 100\ km}$ i.e., the costs in € per passenger (PAX) per 100 km distance travelled. Until the utilization step, the different fuels can be compared by the different costs in $\frac{€}{MW_{LHV}}$. To determine these indicators, the whole pathway is broken down into individual steps. The supply chain that is evaluated in this thesis is depicted in Figure 4.

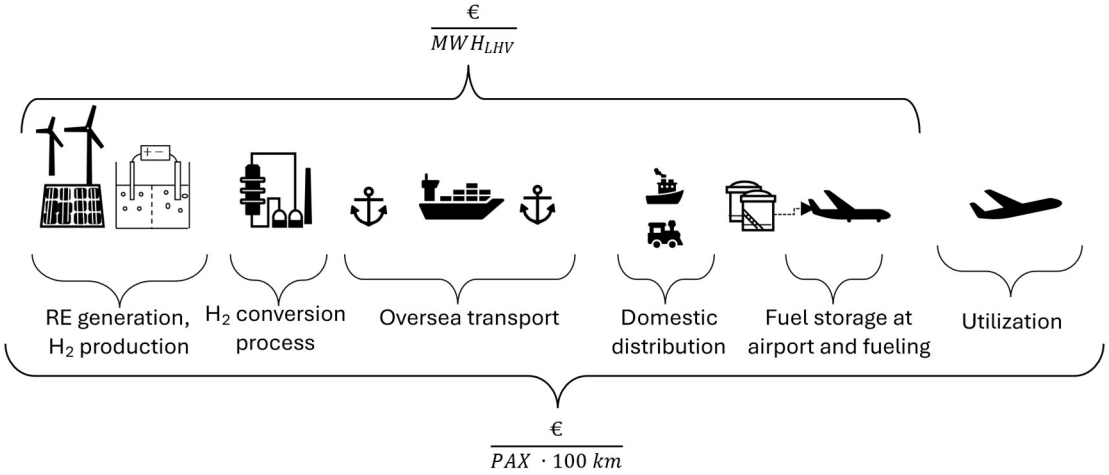

Figure 4: Steps of the evaluated “well-to-wake” supply chain

For the sake of a fair comparison, it is assumed that every fuel is produced via the PtX route. As indicated in Figure 4, the fuel synthesis is spatially separated from the airports and the fuels are transported with a carrier ship. A so-called “sweet spot” is considered as the location where the fuels are synthesized. This expression refers to a location with a high production potential of wind and/or solar energy. It is assumed that this location is at a remote place in the world. Exemplary locations where the realization of the depicted supply chain is at least considered by companies or other governmental institutions are:

- The Magallanes Province in southern Chile (40)
- The Omanian desert (41)
- “Sperrgebiet” in Namibia (42, 43)

The whole supply chain is broken down into the following steps (from left to right)

- **Step A** requires the supply of renewable energy like solar or wind energy to produce hydrogen (nuclear energy or hydropower could also be used, but it is not considered in this thesis). The reference sweet spot is El-Ouatia in Morocco. It is considered that a constant hydrogen mass flow is provided to the subsequent conversion step.
- **Step B** is the actual fuel conversion step i.e., the hydrogen liquefaction unit for **LH_2**, methanation process with the subsequent methane liquefaction unit for **LCH_4** or the **SAF** production process via the Fischer-Tropsch route. In this thesis, if CO_2 is required, it is supplied from air.
- **Step C** step evaluates the oversea transport logistics from the remote location (El-Ouatia in Morocco) to the port of entry (Wilhelmshaven in Germany).
- **Step D** evaluates the domestic distribution via inland waterway transport to Frankfurt and rail transport to Munich.
- **Step E** considers the required changes to the airport infrastructure which are necessary to fuel the corresponding aircraft. A liquefaction unit might be required for cryogenic fuels. Up to this point the steps A – E give the fuel costs in $\frac{€}{MWh_{LHV}}$.
- **Step F** is the actual fuel utilization which is required to evaluate costs in $\frac{€}{PAX\ 100\ km}$. Depending on the size of the aircraft or the fuel type, different aspects have to be considered, e.g. how is the chemical energy converted into propulsion. By combustion in a turbine or via electricity from a hydrogen fuel-cell? Or how is the lower volumetric energy density of LH_2 and LCH_4 and the aspect, that no wet-wing fuel storage is possible affecting the aircraft design and thus the specific energy demand for air travel?

Many papers have been published focusing on individual aspects of the chain depicted in Figure 4. The status of the current literature is presented in subchapter 2.1. But no study so far has evaluated the whole chain from a “well-to-wake” perspective and compared all the viable options from a technical and economical point of view. The aim of this work is to map the influence of the respective sub-steps and to determine to what extent the different steps affect the specific cost of air travel. This transparent assessment enables stakeholders involved to implement and to support the most preferential route to phase out fossil fuels from the aviation industry. The methodology used in this thesis can also be applied to evaluate other industries like the different fuel options for the maritime sector or even be used in the chemical industry to determine which pathways are most suitable to produce chemicals without using fossil feedstocks.

2 Current research status

In this chapter first a literature review of the different relevant technologies is conducted and the current status of the research is summarised. Then, the contribution of this work is outlined how further research will benefit from this thesis.

2.1 Literature review

The literature review is structured in "direction of energy flow" as shown in Figure 4. First the aspect of renewable energy generation and hydrogen production is discussed in subchapter 2.1.1. Then, the aspects of fuel production, general logistics, airport infrastructure and aircraft design are evaluated for LH_2 and LCH_4. Since in the case of SAF only the fuel production changes, the literature review does only consider this part of the chain. Table 4 gives an overview how the development has progressed for each step of the corresponding fuel chain (starting from H_2 and CO_2) and if this specific aspect is the focus of current research activities. Details and references to the statements are given in the respective subchapter.

Table 4: Overview of the respective stage of development

Step	LH_2	LCH_4	SAF
Fuel synthesis based on hydrogen (and CO_2)	Hydrogen liquefaction as niche application for rocket propulsion – Research activities mostly focus on the reduction of the specific energy demand of the liquefaction process.	**Chemical conversion:** State of the art. So-called package units can be supplied from the industry. **Liquefaction:** Industrially established on a large scale.	Small PtX based pilot plants are in operation. Many research papers are available. Fossil based process is state of the art.
Logistics	**Oversea transport:** Since 2022 one concept vessel is in operation with a capacity of 75 t. Many research papers available **Domestic distribution:** Transport via truck is available but niche application	**Oversea transport:** Industrially established on a large scale **Domestic distribution:** First inland waterway vessels are operating on the Rhine Cargo vessels for train transport are available	Industrially established on a large scale
Airport infrastructure	LH_2 storage tanks are niche application for space travel. Many research papers available	LNG storage vessels are state of the art No research papers available	Industrially established on a large scale

Aircraft design	Many research papers available	Some research papers available	Industrially established on a large scale

Some aspects of the following literature review might have already been mentioned in chapter 1, e.g. the methanation process. But to give a wholistic overview of current research activities, some aspects are mentioned twice.

2.1.1 Hydrogen production based on wind and solar energy

The first step in the evaluated chain is the production of renewable electricity that is required for the "power-to-x" process. Components like wind turbines and solar panels are state-of-the-art and incremental technical improvements are not focus of this thesis. Current research activities focus on the overall layout of the plant. The wind turbines, solar panels and also the electrolyzer are all capital-intensive components and thus, hydrogen costs are dominated by the depreciation costs of these components. It is therefore relevant to know, how to determine the installed capacity of each component to retrieve the lowest hydrogen production costs. (The same is valid for the carbon capture system and the actual fuel synthesis, but this subchapter focusses on the hydrogen production). Before the different research activities are discussed, the general issue is described.

A typical course of the solar irradiance of a not further specified location is shown in Figure 5. Even if this curve translates to low energy production costs, as they are currently propagated for countries like Saudi Arabia with a value of 1 ct/kWh_{El} (44), no statement can be made about the hydrogen production costs. If an imaginary electrolyzer is connected to a solar farm that produces electricity with the profile shown in Figure 5, to what relative size should the electrolyzer be sized? If the electrolyzer is able to use the peak production during the middle of the day, it will operate in partial load for most of the time. If it is sized to use only 60 % of the peak production, a large share of the produced electricity has to be curtailed. But what relative installed capacity would result in the lowest hydrogen costs? The methodology how to answer this question is evaluated in many research papers. The following gives an exemplary excerpt of current research activities:

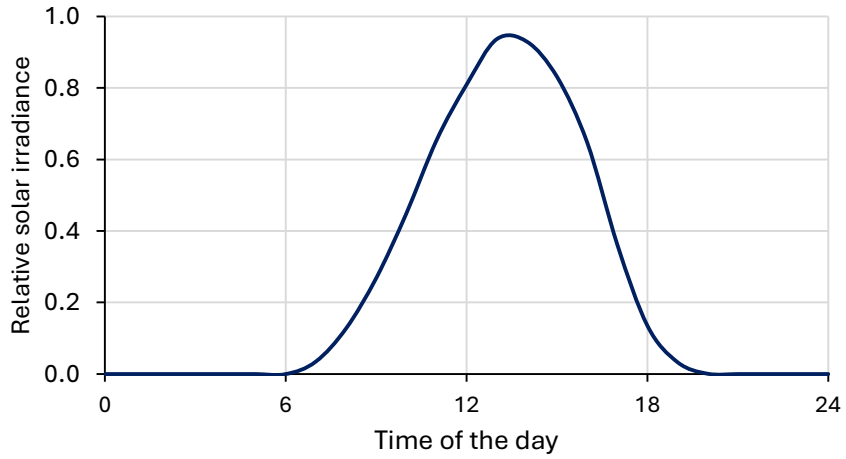

Figure 5: Exemplary solar irradiance curve

Mallapragada et al. evaluated in their study if hydrogen derived from solar energy can be cost competitive in the USA by 2030 (45). They assumed a continuous hydrogen production of 4.17 t/h (including a tolerance of ±10 %) and compared underground storage in salt caverns with storage in pressure vessels to balance the hydrogen supply curve over time. Their results include the installed capacity ratios between the solar farms and the electrolyzer as well as the cost implications of the storage systems. They determined more than 34 sites where the costs are below $ 2.5 per kg. Another study that focusses on hydrogen produced with solar energy has been published by Vartiainen et al. (46). They evaluated 8 locations around the globe but considered (in the opinion of the author) very optimistic cost assumptions for electrolyzer and solar panels. They retrieved costs as low as 1 €/kg for the Atacama Desert and stated, that in the year 2050 even in Helsinki the costs of hydrogen will be below 1 €/kg. A study where the dynamic hydrogen production from a combination of wind and PV is evaluated was published by Schnuelle et al. (47). They considered a dynamic hydrogen production in the northern parts of Germany for different electrolyser technologies as well as from onshore and offshore wind farms. They also considered wind farms that no longer receive a fixed renumeration and therefore, no depreciation costs have to be paid. They retrieved hydrogen production costs in the range of 5.90 – 11.66 €/kg.

Thus, current literature has a cost spread ranging from 1 – 11.66 €/kg. While the costs at the lower end include depreciation costs for solar farms, the costs at the higher end considered a power source where only the operating and maintenance costs were considered. The methodological approach for most of these cost estimations is to describe the plant with *linear equations*. A *linear programming* optimization is then used to determine the plant layout (further details are given in subchapter 3.1). But as it can be seen by the large cost spread, there is a certain disagreement in the scientific literature. How this thesis is contributing to eradicate this uncertainty is described in section 2.2.

So far, the actual plants that have been build had mostly a scientific background. One example is the solar-hydrogen project that was realized in the early 1990's close to "Neunburg vorm Wald" (48). More recently in 2018, a 1 MW PEM electrolyzer has been inaugurated at the DLR site in Lampoldshausen that is directly connected to a local wind farm (49). Larger projects are on verge of becoming realized, some of them at the sweet-spots mentioned in subchapter 1.3.2, another example is the PEM electrolyzer built at BASF, though this electrolyzer does not have a direct connection to a wind farm or solar farm (50).

2.1.2 Utilizing LH_2 in aviation

The research activities focussing on the introduction of LH_2 as fuel for commercial aviation date back to the 1970s and were mostly driven by the oil crisis (51). In a study published by Korycinski in 1978, the LH_2 demand at the airports of Chicago and San Francisco were simulated for a reference year between 1990 and 1995 (52). The study considered the daily LH_2 demand, required changes at the airport infrastructure as well as a brief description of two conceptual 400 passenger aircraft fuelled with LH_2. Obviously, these aircraft were never realized but in recent years LH_2 is again being considered as aviation fuel. This time with the motivation to reduce the aviation industry's GHG emissions.

The current research activities cover a very broad spectrum since almost no aspect of the recent value chain of the aviation industry remains untouched (fuel production, logistics, airport infrastructure, aircraft design and LH_2 utilization).

a) Hydrogen liquefaction

In the past, liquid hydrogen was almost exclusively used as rocket propellant (53). This is rather a niche application with few available alternatives for this particular use-case, thus not too much focus was put on the development of highly efficient hydrogen liquefaction processes. The global hydrogen liquefaction capacity was 335 tons per day (tpd) in the year 2009 (54). Several plants are currently under construction or have been inaugurated in recent years, so that the global capacity should soon be in the order of 500 tpd (55, 56) which is equivalent to roughly 700 MW_{LHV}. In the supply chain shown in Figure 4, the liquefaction unit is required directly after the electrolyzer to convert gaseous hydrogen into its liquid state and most likely at airports as a boil-off management system. Therefore, the efficiency of the liquefaction process has a relevant role in the overall fuel supply chain.

Until today, most hydrogen liquefaction plants are integrated into air separation units where liquid nitrogen is used as refrigerant for the precooling step of hydrogen (Precooling is the first cooling stage down to a temperature of more or less 80 K). These plants have an electric energy demand of roughly 11 kWh to liquefy 1 kg of hydrogen (57).

One area of current research activities is the evaluation how mixed refrigerants can reduce the specific electric energy demand. This has been thoroughly evaluated in a thesis by Eckroll (58). He concluded that the specific energy demand could be reduced to 5.9 kWh/kg when utilizing a mixed refrigerant containing nitrogen and C_1-C_4 n-alkanes.

Another field of research is the evaluation of the cryo-cooling step, thus the cooling step from 80 K down to the actual phase change of hydrogen. There, different cycles and refrigerants have been evaluated. Cardella et al. evaluated an open H_2-cycle and compared it with a cycle utilizing a mixture of Neon and Helium (59). Another thorough overview is given by Ghafri et al. (60). While the sole efficiency of the process is one aspect, the part load behaviour of the plant might be another crucial issue. If the liquefaction plant is located at a remote location behind an electrolyzer, it could be more economic to reaction to load changes than consider a steady hydrogen supply.

b) LH_2 logistics

The logistics of the LH_2 supply chain can be divided in the large-scale oversea transport and domestic distribution. The former has been subject to several studies and projects in the past with the Euro-Quebec Hydro-Hydrogen Pilot Project (EQHHPP) as one example from the early 1990s (61). In this project, it was envisaged to transport LH_2 from Canada to Germany. More recently, Japan has been considered as a country with a LH_2 import infrastructure and a supply from Australia (62). In 2022, the ship "Suiso Frontier" as being the world's first LH_2 carrier completed its first voyage (63). The ship has a capacity of 75 t which is equivalent to a storage volume of roughly 1,060 m^3.

The domestic distribution via trucks is state of the art with capacities of up to 4.5 t per truck delivery (64). Other means of domestic transportation could be inland waterway vessels and railcars (i.e., per train). While no inland waterway vessel for LH_2 exists so far, the railway transport is rather a niche application with few railcars available, according to Verfondern (65).

c) Airport infrastructure

The required changes at the airport infrastructure are evaluated in a study by Hoelzen et al. (66). They compare an underground fuelling system with a truck refuelling system at three different exemplary airports in Germany and evaluate the costs depending on the total hydrogen demand. They concluded that the overall fuel supply costs are dominated by the hydrogen feed costs (69 %) and the costs for hydrogen liquefaction (25 %), while the remaining costs for storage and logistics only have a minor role (6 %). A detailed analysis of the turnaround and refuelling procedure at the airport is performed by Mangold et al. (67). They outline the safety aspects and the necessity of tight connections between the aircraft and the refuelling systems.

d) Aircraft design and LH_2 utilization

The general design of the aircraft is subject to change if LH_2 is utilized instead of kerosene. Since no conventional wet-wing fuel storage is possible, fuel has either to be stored inside the fuselage or in additional tanks mounted to the aircraft, as it is shown in Figure 6. In the former case, the fuselage might become bulkier compared to the commonly known round shape. The following figures show different aircraft concepts that have been proposed in the past.

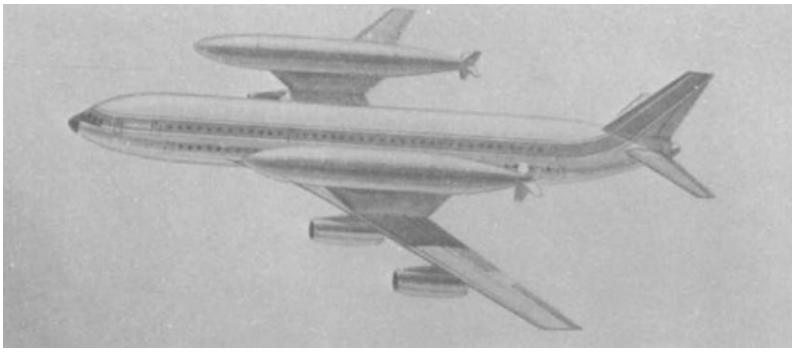

Figure 6: Tube-and-wing design with additional LH_2 tanks – Proposed in 1976 by Brewer (51)

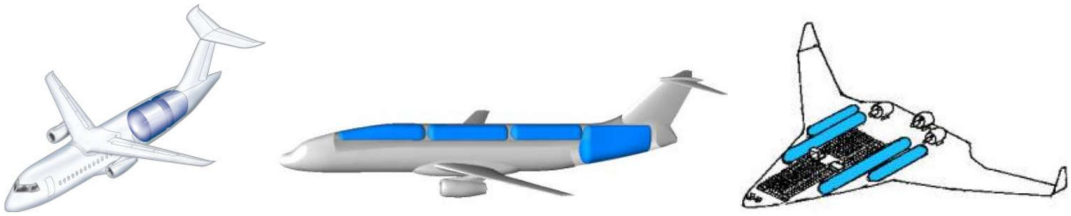

Figure 7: Aircraft concepts from the “Cryoplane” project – Published by Airbus in 2003 (68)

In Figure 7 it is shown, how LH_2 tanks could be distributed inside the aircraft. Especially in the aircraft on the left it is visible, that due to the location of the tanks inside the fuselage, less space is available for cargo and passengers than it would be for a wet-wing fuel storage system. The aircraft in the middle of Figure 7 depicts a bulkier fuselage. Ongoing projects like the ZEROe program by Airbus also work with similar designs and further evaluate more radical concepts like the Blended-wing aircraft depicted on the right in Figure 7 (26). The aircraft design is not only influenced by the implications of the fuel storage concept, but also how hydrogen is utilized. In subchapter 1.2.3 it is mentioned that hydrogen can either be burned like kerosene or utilized in fuel-cells. If the latter is considered, the number of propellers on the wing can drastically increase as it is shown in Figure 8.

Figure 8: Concept regional aircraft from the DLR Exact project - Bild: DLR, CC BY-NC-ND 3.0

The conversion of hydrogen in fuel-cells inside the aircraft require different powertrain concepts compared to conventional aircraft. This is also explained in detail in a publication by Vietze and Weiland (69). To conduct further research and evaluate the dynamic behaviour of the powertrain components inside the aircraft, the German Aerospace Centre (DLR) is building a research facility in Empfingen in the “BALIS” project (70).

Another research area that is connected to the implementation of hydrogen as aviation fuel is the effect on the climate resulting from the utilization. Since in this thesis no life cycle assessment is conducted and non-CO_2 emissions are not evaluated, this area is only mentioned to give an insight of the whole issue but is not further discussed.

In a study by Svensson et al., the dependency of the flight altitude and thus the emissions of water vapor are evaluated (71). Apart from the emissions resulting from utilization, the GHG potential of hydrogen emissions itself (resulting from purging, leakage or slip) also need to be considered, as shown in a paper by Sand et al. (72).

2.1.3 Utilizing LCH_4 in aviation

The research activities focussing on LNG as aviation fuel date back to the 1980s and were driven by the oil crisis and the prediction of the oil-peak to occur in the year 2000 (31). The study published by Carson et al. in 1980 makes a thorough analysis about the competitiveness of LH_2 and LNG compared to kerosene type aviation fuels, though with the sole focus on fossil derived fuels and without the option of hybrid-electric aircraft. Therefore, their conclusions are based on different boundary conditions as they apply in this thesis. As for LH_2, almost every part of the aviation industry would be affected by the introduction of LCH_4 as fuel. Though there is significantly less research

activity ongoing that evaluates the introduction of LCH_4. The fossil variant of LCH_4 (i.e., LNG) is a global commodity and apart from the aircraft design, not too many aspects of the chain require further research before LCH_4 could be introduced as aviation fuel. Thus, research papers focus mostly on new aircraft designs.

a) Methane synthesis and liquefaction

The sole catalytic conversion of H_2 and CO_2 to methane and water is state-of-the-art. Package-units with an integrated reactor can be purchased from the industry, e.g. from MAN Energy solutions (73). Nevertheless, the synthesis based on H_2 and CO_2 (also framed under the expression "Power-to-Gas") was subject to several research projects in the past like the "STORE&GO" project (74). In these projects, not only the synthesis itself but also the evaluation if such a plant is suitable to store energy were evaluated. The car manufacturer Audi also promoted the concept of "Power-to-Gas" to enable their customers to drive the Audi "g-tron" with renewable produced methane. Recent research activities focussed mostly on details of the catalytic mechanisms and improvements of the catalyst (75).

The liquefaction process of methane is state-of-the-art. The global liquefaction capacity of natural gas was 478.4 MTPA in the year 2022 (33). This is equivalent to 758 GW_{LHV} and therefore, around a factor of 1000 times higher compared to the hydrogen liquefaction capacity. Research activities focus on further improvements of the liquefaction process itself, as shown in the dissertation by Bin-Omar (76).

b) LCH_4 / LNG logistics

LNG is used as fossil analogy to LCH_4. The amount of LNG that has been imported by Europe and Asia amounted to more than 375 MTPA in 2022 (33). It is globally available with efficient state-of-the-art logistics even to provide energy security of entire countries. Thus, not too many research activities are available or even required in this area.

The same aspect accounts for the domestic distribution. The inland waterway transport has been demonstrated on the Rhine since 2013 with the vessel "Greenstream" (IMO: 9664990) (77). Also the rail transport of LNG is state of the art (78).

c) Airport infrastructure

Since almost no research papers evaluate the utilization of LCH_4 in the aviation industry, the aspect how it could be stored at the airport or how aircraft could be fuelled is currently not evaluated by researchers. But since large LNG tanks are required at LNG terminals and several truck manufacturers offer LNG-trucks, certain analogies can be taken over from these industries (79).

d) Aircraft design and LCH_4 utilization

In 2012, NASA and Boeing evaluated in the "SUGAR" program (SUGAR as Subsonic Ultra Green Aircraft Research) different LNG fuelled aircraft concepts that could enter the market in the 2040s (80). The aircraft size considered has been the A320/B737 class. They concluded that the total energy demand for a given flight increases by 5.6 % compared to aircraft using kerosene due to the overall heavier aircraft. In 2020, Rompokos et al. evaluated the performance of a modified B737-800 fuelled with LNG. They considered an "above-the-passenger-cabin" tank system, similar to one depicted in the middle of Figure 7 and estimated an energy demand increase of 10 % compared to an aircraft fuelled with kerosene.

A LNG-powered widebody aircraft like the B777 was evaluated in a student thesis conducted at the DLR in 2015 (81). This thesis focussed on technical aspects like the tank configuration, the dimensions of the aircraft and its dependency on aerodynamics and seat capacity. Figure 9 shows an exemplary cross section with the tank location inside the fuselage.

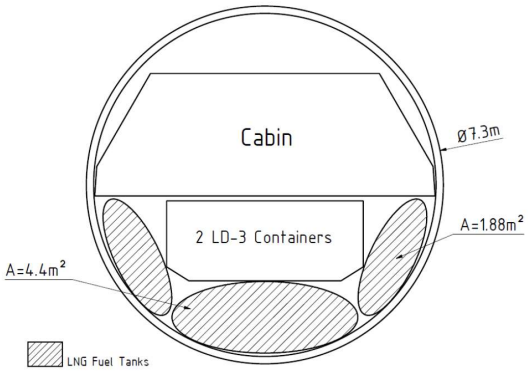

Figure 9: Fuselage cross section of LCH_4 fuelled widebody aircraft – taken from (81) "Layout C-round"

Another approach to introduce LNG as aviation fuel is the concept of a multi-fuel aircraft. This has been proposed by Gibbs et al. (82). With this approach, kerosene could still be stored in the wings of the aircraft and additional LCH_4 tanks could be used to cover the remaining fuel demand of the aircraft. These aircraft types are not considered in this thesis but are included in this chapter to give a complete picture of the current state of research.

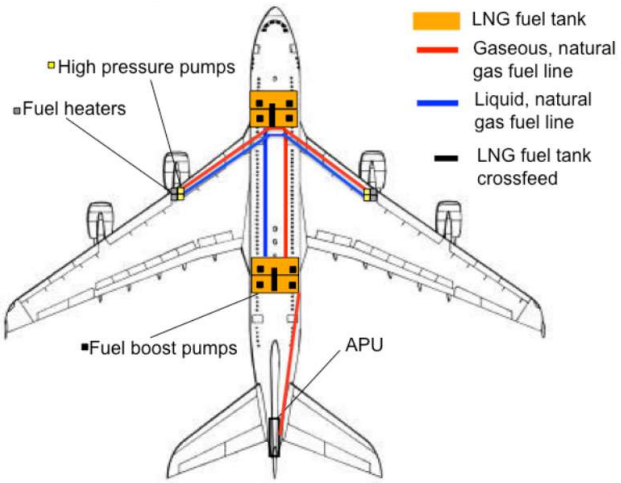

Figure 10: Engine fuel supply system of a concept multi-fuel aircraft (82)
* APU = Auxiliary power unit

2.1.4 Electricity based SAF production processes

The two main processes how kerosene is produced via the PtX route is the Fischer-Tropsch (FT) pathway and the methanol-based pathway. The latter is a rather new technology with ongoing research projects like the “M2SAF” or “KeroSYN100” (83, 84). This pathway is also not certified yet, as it can be seen in Table 2 and is not further considered.

The sole FT reaction according to Equation 4 was discovered in the 1920s and has been incorporated in large production facilities since then. An overview of the historic aspects can be found in a publication by Davis (85). The three largest plants mentioned in a paper by Martinelli et al. have a capacity of more than 140,000 barrels per day (86). All are running on a fossil feedstock where no rWGS reaction is required. Furthermore, it is not stated if the main product of these plants is kerosene. Even though the FT-reaction itself is commercialized on a large-scale, there are still ongoing research activities, especially if the whole process including the reduction of CO_2 to CO is included. Most publication focus on the following aspects:

- CO_2 reduction to CO via rWGS (87, 88), plasma (89) or electrochemical (89)
- CO_2 active FT synthesis (90, 91)
- Catalyst and reactor design with the emphasis of yield improvements (86, 92)

It is noted that the cited literature is only an exemplary excerpt of the available publications. Further aspects that could be considered is the dynamic behaviour of the reactors if the plants are intermittently supplied with hydrogen and CO_2 and how it influences the yield of SAF.

Plants where the whole “electricity based SAF production process” is performed are rare. Close to the airport of Frankfurt, a plant with an annual production capacity of 2,500 t is under construction and will start operation in 2024 (93). As a comparison, the maximum fuel storage capacity of an A380 is 250 t, i.e. 10 % of the annual plant capacity. Another example is the demonstration plant in Werlte in Lower-Saxony with a production capacity of 25 m^3 (roughly 20 t) per year which has been running since 2021 (94). While both plants produce rather small amounts of SAF a year, they act as first projects to demonstrate how SAF can be produced based on hydrogen and CO_2. Further facilities with higher production capacities are planned, but are at an early planning stage (95, 96). The technical concept of the “electricity based SAF production process” has been proven but the cost perspective has not been mentioned in this subchapter so far.

Table 5 gives an overview of the PtX derived SAF costs reported in literature. As a comparison, the price for fossil Jet A-1 was 0.96 €/kg in November 2023 in Europe which is equivalent to 80 €/MWh_{LHV} (97).

Table 5: Overview of PtX based SAF production costs

Authors	**CO_2 source***	**CO_2 costs [€/t]**	**Power costs [€/MWh]**	**FT/SAF costs [€/MWh_{LHV}]**	**Remark**	**Source**
Adelung et al.	MEA	-	76.8	326	Base case	(98)
Albrecht et al.	U	37.8	105	297	PtL Case	(39)
Brynolf et al.	U	30	50	224	2015 Case	(99)
Brynolf et al.	U	30	50	180	2030 Case	(99)
König	MEA	37.76	105	283	Reference case	(21)
Schemme et al.	U	70	98	231	H_2 from pipe	(100)

* U = undefined from a pipe, MEA = via flue gas amine scrubber

Table 5 is only a small excerpt of the available data. A broad overview of the costs for all SAF production technologies, including the ones from Table 2, is given in a review paper by Detsios et al. (101). However, it can be concluded that the production costs of electricity-based fuels are several times higher than the current prices at the airport.

According to Albrecht et al., 70 % of the fuel costs result from the costs for electricity. So, the cost of electricity is the most relevant input parameter for the cost estimation. Electricity is retrieved from the electric grid with a fixed price per MWh in all studies cited in Table 5. Thus, the whole plant is capable of running in a steady state mode at its designated capacity. This consideration might not be applicable for plants built at the sweet-spots mentioned in subchapter 1.3.2.

2.2 Contribution of this work beyond the current research state

In section 2.1 an overview is given about the different aspects of the chain shown in Figure 4. Every aspects involved has been outlined that will be relevant if electricity-based SAF or even cryogenic fuels will be introduced on a large scale in the aviation industry. So far, no study has compared these different approaches on a systemic level. This is performed in this thesis based on evaluating the 6 steps introduced in section 1.3.2. With this approach, the cost reduction potential of every step is openly presented to outline how the costs of air travel could be reduced by further improvements.

The corresponding publications that have been published as part of this thesis do further contribute to a better understanding of:

- How to design a hydrogen production plant with wind energy, solar energy and grid electricity as possible power sources and depending on local weather conditions
- The costs of importing fuels from a sweet spot and the influence of the location of the carbon-source
- How cryogenic fuels can be transported domestically and utilized eventually

2.3 Methodology and scientific approach

Different methodologies are used for the corresponding steps of the evaluated supply chain. For the first step of the supply chain shown in Figure 4, a tool has been developed to determine the most economic plant layout that can provide a constant hydrogen stream to a subsequent conversion unit. This tool has been developed in PyCharm 2021.2 and uses the Gurobi solver to find the optimum solution. Details of this tool and exemplary results for several locations around the world have been published in **Publication I**.

In **Publication II** the first half of the supply chain shown in Figure 4 has been summarized and evaluated. Based on the methodology presented in Publication I, the levelized costs of hydrogen at the exporting site in Morocco are assessed. The corresponding fuel synthesis processes are depicted in ASPEN Plus. The economic evaluation is performed with the DLR-inhouse software TEPET (39). In this publication, a sensitivity analysis is conducted where the influence of the location of the carbon source is evaluated. It is differentiated if CO_2 is captured from air at the exporting site or from a local point source at the importing site. The aspects of the oversea transport of the fuels are based on another publication from the author of this thesis.

The domestic fuel distribution, fuel storage at the airport as well as the utilization in future aircraft are all part of **Publication III**. Another tool has been developed to

determine the required number of transport vessels (via inland water vessel, truck or train) that are required to supply the corresponding fuel to exemplary airports. The fuel demand depends on fuel utilization scenarios where for different flight routes and aircraft categories the share of LH_2, LCH_4 and SAF has to be assumed. The fuel demand of the different aircraft is estimated with data from literature. To estimate the costs of future aircraft two different standardized models are applied.

3 Publications

This thesis is based on the work published in the following journal contributions:

I. Sweet spot analysis for large-scale hydrogen production plants

Moritz Raab, Robin Körner, Ralph-Uwe Dietrich (2022): Techno-economic assessment of renewable hydrogen production and the influence of grid participation.

https://doi.org/10.1016/j.ijhydene.2022.06.038

II. Fuel production and large-scale transport to Germany

Moritz Raab, Ralph-Uwe Dietrich (2023): Techno-economic assessment of different aviation fuel supply pathways including LH_2 and LCH_4 and the influence of the carbon source.

https://doi.org/10.1016/j.enconman.2023.117483

III. Domestic fuel distribution and utilization

Moritz Raab, Wolfgang Grimme, Jon Gibbs, Paula Philippi and Ralph-Uwe Dietrich (2024): Aviation fuels of the future – A techno-economic assessment of distribution, fueling and utilizing electricity-based LH_2, LCH_4 and kerosene (SAF)

https://doi.org/10.1016/j.ecmx.2024.100611

Additionally, the scientific work has been presented at the following national and international conferences:

- Moritz Raab and Ralph-Uwe Dietrich (2020) "Large-scale hydrogen transport - Techno-economic assessment of different pathways" ProcessNet EVT, 04. - 05. March, Frankfurt, Germany.
- Moritz Raab and Ralph-Uwe Dietrich (2022) "Challenges of intermittent hydrogen supply and constant hydrogen demand - A techno-economic assessment of different sweet spots and the influence of grid availability" ProcessNet EVT, 30. March - 1. April, Bamberg, Germany.
- Moritz Raab and Ralph-Uwe Dietrich (2023) "Techno-Economic Assessment of SAF and Other Radical Technological Changes to Decarbonize Aviation". 11th FSC International Conference, 23. - 25. May 2023, Aachen, Germany.

3.1 Publication I

Sweet spot analysis for large-scale hydrogen production plants

Moritz Raab, Robin Körner, Ralph-Uwe Dietrich (2022): Techno-economic assessment of renewable hydrogen production and the influence of grid participation.

https://doi.org/10.1016/j.ijhydene.2022.06.038

Available online at www.sciencedirect.com

ScienceDirect

journal homepage: www.elsevier.com/locate/he

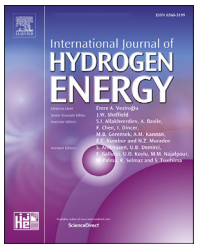

Techno-economic assessment of renewable hydrogen production and the influence of grid participation

Moritz Raab[*], *Robin Körner*, *Ralph-Uwe Dietrich*

German Aerospace Center (DLR), Pfaffenwaldring 38-40, 70569, Stuttgart, Germany

HIGHLIGHTS

- Sweet-spot analysis of hydrogen production facilities for constant hydrogen supply.
- Dynamic evaluation of energy and hydrogen production, as well as hydrogen storage throughout the year.
- Linear programming approach to evaluate minimum hydrogen costs.
- Adapting the share of installed wind and PV capacities depending on the location to minimize hydrogen production costs.

ARTICLE INFO

Article history:
Received 23 February 2022
Received in revised form
25 May 2022
Accepted 5 June 2022
Available online 7 July 2022

Keywords:
Renewable hydrogen production
Sweet spot analysis
Linear programming
Grid assisstance
Green hydrogen

ABSTRACT

Large-scale hydrogen production facilities will be required to supply the chemical energy demand of certain industries in the future. The case for such production plants based on individual adapted PV and wind farms has been addressed in several studies. However, most studies focus on an island solution of the evaluated plant and therefore, do not allow grid assistance which significantly reduce the installed capacity of the corresponding units. To address this issue, we developed a tool with a linear programming approach to evaluate any location around the world for its renewable hydrogen production costs and the influence on the plant layout depending on its interaction with the grid. A detailed techno-economic evaluation has been performed for five locations where hydrogen production costs in the range of 4–6 €$_{2020}$/kg have been retrieved. Furthermore, it is shown that with perspective cost data the costs can further be reduced to 2.50 €$_{2020}$/kg.

Introduction

The usage of fossil based primary energy carriers has caused an increase in the concentration of CO_2 and other greenhouse gases (GHG) in the atmosphere of the earth resulting in global warming and the climate crisis. While there are political instruments implemented around the globe to reduce these emissions, with current measures mankind will most likely fail the goal of the COP21 Paris Agreement limiting global warming to "well below" 2 °C [1,2]. In order to reach the 1.5 °C goal, a rapid electrification of end-use applications, especially in the heating and transportation sectors is required [1]. But there are sectors where a direct electrification is not feasible e.g., the steel industry, aviation or shipping. For these sectors hydrogen and hydrogen-based synthetic fuels will have to

* *Corresponding author.*
E-mail addresses: Moritz.Raab@dlr.de (M. Raab), robin.koerner@dlr.de (R. Körner), Ralph-Uwe.Dietrich@dlr.de (R.-U. Dietrich).
https://doi.org/10.1016/j.ijhydene.2022.06.038

replace fossil chemical energy carries in order to reach the climate goals [1]. This issue is addressed by an enormous increase in global funding for research activities and first demonstration projects regarding all aspects of a global hydrogen economy like the production, distribution, and utilization (directly and via hydrogen-based fuels) [3–5]. For the case of Germany, the hydrogen demand for the year 2030 is predicted to be in the range of 90–110 TWh, of which about 14 TWh can be produced domestically [6]. Hydrogen import options might prevail in the near future while its origin is not determined yet. Countries like Chile and Australia recently got a lot of attention for their high potential to produce renewable energy (RE), such locations are called "sweet spots". A transparent techno-economic based rating of different locations is required and the first step to develop a hydrogen import options map. Further social aspects, e.g. considering the local population and its own development goals, must get addressed as well. The increase of RE-capacity has to be carried out under a fair development partnership [7].

Only countries and regions with a clear climate-protection roadmap, e.g. electrifying their own energy system, should be considered to provide hydrogen or hydrogen-bases fuels to the rest of the world.

If a certain sweet spot is selected to build a hydrogen production plant from local "excess" RE, the layout of the whole plant must be individually designed to the local conditions in order to achieve high capacity factors of the RE sources and due to the high required investments [7]. Furthermore, the intermittency of the renewable power supply and its implications on the consecutive hydrogen conversion step needs to be considered. Cryogenic liquefactions as well as the Fischer-Tropsch synthesis, as an exemplary PtX process, are usually designed to run in a stationary mode; even though recent studies focus on the dynamic behavior of these processes [8,9]. Load changes will considerably reduce the production rate, they can lead to increased thermal stress resulting in higher maintenance costs as well as challenges in the design of the process. In this study a hydrogen production plant with its own RE sources is designed, so that a consecutive conversion step gets supplied with a constant flow of hydrogen. Consequently, storage devices for electricity and hydrogen will be required for such a plant.

Several studies have examined the production costs for green hydrogen. In order to take the fluctuating renewable energy supply into account, a dynamic simulation with an hourly temporal resolution is usually considered. Mallapragada et al. [10] assessed the levelized cost of hydrogen ($LCOH_2$) for the year 2030 for solar energy (PV) based plants with a continuous hydrogen supply of 100 t/d in the US. An "island solution" was considered for every plant, meaning no relevant external mass or energy flows, except the water input and hydrogen output are considered. They identified a set of locations around the US where the $LCOH_2$ were as low as 2.5 $/kg with a plant availability of 95% if a salt cavern could be used as intermediate hydrogen storage. Schnülle et al. [11] assessed the current $LCOH_2$ for northern Germany based on PV, onshore, and offshore windfarms, also focusing on island solutions in their business cases. In their study, a direct link from the power source to the electrolysis is considered, mainly due to the German energy law to avoid higher costs from grid fees and taxes. The minimum costs amount to 4.33 €/kg_{H_2} for the case with an alkaline electrolysis and electricity from a fully depreciated onshore wind farm [11]. Vartiainen et al. [12], while also considering an island solution with an electrolyzer capacity of 100 MW_{el}, estimated the PV based $LCOH_2$ for 10 locations for current costs as well as perspective costs up until the year 2050. Their results indicate that the $LCOH_2$ in the year 2050 are lower than the current $LCOH_2$ based on methane steam reforming, 0.30–0.84 €/kg compared to roughly 1.70 €/kg for every location considered [13]. The year 2050 is also the reference year of the "PtX-Atlas" published by Pfennig et al. [14]. They focused on the $LCOH_2$ of liquid hydrogen in coastal locations and retrieved values of 1.92–4.59 €/kg.

In summary, a lot of research activity has been going on regarding the assessment of hydrogen production based on renewable energy like wind and PV and for island solutions, as can be seen in Table 1. Large-scale hydrogen production plants will interact with the local electric grid, even if they have their own RE sources. In this study, its implications on every step along the production chain will be evaluated and thoroughly discussed. With the participation of the local grid, the hydrogen production costs can be further reduced by omitting the demand for storage equipment to a certain extent. Furthermore, land use and the resulting ecological footprint might be reduced if the installed capacities of the plant can also be decreased.

The aim of this study is a reproducible and transparent assessment of hydrogen production plants designed to minimize each site-specific cost for a constant hydrogen supply including potential grid support. Several sweet spots around the globe are evaluated to consider different climate conditions. Grid assistance leads to the fact that the produced hydrogen will not be 100% renewable, but it might be beneficial from a technical, economic and even ecological point of view. This relationship between partial electric grid support and the optimal dimensioning of the unit operations is the focus of this study. The basic outline of the hydrogen supply plant is depicted in Fig. 1. The consumer might be a liquefaction plant for green hydrogen export or any other PtX-plant.

Methodology of techno-economic evaluation

Definition of the case study

In this study, the layout of a plant is evaluated that continuously supplies an undefined downstream processing plant with hydrogen. To consider different climate conditions, 5 sweet spots around the globe are evaluated. First, a **base case [BC]** is evaluated to retrieve the currently achievable minimal $LCOH_2$, which will be reported in $€_{2020}/kg_{H_2}$. The base case considers the current technical and economic progress and an "island solution" as reference frame. Then, different scenarios are evaluated; to mimic downtime periods of the downstream plant, the **downtime case [DT]** is considered where no hydrogen is delivered to the downstream processing plant for a consecutive time of 760 h. This case is evaluated to see, if purposely overlapping schedulable maintenance works with

Table 1 – Levelized costs of hydrogen - Selection of current and perspective cost predictions.

Author	Reference year	RE supply	Location considered	$LCOH_2$
Schnülle [11]	2020	Wind & PV	Northern Germany	4.33–12.38 €/kg
Vartiainen [12]	2020	PV	Various (focus on high PV potential)	0.93–2.16 €/kg
Vartiainen [12]	2030	PV	Various (focus on high PV potential)	0.60–1.44 €/kg
Mallapragada [10]	2030	PV	USA (10 most favorable sites)	1.98–4.00 $/kg
Pfennig [14]	2050	Wind & PV	Various (global PtX-Atlas)	1.92–4.59 €/kg (liquid)

periods of low RE production potential will be beneficial for the $LCOH_2$, since hydrogen processing plants have usually 8000 operating hours per year [15]. In the cases **G-10** and **G-25** no downtime is considered but the influence on the plant layout is determined when a certain amount of power can be drawn from the electric grid. For the G-10 case, the electric power drawn from the grid is enough to meet 10% of the required hydrogen flow and 25% in the G-25 case, respectively. All cases are listed in Table 2. Additionally, in a sensitivity analysis the future reduction potential of $LCOH_2$ will be outlined by using cost decline predictions. In the sensitivity analysis cost predictions for photovoltaic (PV) cells and electrolyzers are considered, for further details see subchapter 3.1.1 and 3.3. The total annual hydrogen mass flow is taken from a previous study and amounts to 225,500 t/a [16]. This is equivalent to 10% of the minimum hydrogen import demand in the year 2030 according to the German hydrogen strategy [6] and corresponds to 25.74 t_{H_2}/h and a power output of 858 $MW_{H_2, LHV}$. A mass flow in this order of magnitude exceeds the limits of a scale up approach and requires numbering up of the individual process units. In order to retrieve the minimal $LCOH_2$ for every location and scenario, a linear programming approach is used and further introduced in subchapter 2.2. Since the hourly mass flow will not be adapted, the annual mass flow is reduced to 205,936 t in the downtime case.

As already stated, one year with a temporal resolution of 1 h is considered for the dynamic simulation. For the evaluation, discrete mass and energy packages are transferred in between the unit operations of the plant, giving it a pseudo-continuous appearance. An exemplary temporal course and intermediate results are given in chapter S.1.2 in the supplementary information. RE is supplied via wind turbines and PV panels depending on their availability, which is determined from weather data from the individual location. Electric energy is either stored for later use or directly transferred to the electrolysis unit, which can either be a proton exchange membrane (PEM) or alkaline electrolysis. The produced hydrogen is transferred to the consumer or a hydrogen storage unit. The total mass flow to the consumer, meaning the mass flow from the electrolysis unit plus the flow from the storage unit, must be constant for every hour of the year. The whole plant is designed to obtain the lowest $LCOH_2$ achievable. Excess electric energy gets curtailed. If a storage unit is considered, it has the same loading level at the start and the end of the evaluated year. Meaning it can have a loading level of 47% at the beginning but then the loading level at the end of the evaluated year must also be at 47%. There are no upper limits regarding the installed capacities of the unit operations. Relevant data of the considered units can be found in chapter 3 and are summarized in the supplementary information. Transmission and transformation losses of electric energy are neglected. Table 3 lists the basic input values of the scenarios.

Methodology of the techno-economic evaluation

The methodology of the evaluation is based on a previous study focusing on techno-economic assessments (TEA) of chemical production plants and is extended to PV and wind farms [18]. Fixed capital investment (FCI) and partly the operating costs (OPEX) are estimated by using the factor method. The so called "Lang-factors" are the ratio between the costs of an equipment that has been fully installed, designed

Table 3 – General input values for the techno-economic assessments.

	Unit	Value	Source
Hydrogen flow	t/h	25.74	Assumption, based on [16]
Depreciation time	a	20	Assumption, based on [15]
Weighted Average Cost of Capital (WACC) - OECD countries	–	5%	[17]
WACC – non-OECD countries	–	7.5%	[17]

Table 2 – Cases evaluated in the study.

Case	Adaptation to base case
Base case - [BC]	–
Downtime case - [DT]	Downtime of 760 h of the downstream plant is considered – evaluation as island system
Grid connection - [G-10]	Grid supply can meet 10% of the required H_2 flow (2.57 t/h)
Grid connection - [G-25]	Grid supply can meet 25% of the required H_2 flow (6.48 t/h)
Sensitivity - S1	Sensitivity analysis regarding PV costs
Sensitivity - S2	Sensitivity analysis regarding electrolyzer data
Sensitivity - S3	Sensitivity analysis regarding PV and electrolyzer data

incl. cost for building, construction etc. compared to its sole procurement costs [19]. Remaining OPEX arise from participating with the electric grid and labor costs. With the given input data from chapter 3, specific annual costs C_i. (see Equation 1) are determined and adjusted to every location.

In order to determine the plant layout with the lowest $LCOH_2$, a tool has been developed in using Py-Charm 2021.2 and employing the Gurobi solver [20]. The underlying mathematical model determines the lowest $LCOH_2$ by minimizing the *objective function* (Equation 1) with a linear programming approach i.e., the specific annual costs C_i are independent of the corresponding installed capacity:

Equation 1: Objective function of the mathematical model.

$$C_{Total} = C_{PV} \cdot x_1 + C_{Wind} \cdot x_2 + \sum_{Bat} C_{Battery} \cdot x_{3,bat} + C_{Elec} \cdot x_4 + C_{Comp} \cdot x_5 + C_{C-St} \cdot x_6 + C(h)_{Grid} \sum_{h=1}^{8760} E_{Grid,h} \quad (1)$$

The *decision variables* ($x_1 - x_6$) of the objective function are equivalent to the required installed capacities of the corresponding units. These are the variables the solver is adapting to find the lowest $LCOH_2$. A set of *constraints*, i.e., boundary conditions is defined by linear equations which describe all flows, conversions, efficiencies and losses of the entire hydrogen production plant. An exemplary constraint is the requirement of the constant hydrogen flow, i.e., the mass flow from the storage unit plus from the electrolyzer, as shown in Fig. 1, must be equal to 25.74 t/h. Details and equations of the mathematical model like the whole set of *constraints* or the declaration of the *decision variables* can be found in chapter S.1 of the supplementary information.

In addition to the $LCOH_2$, useful intermediate results like the levelized costs of electricity (LCOE) or the capacity utilization factor (CUF) of the PV and wind farms are obtained. The dynamic behavior of the individual units and the storage systems of the plant along the year are also part of the results. However, given that the mathematical model works with the weather data of the entire year instantaneously, it inherently features "perfect foresight". This means for example, that the model knows perfectly when and how much energy is required or needs to be stored to compensate for a time of scarcity in the future, operating in the leanest way. In a more realistic scenario, storage systems might be kept as full as possible during a certain season. This would result in a higher CUF of the PV and wind farms, but also in a greater loss of energy due to possible self-discharge of the storage systems. The schematic flowchart with the corresponding input and exemplary output parameters is depicted in Fig. 2.

Example locations for the evaluation

5 locations around the globe are evaluated. Since the influence of the grid is also evaluated, only countries with a stable grid are considered. The locations are handpicked and selected on an emphasis of high potential for wind and solar energy [21,22]. Some of the locations are already considered for large-scale renewable energy generation or PtX-projects [23–26]. Table 4 lists the location considered and the corresponding coordinates for which the weather data has been retrieved. Different tilt angles for the PV panels are considered, depending on the latitude of the location, to increase the energetic output. The angles are determined by the method of Chinchilla et al. [27].

Unit operations of the hydrogen production plant

In this section, the relevant aspects of the unit operations considered for a process plant, as it is depicted in Fig. 1, are described.

Renewable energy supply

The availability of solar and wind energy is determined by the local and temporal weather conditions. To consider different locations, publicly available data of the weather conditions with 2019 as the reference year and a local resolution of 0.5° × 0.625° is used [35–37]. This is equivalent to 55.6 km × 63.02 km in Pampa Anita, the location closest to the equator, and 55.6 km × 41.65 km in Punta Arenas, the location

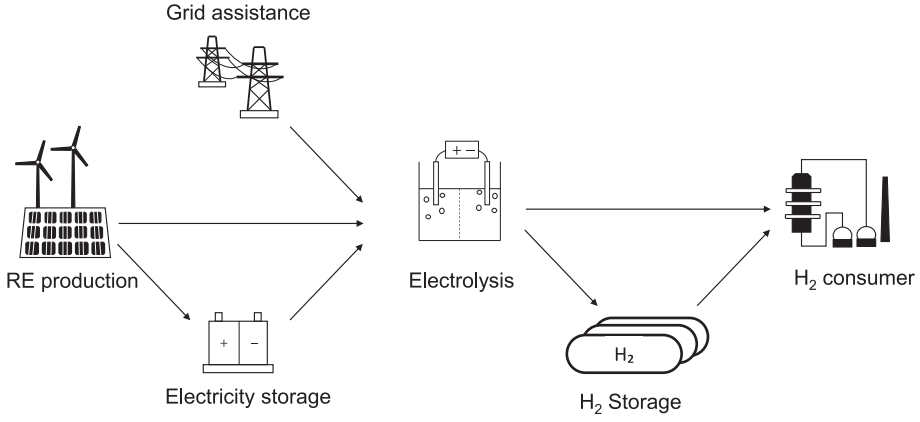

Fig. 1 – Basic process layout of a hydrogen production plant.

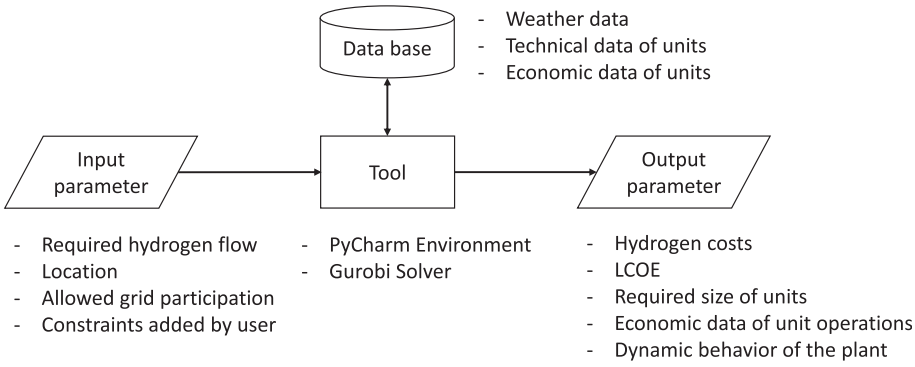

Fig. 2 – Schematic flow chart of the developed tool.

Table 4 – Example locations considered for the evaluation.

Location	Coordinates	PV tilt angle	Grid energy costs [€$_{2020}$/MWh]
Pampa Anita, Chile	−24.928, −69.740	24°	92.86 [28,29]
Punta Arenas, Chile	−53.175, −70.943	39°	92.86
Sakaka, Saudi Arabia	29.744, 40.095	27°	41.96 [30,31]
Almeria, Spain	37.093, −2.357	32°	70.50 [32]
Northampton, Australia	−28.352, 114.630	26°	197.95 [33,34]

furthest away from the equator. Data for utility-scale PV and onshore wind farms are taken from Ref. [17].

Solar energy supply

The input variable for the determination of PV power supply is the sum of direct and diffuse solar irradiance. For simplicity reasons, all PV panels have the same orientation at a certain location and no tracking is considered. Cost data for the investment as well as operating and maintenance (O&M) of utility-scale PV farms in the corresponding countries are taken from a study published by IRENA [17]. Since installed costs are given, no Lang-factors are required. Based on the efficiency, which is considered to be 20.3% [38], the required area of PV panels is estimated. Degradation of the solar panels is neglected. Labor demand amounts to 46.33 full time equivalent (FTE) for each GW of installed PV capacity [26]. For the sensitivity analysis S1 and S3, fixed costs for utility-scale PV with 100 €$_{2020}$/m^2 are assumed. The translated values to USD$_{2020}$/kW as well as all values for the solar energy supply are given in Table S.6 and S.7 of the supplementary information.

Wind energy supply

Local wind speed is the input variable to estimate the wind power supply. The used weather data give the average wind speed for a reference height of 80 m above the ground. For wind turbines with a different hub height, the wind speed is adapted by the power-law approach with an exponent of 1/7, which is commonly used for smooth terrain on land [39]. Two different wind turbines are considered. Technical data from the model V112–3.45 MW® by Vestas is used for wind turbine I [40,41]. For wind turbine II the model GE 2.5 ® by General Electric is considered [42]. Power curves of both turbines are shown in Fig. 3. Both wind turbines have a cut-out wind speed of 25 m/s.

Investment and O&M cost data for the corresponding countries is taken from Ref. [17] and given in Table S.8 and S.9 of the supplementary information. Since installed costs are given, no Lang-factors are required. Labor demand amounts to 87 FTE for each GW of installed wind power capacity [26].

Electricity storage

For the intermittent storage of electric energy, only technologies that are independent of geographic locations will be included in the model, i.e., pumped-hydro storage and compressed-air energy storage are not considered. Fly wheels are excluded due to their high costs and self-discharging rates [43]. Therefore, only battery systems are considered. Data for Li-ion, lead and vanadium redox flow (VRF) batteries is taken from Jülch et al. [44] and listed in Table S.10 and S.11 in the supplementary information.

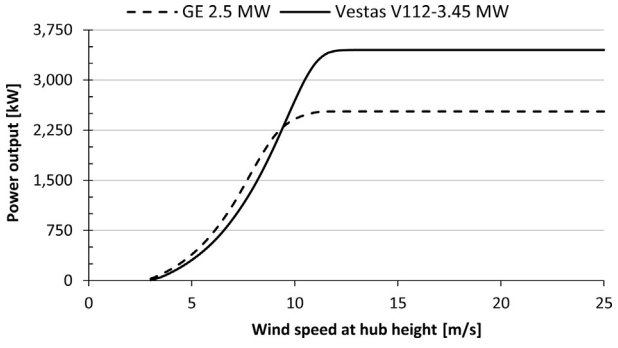

Fig. 3 – Power curves of considered wind turbines.

Hydrogen production

Hydrogen is produced in either an alkaline or PEM electrolyzer unit (AEL or PEM-EL). The alkaline electrolyzer is a mature technology with the global installed capacity reaching the MW-scale [45]. Contrary, there are still challenges that need to be addresses in order to achieve a large-scale implementation of the PEM-EL, e.g., the reduction of iridium loading due to the low availability of the metal [46]. The required electrolyzer capacity in this study reaches the low GW-scale. Currently, most large-scale projects are focused on building electrolyzer units with capacities around 10–100 MW [47–49]. Therefore, cost data for 100 MW units will be considered and the required capacity will be achieved by numbering up. Specific costs are 400 US-$$_{2020}$/kW for an AEL and 500 US-$$_{2020}$/kW for a PEM-EL [50]. To estimate the installed costs of the whole electrolyzer unit, a Lang-factor of 1.62 is considered [51]. For O&M costs, the same assumptions as in Schnülle et al. are used [11]. Furthermore, Schnülle et al. have been shown that water costs have only a small impact on the final hydrogen costs. Therefore, water costs are neglected in this study. For the whole production plant, a load flexibility of 0–100% is considered. This flexibility does not apply to a single electrolyzer but is assumed to apply to the entire system as several units will be operated in parallel. For simplicity reasons, the efficiency is considered to be independent of the load and no electricity demand is considered for stand-by. The AEL requires 51.9 kWh/kg$_{H_2}$ and the PEM-EL 54.3 kWh/kg$_{H_2}$. Since the electrolysis is a highly automated process, the required labor demand is rather low and no data from literature could be obtained. It is assumed that two people per shift are required for every 100 MW of installed electrolyzer capacity. Regarding the sensitivity analysis, Vartiainen gives different values for utility-scale CAPEX for the years 2030–2050 with costs decreasing from 240 €/kW$_{el}$ to 80 €/kW$_{el}$ [12]. The value of 80 €/kW$_{el}$ is considered to be too optimistic in the authors opinion. Therefore, the system costs of 160 €/kW$_{el}$ with an efficiency of 48 kWh/kg$_H$ are chosen as a very optimistic scenario for the sensitivity analysis S2 and S3. Input data for the hydrogen production is summarized in table S.12 and S.13 of the supplementary information.

Hydrogen compression and storage

As for the electricity storage, only technologies that are independent of the geographic locations are considered. Therefore, storage tanks with a pressure level of 250 bar are considered for the intermittent hydrogen storage. Higher pressures are not beneficial from an economic point of view [52]. In the required compression step, a maximum pressure ratio of 3 is assumed per stage [53]. For simplicity reasons, the pressure after the compressor step is always 250 bar. Hydrogen losses of 0.8% are considered in the compression step due to leakage from the sealings [54]. Cost data for the compressor is taken from literature for the size of a 4000 kW reciprocating compressor [53]. This size has been chosen as a compromise between economy of scale and redundancy. The procurement costs for the storage containers are 700 $$_{2020}$/kg$_{H_2}$ [55]. The Lang-factor for the storage is assumed to be 2 [56]. A labor demand of 1 person per shift and 5 t of hydrogen storage capacity is assumed for surveillance. Input data for hydrogen compression and storage is summarized in Table S.14 and S.15 of the supplementary information.

Results and discussion

A TEA of a hydrogen production plant for several locations was conducted with the goal to minimize the levelized costs of hydrogen for every considered case. The individual technical aspects as well as costs for every unit operation of the plant were estimated with data from the given references. This section gives an overview over the key findings. Detailed results can be found in the supplementary information.

Technical evaluation

The aim of generating large amounts of hydrogen is the transformation of renewable electric energy into a versatile chemical that can be utilized elsewhere. Therefore, it is relevant to know how the renewable energy can be used the most efficient way. Depending on the different climatic conditions and the predefined cases from Table 2 the required installation capacities change, also leading to different utilization factors of the corresponding units. Fig. 4 shows the required installed capacities of the RE sources of the plant layout with the lowest LCOH$_2$ for the different locations and the defined cases. The dashed grey horizontal line indicates the power demand of a constantly running alkaline electrolyzer that generates the required hydrogen mass flow of 25.74 t/h.

It can be seen how the tool adapts the most economic plant layout to the different climatic conditions and cases. While PV is preferred as RE supply for both in Pampa Anita and Almeria, in Punta Arenas and Northampton wind energy is preferred with the former using it exclusively. In every run wind turbine II (adapted on GE 2.5) is the more economic option. The base case is almost always the case with the highest installed capacity of RE generation. Enabling the plant to draw a certain electric power demand from the grid leads to a decrease of the required capacity of RE generation, while the ratio of installed PV to wind capacity is almost unaffected by this. For the downtime case, the installed capacity decreases in Punta Arenas, Almeria and Northampton compared to the base case while it increases in Sakaka. In Pampa Anita almost no change is observable. Furthermore, in Sakaka it can be seen that the ratio between installed PV and wind capacity changes. Since the installed RE capacity exceeds the size of the electrolyzer in every location, RE has to be curtailed if the RE sources run at full capacity. In Fig. 5 the different RE utilization rates for the different cases and locations are shown.

It can be seen that the ratio of utilized RE increases if grid participation is possible. This meets the expectation because the plant does not need to be as over-dimensioned as in the base case. Increasing storage capacity and thus increasing the utilization rate in the base case would lead to higher LCOH$_2$. Therefore, increasing the utilization rate in the base case is not economically beneficial. Again, for the downtime case no clear trend is observed. The utilization ratio even decreases in Pampa Anita. Since it is the aim to convert RE into hydrogen, it is relevant to know how much grey energy from the grid is

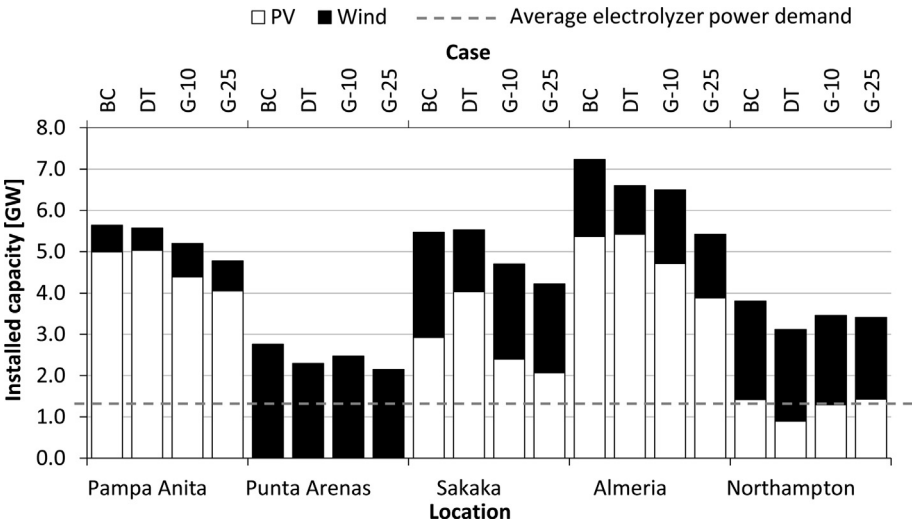

Fig. 4 – Installed PV and wind farm capacity for the different locations and cases.

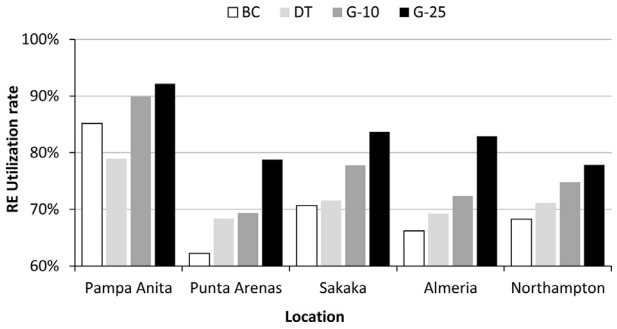

Fig. 5 – Utilization rate of RE for the different locations and cases.

Table 5 – Percentage of grid energy used for hydrogen production.

Location	G-10	G-25
Pampa Anita	2.0%	7.6%
Punta Arenas	0.4%	1.7%
Sakaka	0.7%	3.3%
Almeria	0.8%	4.8%
Northampton	0.5%	1.7%

used in the G-10 and G-25 cases. The share of used grid energy compared to the total amount of energy used is listed in Table 5. Even in the G-25 case less than 8% of the used energy is drawn from the grid.

Electricity storage was not considered by the tool in every location for every case. The reason behind this will be discussed in subchapter 4.3. Furthermore, only the alkaline electrolysis is used in every evaluation since it is more economic. The installed electrolyzer capacity is shown in Fig. 6. As in Fig. 4, the dashed grey horizontal line indicates the power demand of a constantly running alkaline electrolyzer that generates the required hydrogen mass flow of 25.74 t/h. The actual electrolyzer capacity has to be over-dimensioned for times where the electrolyzer is idle. Pampa Anita and Almeria, both locations with a high share of PV for installed RE capacity, have larger electrolyzer capacities than locations that focus on wind energy. This also meets the expectation because overproduction and storage are required to supply the downstream plant with hydrogen during the night. While the electrolyzer in Punta Arenas is only oversized by 38% for the base case, this value rises to 168% in Pampa Anita.

A reduction of electrolyzer capacity can be seen for all cases with grid participation and is more prominent for locations with a high installed PV capacity, especially in Almeria where the electrolyzer capacity is 0.65 GW (−18.3%) lower in the G-25 case than the base case. The installed electrolyzer capacity in Punta Arenas is already close to the minimum required size, so the reduction potential is also low compared to other locations. The utilization ratio of the electrolyzers is shown in Fig. 7. Since the produced amount of hydrogen is the same for all locations, the correlation between a higher installed capacity and a lower utilization ratio is expected.

In order to overcome the intermittency of the RE supply and therefore the hydrogen production, compressed hydrogen storage was chosen for the most economic plant layout in every evaluation. The required storage capacity is shown in Fig. 8. On the right axis the maximum duration is given, how long the storage tanks could supply the downstream processing plant with hydrogen. If the storage tanks were fully loaded and the only hydrogen source for the downstream plant.

It can be seen that locations with a high amount of installed PV capacity tend to require a smaller storage capacity. Especially in Pampa Anita the required capacity is rather small and can even be halved by enabling the usage of grid energy. Punta Arenas requires the largest storage capacity. This might be because it only relies on wind energy as RE source and that the option is more economic than installing additional PV farms. The size of the storage capacity is not the only decisive factor. Similar to the electric energy storage the

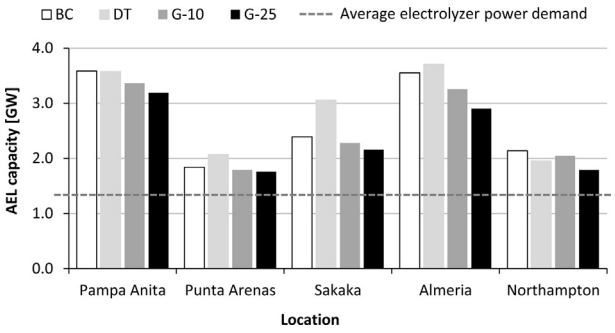

Fig. 6 – Installed electrolyzer capacity for the different locations and cases.

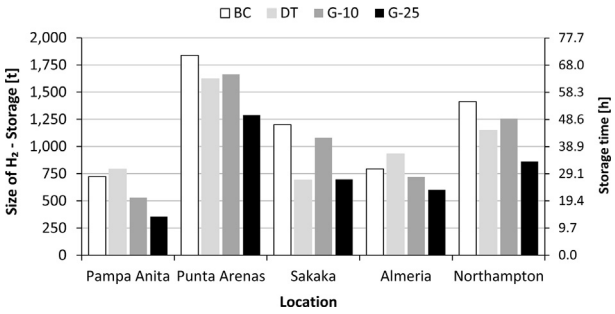

Fig. 8 – Required compressed hydrogen storage capacity for the different locations and cases.

maximum charging rate is also relevant. This value is a result from the model and is determined by the amount of installed compressor capacity. The results are depicted in Fig. 9. Surprisingly, the required capacity of the compressor increases for the cases with grid assistance. Furthermore, the locations with a small required storage capacity have a higher compression capacity and thus, a higher "charging" rate for the compressed hydrogen storage. For locations with a high share of RE supplied from PV farms, the mass flow to the storage facilities can be up to twice as high as the mass flow to the downstream processing plant. This is indicated by the right axis in Fig. 9. The large required compression capacities for these locations are in accordance with the results from Fig. 6 where the required capacities of the electrolyzers are shown. In peak production times, the hydrogen produced from a strongly over-dimensioned electrolyzer also has to be processed in a certain way. A detailed analysis on the utilization of the storage devices can be found in chapter S.4 where the amount of hydrogen stored over the course of the year is depicted in a sorted and descending order.

Economic evaluation

For the economic evaluation the FCI and the resulting depreciation costs as well as OPEX are estimated. Based on those, the levelized costs of hydrogen are given in $€_{2020}/kg_{H_2}$. Fig. 10 shows the absolute and specific FCI for the different locations and pathways.

The specific values on the right axis of Fig. 10 are based on the annual amount of 225,500 tons of hydrogen. In order to produce hydrogen in this scale, the required investments are roughly in the range of 7–9 billion € for the base case. Since this case requires the highest installed capacities for the different unit operations, it also has the highest FCI for every location. In most locations the RE supply is clearly the most dominant cost contributor of the FCI. In Punta Arenas the RE supply still accounts for roughly half of the FCI. The share of hydrogen storage is also very high due to the aforementioned reasons. With the possibility to use electric energy from the grid, the FCI is reduced in every location. For the G-10 case, the reduction amounts to 8.1–9.1% for the different locations and reaches 16.9–22.4% in the G-25 case. The levelized costs of hydrogen are shown in Fig. 11.

Except for the location of Northampton, the DT case is more expensive than the base case. Especially for Pampa Anita the consideration of a downtime has a negative effect on the $LCOH_2$. Therefore, this case is not further considered in the sensitivity analysis. The effect of grid participation reduces the $LCOH_2$ in every location. The costs of electricity from the grid are almost negligible for the G-10 case in every location. Only for the G-25 case in Pampa Anita they are roughly as relevant as the costs for hydrogen storage and compression. In both cases, G-10 and G-25, the smaller

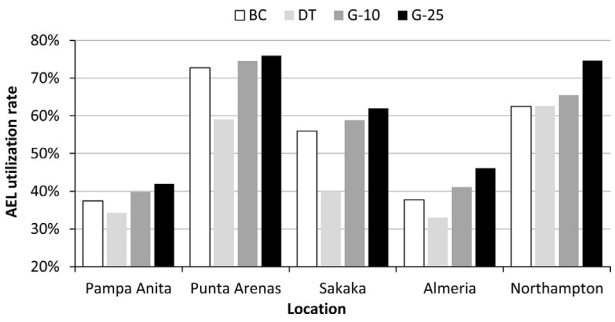

Fig. 7 – Utilization ratio of the electrolyzers for the different locations and cases.

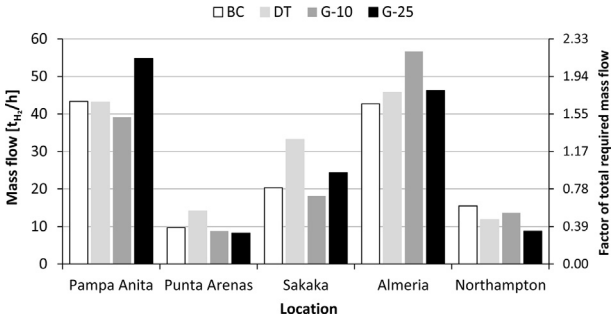

Fig. 9 – Installed compression capacity for the different locations and cases.

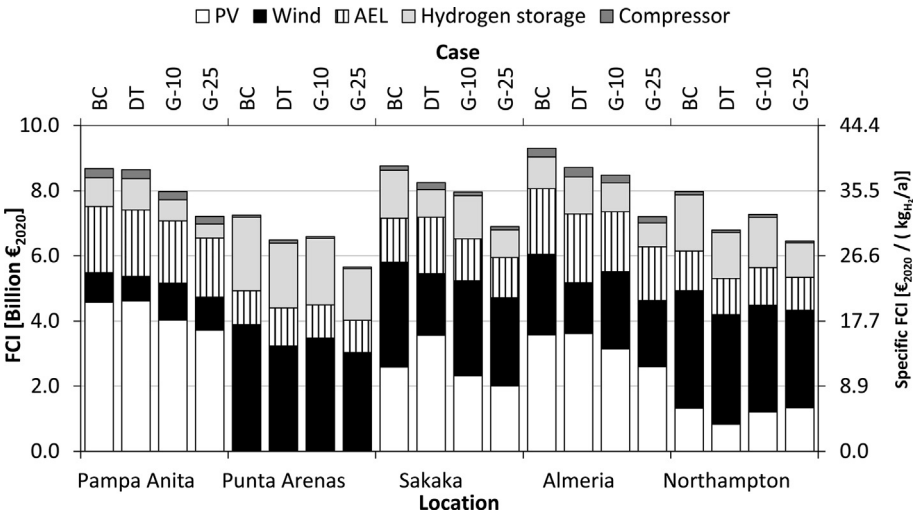

Fig. 10 – FCI for the hydrogen production plant for the different locations and cases.

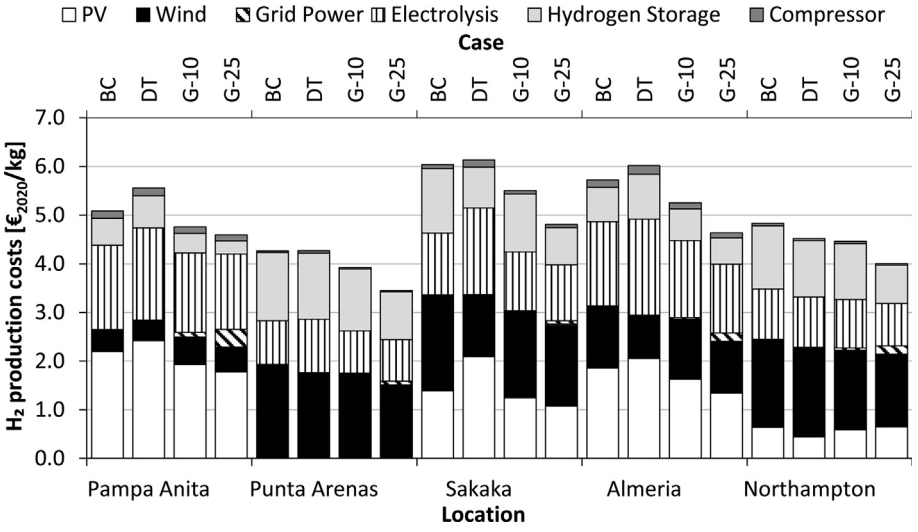

Fig. 11 – $LCOH_2$ for the different locations and cases.

installed capacity, as depicted in Fig. 4, outweighs the cost of electricity from the grid and causes a reduction of the $LCOH_2$. In general, the $LCOH_2$ are lowest in Punta Arenas with 3.45 €/kg_{H_2} in the G-25 case as the most economic option.

The results of the sensitivity analysis introduced in Table 2 are depicted in Fig. 12. In the analysis, the $LCOH_2$ retrieved with current cost (**CC**) data are compared with $LCOH_2$ retrieved considering perspective costs for PV (**S1**), the electrolyzer (**S2**) and for both (**S3**). The total height of the individual columns corresponds to the current cost scenario shown in Fig. 11. The cost altering effect is shown for every individual sensitivity. To evaluate the cost reduction potential, the black colored part of the column plus the corresponding boxes above the part have to be considered. It can be seen for Punta Arenas that no cost reduction from CC to S1 and from S2 to S3 is visible in the diagram. The location relies only on wind power in every evaluation and therefore, the current $LCOH_2$ are equal to $LCOH_2$ of S1. The same applies to the $LCOH_2$ of S2 and S3, respectively. The reduction of electrolyzer costs in S2 has a stronger influence on the $LCOH_2$ than lower costs for PV in S1 for every case in every location. It is most prominent in Almeria followed by Pampa Anita. This is in accordance with the results shown in Fig. 6 since both locations have the largest installed electrolyzer capacity and the lowest utilization rate of the electrolyzer. In the S3 sensitivity it can be seen that all $LCOH_2$ are below 4 €/kg_{H_2} with most values in the range between 3 and 4 €/kg_{H_2}. Only in Chile and Northampton in the G-25 case the costs reach values below 3 €/kg_{H_2} with 2.50 €/kg_{H_2} in Pampa Anita for the case of G-25 as the most economic option of S3. One aspect that applies for

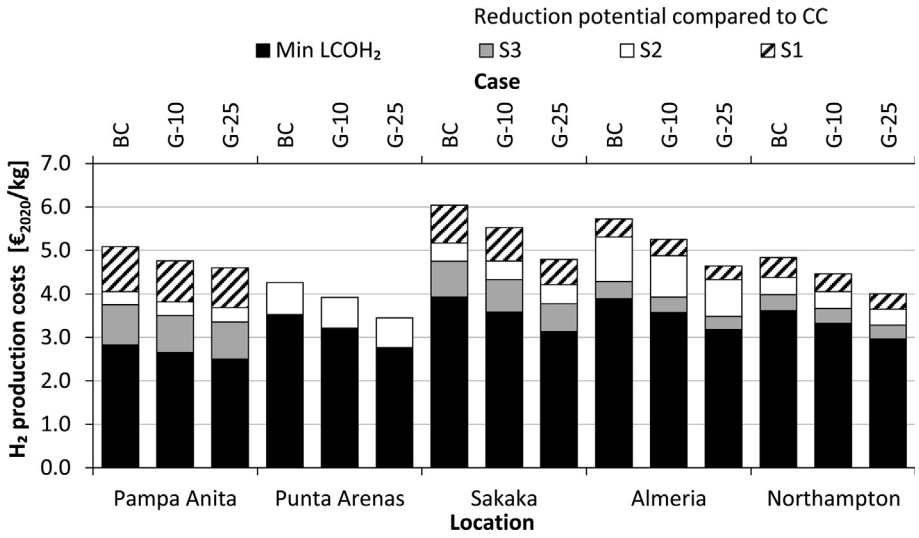

Fig. 12 – Reduction potential of different sensitivities on the $LCOH_2$.

every sensitivity is a change in the merit order of the most economic option, e.g., when future costs for PV and the electrolyzer are considered (S3), hydrogen can be produced more economical in Pampa Anita than in Punta Arenas. This is not the case using current costs or in the S2 evaluation. Detailed results of the sensitivity can be found in chapter S.4 of the supplementary information.

Discussion

With the developed tool the layout of a plant producing hydrogen from RE and grid electricity can be determined. It is shown that with the current technological progress and the conditions of the base case, $LCOH_2$ between 4 and 6 €$_{2020}$/kg are feasible. One major finding of this study is the advantage that grid assistance has appreciable impact on the technical and economic key performance indicators. The grid connection leads to lower installed capacities of the unit operations while increasing their utilization rate. Especially for the G-25 case in Punta Arenas, where only 1.7% of the total energy is drawn from the grid, the $LCOH_2$ are reduced by almost 20% compared to the base case. Therefore, when such a plant is built in the future it should be expected to interact with the local grid to bridge times with low local RE supply and even sell excess energy to the grid instead of curtailing it. In subchapter 4.1 it is stated that no electricity storage is used in the evaluations. The aspect that electricity storage is not economic compared to hydrogen storage has already been explained by Mallapragada [10] For a comparison it has to be considered if it is more economic to store the electric energy to produce one kg of hydrogen or storing the actual produced hydrogen. Perspective data available in literature reach values of roughly \$ 70/kWh$_{el}$ for lithium battery systems for the year 2050 [57]. This corresponds to \$ 2333.3/kg$_{H_2}$ with the LHV of 33.33 kWh/kg$_{H_2}$. So even without considering the efficiency losses from the electrolyzer and using optimistic cost data, it is four times more expensive than the specific costs for storing compressed hydrogen with roughly 613 €$_{2020}$/kg$_{H_2}$, (neglecting the different reference years and simplifying the exchange rate). Therefore, focusing on compressed hydrogen storage to achieve a constant hydrogen supply is the more economic option. Nevertheless, this whole aspect strongly depends on the simplification that the electric energy demand for standby during dark wind lulls and the control systems are neglected. If a hydrogen production plant is installed in island mode without a connection to a local grid, at least some sort of electricity storage or a back-up power supply will be required.

The results of the base case from this study confirm the outcomes of previous studies for the installation year 2020. Schnülle et at. received minimum $LCOH_2$ of 4.33 €$_{2020}$/kg with onshore wind turbines after their remuneration period [11]. While Mallapragada estimated $LCOH_2$ of 2.5 \$/kg for 2030 with perspective cost data and a salt cavern for intermediate hydrogen storage [10]. This is in accordance with the results from the sensitivity analysis shown in Fig. 12, especially, if the given accuracy of the applied cost estimation and the influence of the different locations are considered.

Several aspects have to be acknowledged that influence the presented results. One aspect is the stiff requirement of a constant mass flow over the whole period of time. The evaluated hydrogen production plant is suppling an undefined downstream plant. For this study, only the hydrogen production plant was considered to be flexible which corresponds to a scenario with maximum $LCOH_2$. If a range is required instead of a fixed value, e.g., a mass flow of 25.74 t/h ± 15% (21.9–29.6 t/h) the required storage demand and subsequently the $LCOH_2$ could be reduced. Another aspect is the weighted average cost of capital (WACC) since the gained $LCOH_2$ are dominated by the depreciation of the FCI. With the given mass flow, a WACC of 5% and 20 years as depreciation time, 0.134 €/kg$_{H_2}$ per billion € investment account for the cost of capital. This value increases to 0.213 €/kg$_{H_2}$ per billion € investment for the WACC of 7.5% in Saudi Arabia. Recently, an increase of the inflation rate was observed accompanied with insecurities

regarding the interest rate policies. This could also influence the WACC of the different countries and thus influence the merit order of a ranking based solely on $LCOH_2$. With the required FCIs from Fig. 10 that are in the range between 5.5 and 9 billion €, the share of costs for capital can reach values of up to 25% from the $LCOH_2$. An aspect that could reduce the $LCOH_2$ is the consideration of local geographic features e.g. the usage of salt caverns for hydrogen storage. The specific costs for hydrogen storage in salt caverns is in the range of 1.41–11.42 €/kg_{H_2} [58,59] and significantly lower compared to the specific costs for hydrogen storage in pressure tanks with roughly 613 €$_{2020}$/kg_{H_2}. Since the share of costs for hydrogen storage reaches values up to 33%, as shown in Fig. 11, this cost reduction potential must not be neglected.

Other uncertainties in the calculation originate from simplifications, e.g.: in a future study it could be evaluated whether the costs for water can really be neglected for locations like Pampa Anita or Sakaka since the hydrogen mass flow corresponds to a water flow of 2300 t/h.

Furthermore, transmission and transformation losses of electric energy are neglected and there is no difference considered in the form of electricity (AC or DC). However, the simplifications do not substantially influence the results of the mathematical model and how the interaction with the electric gird reduces the $LCOH_2$. One of the most important input variables are the weather data. for which the year 2019 is used as the reference year. Furthermore, as stated in section Methodology of the techno-economic evaluation the mathematical model has "perfect foresight" of the used weather data while an operator of a real plant can only rely on weather forecasts and seasonable changes. Another aspect that has not been considered regarding the usage of wind energy is the influence of turbulent weather conditions like wind gusts. In every case wind turbine II is more economic which might change when actual cost data for the wind turbines is used or if other aspects limit the selection, e.g., regarding wind classes and allowed turbulences. These aspects could be addressed by further research.

The EU has set the goal to produce green hydrogen with costs lower than 1.80 €/kg by the year 2030 [60]. The results of Fig. 12 indicate that there are still aspects that need to be addressed to reach this goal. But it seems reachable since the lowest costs amount to 2.50 €$_{2020}$/kg_{H_2} in Pampa Anita in the G-25 case and the S3 sensitivity. By considering additional technical progress, including geographic features like salt cavern for hydrogen storage, a reduction in the WACC and softening the requirement of the constant mass flow, the goal of 1.80 €/kg can be achieved.

However, the costs from Vartiainen, 0.30–0.84 €/kg for the year 2050, seem to be very ambitious but cannot be ruled out if the costs for PV and the electrolyzer will develop in the presented manner of their study [12]. The same challenge applies to the target of \$1/kg_{H_2} that has slightly higher costs but is supposed to be reached by the year 2030 [61].

Technical progress can be expected for every unit of the plant layout, e.g., bifacial solar cells or the consideration of a tracking system which could decrease the costs of solar electricity. By implementing new data to the mathematical model, the tool can automatically determine the improvements and estimate the adapted $LCOH_2$.

Conclusion

In this study a method is described to automatically retrieve the layout of a cost optimized hydrogen production plant for different locations around the world. The developed tool is able to determine the cost-optimized size of RE production capacity, electrolyzer, compressor and H_2 storage capacity for a constant supply of 25.74 t/h to a downstream plant (225,500 t/a). The operation of such a plant in an island mode is neither realistic nor beneficial, since the plant has to be drastically over dimensioned in order to supply hydrogen 100% of the time. A certain amount of grid assistance was able to reduce the required installed capacities of the individual units and thus also reduce the $LCOH_2$. Technical and economic aspects of the different geographic locations have been presented and can be adapted for cost estimations of different scenarios or for further future costs developments. To the knowledge of the authors no study has been published where the cost calculation is described as detailed and reproducible and the influence of grid assistance on the plant layout has been discussed.

Utilizing current knowledge about the technical progress and best practice chemical process cost engineering methodology the lowest achievable current costs for the considered locations are 3.45 €$_{2020}$/kg_{H_2} in Punta Arenas in the G-25 case. Future costs in the range of 2.50–4 €$_{2020}$/kg_{H_2} can be expected for all evaluated locations just by considering progress for PV panels and the alkaline electrolyzer, as shown in Fig. 12 for the sensitivity S3. Based on the results shown in this study, a life cycle assessment of such a hydrogen production plant will be essential to evaluate the impacts of grid participation. To seriously address questions like: How "green" is the produced hydrogen and do the reduced installed RE capacities outweigh the share of grey energy from the grid? Furthermore, hydrogen leakage must also be considered, since hydrogen can act as an indirect greenhouse gas by extending the lifetime of methane in the atmosphere [62]. Additional work is required and will be addressed in future studies.

Imprecisions of the presented methodology have to be reduced in future research to increase the resilience of the study results. Lang-factors should be validated for each unit individually, especially regarding the electrolyzer where a lot of studies often neglect installation costs. Future research could also implement additional technologies. In this study only one-axis and non-tracking PV panels have been considered and no geographically bound units like a salt-cavern were evaluated. Furthermore, softening the strict requirement of the constant mass flow might be provided by actual H_2 consumers. Apart from considering aspects that might further decrease the $LCOH_2$ it will be relevant to understand the future hydrogen consumer's perspective and how a customer wants to achieve its CO_2 abatement goals with the least costs and the highest process and delivery safety.

Declaration of competing interest

The authors declare that they have no known competing financial interests or personal relationships that could have appeared to influence the work reported in this paper.

Appendix A. Supplementary data

Supplementary data to this article can be found online at https://doi.org/10.1016/j.ijhydene.2022.06.038.

Abbreviations

AEL	Alkaline electrolyzer
BC	Base case
CAPEX	Capital expenditures
CC	Current costs
DT	Downtime (refereeing to downtime case)
FCI	Fixed capital investment
FTE	Full time equivalent
GHG	Greenhouse gases
LCOE	Levelized cost of electricity
$LCOH_2$	Levelized cost of hydrogen
OPEX	Operating expenditures
O&M	Operating and maintenance costs
PEM-EL	Proton exchange membrane – electrolyzer
PtX	Power to X
PV	Photovoltaic (referring to solar energy)
RE	Renewable energy
TEA	Techno-economic assessment
WACC	Weighted average cost of capital

REFERENCES

[1] IRENA. World. Energy transitions outlook: 1.5°C pathway 2021. https://www.irena.org/-/media/Files/IRENA/Agency/Publication/2021/Jun/IRENA_World_Energy_Transitions_Outlook_2021.

[2] Sognnaes I, Gambhir A, van de Ven D-J, Nikas A, Anger-Kraavi A, Bui H, et al. A multi-model analysis of long-term emissions and warming implications of current mitigation efforts. Nat Clim Change 2021;11(12):1055–62. https://doi.org/10.1038/s41558-021-01206-3.

[3] Casey J. Power Technology. Siemens begins work on 8.75 MW green hydrogen plant in Germany. https://www.power-technology.com/news/siemens-begins-work-on-8-75mw-green-hydrogen-plant-in-germany/. 2021. [Accessed 23 November 2021].

[4] Morison R, Bloomberg LP. Giant offshore Irish wind farm planned for green hydrogen. 2021. https://www.bloomberg.com/news/articles/2021-11-22/giant-offshore-wind-farm-planned-in-ireland-for-green-hydrogen. [Accessed 23 November 2021].

[5] Paddison L. The Guardian. Oman plans to build world's largest green hydrogen plant. https://www.theguardian.com/world/2021/may/27/oman-plans-to-build-worlds-largest-green-hydrogen-plant. [Accessed 23 November 2021].

[6] Die BMWi. Nationale wasserstoffstrategie. 2020. https://www.bmwi.de/Redaktion/DE/Publikationen/Energie/die-nationale-wasserstoffstrategie.pdf.

[7] Knipperts A. Neue Energie für globale Partnerschaften?. 2021. https://bdi.eu/publikation/news/neue-energie-fuer-globale-partnerschaften-wasserstoff-energie-h2/.

[8] Loewert M, Pfeifer P. Dynamically operated fischer-tropsch synthesis in PtL-Part 1: system response on intermittent feed. ChemEngineering 2020;4(2). https://doi.org/10.3390/chemengineering4020021.

[9] Klein H, Fritsch P, Haider P, Kender R, Rößler F, Rehfeldt S, et al. Flexible Operation of Air Separation Units 2021;8(4):357–74. https://onlinelibrary.wiley.com/doi/abs/10.1002/cben.202100023.

[10] Mallapragada DS, Gençer E, Insinger P, Keith DW, O'Sullivan FM. Can industrial-scale solar hydrogen supplied from commodity technologies Be cost competitive by 2030? Cell Reports Physical Science 2020;1(9):100174. https://doi.org/10.1016/j.xcrp.2020.100174.

[11] Schnuelle C, Wassermann T, Fuhrlaender D, Zondervan E. Dynamic hydrogen production from PV & wind direct electricity supply – modeling and techno-economic assessment. Int J Hydrogen Energy 2020;45(55):29938–52. https://doi.org/10.1016/j.ijhydene.2020.08.044.

[12] Vartiainen E, Breyer C, Moser D, Román Medina E, Busto C, Masson G, et al. True cost of solar hydrogen. Sol. RRL 2021;6:2100487. https://doi.org/10.1002/solr.202100487.

[13] Ausfelder F, Dura H. 3. Roadmap des Kopernikus-Projektes P2X Phase II. 2021. https://www.kopernikus-projekte.de/lw_resource/datapool/systemfiles/cbox/1683/live/lw_datei/dec_p2x_ii_v06_online_small.pdf.

[14] Pfennig M, Bonin M, Gerhardt N. PtX-Atlas: weltweite Potenziale für die Erzeugung von grünem Wasserstoff und klimaneutralen synthetischen Kraft-und Brennstoffen , Teilbericht im Rahmen des Projektes: DeV-KopSys. 2021. https://www.iee.fraunhofer.de/content/dam/iee/energiesystemtechnik/de/Dokumente/Veroeffentlichungen/FraunhoferIEE-PtX-Atlas_Hintergrundpapier_final.pdf.

[15] Schemme S, Breuer JL, Köller M, Meschede S, Walman F, Samsun RC, et al. H2-based synthetic fuels: a techno-economic comparison of alcohol, ether and hydrocarbon production. Int J Hydrogen Energy 2020;45(8):5395–414. https://doi.org/10.1016/j.ijhydene.2019.05.028.

[16] Raab M, Maier S, Dietrich R-U. Comparative techno-economic assessment of a large-scale hydrogen transport via liquid transport media. Int J Hydrogen Energy 2021;46(21):11956–68. https://doi.org/10.1016/j.ijhydene.2020.12.213.

[17] IRENA. Renewable. Power generation costs in 2020. 2021. https://www.irena.org/publications/2021/Jun/Renewable-Power-Costs-in-2020.

[18] Albrecht FG, König DH, Baucks N, Dietrich R-U. A standardized methodology for the techno-economic evaluation of alternative fuels – a case study. Fuel 2017;194:511–26. https://doi.org/10.1016/j.fuel.2016.12.003.

[19] Lang H. Cost relationships in preliminary cost estimation. Chem Eng 1947;54(10):117–21.

[20] Gurobi optimization, LLC - Gurobi optimizer reference manual. 2021. https://www.gurobi.com/wp-content/plugins/hd_documentations/documentation/9.0/refman.pdf. [Accessed 1 September 2021]. accessed.

[21] Lu X, McElroy MB, Kiviluoma J. Global potential for wind-generated electricity. Proc Natl Acad Sci USA 2009;106(27):10933–8. https://doi.org/10.1073/pnas.0904101106. https://www.pnas.org/content/pnas/106/27/10933.full.pdf.

[22] Gsa 2.6 - global solar atlas. 2021. https://globalsolaratlas.info. [Accessed 1 August 2021].

[23] Gräve P. Porsche. Baubeginn für weltweit erste integrierte kommerzielle Anlage zur Herstellung von eFuels. https://newsroom.porsche.com/de/2021/unternehmen/porsche-baubeginn-kommerzielle-anlage-herstellung-co2-neutrale-kraftstoffe-chile-25681.html. 2021.
[24] Power-Technology. Sakaka photovoltaic solar project. https://www.power-technology.com/projects/sakaka-photovoltaic-solar-project/. 2021. [Accessed 3 February 2022].
[25] DLR-SF. CIEMAT plataforma solar de Almería - europe's biggest test center for concentrating solar power (CSP). https://www.dlr.de/sf/de/desktopdefault.aspx/tabid-7176/11942_read-28189/. 03.02.2022.
[26] Chapman AJ, Fraser T, Itaoka K. Hydrogen import pathway comparison framework incorporating cost and social preference: case studies from Australia to Japan. Int J Energy Res 2017;41(14):2374–91. https://doi.org/10.1002/er.3807.
[27] Chinchilla M, Santos-Martín D, Carpintero-Rentería M, Lemon S. Worldwide annual optimum tilt angle model for solar collectors and photovoltaic systems in the absence of site meteorological data. Appl Energy 2021;281:116056. https://doi.org/10.1016/j.apenergy.2020.116056.
[28] Statista. Average market price of electricity in Chile from January 2019 to October 2021. https://www.statista.com/statistics/1029737/chile-electricity-average-m/. 2021. [Accessed 28 December 2021].
[29] ExchangeRates. Euro to Chilean peso spot exchange rates for. 2019. https://www.exchangerates.org.uk/EUR-CLP-spot-exchange-rates-history-2019.html. 2021. [Accessed 15 December 2021].
[30] SaudiElectricityCompany. Tariffs & connection fees. https://www.se.com.sa/en-us/customers/Pages/TariffRates.aspx. 2022. [Accessed 5 January 2022].
[31] ExchangeRates. Euro to Saudi riyal spot exchange rates for 2020. https://www.exchangerates.org.uk/EUR-SAR-spot-exchange-rates-history-2020.html. 2021. [Accessed 15 December 2021].
[32] Prices Statista. of electricity for industry in Spain from 2008 to 2020, https://www.statista.com/statistics/595813/electricity-industry-price-spain/. 2022. [Accessed 5 January 2022].
[33] Horizon power - electricity prices. https://www.horizonpower.com.au/manage-my-account/pricing/#for-business. 2022. [Accessed 5 January 2022].
[34] ExchangeRates. Euro to Australian dollar spot exchange rates for 2020. https://www.exchangerates.org.uk/EUR-AUD-spot-exchange-rates-history-2020.html. 2021. [Accessed 15 December 2021].
[35] Pfenninger S, Staffell I. Long-term patterns of European PV output using 30 years of validated hourly reanalysis and satellite data. Energy 2016;114:1251–65. https://doi.org/10.1016/j.energy.2016.08.060.
[36] Staffell I, Pfenninger S. Renewables. ninja. https://www.renewables.ninja/. 2021. [Accessed 10 November 2021].
[37] Staffell I, Pfenninger S. Using bias-corrected reanalysis to simulate current and future wind power output. Energy 2016;114:1224–39. https://doi.org/10.1016/j.energy.2016.08.068.
[38] Xu Z, Xu X, Cui C, Huang H. A new uniformity coefficient parameter for the quantitative characterization of a textured wafer surface and its relationship with the photovoltaic conversion efficiency of monocrystalline silicon cells. Sol Energy 2019;191:210–8. https://doi.org/10.1016/j.solener.2019.08.028.
[39] Hsu SA, Meindl EA, Gilhousen DB. Determining the power-law wind-profile exponent under near-neutral stability conditions at sea. J Journal of Applied Meteorology and Climatology 1994;33(6):757–65. https://doi.org/10.1175/1520-0450(1994)033<0757:DTPLWP>2.0.CO. 2.
[40] Vestas. V112-3.45 MW®. https://www.vestas.com/en/products/4-mw-platform/V112-3-45-MW. 2021. [Accessed 15 December 2021].
[41] Wind turbine models - Vestas V112-3.45. https://www.wind-turbine-models.com/turbines/1247-vestas-v112-3.45. 2021. [Accessed 15 December 2021].
[42] Wind turbine models - GE general electric GE 2.5 - 120. 2021. https://www.wind-turbine-models.com/turbines/310-ge-general-electric-ge-2.5-120.
[43] IRENA. Electricity storage and renewables: costs and markets to 2030. 2017. https://www.irena.org/publications/2017/oct/electricity-storage-and-renewables-costs-and-markets.
[44] Jülch V. Comparison of electricity storage options using levelized cost of storage (LCOS) method. Appl Energy 2016;183:1594–606. https://doi.org/10.1016/j.apenergy.2016.08.165.
[45] Shiva Kumar S, Himabindu V. Hydrogen production by PEM water electrolysis – a review. Materials Science for Energy Technologies 2019;2(3):442–54. https://doi.org/10.1016/j.mset.2019.03.002.
[46] Bernt M, Hartig-Weiß A, Tovini MF, El-Sayed HA, Schramm C, Schröter J, et al. Current challenges in catalyst development for PEM water electrolyzers. Chem Ing Tech 2020;92(1–2):31–9. https://doi.org/10.1002/cite.201900101. https://onlinelibrary.wiley.com/doi/abs/10.1002/cite.201900101.
[47] Asahi Kasei's "aqualizer" starts producing green hydrogen in Japan. Membr Technol 2020;2020(5):2. https://www.sciencedirect.com/science/article/pii/S095821182030077X.
[48] Radowitz B. Linde to build 'world's largest electrolyser' to produce green hydrogen 2021. https://www.rechargenews.com/transition/linde-to-build-world-s-largest-electrolyser-to-produce-green-hydrogen/2-1-944080.
[49] Shell. Shell starts up Europe's largest PEM green hydrogen electrolyser 2021. https://www.shell.com/media/news-and-media-releases/2021/shell-starts-up-europes-largest-pem-green-hydrogen-electrolyser.html.
[50] Green IRENA. Hydrogen cost reduction. https://www.irena.org/publications/2020/Dec/Green-hydrogen-cost-reduction; 2020.
[51] Zauner A, Böhm H, Rosenfeld DC, Tichler R. Innovative large-scale energy storage technologies and Power-to-Gas concepts after optimization - D7. 7. Analysis on future technology options on techno-economic optimization. 2019.
[52] Baldwin D. Hexagon lincoln. Proceedings of DOE hydrogen compression, storage, and dispensing cost reduction workshop. 2013. http://www1.eere.energy.gov/hydrogenandfuelcells/pdfs/csd_workshop_8_baldwin.pdf. [Accessed 1 October 2022].
[53] Woods DR. Rules of thumb in engineering practice. John Wiley & Sons; 2007.
[54] Stolzenburg K, Berstad D, Decker L, Elliott A, Haberstroh C, Hatto C, et al. Efficient liquefaction of hydrogen: results of the IDEALHY project. 7 – 9 november 2013. Stralsund/Germany2013. p. 8, https://www.idealhy.eu/uploads/documents/IDEALHY_XX_Energie-Symposium_2013_web.pdf.
[55] Abdin Z, Tang C, Liu Y, Catchpole K. Large-scale stationary hydrogen storage via liquid organic hydrogen carriers. iScience 2021;24(9):102966. https://doi.org/10.1016/j.isci.2021.102966.
[56] Personal communication with expert for hydrogen fuelling stations. 2021.
[57] Mauler L, Duffner F, Zeier WG, Leker J. Battery cost forecasting: a review of methods and results with an outlook

to 2050. Energy Environ Sci 2021;14(9):4712–39. https://doi.org/10.1039/D1EE01530C.

[58] Elberry AM, Thakur J, Santasalo-Aarnio A, Larmi M. Large-scale compressed hydrogen storage as part of renewable electricity storage systems. Int J Hydrogen Energy 2021;46(29):15671–90. https://doi.org/10.1016/j.ijhydene.2021.02.080.

[59] Friedrich KA, Noack C. Power-to-Hydrogen: technische und Ökonomische Bewertung von Wasserstoff als Energieträger und–Speicher Ergebnisse der Studie Plan-DelyKad. 2014.

[60] Opening EU. keynote by President von der Leyen at the European Hydrogen Week 2021. https://ec.europa.eu/commission/presscorner/detail/en/speech_21_6421. 2021. [Accessed 30 January 2022].

[61] Collins L. RECHARGE. 'Producing green hydrogen for $1/kg is achievable in some countries by 2030': WoodMac. https://www.rechargenews.com/energy-transition/producing-green-hydrogen-for-1-kg-is-achievable-in-some-countries-by-2030-woodmac/2-1-1118580. 2021. [Accessed 30 January 2022].

[62] Ocko IB, Hamburg SP. Climate consequences of hydrogen leakage. Atmos Chem Phys Discuss 2022;2022:1–25. https://acp.copernicus.org/preprints/acp-2022-91/.

3.2 Publication II

Fuel production and large-scale transport to Germany

Moritz Raab, Ralph-Uwe Dietrich (2023): Techno-economic assessment of different aviation fuel supply pathways including LH_2 and LCH_4 and the influence of the carbon source.

https://doi.org/10.1016/j.enconman.2023.117483

Energy Conversion and Management 293 (2023) 117483

Contents lists available at ScienceDirect

Energy Conversion and Management

journal homepage: www.elsevier.com/locate/enconman

Techno-economic assessment of different aviation fuel supply pathways including LH_2 and LCH_4 and the influence of the carbon source

Moritz Raab *, Ralph-Uwe Dietrich

German Aerospace Center (DLR), Pfaffenwaldring 38-40, 70569 Stuttgart, Germany

ARTICLE INFO

Keywords:
Techno-economic assessment
LH2
LOHC
LNG
Aviation
SAF

ABSTRACT

Sustainable Jet A-1 and radical technological changes are required to decrease the CO_2 emissions of the aviation industry. While the CO_2 reduction potential of electric aircraft is limited, the implementation of LH_2 and LCH_4 are exemplary radical technological changes with large potential impact. Recent studies have evaluated conceptual designs for planes utilizing LH_2 and LCH_4. Also, the costs of sustainable Jet A-1 and green hydrogen have been evaluated in different studies. However, most studies focus on one fuel and its production costs and do not include the production at a sweet spot and the subsequent logistic to the destination. To address this issue and present novel research results, we conducted a holistic techno-economic assessment for the different fuels that could be implemented in the aviation industry; LH_2, LCH_4 and sustainable Jet A-1. Based on renewable hydrogen produced in Morocco, we compared the aspects of a local fuel synthesis with the synthesis in Germany. CO_2 is supplied from ambient air in Morocco and from a local point source in Germany. For the latter, we considered a hydrogen transport via LH_2 or LOHC, with a direct integration of the LOHC dehydrogenation into the fuel synthesis plant. We outlined the cost composition of every fuel supply chain and retrieved LH_2 import costs of 157 €/MWh while the cost range for LCH_4 is 217–228 €/MWh. SAF has the highest net production costs of 279–302 €/MWh.

1. Introduction

The aviation industry faces the challenge to decrease its CO_2 emissions while at the same time the worldwide demand for travel is predicted to increase. FCH JU Europe (now reestablished as Clean Hydrogen JU) outlined several scenarios how these emissions will develop in the future, as shown in Fig. 1 [1].

Efficiency improvements of planes do not lead to emission reductions in these scenarios. Only sustainable aviation fuels (SAF) and radical technological changes are able to achieve the "-50 % vs. 2005 target" from the Air Transport Action Group (ATAG) or even the net zero target for the year 2050 [1]. Exemplary radical technological changes are the utilization of liquid hydrogen (LH_2) or the direct electrification of aircraft propulsion systems. While every approach that reduces CO_2 emissions should be considered, it has to be evaluated where most emissions occur. Therefore, the emissions from the sole passenger aviation industry (excluding e.g.: cargo) depending on the plane segment and range is depicted in Fig. 2 with data from 2018 where the CO_2 emissions amounted to 766 Mt_{CO_2} [2].

In Fig. 2 it is shown that planes with a capacity of up to 80 passengers contributed to less than 4 % of the total emissions. This is the size were most research activities of electrified aircraft is focused. This research is relevant to reach the net zero target of the year 2050, but it also cannot completely decarbonize the aviation sector. Larger planes with a capacity of more than 166 passengers designed for medium to long range distances caused almost two thirds of the emissions. Flights with a distance above 2000 km released more than 80 % of the CO_2 emissions. Since the electrification of these flights is currently not technically feasible, it cannot be considered as a radical technological change that will vastly decarbonize the aviation industry. Therefore, only SAF (equivalent to sustainable Jet A-1) and other chemical energy carriers (LCH_4 and LH_2) are considered in this study.

The production and utilization of SAF is well-known with several certified production processes and a current blending limit of up to 50 % according to the ASTM-5766 [1]. It includes the Fischer Tropsch (FT) synthesis, where so far only fossil based processes have been realized on a larger scale with the Shell GTL plant as a prominent example [3]. The electricity-based production via Power-to-X (PtX) processes has received a lot of attention in recent years and lead to first production plants [4–6]. In 2021, a small-scale plant has started production in Werlte, Germany with a capacity of 360 t/a [7]. Two exemplary larger projects

* Corresponding author.
E-mail addresses: Moritz.Raab@dlr.de (M. Raab), Ralph-Uwe.Dietrich@dlr.de (R.-U. Dietrich).

https://doi.org/10.1016/j.enconman.2023.117483
Received 6 April 2023; Received in revised form 17 July 2023; Accepted 28 July 2023
Available online 10 August 2023

Nomenclature

BT	Benzyl toluene
CAPEX	Capital expenditures
COP	Coefficient of performance
DAC	Direct air capture
FT	Fischer-Tropsch
HPP	Hydrogen production plant
LCH_4	Liquid methane
LH_2	Liquid hydrogen
LHV	Lower heating value
LNG	Liquefied natural gas
LOHC	Liquid organic hydrogen carrier
MEA	Monoethanolamine
MTPA	Mega tons per annum (usually referring to the capacity of a CH_4 liquefaction plant)
MtK	Methanol-to-kerosene
OPEX	Operating expenditures
PtX	Power to X
SAF	Sustainable aviation fuel (considers renewable fuel with Jet A-1 specifications)
TEA	Techno economic assessment
TPD	Tons per day (usually referring to the capacity of a H_2 liquefaction plant)

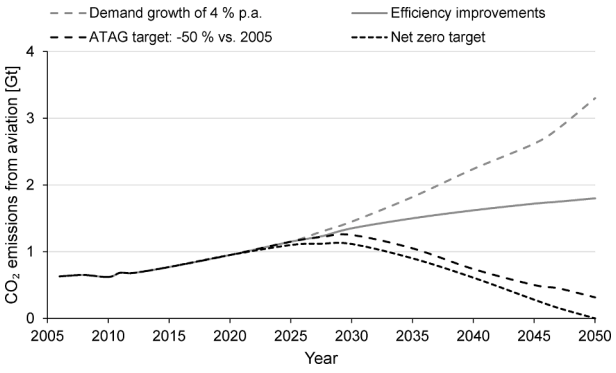

Fig. 1. Projected CO_2 emissions from the aviation industry [1].

are the joint venture "P2X-Portugal" with a capacity of 40,000 t/a and the "Green Fuels Hamburg" consortium with a capacity of 10,000 t/a, respectively [8–9]. Apart from the FT synthesis the so called "Methanol route" or Methanol-to-kerosene (MtK) process has been evaluated as an alternative for the FT synthesis [10–11]. This pathway has not been certified yet. Since SAF has almost the same properties as fossil kerosene, only minor changes have to be made in order for its full implementation. The main hurdles for a large-scale introduction of SAF so far are high costs as well as the availability of the educts for the production i.e. renewable electricity and biomass [5,12].

Implementing LH_2 as jet fuel is a more drastic approach to decarbonize the aviation industry. LH_2 has the major advantage that no CO_2 emissions result from its utilization, though non-CO_2 effects still have to be considered [13–14]. While with SAF, only the fuel source is changed, LH_2 effects the whole supply chain and would also require different plane designs and a new airport infrastructure. But by considering the whole supply chain, it still might be a more efficient and more economic option to introduce LH_2 to the aviation industry than the sole reliance on SAF. The utilization of LH_2 as alternative aviation fuel was first demonstrated in the 1950 s with a B-57 by NASA and was repeated in the former USSR in 1988 with a Tu-155 [15]. Both planes had one of their engines running on LH_2 as propellant. The emphasis was probably not the decarbonization of the aviation sector and due to the challenges of a cryogenic supply chain it is not surprising that LH_2 was not introduced into the market. Several studies focusing on LH_2 as aviation fuel have been published since these experiments. In the early 2000 s, in the Cryoplane project led by Airbus, different plane configurations were evaluated including a blended wing body (BWB) or even a triple deck long range aircraft [16–17]. In 2020, Airbus introduced the ZEROe program with the goal to develop the first zero emission commercial aircraft until the year 2035 [18]. Hydrogen can also be used in fuel cells for electrified propulsion systems. Aircraft with this technology are in an early development stage and are further developed in different research projects and start-up companies [19–21].

Another radical technological change is the introduction of LNG or liquid methane (LCH_4) as an aviation fuel. The aspect that fossil LNG can be suitable and more economic than kerosene has been shown in several studies [22–24]. As with LH_2, experiments with planes have been conducted in the past. In the year 1989, the aforementioned Tu-155 tested LNG as alternative aviation fuel [25]. NASA evaluated the usage of methane and designed planes with different cryo-tank concepts in the late 1970 s [26]. More recently, NASA published a study about LNG and LH_2 plane configurations and airport infrastructures highlighting the advantages like lower emissions (except methane slip) and lower costs

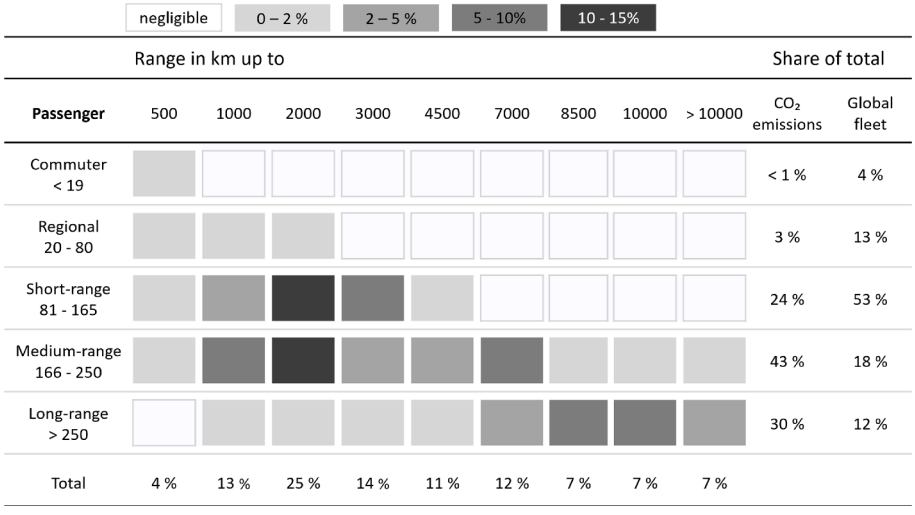

Fig. 2. CO_2 emissions of civil aviation per segment and range for the year 2018 [1].

compared to fossil kerosene as well as the significant challenges of the different supply chain [27]. Today, there is one start-up company focusing on commuter-sized LNG based aircraft, but service is not expected to begin before 2024 [28]. LCH_4 does require a carbon source, further chemical synthesis steps and is also a cryogenic liquid. But the synthesis is less complex than for SAF and the boiling point of methane is not as low as for LH_2. Furthermore, the volumetric energy density relative to SAF is only 24 % for LH_2, while it is 61 % for LCH_4 as shown in Table 8. So spatial limitations are not as critical for LCH_4 as for LH_2. This aspect is especially relevant for long-haul flights.

So far, the introduction of LH_2 and LCH_4 has failed. Mainly because there was no necessity to introduce them and it involved major technical and financial risks since several parties would have to be involved like fuel suppliers, airports, airlines, aircraft manufactures etc. But to reduce its CO_2 emissions the aviation industry has to move away from a business model based on fossil kerosene and introduce radical technological changes. Since every fuel has to be produced renewable, the technical and economic differences of the production processes from LH_2, LCH_4 and SAF become more relevant. This work focuses on the supply chain on how to provide a future sustainable aviation industry with these renewable fuels and therefore, belongs to studies that focus on the realization of a worldwide hydrogen economy [29]. Among others, the research questions involved are: How efficient can the different fuels be produced? What are the costs and how do these costs influence the fuel related expenses per passenger? This lays the groundwork for future socio-economic evaluations. The whole supply chain is depicted in Fig. 3, though this paper focuses on the first half of the supply chain. It is assumed, that these fuels have to be imported from a country with a high production potential of renewable energy, a so-called sweet spot. Three cases are evaluated; with **case A** where fuel synthesis is located at the sweet spot and **cases B** and **C** where the fuel synthesis is located in the importing site. There, two different hydrogen transport options are considered. The direct comparison of these three fuels as well as the evaluation of the different production sites and hydrogen transport pathways are the novelty of this research. The aspects domestic fuel distribution and storage at airport and plane fueling will be evaluated in a future study.

2. Methodology of techno-economic evaluation

2.1. Definition of the case study

In this study, the supply chain for the possible aviation fuels LH_2, LCH_4 and SAF are evaluated with the emphasis to outline the advantages and disadvantages of these perspective fuels from the manufacturers point of view. Furthermore, it is evaluated how the location of the carbon source influences the results. The different pathways are shown in Fig. 4. The reference year is 2030, meaning perspective input data is used. It is highly unlikely, that there will already be a significant number of commercial planes flying with LH_2 or LCH_4. But estimations for the year 2050 often use too optimistic costs and efficiencies and since there are too many unforeseeable aspects the year 2030 is chosen. For **case A** it is assumed that no local point source can be used and CO_2 has to be supplied from air via a direct air capture (DAC) unit. In the other cases CO_2 is supplied via an amine scrubber integrated to a waste incineration plant. In **case B** hydrogen is imported via hydrogenated benzyl toluene (BT), a so called liquid organic hydrogen carrier (LOHC), for the synthesis of LCH_4 and SAF. In **case C** LH_2 is used in the fuel synthesis. This study only focusses on the technical and economic aspects, the debate on how to allocate the CO_2 emissions when the fuel is burned are not addressed. A detailed view of the considered pathways as well as the system boundaries is shown in Fig. 4.

Every pathway begins with a constant hydrogen feed of 25.74 t_{H_2}/h, so that losses along the pathway can be easier compared. This amounts to 225 kt_{H_2}/a, an order of magnitude that is expected to be required for medium and larger airports in 2050 [30]. Techno-economic assessments (TEA) of plants that provide a constant hydrogen supply based on renewable energy have been evaluated in a previous study [31]. For this study, El Ouatia in Morocco is considered as an exemplary exporting location. The area is not densely populated and no hills are around that could otherwise cause spatial limitations, though every location around the world could be evaluated with this methodology. For **case A** it is considered that the electricity demand of the fuel production units is partially supplied from excess renewable energy from the hydrogen production plant (HPP) for no further charge, remaining power is supplied from the grid. For **case B** and **C**, the electric power demand is drawn from the grid. In every case, storage facilities after the conversion units, the harbor infrastructure, a transport carrier that is exclusively used to ship the fuels as well as the required harbor infrastructure and storage facilities at the destination are included in the evaluation. Wilhelmshaven is chosen as an exemplary destination, since the German LNG receiving terminals have been constructed there. The domestic transport to the airports will be evaluated in a future study.

2.2. Methodology of the techno-economic evaluation

Literature data is used to depict the thermochemical conversion steps in ASPEN Plus®. The results of these process simulations are the basis for

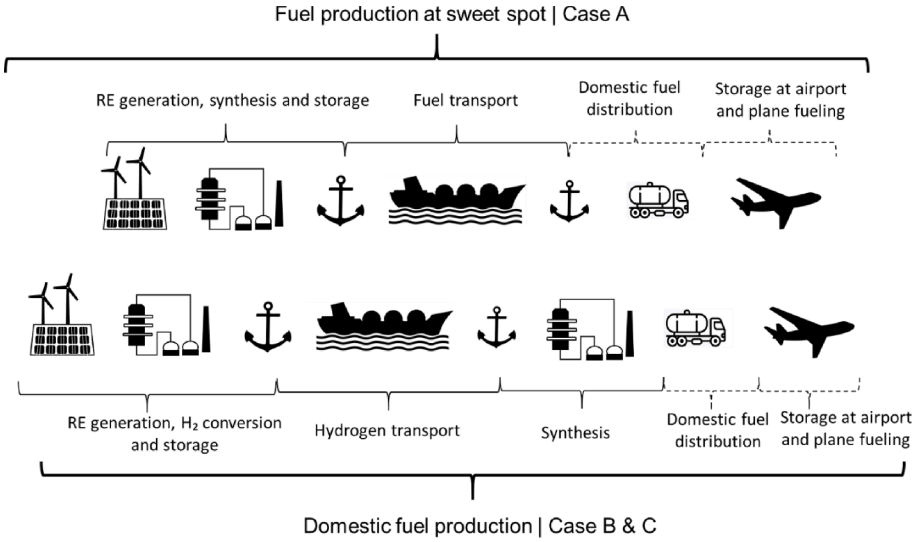

Fig. 3. System boundaries of a renewable aviation fuel supply chain | sweet spot and domestic synthesis.

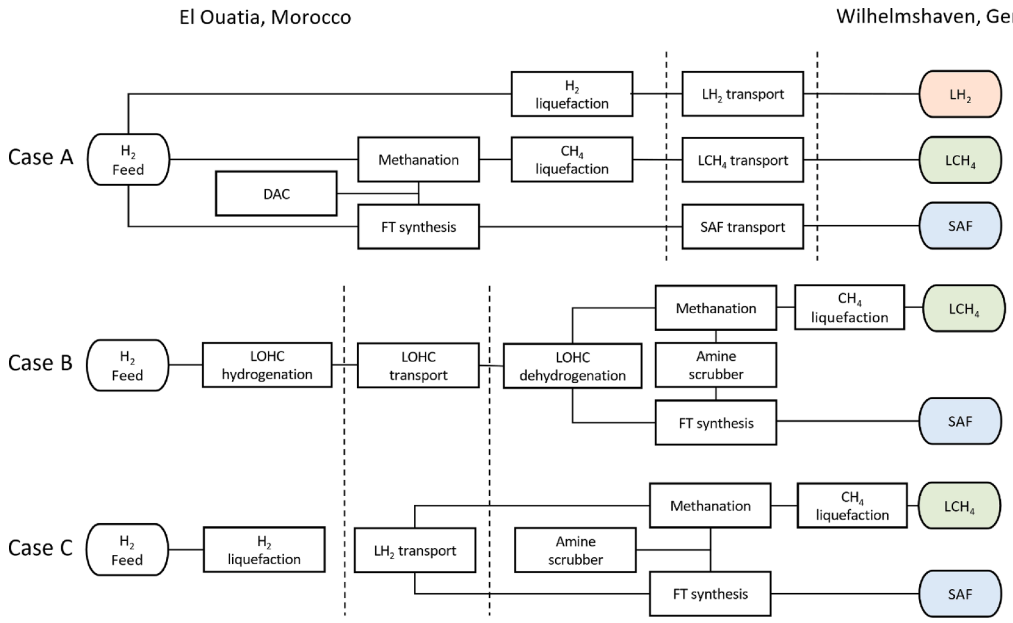

Fig. 4. Process steps of the evaluated pathways.

the techno-economic assessment which is conducted with the DLR in-house software TEPET [12]. Intercontinental shipping of the corresponding fuels is evaluated as published in a previous study [32]. The general methodological approach of the TEA has been described by Albrecht et al. [33]. Detailed input data of the corresponding pathways are described in chapter 3. Fixed capital investment (FCI) and to a certain extend operating expenditures (OPEX) are determined by using the factor method. The factors are given in the supplementary information. Remaining OPEX is estimated by the costs for the used materials, costs for labor and waste disposal. Costs for educts, utilities and labor are listed in Table S.1. Apart from different costs for labor, electricity and the corresponding interest rates, no further regional factors are considered. The final results will be given in $€_{2020}/MWh_{LHV}$ and have an accuracy level of ± 30 % due to the applied methodology. The boundary conditions are listed in Table 1.

2.3. Effects on commercial aviation

To conduct further socio-economic research, it is relevant to know how the utilization of renewable fuels influences the share of fuel-costs per flight. To evaluate how these fuels compare with each other, a simplified approach is followed. Based on an available online calculator that determines the personal carbon footprint of a certain flight, the kerosene demand per person per flight is retrieved [37]. Apart from flights that depart in Germany, further routes with a high passenger volume are included. These routes do not fit in the evaluated cases, but are included to give a broader and more general overview. For every flight only one-way, economy class, a scheduled flight and a typical modern plane type is assumed. Then, a ratio of 3.16 kg CO_2 emitted per burned kg of Jet A-1 is considered. With this data, the demand of SAF and cryogenic fuels is estimated based on the simplification that the specific energy demand does not change, even though it most likely would [1]. The results are shown in chapter 4.3. The considered flight paths are listed in Table 2 with the estimated energy demand and current fuel costs based on values from IATA [38] and Table 8.

Table 1
Boundary conditions of the case study.

	Unit	Value	Source
Hydrogen feed	t/h	25.74	[34]
Depreciation time	a	20	Assumption, based on[5]
Plant availability	h/a	8,760	Assumption, based on[31]
Sea distance	NM	2,000	[35]
Interest rate - Morocco	%	7.5	[36]
Interest rate - Germany / Carrier	%	5	[36]

3. Input data of aviation fuel supply pathways

In this section the synthesis steps as well as the aspects of fuel logistics are described. Block flow diagrams of the individual steps and detailed input data are provided in the supplementary information.

3.1. Feedstock supply for aviation fuel production

3.1.1. Hydrogen source

Future renewable aviation fuels will largely depend on green hydrogen. The hydrogen production plant (HPP) is shown in Fig. 5. To retrieve the minimum production costs based on the local weather conditions a linear programming cost optimization methodology was introduced in a previous study [31]. The HPP of this study comprises.

- an optimized PV farm and wind mills installation based on local solar radiation and wind profile using El Ouatia in Morocco as an example for a sweet spot location
- Alkaline electrolyzer and H_2 storage capacity for a fixed steady-state supply.

In the previous study it was shown, how the interaction of such a plant with the local grid reduces the required installed capacity of the units in the HPP [31]. The future Moroccan grid support is an open parameter for this study. A support in the range of 0 – 25 % is assumed i. e. the maximum power that can be drawn from the grid at any given time is sufficient to produce 0 – 25 % of the required hydrogen flow of 25.74 t/h. This flexibility leads to current hydrogen production costs of 4.10 – 4.89 $€_{2020}/kg_{H_2}$. For perspective data for PV modules and electrolyzers, future costs of 3.05 – 3.55 $€_{2020}/kg_{H_2}$ can be expected.

The reference year is 2030 as previously mentioned. Since it can be assumed, that large productions plant will be connected to an electric grid, hydrogen cost of 3.05 $€_{2020}/kg_{H_2}$ are considered for every pathway. To put that into perspective; some studies consider very ambitious costs and even reduction potentials, especially regarding PV farms and electrolyzers, leading to current cost estimations of less than 2.50 $€/kg_{H_2}$ that

Table 2
Exemplary flight paths and their kerosene demand per person.

ID	From	To	Plane	Distance [km]	CO_2emitted [kg]	Kerosene demand [kg]	Energetic content [MWh_{th}]	Fuel costs 2019 [€$_{2019}$]	Fuel costs 2022 [€$_{2022}$]
1	MUC	HAM	A320 neo	649	43	13.6	0.16	8	14
2	CJU	GMP	A321 neo	1,002	66	20.9	0.25	12	22
3	JFK	LAX	737-Max 9	4,022	181	57.3	0.68	32	60
4	LHR	JFK	A350-900	5,586	311	98.4	1.18	55	103
5	FRA	GRU	777-300ER	9,840	656	207.5	2.48	117	217
6	LHR	PER	787–8	14,574	1079	341.5	4.08	192	357

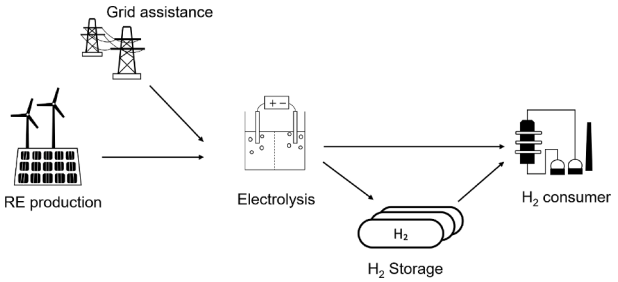

Fig. 5. Plant layout of the hydrogen production plant (HPP).

can further be reduced to 0.7 €/kg_{H_2} in Germany [39]. Other studies predict higher current costs of 4.33 €/kg_{H_2}, even when considering wind farms that no longer receive a fixed remuneration [40]. Since the plausibility of future costs can only be confirmed to a certain extent, the hydrogen feed costs will not be further discussed. The specific perspective energy demand of the electrolyzer is 48 kWh_{el}/kg_{H_2} with liquid water as feedstock [31]. Thus, the electrolyzer has a cooling demand of roughly 8 kWh_{th}/kg_{H_2}. It is considered, that 5.5 kWh_{th}/kg_{H_2} of low temperature heat can be recycled via lye cooling at a temperature level of 70 °C, as shown by Huang et al. [41]. This heat is upgraded via a heat pump for the thermal energy demand of the DAC unit.

3.1.2. Carbon source

3.1.2.1. Direct air capture (DAC). A low temperature DAC unit as described in Fasihi et al. [42] is used as CO_2 source in Morocco. Since the retrieved CO_2 cannot directly be used for the synthesis process due to impurities, a consecutive CO_2 liquefaction unit is considered as in Ausfelder et al. [43]. Technical and economic input data for the DAC unit is taken from Ausfelder et al. The DAC is simulated as a black-box unit. Heat is provided via steam at 120 °C and is required for the endothermic desorption process of CO_2 from the adsorbent resin. Unfortunately, it was not possible to conduct a more detailed heat integration of the DAC with different temperature levels due to lack of detailed input data.

3.1.2.2. Amine scrubbing (MEA scrubber). CO_2 is washed from the exhaust gases of the waste incineration plant via an amine scrubber utilizing monoethanolamine (MEA) [44]. The average exhaust gas composition is taken from [45] and contains 10 $\%_V$ CO_2. The process is depicted in ASPEN Plus® with an equilibrium-based model with input data taken from Kothandaraman and utilizes steam at a temperature level of 125 °C in the desorption column [44]. Degradation of MEA amounts to 0.5 kg MEA per ton of CO_2 captured [46]. Costs for the required equipment of the units is taken from Goff et al. and Woods [47–48]. Specific costs for MEA is taken from a chemical online store-Jokora. Monoethanolamin 99% [49].

Both processes require heat to release the captured CO_2. Heat is supplied in the form of steam at a temperature level of 120 °C and 125 °C, respectively, which is generated via heat integration of the synthesis processes. If the heat of the process is not sufficient, heat pumps with n-butane as refrigerant are considered to utilize lower temperature levels.

3.2. Synthesis of aviation fuels

3.2.1. Hydrogen liquefaction and storage

A large-scale hydrogen oversea transport via LH_2 has been described in a previous study [32]. As in Raab et al. [32], a specific energy demand for the liquefaction of 7 kWh/kg_{H_2} as well as hydrogen losses of 1.65 % from the feed stream during the liquefaction process are considered. With the given feed stream, the required liquefaction capacity amounts to 618 tons per day (tpd). This is rather much compared to the worldwide installed liquefaction capacity of 350 tpd in the year 2020. Three parallel liquefaction plants with a capacity of 225.5 tpd each are considered.

3.2.2. LOHC hydrogenation, logistics and dehydrogenation

The LOHC system *H*00/H12-BT is used to transport hydrogen to Germany for domestic fuel synthesis. With *H*00-BT as dehydrogenated and H12-BT as fully hydrogenated version of the carrier molecule. The involved chemical reaction is shown in Equation (1) with *ortho*-BT as exemplary isomer. The reaction conditions are based on Ausfelder et al. [43]. The exothermic hydrogenation is conducted at 250 °C. The heat released in the reaction is used for steam production and subsequent electric power generation in a steam turbine. The dehydrogenation reaction occurs at 300 °C. No side reactions are considered in the simulation model but losses of recycled BT of 0.1 % per turn are considered.

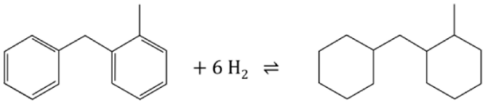

(1)

Eq. (1): De/hydrogenation of ortho BT.

Tube bundle reactors are considered for both, the hydrogenation and the dehydrogenation reaction with 0.3 $\%_{wt}$ Pt/Al_2O_3 as catalyst [50].

3.2.3. Methane synthesis and liquefaction

The methanation of CO_2 according to Eq. (2) was first described by Sabatier [51]. With the reaction enthalpy and the values of the LHV given in Table 8 it can be determined, that under ideal conditions 82.9 % of the chemical energy stored in hydrogen is transferred to chemical energy stored in methane. This ratio is relevant in the explanation of the results in chapter 4.

$$CO_2 + 4\,H_2 \rightleftharpoons CH_4 + 2\,H_2O_{(g)}\ \Delta H^0 = -164\,\frac{kJ}{mol} \quad (2)$$

Eq. (2): CO_2 methanation.

Two different process designs are considered. For the **case A** and **C**, an adiabatic fixed-bed reactor concept is depicted in ASPEN Plus. This process design is commercialized by Haldor Topsøe in the TREMP process [52]. A combined approach for CO_2 methanation and LOHC dehydrogenation is considered in **case B**, as shown in Fig. 6.

In a tube bundle reactor both the methanation and the LOHC dehydrogenation happen simultaneous. On the shell side, water is used as heat transfer fluid. Water evaporates at the outer tube where the

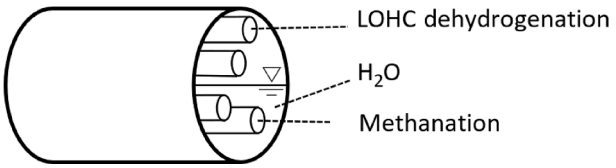

Fig. 6. Reactor concept for combined methanation und LOHC dehydrogenation.

methanation occurs and condenses on the tubes where LOHC dehydrogenation occurs. By regulating the pressure on the shell side, the temperature level can be controlled. For the simulation it is assumed, that a temperature gradient of 10 K is required for the dehydrogenation of LOHC. Therefore, the pressure on the shell side amounts to 98 bar. The heat released in the methanation reaction is 41 kJ/mol_{H_2}. While the heat demand of the endothermic dehydrogenation i.e. the backwards reaction of the reaction shown in Eq. (1), is roughly 65 kJ/mol_{H_2} for ideal conditions. Thus, this concept is not sufficient to dehydrogenate all of the required H12-BT. Kinetic data for the adiabatic TREMP process is taken from Rönsch [53]. Kinetic data from Koschany et al. is used for the isothermal approach with simultaneous LOHC dehydrogenation [54]. After the methanation process remaining water and CO_2 is stripped from the product stream via adsorption to avoid blockages in the subsequent liquefaction unit. There, a propane cooled mixed refrigerant (C3MR) process is used to liquefy methane, as shown in the by Bin-Omar [55]. This technology is state of the art for methane liquefaction processes [56]. With the given hydrogen feed of 25.74 t_{H_2}/h and a conversion efficiency of 100 % the amount of methane that has to be liquefied is 51.2 t_{CH_4}/h. This is equivalent to 0.45 million tons per annum (MTPA) which is rather small compared to other on-shore liquefaction plants ranging from 4 − 8 MTPA [56]. Technical and economic data is taken from [55]. Costs are adapted with a scaling factor of 0.7.

3.2.4. SAF production via Fischer-Tropsch synthesis

The process conditions of the FT synthesis unit are based on studies by Albrecht et al. [33] and Adelung et al. [57]. The whole process is the most complex in this study since it contains several individual steps that are all interconnected. Namely: the reverse water–gas-shit (rWGS) unit, the actual synthesis, a hydrocracker as well as a distillation process. Two main chemical reactions are involved [57].

$$CO_2 + H_2 \rightleftharpoons CO + H_2O_{(g)} \quad \Delta H^0 = 41 \frac{kJ}{mol} \tag{3}$$

Eq. (3): rWGS reaction

$$CO + 2H_2 \rightarrow (-CH_2-) + H_2O_{(g)} \quad \Delta H^0 = -152 \frac{kJ}{mol} \tag{4}$$

Eq. (4): FT synthesis.

The rWGS unit is required to reduce CO_2 to CO, because the catalyst considered in the synthesis is unable to activate CO_2. The influence of the rWGS conditions on the remaining process is shown in a study by Adelung et al. [57]. For this study the pressure in the rWGS unit is set to 5 bars. Only n-alkanes from CH_4 up to $C_{34}H_{70}$ are considered as possible products of the FT synthesis. The share of products is described via the "Anderson–Schulz–Flory (ASF)" distribution with chain growth probability of 85 %. Methane yield is adapted and amounts to 12 %. This is a simplified approach, especially since real Jet A-1 contains a mixture of n-alkane, *iso*-alkanes, cycloalkanes and aromatics [58–59]. Numerous variables influence the product distribution e.g. temperature [60], catalyst support [61], residence time [60,62], time on stream [63] or inert gases in the stream [64–65]. Thus, a simplified approach is used to depict the process in a more generic way. As in Albrecht et al. a hydrocracker is considered based on [66] to break heavier compounds into smaller hydrocarbons. In the distillation process, the final product is separated into the SAF fraction and a lighter fraction.

Unreacted gas after the reactors is partially recycled back to the first reactor, partially to the rWGS and to a certain extent to a burner that is required to provide the high temperature for the rWGS unit. The burner is supplied with oxygen so that some of the exhaust gases can also be recycled. To depict the recycling ratios, a carbon flow Sankey diagram of **case A** is provided in the supplementary information.

The heat from the reaction is used to generate steam, which in **case A** and **C** is directly used for the DAC and the amine scrubber, respectively. In **case B,** steam is required at a temperature level of 310 °C which is significantly higher than 220 °C that is provided from the heat of reaction. To overcome this, a novel approach of a high temperature steam heat pump is considered, as it is followed by the DLR in a first pilot plant called "ZiRa" [67].

3.3. Harbor infrastructure and oversea transport

For every pathway the required harbor infrastructure as well as the actual ships are included in the evaluation. This includes:

- Jetty
- Storage tanks
- Loading and unloading lines from the tanks to the ship
- Flares when LH_2 and LCH_4 is shipped
- Fuel carrier

It is unlikely that the jetty will be used exclusively for shipping the fuel in the considered pathways, especially in case of the importing country. But for the sake of a fair comparison, it is considered in every pathway for both locations. Costs are taken from [68]. The dimensions of the fuel carriers as well as the storage tanks are designed in a manner, that roughly 20 return trips of the carriers are required and that the ships are utilized 80 % of the time. The storage tanks are slightly over dimensioned in order to consider contingencies. Storages for cryogenic liquids are designed that 4–98 % of the total volume can be used i.e. the minimal storage level is 4 % in order to keep the vessel cool. LNG storage container are used as reference vessels for LH_2. 5 m^3 of the cryogenic liquids are lost in every loading and unloading procedure to cool the lines, while losses during these procedures are neglected for LOHC and the SAF-pathway. Lengths of the loading lines of1,200 m are considered with specific costs of 50,000 €/m for cryogenic liquids and 45,000 €/m for hydrocarbons [32].

4. Results and discussion

This work focuses on aspects how a future aviation industry can be supplied with LH_2, LCH_4 and SAF, and how these fuels differ regarding their supply chain. In this chapter, first the technical results are shown in subchapter 4.1 with a distinction between the cases. The resulting costs are shown in subchapter 4.2, where the costs are differentiated between LH_2, LCH_4 and SAF.

4.1. Technical evaluation

To indicate how much energy is required to produce and transport the considered aviation fuels, flow diagrams (similar to Sankey diagrams) are used to depict the average power inputs and outputs of the different steps. For reasons of clarity, only streams transferring thermal energy that is used in the process, chemical energy and electric energy are shown. The first step in every pathway is the HPP mentioned in subchapter 3.1.1 with the values of the averaged flows given in Table 3. The column "Label" refers to the labels in Figs. 7–9. The installed capacities of the corresponding units of the HPP are shown in the SI. A certain over dimensioning of these units is required to achieve the constant hydrogen supply of 25.74 t/h. This leads to unavoidable curtailment of renewable electricity. Some of this curtailed electricity is used in the conversion processes, as shown in the following figures.

Table 3
Annual-average power input and output of the hydrogen production plant (HPP).

Stream	Label	Unit	Value
PV power output	PV	MW	653.8
Wind power output	Wind	MW	769.3
Grid power for AEL	Grid el. for AEL	MW	35.2
Compression power	1	MW	8.8
Curtailed electricity	2	MW	214.0
Power used in AEL	AEL	MW	1,235.5
Hydrogen feed flow	H_2 feed	MW_{LHV}	857.9

4.1.1. Case A - Synthesis at the sweet spot

In the following figures, "H_2 feed" refers to the gaseous hydrogen feed of 25.74 t/h. Fig. 7 shows the power flow diagram of the LH_2-pathway including the HPP, the liquefaction as well as the transport to Germany. The values of the corresponding streams are listed in Table 3 and Table 4.

The different shares of "PV", "Wind" and "Grid el. for AEL" are determined via the linear programming cost optimization methodology published in [31]. They refer to the average electricity flow towards the HPP. Most of the electricity is transferred to the node "AEL" where hydrogen is produced. A small share of the electricity, stream "1", is required in compression units for the H_2 storage shown in Fig. 5. Stream "2" is the average electric power that is curtailed. These streams are identical for every pathway in every case, the remaining streams do differ. Stream "3" shows the average power flow that is curtailed by the HPP but is used in the subsequent liquefaction process. The electric power demand is only met to a certain extent by this stream, remaining electricity demand for the conversion step is taken from the grid. The energetic losses at the "AEL" node result from the difference between the specific electricity demand of the electrolysis at the input (48 kWh_{el}/kg_{H_2}) and the energetic content of hydrogen as output (LHV = 33 kWh_{th}/kg_{H_2}). The node "Final LH_2" is the final amount of liquid hydrogen that arrives in the storage tanks in Wilhelmshaven. This node is also the feed stream for the LCH_4 and SAF-pathway of **case C**. Some of the produced hydrogen is lost in the liquefaction process and some is lost during the loading and unloading from the carrier (summarized in "Losses from handling"). The energy demand to power the LH_2 carrier is met by using the boil-off during transport, this is shown with the node "Shipping".

The power flow diagram depicted in Fig. 8 shows the LCH_4-pathway with a DAC unit as carbon source. The values of the corresponding streams are listed in Table 3 and Table 4.

Every pathway starts with the same hydrogen feed, so the streams of

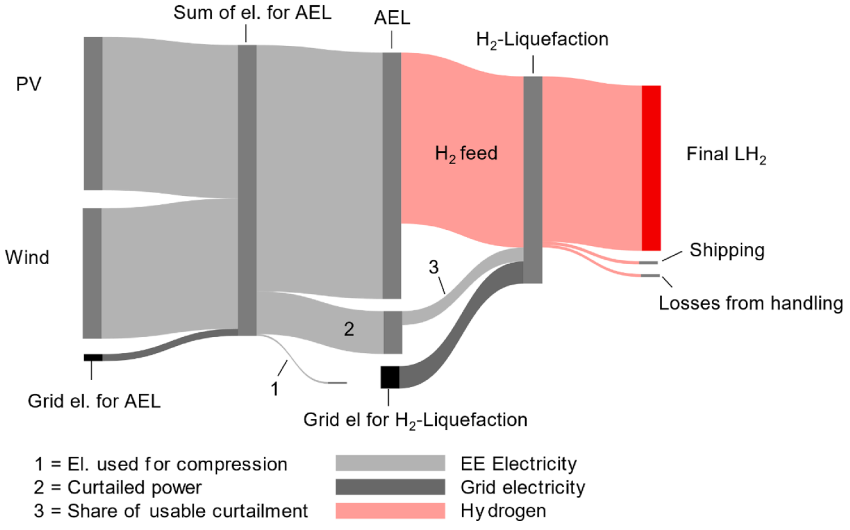

Fig. 7. Power flow diagram for the LH_2 pathway.

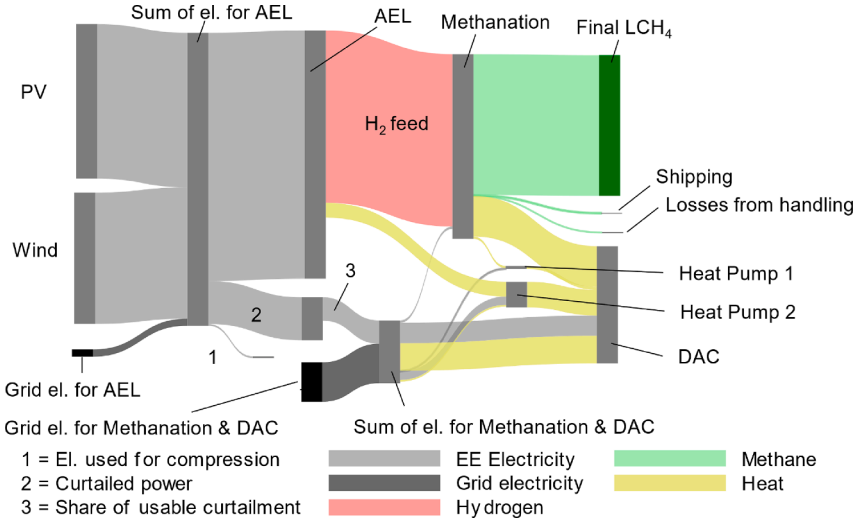

Fig. 8. Power flow diagram for the LCH_4 pathway – Case A.

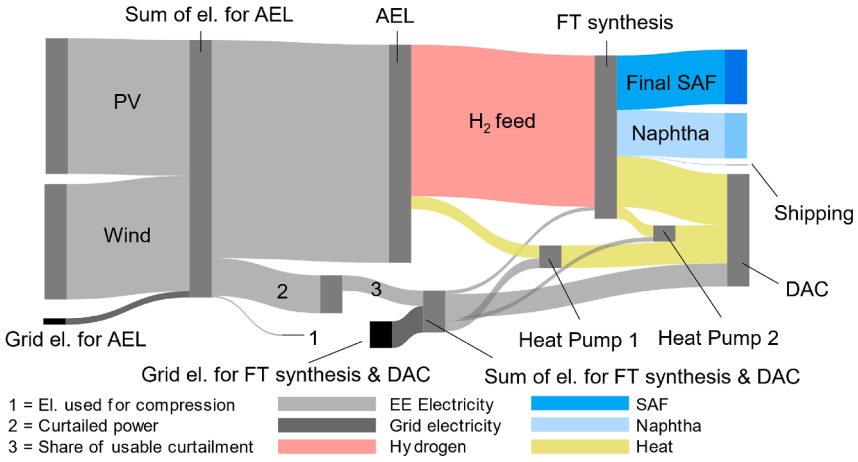

Fig. 9. Power flow diagram for the SAF pathway – Case A.

Table 4
Average input and output power streams - Case A.

Case A	Unit	LH_2	LCH_4	SAF
Total el. power demand	MW	180.2	312.5	241.5
Used curtailed power from HPP	MW	68.9	116.4	91.2
Additional grid power used	MW	111.3	196.1	150.3
Total heat demand DAC	MW	–	490.1	528.2
Total electricity demand DAC	MW	–	101.2	109.1
Power demand for shipping	MW_{LHV}	15.5	4.3	4.4
Final product (incl. side product)	MW_{LHV}	828.4	701.2	298.0 (558.2)
H_2 to fuel efficiency (incl. transport)	%	96.6	81.7	34.7 (65.1)
Total efficiency (incl. side product)	%	52.8	42.4	18.5 (34.7)

the HPP are the same as in Fig. 7. The electric power demand of the methanation process is summarized in node "Sum of el. for Methanation & DAC". Most of the power demand is taken from the grid, a smaller amount of electricity is usable curtailment from the HPP (stream "3"). Most of the electric power demand is directly or indirectly used to supply the process with CO_2. Electric power is used in two heat pumps which are required to utilize low temperature heat for the DAC unit. The heat pumps are utilizing low-grade thermal energy from lye cooling of the electrolysis and from the process streams of the methanation. Furthermore, electric power is used to move air through the DAC units and as direct electric heat source. This high effort of thermal management is due to the high thermal power demand of the DAC of roughly 3.5 MWh_{th}/t_{CO_2}. It appears, that there is more power leaving the "Methanation" node than entering it, this is due to the fact that the "H_2 feed" is based on the LHV of hydrogen and the heat utilized in the DAC unit derives from condensing water out of the product streams. If more detailed data of the DAC unit were available, heat could be integrated at different temperature levels, leading to a less complex flow diagram and a lower electricity demand. The difference between the chemical in- and output of the methanation node results from the chemical conversion of hydrogen to methane, as previously mentioned in chapter 3.2.3. The real value is slightly lower, as shown in Table 4.

The power flow diagram depicted in Fig. 9 shows the SAF-pathway with a DAC unit as carbon source.

Every pathway starts with the same hydrogen feed, so the streams of the HPP are the same as in Fig. 7. As mentioned in subchapter 3.2.4, a simplified model of the FT synthesis is used. Therefore, a generic SAF product and Naphtha side product are retrieved. Again, two heat pumps are required to utilize low temperature heat in the DAC unit. The amount of chemical energy converted into a product is slightly lower than in the LCH_4-pathway. This results from the required high temperature of the rWGS reactor that is provided by burning some of the lighter products of the synthesis. These compounds could otherwise be recycled to the rWGS reactor. The mean power flows of all pathways of **case A** are listed in Table 4.

Total efficiency is defined as the chemical energy at the destination based on the LHV divided by the electricity input. The electric input is the sum of "PV power output", "Wind power output", "Grid power for AEL" and the corresponding "Additional grid power used" listen in Table 3 and includes the electricity demand for the whole process including the CO_2 supply. *H_2* to fuel efficiency is the ratio of the chemical energy at the destination divided by initial H_2 feed, both based on LHV. For the results of the SAF pathways, the efficiencies are differentiated between only SAF and SAF + Naphtha.

4.1.2. Case B - Synthesis based on LOHC-hydrogen

As shown in Fig. 3, in the pathways of **case B** the fuel is synthesized at the importing site and hydrogen is transported via LOHC. In Fig. 10 the power flow for LCH_4 is shown excluding flows of the HPP.

Steam is produced during H0-BT hydrogenation and used to generate electricity in a steam turbine (stream "4″). At the receiving site, the first step is the node "LOHC dehyd.", the dehydrogenation of H12-BT. This step requires heat at 300 °C. It is partially supplied via the exothermic methanation, hence the recycle stream "Heat for dehydrogenation" which covers 61 % of the required heat. Remaining heat for dehydrogenation is supplied via electric heating. Another heat demanding step is the reboiler of the desorption column in the MEA scrubber. Remaining heat of the process is not sufficient to cover the heat demand of the MEA scrubber. Therefore, a heat pump is used to utilize the heat released from cooling the process streams down to 80 °C. The specific heat demand of the MEA scrubber is 3.7 MJ_{th}/kg_{CO_2} according to the process simulation. This equals to a steam demand of 1.6 kg/kg_{CO_2}. The specific heat demand of LOHC dehydrogenation amounts to 10.8 kWh_{th}/kg_{H_2}. Fig. 11 shows

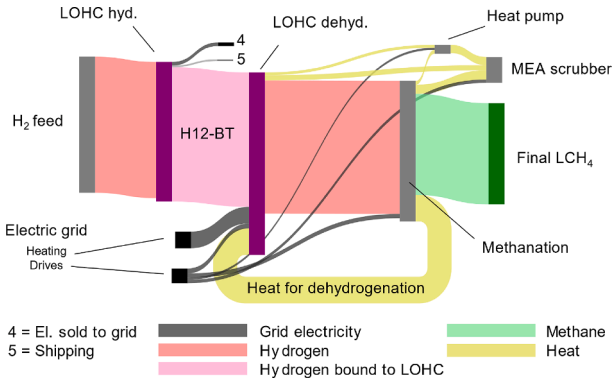

Fig. 10. Power flow diagram for the LCH_4 pathway - Case B via LOHC.

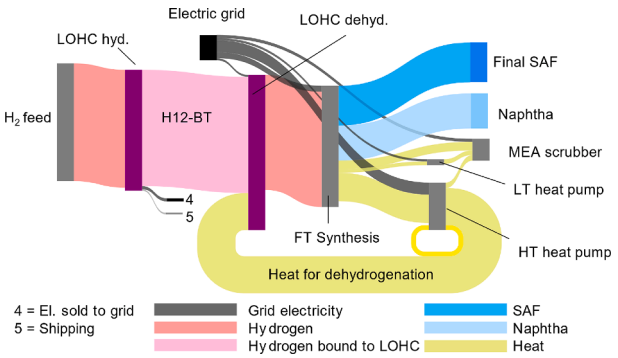

Fig. 11. Power flow diagram of the SAF pathway - Case B via LOHC.

Table 5
Average input and output power streams - Case B - LOHC.

Case B - LOHC	Unit	LCH_4	SAF
Power used for shipping	MW_{LHV}	10.4	10.4
Hydrogen feed to synthesis	MW	838.9	838.9
Heat demand of dehydrogenation	MW	271.8	271.8
Heat demand MEA scrubber	MW_{th}	142.0	151.3
Power demand of LT - HP (C4)	MW	14.4	9.3
Power demand of HT - HP (H_2O)	MW	–	88.8
Power demand for liquefaction	MW	23.0	–
Total power demand	MW	200.7	176.1
Final product (incl. side product)	MW_{LHV}	650.7	290.2 (546)
Production efficiency in Germany	%	62.6	28.6 (53.8)
Total efficiency incl. H_2 import(incl. side product)	%	39.8	18.0 (33.9)

the power flow for SAF via LOHC, also excluding the flows of the HPP.

Compared to the LCH_4 pathway, no electric heating is required. Electricity is only used to power engines and other drives. “LT heat pump” is the heat pump using n-butane. “HT heat pump” is the high temperature heat pump mentioned in subchapter 3.2.4. In this unit, the heat of the FT synthesis is upgraded so it can be used in the dehydrogenation process with a resulting coefficient of performance (COP) of 2.35. A small amount of heat from the HT heat pump is also transferred to the HT heat pump. This heat comes from interstage cooling of the compressors that increase the pressure of the steam. Due to the properties of water a lot of heat is produced during steam compression, this is shown in a T,s diagram in the SI. The average power flows of both pathways from **case B** are listed in Table 5.

4.1.3. Case C - Synthesis based on LH_2

Instead of utilizing a chemical compound for the hydrogen transport, imported LH_2 is used for the synthesis in **case C**. The flow diagram for LCH_4 is shown in Fig. 12.

“LH_2 feed” corresponds to the “Final LH_2” stream shown in Fig. 7. Since heat released from the exothermic reaction is not required elsewhere, steam is generated and fed to steam turbines. Therefore, no external electricity is required for the methanation process. Only the electric drives in the MEA scrubber require external electricity. Furthermore, no active liquefaction is required since the low temperature of the LH_2 feed is used to liquify methane. Fig. 13 shows the power flow diagram for SAF with LH_2 as feed.

As in the LCH_4 pathway for **case C**, no complex heat management system or heat pumps are required in the process. The mean power flows of all pathways of **case C** are listed in Table 6.

4.2. Economic evaluation

In this subchapter, the cost breakdowns of the supply chain for the different aviation fuels are shown. For every pathway hydrogen cost of

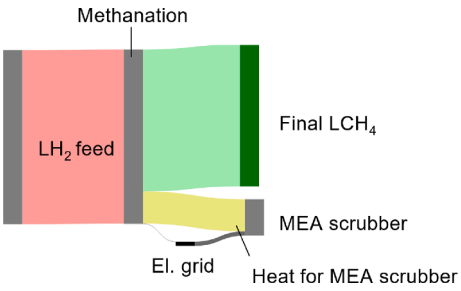

Fig. 12. Power flow diagram for the LCH_4 pathway - Case C via LH_2.

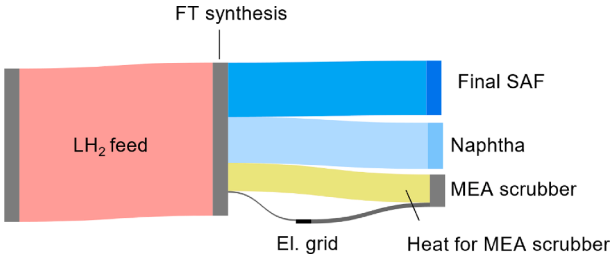

Fig. 13. Power flow diagram for the SAF pathway - Case C via LH_2.

Table 6
Average input and output power streams - Case C - LH_2.

Case C - LH_2	Unit	LCH_4	SAF
Hydrogen feed to synthesis	MW	828.4	828.4
Heat demand MEA scrubber	MW	140.4	149.6
Total power demand	MW	15.85	39.6
Final product (incl. side product)	MW_{LHV}	675.13	286.4 (536.3)
Production efficiency in Germany	%	80.0	33.0 (61.8)
Total efficiency incl. LH_2 import(incl. side product)	%	43%	17.8 (33.3)

3.05 $€_{2020}/kg_{H_2}$ from the HPP are considered, which is equivalent to 91.50 $€_{2020}/MWh_{LHV}$. If not stated otherwise, costs are given in $€_{2020}$ and energy specific costs are based on the lower heating value. These subscripts will be left out in this subchapter.

The cost elements of hydrogen from the HPP are given in the SI.

4.2.1. Liquid hydrogen

The cost breakdown of the LH_2 pathway are shown in Fig. 14. To better display the different elements, the ordinate does not start at the value of 0 but at 80 €/MWh. The final costs are 157 €/MWh which corresponds to 5.23 $€/kg_{H_2}$, these are the feed cost for the production of LCH_4 and SAF in **case C**.

From Fig. 14 it can be seen the total costs are dominated by the hydrogen supply, which account for roughly 60 % of the total costs. The second largest cost contributor is the cost for electricity, although only costs for electricity from the grid for the liquefaction process are considered and 38 % of the power demand is met by excess electricity from the HPP, as shown in Fig. 7. In general, it can be seen that the costs for the logistics i.e. storage, harbor and the LH_2 sum up to roughly 17 €/MWh meaning to slightly more than 10 % of the costs of the supply chain shown in Fig. 3.

4.2.2. CO_2 from MEA and hydrogen transport via LOHC

The results of **case B** and **C** include CO_2 from an amine scrubber. Detailed economic results of this process are shown in Fig. 15. Costs of the energy required in the desorber column are not included, since it is taken from the exothermic fuel synthesis. It can be seen, that the costs are dominated by OPEX where the largest share is the cost of electricity. In total 150.6 kWh_{el}/t_{CO_2} are required of which 85 % are needed in a first

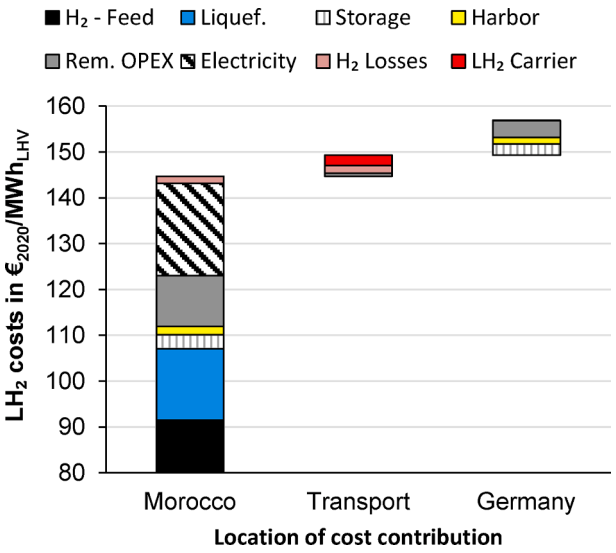

Fig. 14. Costs of the LH_2 pathway.

compressor stage to move the exhaust gas through the absorber column. Further 14 % are needed in a compressor after the desorber column to increase the pressure to 3 bar. The total supply costs of CO_2 amount to 44.4 €/t_{CO_2}.

In **case B** hydrogen is supplied via LOHC. In the SAF pathway LOHC is dehydrogenated in reactors that are specially designed for that purpose. In the LCH_4 pathway a certain amount is dehydrogenated in the combined reactors shown in Fig. 6. Remaining LOHC is dehydrogenated in individual dehydrogenation reactors. Results of the hydrogen supply costs via LOHC are shown in Fig. 16 without the costs for the dehydrogenation energy demand but with the distinction between the SAF and the LCH_4 pathway. In the latter, no reactor costs are included. To better display the different cost elements, the ordinate does not start at the value of 0 but at 90 €/MWh. The different values for electricity results from the different pressure at which hydrogen is transferred to the synthesis unit. 11 bar and 6 bar in the LCH_4-pathway and the SAF-pathway, respectively.

4.2.3. *Liquid methane*

The cost breakdown of the different LCH_4 pathways are shown in Fig. 17. To better display the different elements, the ordinate does not start at the value of 0 but at 100 €/MWh. The three columns on the left

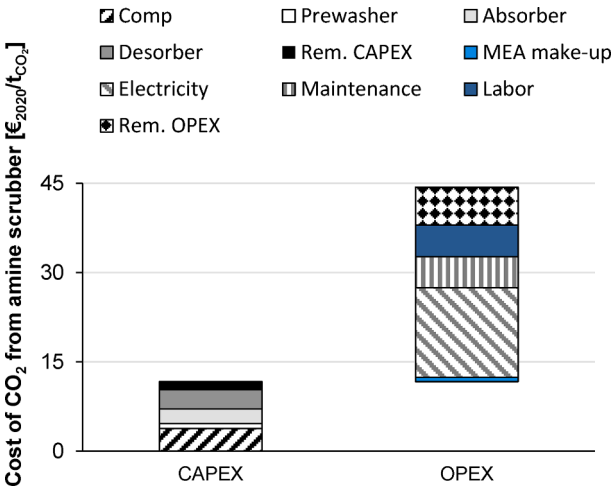

Fig. 15. Cost breakdown of CO_2 from amine scrubber (excl. energy for desorption).

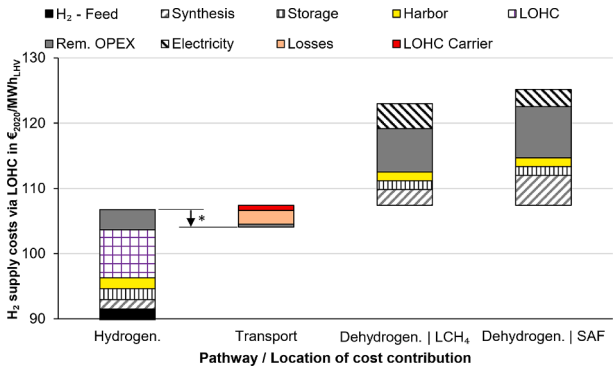

Fig. 16. Hydrogen supply costs via LOHC excl. dehyd. energy | *Cost reduction results from selling electricity.

indicate the different steps of **case A**. The two columns on the right represent **case B** and **case C**. The first noticeable aspect is that the hydrogen feed of 91.50 €/MWh accounts for 111 €/MWh in **case A**. This is due to the energetic losses that result from the methanation reaction itself, as mentioned in 3.2.3. The largest share of the costs in Morocco are the hydrogen feed costs. They make up 50 % of the total costs, followed by electricity and the depreciation of the DAC unit with a share of 19 % and 11 %, respectively. Though the lion-share of electricity is used in the DAC as shown in Fig. 8. Costs for the transport of LCH_4 as well as the receiving terminal in Germany have a rather small influence on the costs in **case A** with a share of 1.6 % and 1.1 %, respectively.

While the hydrogen feed costs are the highest in **case C**, it has the lowest total production costs. No external electricity is required in the synthesis, only the MEA scrubber requires electricity but the costs are considered in the CO_2 supply costs, which account to 9 €/MW. The hydrogen feed costs in **case B** do not include the additional thermal energy demand of the dehydrogenation that is required for the share that cannot be dehydrogenated with the reactor concept shown in Fig. 6 nor the additional dehydrogenation reactors. Due to the additional reactors, the demand for the liquefaction unit and the electric energy demand **case B** is the least economic option for the LCH_4 pathway. In general, the total costs of **case A** and **case C** are quite close to each other with a value of 220 €/MWh and 217 €/MWh, respectively. **Case B** is more expensive with 229 €/MWh.

4.2.4. *SAF*

The cost breakdown of the different SAF pathways are shown in Fig. 18. To better display the different cost elements, the ordinate does not start at the value of 0 but at 130 €/MWh. As for LCH_4, the three columns on the left indicate the different steps of **case A**. The two

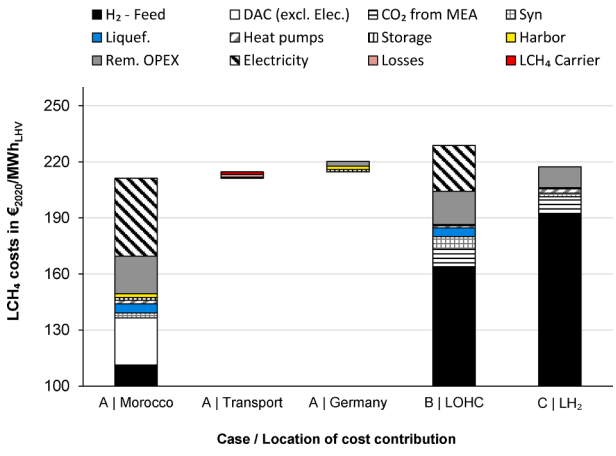

Fig. 17. Costs of the different LCH_4 pathways.

columns on the right represent **case B** and **case C**. The column of the hydrogen feed accounts for roughly 139 €/MWh in **case A,** resulting in a share of 50 % of the total costs. The increase from 91.50 €/MWh to 139 €/MWh corelates with the energetic losses from the FT synthesis, equivalent to the methanation process. The share of electricity costs in the total costs amount to 40 €/MWh, resulting in a share of 19 % of the costs in **case A**. They result mostly from the power demand of the DAC as shown in Fig. 9. The depreciation costs of the DAC unit have a share of 12 % with 34 €/MWh. As for LCH_4, the overall costs of the transport and the receiving terminal have a small influence with a share of 1.1 % and 1.6 % of the total costs, respectively.

While **case C** is the most economic option for LCH_4, it is the most expensive for SAF. The lower share of costs for CO_2, 12 €/MWh for domestic production compared to 74 €/MWh in **case A**, do not outweigh the high hydrogen feed costs 239 €/MWh in **case C**. In **case B**, the advantage of lower CO_2 costs are canceled out by the additional electricity demand for the LOHC dehydrogenation. The final costs for **case A** are the lowest with 277 €/MWh, followed by 298 €/MWh in **case B** and 302 €/MWh in **case C.**

4.2.5. Comparison with other research

The techno-economic evaluation of PtX-processes have been investigated by numerous other researchers before. In Table 7 the outcomes of some studies are listed and compared with the findings of this work. This list is an excerpt of the currently available data and even after a thorough research it cannot be claimed to be complete. Depending on the availability, the corresponding input data as well as intermediate results are listed too. In every research paper, different assumptions have been made for the evaluation. Aspects like the carbon source, the interest rate or annual full load hours lead to different results even when the same costs for hydrogen or electricity are considered. Furthermore, the products also differ. The upgrading step from the FT synthesis to SAF is not always included, thus the column header "FT / SAF". While for methane, different remaining hydrogen concentrations or the presence of a liquefaction step also influence the results. The following aspects can be derived with the values from Table 7.

- The conversion of electric energy in chemical energy in the form of hydrogen leads at least to a doubling of the specific energy costs. Thus, the remark "H_2 from pipe" where a fixed hydrogen price is assumed.
- If both methane and liquid hydrocarbons are produced, methane is cheaper to produce. In the case of Tremel et al. and Zhang et al. the fuels are produced simultaneous in a hybrid plant [69–70].
- The increase of the specific energy costs from hydrogen to methane is in the order of 40–50 % for comparably cheap CO_2 sources. For cases with a DAC the increase is in the order of 140°%. It has to be noted, that the DAC is not a mature technology and further improvements influence this value.
- The increase of the specific energy costs from hydrogen to liquid hydrocarbons (thus a precursor for SAF) via the FT synthesis is at least 60 % for comparably cheap CO_2 sources. In some studies, the value is almost doubled.

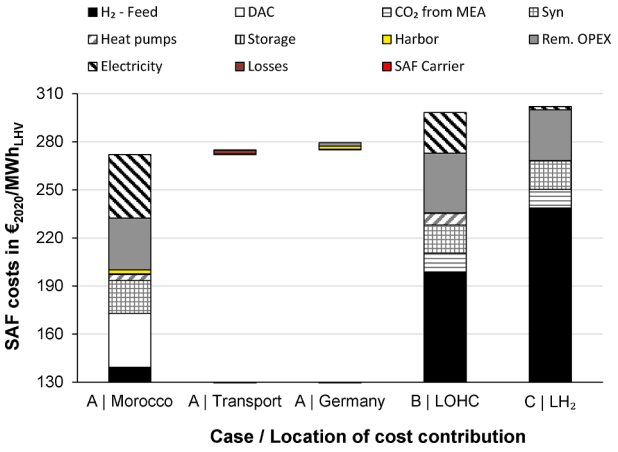

Fig. 18. Costs of the different SAF pathways.

4.3. Fuel comparison

To compare the different fuels, the costs of the results from **case A** are shown in Fig. 19. To better display the different cost elements, the ordinate does not start at the value of 0 but at 80 $€_{2020}/MWh_{LHV}$.

It is shown, how the costs increase with the complexity of the fuel production process and how the share of hydrogen costs increases due to the reaction enthalpies. The total costs increase by 40 % per energy unit if LCH_4 is produced instead of LH_2, this value increase to 78 % in the case of SAF. Costs for the DAC units result in 25 and 34 $€_{2020}/MWh_{LHV}$ for LCH_4 and SAF, respectively. Costs for losses along the pathway, harbor infrastructure and the carriers have a small influence on the total costs. Excluded from this study are the costs further down the supply chain. The values in Fig. 19 do not consider the transport to the airport or the fueling logistics at the airport itself. There, other aspects not included in this TEA so far can have an influence on these ratios. As an example, the different volumetric energy densities of the fuels have to be considered as well. Table 8 lists the properties of LH_2, LCH_4 and SAF.

The volumetric energy content of LH_2 amounts to only 24 % compared to SAF, excluding the required insulation of a cryogenic tank. This does not only play a major role during the logistics but also on the utilization of the fuel in planes itself. While the former aspect will be evaluated in a future study, the latter is subject of numerous studies, as it has been outlined in chapter 1. Furthermore, the specific energy demand of planes using LH_2 is not the same as for planes utilizing SAF or fossil kerosene [77–78]. But for a first rough estimation to evaluate how renewable fuels influence the socio-economic aspects of the aviation industry, it is assumed that the specific energy demand of planes utilizing cryogenic fuels is equal to conventional planes. With the values given in Fig. 19 and the energy content of the fuels from Table 8, the share of fuel costs for future air travel can be determined. The exemplary flight paths from Table 2 are chosen and the results are listed in Table 9, where the cost equivalent for the different fuels based on the required energy of the corresponding flight is listed. Not considered is the aspect of the technical feasibility i.e. if it is even possible to use a LH_2 powered plane to fly a given distance. The values in Table 9 indicate, that the introduction of renewable fuels in the aviation industry will have a high influence on the market. Even for LH_2 where a different energy demand is not considered in these values, the fuel cost share increases by at least a factor of three when compared with 2019 values.

4.4. Discussion

In this study a cost estimation method has been applied that gives the results with an assumed accuracy of ± 30 % [79]. Since for the hydrogen feed costs and the DAC perspective data is considered, the uncertainty window of the final results is higher. Nevertheless, several aspects can be concluded from the results.

The most relevant input parameter is the cost of hydrogen. This value determines the general costs of all considered aviation fuels. The value has been retrieved by applying the method from an earlier study [31], therefore a reduction or optimization of these costs are not part of this study. In the LH_2-pathway the same volume-specific costs for the carrier and storage facilities as for LCH_4 have been used. While this is a simplified approach and the costs for LH_2 equipment might be higher, this simplification does not have a major influence on the final results, as it can be seen in Fig. 14. Also, even though the infrastructure is completely considered in every pathway it only has a small influence on the outcomes. The lack of proper input data for the heat integration of

Table 7
Literature overview for similar PtX production processes.

Author	Carbon source *	Carbon cost [€/t_{CO_2}]	Power [€/MWh_{el}]	H_2 [€/MWh_{LHV}]	CH_4 [€/MWh_{LHV}]	FT / SAF [€/MWh_{LHV}]	Remark	Source
Adelung et al.	MEA		76.8	164		326	Base case	[71]
Albrecht et al.	U	37.8	105			297	PtL case – 11 t/h	[33]
Albrecht et al.	BM	97.4 €/t_{BM}	105			242	PBtL case	[33]
Brynolf et al.	U	30	50	137	198	224	2015 case	[72]
Brynolf et al.	U	30	50	113	162	180	2030 case	[72]
Decker	U	70	38–75	98–187		184–288		[73]
Park et al.	U			150 $	215 $			[74]
Peters et al.	MEA	35		165	253		H_2 via wind power	[75]
Peters et al.	U	88		165	279		H_2 via wind power	[75]
Peters et al.	DAC	800		165	396		H_2 via wind power	[75]
Schemme et al.	U	70	98	138		231	H_2 from pipe	[5]
Tremel et al.	U	50		90	169	169–195	H_2 from pipe	[69]
Zang et al.	U	17.3 $	70 $	60 $		149 $	H_2 from pipe	[76]
Zhang et al.	U	35 $	63 $	75 $		145 $	Base case H_2 from pipe	[70]
Zhang et al.	U	35 $	63 $	75 $	111 $	138 $	Hybrid PtL/PtG-0 H_2 from pipe	[70]
Case A	DAC			91.5	220	277	H_2 costs are feed costs	
Case B	MEA	44.4 **	100	123/125 EE	229	298	H_2 costs are feed costs	
Case C	MEA	44.4 **	100	157	217	302	H_2 costs are feed costs	

* U = undefined via pipe, MEA = via flue gas amine scrubber, BM = biomass, DAC = From air via direct air capture.
** Excluding thermal energy for MEA-CO_2 desorption.
$ Costs given in US-$.
EE = Energy demand for dehydrogenation excluded.

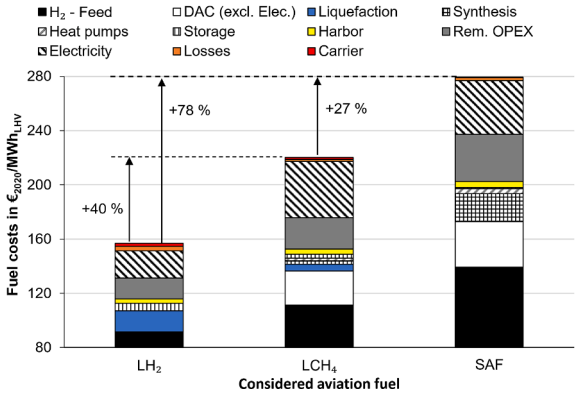

Fig. 19. Cost comparison of aviation fuels | Case A.

Table 8
Comparison of the fuel properties.

Aspect	Unit	LH_2	LCH_4	SAF
Density (liq. / @ 1 bar)	kg/m^3	70.8	422.6	810*
Boiling point @ 1 bar	°C	−252	−161	> 150
Lower heating value	kJ/mol	241.8	802	≈ 535 – 630**
Energy density - volumetric	MJ_{LHV}/m^3	8.50	21.13	34.83
Energy content - mass specific	MJ_{LHV}/kg	120	50	43*
Relative (to SAF) energetic density – volumetric	–	0.24	0.61	1
Relative (to SAF) energetic content – by mass	–	2.79	1.16	1

* Since Jet A-1 is a mixture, mean values are used.
** Average value per carbon atom - based on [59].

the DAC unit was not beneficial for the results of the pathway in **case A**. With an improved heat integration, the energy demand of the DAC units could be reduced. This would lead to lower production costs for LCH_4 and SAF, where electricity is so far the second highest cost contributor. In general, reducing the electric or thermal energy demand of the DAC and increasing the lifetime of the amine-functionalized resin are relevant factors that are beneficial for the costs. Therefore, more research is required in the field of DAC systems to decrease the CO_2 supply costs. The costs of the synthesis unit for LCH_4 and SAF have a subordinate role in the total supply costs, especially for LCH_4. The same statement is valid for the cost of transport and the receiving terminal in Wilhelmshaven.

In **case B** the fuels are synthesized at the receiving terminal. The required hydrogen has been imported via a LOHC. For LCH_4 a novel reactor design has been considered, while for SAF an innovative heat pump concept was evaluated. Therefore, for the results of **case B**, the uncertainty window of the final results is most likely larger than ± 30 %. But with the implementation of the high temperature heat pump an exemplary use case for a such a system with water as refrigerant is shown.

In **case C** the fuels are also synthesized at the receiving terminal. The required hydrogen is imported as LH_2 as in case A. For the production of LCH_4, a novel approach to liquify methane with LH_2 in a heat exchanger is evaluated and thus, no further external electricity is used in the methane liquefaction process. Contrary, in the FT synthesis, the low temperature of LH_2 is not further utilized since it would be out of scope of the actual fuel synthesis. But the implementation of a cryogenic exergy recovery system as proposed by Fyke et al. might be beneficial for the SAF production costs [80].

The results of this study and similar research are listed in Table 7. When the values of **case C** are compared with the results of Adelung et al. and Park et. al., they seem to be in accordance [71,74]. But for the case of Adelung et al, the costs for the C_{5+} product are reduced by 31 €/MWh due to the revenue of selling side products like district heating, LPG and oxygen. While in **case C** the final costs are based only on the liquid hydrocarbon fraction. The overall higher costs in Adelung et al. could be explained with the slightly higher interest rate of 7 % compared to 5 %. This shows the relevance of transparent input data as well as intermediate results, so that differences in the outcomes can be evaluated. Two further observations are highlighted. First; while Peters et al. and **case C** have comparable hydrogen feed costs, the costs for methane retrieved by Peters et al. are at least 17 % higher, even though the costs for CO_2 are slightly lower. Second; the ratio between the SAF/ FT-product and hydrogen energy-specific costs are roughly 1.65 in the

Table 9
Costs for renewable aviation fuel on exemplary flight paths | per person and one-way.

ID	From	To	Energetic content [MWh_{th}]	Fossil fuel costs 2019 [€$_{2019}$]	Fossil fuel costs 2022 [€$_{2022}$]	Equiv. cost LH_2 [€$_{2020}$]	Equiv. cost LCH_4 [€$_{2020}$]	Equiv. cost SAF [€$_{2020}$]
1	MUC	HAM	0.16	8	14	25	35	45
2	CJU	GMP	0.25	12	22	39	55	70
3	JFK	LAX	0.68	32	60	107	150	190
4	LHR	JFK	1.18	55	103	185	260	330
5	FRA	GRU	2.48	117	217	389	546	693
6	LHR	PER	4.08	192	357	640	898	1140

2015 case of Brynolf et al. and for Schemme et. al (224/137 ≈ 231/138 ≈ 1.65), while it is roughly 1.95 for Adelung et al. and in **case C** (302/157 ≈ 326/164 ≈ 1.95). Both observations cannot be further evaluated due to the lack of further data. The first could be explained with higher costs for electricity or CAPEX. But especially the second observation is counterintuitive. In general, the energy-specific cost ratio between the product and hydrogen should increase for low hydrogen costs, since the remaining costs play a more dominant role.

Regarding the absolute values, the results show that LH_2 is the most economic fuel, followed by LCH_4 and SAF. Which is expected since the basis for every fuel is the supply of gaseous hydrogen and the complexity of the conversion procceses are in accoredance with the ranking of the costs. Furthermore, due the reaction enthalpies some of the energy stored in hydrogen is converted into heat and the hydrogen liquefaction process is powered by external electricity, i.e. no energy in the form of the provided hydrogen is lost. Some of the heat released during the synthesis reactions can be recovered in the form of steam and electricity in a subsequent steam turbine. But it is not sufficient to cover the electricity demand of the CO_2 supply, the methane liquefaction or the synthesis process itself. In the SAF production, the heat demand of the endothermic rWGS reaction is covered by burning some of the light gases produced in the process. If the heat of the rWGS is supplied by electricity instead of burning some of the light gases, the efficiency of the whole supply chain could be increased.

Apart from the applied methodology and the process design, the technical input parameters and the used simulation software have to be addressed in the discussion. The hydrogen transport pathways via LH_2 and LOHC are not very complex processes to simulate in ASPEN Plus since a simplified liquefaction process is used and for the hydrogenation and dehydrogenation no side reactions are considered. The chemical aspects of the methanation process can also be depicted with small efforts, only the heat integration required to supply steam for the amine scrubber is a more complex but manageable issue for the software. For the production of SAF, the limits of the software were reached. A simplified simulation model is applied in the FT synthesis. Increasing the number of components is not beneficial if there are too many recycle streams in the process. The carbon flow of the FT synthesis of case A is shown in the supplementary information where it can be seen that several recycle streams are considered. This already led to an unstable behavior of the software. While this has only a minor effect on the outcomes it opposes a challenge for further sensitivity studies. One aspect that has not been discussed so far is how to deal with the large side-product stream of the SAF-pathways. If they represent products of a high value that can be sold with a high margin, they could be beneficial for the overall economics of the process. Otherwise with improvements in catalyst development, the share of undesired side-products could be reduced but not completely be avoided. Remaining side products can be upgraded in an alkylation unit. But state-of-the art processes utilize sulfuric or even hydrofluoric acid and modern solid-acid based process face issues with catalyst life. Therefore, research questions should be addressed not only to develop better catalysts for the FT synthesis but also to develop efficient alkylation processes with non-hazardous chemicals to improve the carbon-yield of the FT process.

5. Conclusion and outlook

In this study a comparative techno-economic evaluation for different aviation fuel supply options has been conducted. To the knowledge of the author, so far, no study has evaluated the supply of LH_2, LCH_4 and SAF (SAF as e-kerosene) where the remote hydrogen production plant (HHP) is included in the battery limit of the evaluation and where the influence of the location of the carbon source has been compared. It has been shown in Fig. 19, that LH_2 is the most economic option of remotely produced renewable aviation fuel. The production of LCH_4 is roughly 40 % more costly as for LH_2, however the cost difference between remote (**case A**) and domestic synthesis using LH_2 (**case C**) is negligible. The energy import of SAF/e-kerosene is 78 % more costly as for LH_2. The cost assessment shows an advantage for remote production (**case A**), because of considerably lower hydrogen feed costs compared to **case B** and **case C**. It can be concluded, that if the aviation industry decides to introduce LH_2 as a viable fuel option, the introduction of LCH_4 should also be considered from a techno-economic point of view.

Future research should evaluate the change of the specific energy demand of planes utilizing cryogenic fuels. The efficiency of converting energy into mileage is not the same for every considered fuel or plane type, respectively. The distinct cost advantage of LH_2 allows a certain higher specific energy demand or higher costs of hydrogen airplanes. To retrieve the breakeven point, the remaining aspects of Fig. 3 have to be assessed. Further research questions like the ecological impacts of introducing cryogenic fuels and effects of non-CO_2 emissions involved in the whole supply chain also have to be addressed. Especially if LCH_4 is introduced, research should focus on methane slip during the utilization as well as during the whole supply chain.

Furthermore, the ranking shown in Fig. 19 is valid for hydrogen-based fuels. This ranking does not change even if further research can increase the efficiency of the DAC units or an electric rWGS is used. But LCH_4 or SAF based on biomass like the already certified production processes can have lower production costs [12]. Though the scalability of these production processes also has to be considered. This is relevant to evaluate the drastic increase of the costs for fuel as shown in Table 9 and the resulting socio-economic consequences.

CRediT authorship contribution statement

Moritz Raab: Conceptualization, Methodology, Software, Investigation. **Ralph-Uwe Dietrich:** Supervision, Validation, Writing – review & editing, Resources.

Declaration of Competing Interest

The authors declare that they have no known competing financial interests or personal relationships that could have appeared to influence the work reported in this paper.

Data availability

Data will be made available on request.

Appendix A. Supplementary material

Supplementary data to this article can be found online at https://doi.org/10.1016/j.enconman.2023.117483.

References

[1] Fuel Cells and Hydrogen 2 Joint Undertaking, Hydrogen-powered aviation : a fact-based study of hydrogen technology, economics, and climate impact by 2050: Publications Office; 2020. [Available from https://op.europa.eu/en/publication-detail/-/publication/55fe3eb1-cc8a-11ea-adf7-01aa75ed71a1/language-en].

[2] Graver B, Rutherford D, Zheng S. CO_2 Emissions from Commercial Aviation: 2013, 2018, and 2019. ICCT; 2020. https://theicct.org/sites/default/files/publications/CO2-commercial-aviation-oct2020.pdf.

[3] Shell Global | PEARL GTL - OVERVIEW [Available from: https://www.shell.com/about-us/major-projects/pearl-gtl/pearl-gtl-an-overview.html. [Accessed 17.08.2022].

[4] Habermeyer F, Kurkela E, Maier S, Dietrich R-U. Techno-Economic Analysis of a Flexible Process Concept for the Production of Transport Fuels and Heat from Biomass and Renewable Electricity. Front Energy Res 2021. https://doi.org/10.3389/fenrg.2021.723774.

[5] Schemme S, Breuer JL, Köller M, Meschede S, Walman F, Samsun RC, et al. H2-based synthetic fuels: A techno-economic comparison of alcohol, ether and hydrocarbon production. Int J Hydrogen Energy 2020. https://doi.org/10.1016/j.ijhydene.2019.05.028.

[6] Projekt PowerFuel - CO2 aus der Luft wird zu klimafreundlichem Kraftstoff [Available from: https://www.energiesystem-forschung.de/forschen/projekte/powerfuel. [Accessed 17.08.2022].

[7] Scheuermann A. Lufthansa, Atmosfair und EWE starten erste Anlage für klimaneutrales Kerosin 2021 [Available from: https://www.chemietechnik.de/anlagenbau/lufthansa-atmosfair-und-ewe-starten-erste-anlage-fuer-klimaneutrales-kerosin-683.html. [Accessed 17.08.2022].

[8] Collins L. Green hydrogen + captured CO2 | 'Unique and powerful' joint venture aims to produce 80,000 tonnes of aviation e-fuel annually2021 17.08.2022. Available from: https://www.rechargenews.com/energy-transition/green-hydrogen-captured-co2-unique-and-powerful-joint-venture-aims-to-produce-80-000-tonnes-of-aviation-e-fuel-annually/2-1-1266267.

[9] Wintgens. Green Fuels Hamburg industrial production of sustainable aviation fuels for climate-neutral aviation2022 17.08.2022. Available from: https://www.uniper.energy/news/green-fuels-hamburg-industrial-production-of-sustainable-aviation-fuels-for-climate-neutral-aviation.

[10] KEROSyN100 - Die Defossilisierung der Luftfahrt [Available from: https://www.kerosyn100.de/. [Accessed 17.08.2022].

[11] Wassermann T, Schnuelle C, Kenkel P, Zondervan E. Power-to-Methanol at Refineries as a Precursor to Green Jet Fuel Production: a Simulation and Assessment Study. Comput Aided Chem Eng 2020;48:1453–8. https://doi.org/10.1016/B978-0-12-823377-1.50243-3.

[12] Maier S, Tuomi S, Kihlman J, Kurkela E, Dietrich R-U. Techno-economically-driven identification of ideal plant configurations for a new biomass-to-liquid process – A case study for Central-Europe. Energ Conver Manage 2021;247:114651. https://doi.org/10.1016/j.enconman.2021.114651.

[13] Nojoumi H, Dincer I, Naterer GF. Greenhouse gas emissions assessment of hydrogen and kerosene-fueled aircraft propulsion. Int J Hydrogen Energy 2009;34(3):1363–9. https://doi.org/10.1016/j.ijhydene.2008.11.017.

[14] Svensson F, Hasselrot A, Moldanova J. Reduced environmental impact by lowered cruise altitude for liquid hydrogen-fuelled aircraft. Aerosp Sci Technol 2004;8(4):307–20. https://doi.org/10.1016/j.ast.2004.02.004.

[15] Winter CJ. Hydrogen in high-speed air transportation. Int J Hydrogen Energy 1990;15(8):579–95. https://doi.org/10.1016/0360-3199(80)90006-3.

[16] CORDIS. Liquid hydrogen fuelled aircraft - system analysis (CRYOPLANE) 2000 [Available from: https://cordis.europa.eu/project/id/G4RD-CT-2000-00192/de. [Accessed 17.08.2022].

[17] Westenberger, A. (2003). Cryoplane–Hydrogen Aircraft. H2 Expo (11 October Hamburg 2003).

[18] AIRBUS. The ZEROe demonstrator has arrived 2022 17.08.2022. Available from: https://www.airbus.com/en/newsroom/stories/2022-02-the-zeroe-demonstrator-has-arrived.

[19] H2Fly GmbH [Available from: https://www.h2fly.de/. [Accessed 17.08].

[20] Lilium - Building radically better ways of moving [Available from: https://lilium.com/. [Accessed 17.08.2022].

[21] DLR. Konzeptstudie für ökoeffizientes Fliegen 2020 17.08.2022. Available from: https://www.dlr.de/content/de/artikel/news/2020/02/20200504_konzeptstudie-fuer-oekoeffizientes-fliegen.html.

[22] Gibbs J, Nagel B. Design, economic competitiveness, and profitability of a 2025 LNG fueled turboprop for the LNG air transportation system. 54th AIAA Aerospace Sciences Meeting; 2016.

[23] Conroy T, Lim Ee Wei K, Bil C, Dorrington G. Liquefied natural gas aircraft: A life cycle costing perspective. 52nd Aerospace Sciences Meeting. 2014. DOI:10.2514/6.2014-0182.

[24] Rompokos P, Kissoon S, Roumeliotis I, Nalianda D, Nikolaidis T, Rolt A. Liquefied natural gas for civil aviation. Energies 2020;13(22):5925. https://doi.org/10.3390/en13225925.

[25] Yahyaoui M, Anantha-Subramanian A, Lombaërt-Valot I. The Use of LNG as Aviation Fuel: Combustion and Emission. 13th International Energy Conversion Engineering Conference; 2015.

[26] Carson L, Davis G, Versaw E, Cunnington Jr G, Daniels E. Study of methane fuel for subsonic transport aircraft. 1980.

[27] Bradley MK, Droney CK. Subsonic ultra green aircraft research phase II: N+ 4 advanced concept development. 2012.

[28] Savion Aerospace [Available from: https://www.flysavion.com/. [Accessed 16.07.2022].

[29] Hoang AT, Pandey A, Lichtfouse E, Bui VG, Veza I, Nguyen HL, et al. Green hydrogen economy: Prospects and policies in Vietnam. Int J Hydrogen Energy 2023. https://doi.org/10.1016/j.ijhydene.2023.05.306.

[30] Hoelzen J, Flohr M, Silberhorn D, Mangold J, Bensmann A, Hanke-Rauschenbach R. H2-powered aviation at airports – Design and economics of LH2 refueling systems. Energy Convers Manage: X 2022;14:100206. https://doi.org/10.1016/j.ecmx.2022.100206.

[31] Raab M, Körner R, Dietrich R-U. Techno-economic assessment of renewable hydrogen production and the influence of grid participation. Int J Hydrogen Energy 2022;47(63):26798–811. https://doi.org/10.1016/j.ijhydene.2022.06.038.

[32] Raab M, Maier S, Dietrich R-U. Comparative techno-economic assessment of a large-scale hydrogen transport via liquid transport media. Int J Hydrogen Energy 2021;46(21):11956–68. https://doi.org/10.1016/j.ijhydene.2020.12.213.

[33] Albrecht FG, König DH, Baucks N, Dietrich R-U. A standardized methodology for the techno-economic evaluation of alternative fuels – A case study. Fuel 2017;194:511–26. https://doi.org/10.1016/j.fuel.2016.12.003.

[34] Yoshino Y, Harada E, Inoue K, Yoshimura K, Yamashita S, Hakamada K. Feasibility Study of "CO2 Free Hydrogen Chain" Utilizing Australian Brown Coal Linked with CCS. Energy Procedia 2012;29:701–9.

[35] Sea-Distances. 2020 [Available from: https://sea-distances.org/. [Accessed 23.02.2020].

[36] IRENA. Renewable Power Generation Costs in 2020 2021. Available from: https://www.irena.org/publications/2021/Jun/Renewable-Power-Costs-in-2020.

[37] Atmosfair. Ergebnisse Emissionsberechnung: [Available from: https://www.atmosfair.de/de/kompensieren/flug/. [Accessed 24.01.2023].

[38] IATA. Jet Fuel Price Monitor 2023 [Available from: https://www.iata.org/en/publications/economics/fuel-monitor/. [Accessed 26.01.2023].

[39] Vartiainen E, Breyer C, Moser D, Román Medina E, Busto C, Masson G, et al. True Cost of Solar Hydrogen. Solar RRL 2022;6(5):2100487. https://doi.org/10.1002/solr.202100487.

[40] Schnuelle C, Wassermann T, Fuhrlaender D, Zondervan E. Dynamic hydrogen production from PV & wind direct electricity supply – Modeling and techno-economic assessment. Int J Hydrogen Energy 2020;45(55):29938–52. https://doi.org/10.1016/j.ijhydene.2020.08.044.

[41] Huang C, Zong Y, You S, Træholt C. Economic model predictive control for multi-energy system considering hydrogen-thermal-electric dynamics and waste heat recovery of MW-level alkaline electrolyzer. Energ Conver Manage 2022;265:115697. https://doi.org/10.1016/j.enconman.2022.115697.

[42] Fasihi M, Efimova O, Breyer C. Techno-economic assessment of CO2 direct air capture plants. J Clean Prod 2019;224:957–80. https://doi.org/10.1016/j.jclepro.2019.03.086.

[43] Ausfelder F, Tran DD. 4. Roadmap des Kopernikus-Projektes "P2X": Phase II 2022. [Available from https://www.kopernikus-projekte.de/projekte/p2x].

[44] Kothandaraman A. Carbon Dioxide Capture by Chemical Absorption: A Solvent Comparison Study. MIT; 2010.

[45] Deuerling CF. Untersuchungen zum Einfluss von Rauchgas-Aerosolen in Müll-und Biomasse-Verbrennungsanlagen auf die Hochtemperatur-Korrosion der Überhitzer. Logos Verlag Berlin GmbH; 2009.

[46] Goff GS, Rochelle GT. Monoethanolamine Degradation: O2 Mass Transfer Effects under CO2 Capture Conditions. Ind Eng Chem Res 2004;43(20):6400–8. https://doi.org/10.1021/ie0400245.

[47] Woods DR. Rules of thumb in engineering practice: John Wiley & Sons; 2007.

[48] Timmerhaus KD, Peters MS, West RE. Plant Design and Economics for Chemical Engineers - Fifth edition; 2002.

[49] Jokora. Monoethanolamin 99% (2-Aminoethanol) (Kombinations-IBC a. 1000 kg) 2022 [Available from: https://www.jokora.de/organik/monoethanolamin/monoethanolamin-99-2-aminoethanol-kombinations-ibc-a.-1000-kg. [Accessed 17.11.2022].

[50] Rüde T, Dürr S, Preuster P, Wolf M, Wasserscheid P. Benzyltoluene/perhydro benzyltoluene – pushing the performance limits of pure hydrocarbon liquid organic hydrogen carrier (LOHC) systems. Sustainable Energy Fuels 2022;6(6):1541–53. https://doi.org/10.1039/D1SE01767E.

[51] Sabatier P, Senderens J. Direct hydrogenation of oxides of carbon in presence of various finely divided metals. 1902; 134(1): 689–91.

[52] Rönsch S, Schneider J, Matthischke S, Schlüter M, Götz M, Lefebvre J, et al. Review on methanation – From fundamentals to current projects. Fuel 2016;166:276–96.

[53] Rönsch S, Köchermann J, Schneider J, Matthischke S. Global Reaction Kinetics of CO and CO2 Methanation for Dynamic Process Modeling. Chem Eng Technol 2016;39(2):208–18. https://doi.org/10.1002/ceat.201500327.

[54] Koschany F, Schlereth D, Hinrichsen O. On the kinetics of the methanation of carbon dioxide on coprecipitated NiAl(O)x. Appl Catal B 2016;181:504–16. https://doi.org/10.1016/j.apcatb.2015.07.026.

[55] Omar MNB. Thermodynamic and Economic Evaluation of Existing and Perspective Processes for Liquefaction of Natural Gas in Malaysia: Technische Universitaet Berlin (Germany); 2016. [Available from https://doi.org/10.14279/depositonce-5565].

[56] Kang. 2021 World LNG Report. IGU; 2021.
[57] Adelung S, Maier S, Dietrich R-U. Impact of the reverse water-gas shift operating conditions on the Power-to-Liquid process efficiency. Sustainable Energy Technol Assess 2021;43:100897. https://doi.org/10.1016/j.seta.2020.100897.
[58] Hartmann M. Erzeugung von Wasserstoff mittels katalytischer Partialoxidation höherer Kohlenwasserstoffe an Rhodium: KIT Scientific Publishing; 2009. [Available from https://www.itcp.kit.edu/deutschmann/img/content/09_MarcoHartmann_Dr_rernat_UKA.pdf].
[59] Greg Hemighaus TB, John Bacha, Fred Barnes MF, Lew Gibbs, Nancy Hogue, Jacqueline Jones, David Lesnini, John Lind and Jack Morris. Aviation Fuels Technical Review. Chevron: Chevron Products Company; 2007. https://www.chevron.com/-/media/chevron/operations/documents/aviation-tech-review.pdf.
[60] Akbarzadeh O, Alshahateet SF, Mohd Zabidi NA, Moosavi S, Kordijazi A, Babadi AA, et al. Effect of Temperature, Syngas Space Velocity and Catalyst Stability of Co-Mn/CNT Bimetallic Catalyst on Fischer Tropsch Synthesis Performance. Catalysts 2021;11(7):846. https://www.mdpi.com/2073-4344/11/7/846.
[61] Rahmati M, Huang B, Mortensen MK, Keyvanloo K, Fletcher TH, Woodfield BF, et al. Effect of different alumina supports on performance of cobalt Fischer-Tropsch catalysts. J Catal 2018;359:92–100. https://doi.org/10.1016/j.jcat.2017.12.022.
[62] Gorimbo J, Muleja A, Liu X, Hildebrandt D. Fischer-Tropsch synthesis: product distribution, operating conditions, iron catalyst deactivation and catalyst speciation. Int J Ind Chem 2018;9(4):317–33. https://doi.org/10.1007/s40090-018-0161-4.
[63] Silva DO, Scholten JD, Gelesky MA, Teixeira SR, Dos Santos ACB, Souza-Aguiar EF, et al. Catalytic Gas-to-Liquid Processing Using Cobalt Nanoparticles Dispersed in Imidazolium Ionic Liquids. ChemSusChem 2008;1(4):291–4. https://doi.org/10.1002/cssc.200800022.
[64] Muleja AA, Yao Y, Glasser D, Hildebrandt D. A study of Fischer-Tropsch synthesis: Product distribution of the light hydrocarbons. Appl Catal A 2016:217–26. https://doi.org/10.1016/j.apcata.2016.03.015.
[65] Rytter E, Holmen A. Perspectives on the Effect of Water in Cobalt Fischer-Tropsch Synthesis. ACS Catal 2017;7(8):5321–8. https://doi.org/10.1021/acscatal.7b01525.
[66] Liu Y, Murata K, Okabe K, Inaba M, Takahara I, Hanaoka T, et al. Selective Hydrocracking of Fischer-Tropsch Waxes to High-quality Diesel Fuel Over Pt-promoted Polyoxocation-pillared Montmorillonites. Top Catal 2009;52(6):597–608. https://doi.org/10.1007/s11244-009-9239-8.
[67] Finger S, Abu Khass O. The DLR High Temperature Heat Pump Pilot Plants 2021. [Available from https://elib.dlr.de/145429/1/DLR_EHPS.pdf].
[68] Smith R. Comparatice research on LNG receiving terminals and FSRU. The University of Western Australia; 2017. https://www.jtsi.wa.gov.au/docs/default-source/LNG-2017-Graduation-Presentations/comparative-research-on-lng-receiving-terminals-and-fsru.pdf.
[69] Tremel A, Wasserscheid P, Baldauf M, Hammer T. Techno-economic analysis for the synthesis of liquid and gaseous fuels based on hydrogen production via electrolysis. Int J Hydrogen Energy 2015;40(35):11457–64. https://doi.org/10.1016/j.ijhydene.2015.01.097.
[70] Zhang C, Gao R, Jun K-W, Kim SK, Hwang S-M, Park H-G, et al. Direct conversion of carbon dioxide to liquid fuels and synthetic natural gas using renewable power: Techno-economic analysis. J CO2 Util 2019;34:293–302. https://doi.org/10.1016/j.jcou.2019.07.005.
[71] Adelung S. Global sensitivity and uncertainty analysis of a Fischer-Tropsch based Power-to-Liquid process. J CO2 Util 2022;65:102171. https://doi.org/10.1016/j.jcou.2022.102171.
[72] Brynolf S, Taljegard M, Grahn M, Hansson J. Electrofuels for the transport sector: A review of production costs. Renew Sustain Energy Rev 2018;81:1887–905. https://doi.org/10.1016/j.rser.2017.05.288.
[73] Decker M, Schorn F, Samsun RC, Peters R, Stolten D. Off-grid power-to-fuel systems for a market launch scenario – A techno-economic assessment. Appl Energy 2019;250:1099–109. https://doi.org/10.1016/j.apenergy.2019.05.085.
[74] Park S, Choi K, Lee C, Kim S, Yoo Y, Chang D. Techno-economic analysis of adiabatic four-stage CO2 methanation process for optimization and evaluation of power-to-gas technology. Int J Hydrogen Energy 2021;46(41):21303–17. https://doi.org/10.1016/j.ijhydene.2021.04.015.
[75] Peters R, Baltruweit M, Grube T, Samsun RC, Stolten D. A techno economic analysis of the power to gas route. J CO2 Util 2019;34:616–34. https://doi.org/10.1016/j.jcou.2019.07.009.
[76] Zang G, Sun P, Elgowainy AA, Bafana A, Wang M. Performance and cost analysis of liquid fuel production from H2 and CO2 based on the Fischer-Tropsch process. J CO2 Util 2021;46:101459. https://doi.org/10.1016/j.jcou.2021.101459.
[77] FCH JU Europe. Hydrogen Powered Aviation: A Fact-based Study of Hydrogen Technology, Economics, and Climate Impact by 2050. 2020.doi:10.2843/471510.
[78] Hoelzen J, Silberhorn D, Zill T, Bensmann B, Hanke-Rauschenbach R. Hydrogen-powered aviation and its reliance on green hydrogen infrastructure – Review and research gaps. Int J Hydrogen Energy 2022;47(5):3108–30. https://doi.org/10.1016/j.ijhydene.2021.10.239.
[79] Peter Christensen LRD, Jennifer Bates. COST ESTIMATE CLASSIFICATION SYSTEM – AS APPLIED IN ENGINEERING, PROCUREMENT, AND CONSTRUCTION FOR THE PROCESS INDUSTRIES2005. [Available from: https://www.costengineering.eu/Downloads/articles/AACE_CLASSIFICATION_SYSTEM.pdf].
[80] Fyke A, Li D, Crane P, Scott DS. Recovery of thermomechanical exergy from cryofuels. Int J Hydrogen Energy 1997;22(4):435–40. https://doi.org/10.1016/S0360-3199(96)00104-8.

3.3 Publication III

Domestic fuel distribution and utilization

Moritz Raab, Wolfgang Grimme, Jon Gibbs, Paula Philippi and Ralph-Uwe Dietrich (2024): Aviation fuels of the future – A techno-economic assessment of distribution, fueling and utilizing electricity-based LH_2, LCH_4 and kerosene (SAF)

https://doi.org/10.1016/j.ecmx.2024.100611

Energy Conversion and Management: X 23 (2024) 100611

Contents lists available at ScienceDirect

Energy Conversion and Management: X

journal homepage: www.sciencedirect.com/journal/energy-conversion-and-management-x

Aviation fuels of the future – A techno-economic assessment of distribution, fueling and utilizing electricity-based LH2, LCH4 and kerosene (SAF)

Moritz Raab [a,*], Ralph-Uwe Dietrich [a], Paula Philippi [a], Jonathan Gibbs [c], Wolfgang Grimme [b]

[a] German Aerospace Center (DLR), Pfaffenwaldring 38-40, 70569 Stuttgart, Germany
[b] German Aerospace Center (DLR), Institute of Air Transport, Department of Air Transport Economics, Linder Hoehe, 51147 Cologne, Germany
[c] Savion Aerospace Pty Ltd, L 5 111 Cecil St, South Melbourne, Australia

A B S T R A C T

This paper investigates the techno-economic implications on air travel when fossil-based kerosene is phased out of the market, specifically focusing on the comparison between liquid hydrogen, liquid methane and renewable kerosene for ten exemplary flight routes to estimate the cost of air travel per passenger and 100 km distance travelled $\left(\frac{€_{2020}}{PAX100km}\right)$ for every fuel type. By considering the entire supply chain, including hydrogen production from renewable sources, synthesis, oversea transport, domestic distribution, and utilization, this study addresses the overarching question of whether it is more economical to change the fuel source or the fuel itself to reduce fossil kerosene usage in the aviation industry. It is demonstrated that aircraft acquisition costs play a minor role compared to fuel supply costs and specific fuel demand. The study shows that for electricity-based fuels, liquid hydrogen is the most economic option, even with a potential energy penalty, followed by liquid methane and renewable kerosene. The results for an aircraft with a capacity 180 passengers are 3.08, 4.57 and 5.11 $\frac{€}{PAX100km}$ for liquid hydrogen, liquid methane and renewable kerosene, respectively. Challenges regarding storage and isolation requirements for cryogenic fuels in aviation are discussed, with assumptions made that these obstacles can be overcome to realize economic benefits. Additionally, the study suggests potential shifts in aircraft size selection by airlines to mitigate rising fuel prices in the future. The study advocates for the aviation industry's openness to new fuels like liquid hydrogen and liquid methane to alleviate the cost increase associated with phasing out fossil kerosene.

Introduction

Different groups from the aviation industry, like the "International Civil Aviation Organization" (ICAO) or the "Air Transport Action Group" (ATAG), announced their CO_2 emission reduction targets in the past [1,2]. Exemplary goals are the "50 % emissions reduction", referring to 2005 levels or the net-zero target as the ultimate target. To depict the implications of these targets, the CO_2 emissions of the aviation industry from the last 20 years as well as predicted emissions according to the corresponding target/actions are shown in Fig. 1 [2]. The main contribution to reduce CO_2 emissions is expected to come from the reduced consumption of fossil fuels, which leads to the question: What are the alternatives?

Fuel alternatives for the aviation industry

Currently the commercial aviation industry relies primarily on kerosene (ignoring the differences between Jet A and Jet A-1), a mixture of hydrocarbons with a carbon number between 8 and 16 [3]. It is mainly derived from crude oil via distillation and to a lesser extent from biomass–based processes as specified by ASTM–5766. The substitution of fossil kerosene with renewable kerosene (SAF for sustainable aviation fuel) is an approach to decarbonize the aviation industry where only the fuel source is changed, leaving all other aspects more or less untouched. Numerous studies have evaluated the synthesis of SAF via biomass-based processes, electricity-based processes or a combination of both [4–6]. A holistic evaluation has been conducted by Su–ungkavatin et al. [7]. In their study they also evaluate current regulatory frameworks like the EU initiative "ReFuelEU Aviation" [8]. This regulation requires a minimum SAF share of 2 % for the flights departing in the EU from 2025 onwards. The share will increase to 6 % in 2030 and to eventually to 70 % in 2050. Currently, the SAF share for an individual flight is limited to 50 % [9], although higher values are aspired and even required to reach the 70 % goal by 2050. A share of 100 % SAF has already been demonstrated [10].

The introduction of liquid hydrogen (LH_2) as an aviation fuel is a more drastic approach to decarbonize the aviation industry. It will affect

* Corresponding author.
E-mail address: Moritz.Raab@dlr.de (M. Raab).

https://doi.org/10.1016/j.ecmx.2024.100611
Received 9 February 2024; Received in revised form 28 April 2024; Accepted 29 April 2024
Available online 7 May 2024

Nomenclature

Abbreviations

BWB	Blended-wing body
CAPEX	Capital expenditures
EU	European Union
FC	Flight cycles
FH	Flight hours
FMS	Flight movement scenario
FT	Fischer Tropsch
FUS	Fuel utilization scenario
IATA	International Air Transport Association
ICCT	International Council on Clean Transportation
iLUC	Indirect land use change
IGU	International Gas Union
IMO	International Maritime Organization
IPCC	Intergovernmental Panel on Climate Change
LCH_4	Liquid methane
LF	Load factor
LH_2	Liquid hydrogen
LHV	Lower heating value
LNG	Liquefied natural gas
LOV	Limit of validity
MFR	Manufacturing
OPEX	Operating expenditures
PAX	Passenger
PtX	Power to X
RE	Renewable energy
R&D	Research and development
SAF	Sustainable aviation fuel (considers renewable fuel with Jet A-1 specifications)
SI	Supplementary information
TBW	Truss-braced wing
TFU	Theoretical first unit
tpa	tons per annum

Subscripts (together with an exemplary unit)

MWh_{LHV}	Used to indicate which heating value is used
$€_{xy}$/ $\$_{xy}$	"xy" is referring to the purchase power of the currency in the given year
FC_{Calc}	"Calculated", refers to the value that is ultimately used
$CAPEX_{Flight}$	Refers to the expenditures per flight

Latin symbols

d	Distance of the pipeline network in km
$\dot{M}$	Mass flow in t/h

Airport IATA codes

MUC	Munich
FRA	Frankfurt
CDG	Paris
MAD	Madrid
IST	Istanbul
KEF	Keflavík (close to Reykjavík)
CAI	Cairo
IKA	Teheran
DOH	Doha
JFK	New York
BKK	Bangkok

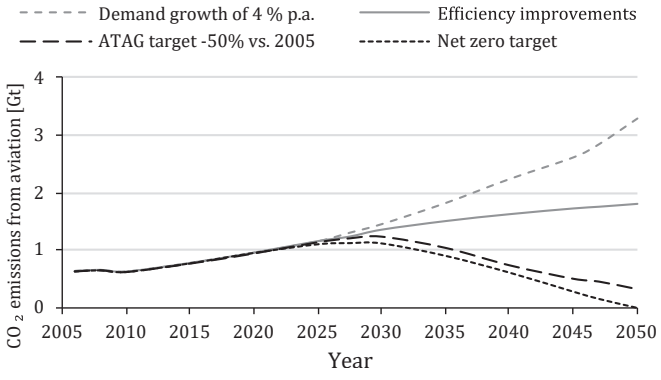

Fig. 1. Projected net CO_2 emissions from the aviation industry (neglecting the COVID 19 effects) (2).

every stakeholder group in the commercial aviation industry and in the current chain ranging from the fuel source to its utilization. Aircraft manufactures will have to design different aircraft, that might even be powered with fuel cells instead of turbines. Airports will have to invest in new fuel tanks and distribution infrastructure and the fuel supply to the airports has to change as well. First studies that evaluated the implications of introducing LH_2 as aviation fuel date back to the 1970 s [11]. A study published by Korycinski in 1978 evaluated the LH_2 demand at the airports of Chicago and San Francisco for a reference year between 1990 and 1995 [12]. Their study considered the daily LH_2 demand, required changes in airport infrastructure and a brief description of two conceptual 400 passenger (PAX) aircraft using LH_2. More recently, Hoelzen et al. evaluated the fuel supply system for different airports in Germany and concluded that depending on the demand a supply via a pipeline system or a truck system is the more economical option [13]. A detailed analysis of the turnaround and refuelling procedure at the airport is performed by Mangold et al. [14]. They outline the safety aspects and the need for tight connections between the aircraft and the refuelling systems. More detailed studies on aircraft design have been carried out by Airbus in the early 2000 s in the "Cryoplane" project and with the ZEROe program launched in 2020 [15–17]. Several smaller companies are working on the development of aircraft utilizing LH_2, such as "ZeroAvia", "H2Fly" and "Deutsche Aircraft". As LH_2 will need to be available at all the airports where these aircraft will operate, an overarching strategy is needed to avoid a chicken-and-egg problem.

The introduction of liquefied natural gas (LNG) as an aviation fuel was also explored by NASA in the 1970 s and recently proposed in a "Think paper" by EUROCONTROL [18,19]. A more recent program by NASA and Boeing evaluated different LNG–fuelled aircraft concepts that could enter the market in the 2040 s [20]. LCH_4, as the main component of LNG, has the advantage that LNG is already a globally available commodity. In addition, the synthesis of methane from biomass and electricity is less complex than the synthesis of SAF. Like hydrogen, it also has to be liquefied and would be a cryogenic fuel, requiring tremendous changes to the airport infrastructure. It is therefore not surprising that there has been no change in the fuel diversity, given the huge investments required. Simply because there has been no demand for change in the commercial aviation industry so far. This may change in the future if the economic or other incentives are high enough.

1.2. Research objective.

The three fuels considered in this study are LH_2, LCH_4 and SAF. Only the production pathway via the electricity based "Power-to-X" pathway is considered. While fuels based on biogenic components are a suitable option, their production capacity is limited. The "International Council on Clean Transportation" (ICCT) published a working-paper in 2021 assessing the production potential of SAF based on waste fats, used

cooking oils, cover crops, agricultural and forestry residues [21]. They concluded, that in the year 2030 only 5.5 % of EU–wide SAF demand could be produced from these feedstocks within the EU. The "Intergovernmental Panel on Climate Change" (IPCC) is more conservative and in its latest report provides a value of only 2 % [22]. Furthermore, biofuel feedstocks with "high indirect land use change (high iLUC)" biofuel feedstocks are expected to be phased out by 2030 [23]. This will affect the availability of palm oil as a feedstock, as it has been considered by Pipitone et al. [24].

The aim of this study is to provide a techno-economic analysis of how the cost of air travel will be affected by a full transition to electricity-based fuels and how the costs will differ whether LH_2, LCH_4 or SAF are used for specific flight routes. While the abbreviation SAF stands for "sustainable aviation fuel" which can be produced in many ways, in this study, it is used for a substance with the same properties as kerosene that is produced via the Fischer-Tropsch synthesis and CO_2 that has been retrieved from ambient air. For the analysis, it is required to consider the whole chain from the renewable electricity supply up to fuel utilization. This is necessary in order to conduct a subsequent comparison based on the same input variables. The chain is illustrated in Fig. 2. Morocco is considered as exemplary fuel-exporting country with Germany as importing country. In a previous study, the first part of the chain, i.e. the methodological approach regarding electricity generation and hydrogen production based on local weather conditions was presented [25] (indicated as "RE generation and H_2 production" in Fig. 2). Another study evaluated, the steps considering the fuel synthesis and overseas transport to Germany [26]. In this study, the focus is on the remaining steps to evaluate the final cost for air travel which are expressed in costs per passenger (PAX) and per 100 km of flight distance i.e., $\frac{€}{PAX100km}$. This is achieved by including the fuel utilization into the evaluation, otherwise the comparison can only be conducted based on costs per energy supplied for every fuel type i.e., $\frac{€}{MWH_{LHV}}$. To date, no study has conducted this direct comparison of electricity-based LH_2, LCH_4 or SAF. In particular, LCH_4 has either not been considered, as by the IPCC [22] or has been excluded from the list of potential aviation fuels, as by Dray et al. [27]. Although the utilization of LH_2 and LCH_4 has been demonstrated in the past, both fuels are far from being ready to use in the aviation industry. Therefore, a fair and transparent assessment could help the stakeholders involved to implement and to support the most preferential route to phase out fossil fuels from the aviation industry. This is done in this study from a techno-economic perspective, the actual reduction of CO_2 emissions cannot be quantified with this study as since no life cycle assessment is conducted.

Methodology

In this study, a comparative techno-economic assessment is conducted for the aviation fuels LH_2, LCH_4 and SAF, evaluating the steps of domestic distribution, fuel storage at the airport, fuelling and fuel utilization. In Germany, fuel is transported from Wilhelmshaven to the airports of Frankfurt and Munich. The costs are 157 €/MWh for LH_2, 220 €/MWh for LCH_4 and 279 €/MWh for SAF at the interface "importing harbour – domestic distribution" [26]. Different methodologies are applied to consider the respective steps and are described in this chapter. The most relevant input data is provided in chapter 3, remaining input is given in the section S.1 of the supplementary information (SI). The aim is to determine the technical and economic aspects under the assumption that the airports are supplied exclusively via the fuel supply chain depicted in Fig. 2. Perspective data is considered for the unit operations and costs are given in $€_{2020}$, as in Raab and Dietrich [26]. Aspects that are independent of the fuel type such as taxes, fees etc., are neglected. The evaluation is divided into two parts.

1. Determination of minimum fuel supply costs

Several scenarios are considered to evaluate how the annual fuel demand influences the costs for domestic distribution, fuel storage at the airport and fuelling. They are listed in Table 1. Based on these scenarios, the required changes at the airport infrastructure are estimated. Up to this point of the fuel chain a comparison of the different fuels is feasible in $\frac{€}{MW_{LHV}}$, as indicated in Fig. 2. The results of this first part are presented in section 4.1.

2. Estimating the specific costs for flying

The costs for air travel are determined in $\frac{€}{PAX\ 100\ km}$ by including the depreciation costs for different future aircraft types and the fuel demand for 10 exemplary flight routes. The flight routes are listed in Table 3. The results of this second part are presented in section 4.2. A detailed breakdown for an exemplary route and aircraft size is given in the SI. In

Table 1
Evaluated fuel utilization scenarios (FUS) to determine the minimum fuel supply costs.

Aircraft type PAX capacity	#1	#2	#3	#4	#5	#6
Commuter & Regional 0–100	SAF	LH_2	LH_2	LH_2	LH_2	LCH_4
Small 101–210	SAF	LH_2	LCH_4	LH_2	LH_2	LCH_4
Medium 211—300	SAF	SAF	LCH_4	LCH_4	LH_2	LCH_4
Large > 300	SAF	SAF	SAF	LCH_4	LH_2	LCH_4

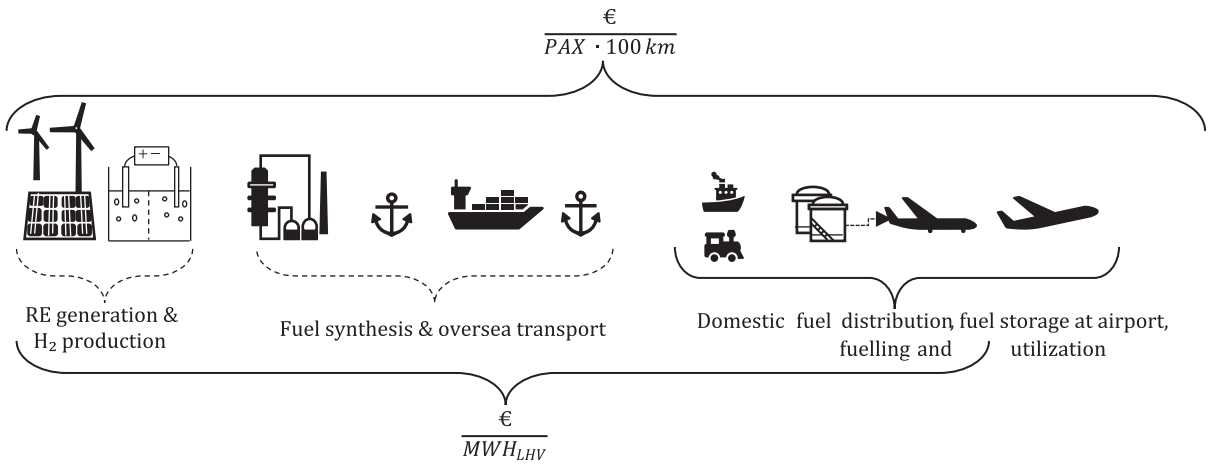

Fig. 2. Overall system boundaries of the renewable aviation fuel chain considered. Focus of this study is from domestic fuel distribution until utilization.

addition, the effect of the SAF supply costs on current ticket prices is estimated using real data from the 10 exemplary flight routes. These results are provided in section 4.3.

Determination of fuel supply costs

The fuel supply costs are evaluated by the methodology shown in Fig. 3. It is based on a flight movement scenario (FMS) for the year 2050 for two exemplary airports, Munich (MUC) and Frankfurt (FRA).

The development of the FMS is not part of this study but a relevant input dataset. Therefore, details of the FMS development are described in section 2.1.1. The FMS is a dataset containing all the flight movements from a given year. It includes the number of departures, the destination airport for each flight as well as the aircraft seat capacity and only considers kerosene as aviation fuel. This dataset is used to evaluate individual fuel utilization scenarios (FUS). There, each flight is assigned a specific fuel (LH_2, LCH_4 or SAF). For each evaluated FUS, the aspects of "Domestic fuel distribution, fuel storage at airport and fuelling" are re-evaluated. Inland waterway transport is considered for Frankfurt and railway transport for Munich. Specific input data is taken from literature and described in section 3.1. The investments required for domestic transport is depreciated over 20 years using an interest rate (WACC) of 5 %. The operating costs consider the required labour, energy costs and indirect costs for insurance, overhead factors etc. It is assumed, that the fuel for the flights is imported exclusively via the supply chain depicted in Fig. 2. The results include the total annual fuel demand, the required airport infrastructure for storage and fuelling and, if economically viable, reliquefication facilities at the airport.

Flight movement scenario

Flight movement scenarios are modelled using a multi-stage approach.

1. The first step is an econometric forecasting model of future air transport demand, focusing on passengers and flight movements. This approach uses various external forecasts on the development of the economy e.g., per capita income, population and fuel prices. Historical relationships between air transport development and the above external factors can be described by demand elasticities (e.g., price and income elasticities), which are estimated on a long time series over two decades to calibrate the air transport demand model. The methodological approach is described in detail by Gelhausen et al. [28]. Passenger demand estimates are combined with a seat load factor forecast in order to account for improvements in the efficiency of the air transport system and to forecast the number of seats offered. The output of this first stage of the forecasting model is the number of seats and the number of flight movements on each airport pair globally, in five–year increments up to 2050.
2. In a second modelling step, specific aircraft types are assigned to each airport pair. The starting point for this model is the base year aircraft fleet (as provided by the commercial database Cirium Fleets Analyzer [29]) and its allocation to airport pairs (as provided by the global flight schedules database OAG [30]). For each five-year period, aircraft retirements are calculated using ICAO's retirement model, based on a logistic regression for each aircraft category (turboprops and regional, narrowbody and widebody jets), as shown by Schaefer [31]. New aircraft to replace retired aircraft and to accommodate growth are drawn from a pool of aircraft representing the state-of-the-art in each forecast period. This approach allows for an accurate modelling of the market diffusion of more fuel-efficient aircraft and the fleet rollover over time. It also allows the modelling of different technological scenarios, such as the system-wide effects of the introduction of aircraft with varying propulsion technologies.
3. In a third step, the energy consumption is calculated for each combination of aircraft type and airport pair. This step uses the commercial flight performance software Piano-X, which models the fuel consumption of more than 100 civil aircraft types based on various sources like flight data recorders. For future aircraft types, assumptions have been made about efficiency improvements, based on technology roadmaps and studies such as Flightpath 2050 [32].

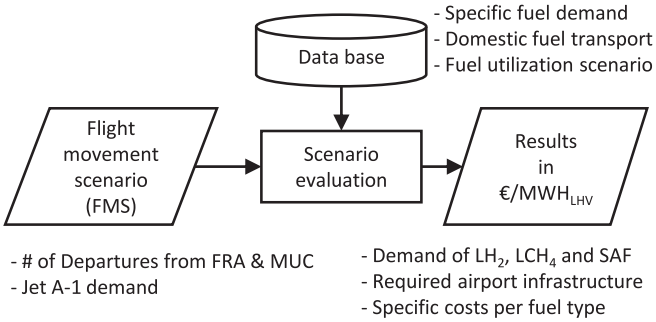

Fig. 3. Applied methodology to determine the fuel supply costs.

The output of the model is a dataset that includes the energy demand for each airport, the number of passengers departing from an airport, the number of flights etc. An exemplary visualization of the dataset is shown in Fig. 4 for Frankfurt for the year 2050.

Fuel demand evaluation

The FMS determines the fuel demand and therefore the chemical energy demand for a given year for a 100 % SAF scenario. In order to assess how the fuel demand changes with the introduction of LH_2 or LCH_4, two aspects are considered:

- The share of LH_2, LCH_4 and SAF for a given aircraft size and distance flown
- The different specific energy demand when cryogenic fuels are used instead of SAF

It is not possible to predict which aircraft types will be developed by the year 2050 and how these aircraft will be propelled. Therefore, for the first aspect different FUS have to be evaluated, assuming the appropriate fuel type for a given aircraft size and flight distance. The resolution of these scenarios is similar to the input shown in Fig. 4, except that the commuter and regional sized aircraft are summarized in one category. Therefore, for 11 different flight distance groups and 4 different aircraft categories the share of LH_2, LCH_4 and SAF has to be assumed for each FUS. Dual-fuel capable aircraft as proposed by Withers et al. [33] are not included in this study. Furthermore, as airlines are likely to prefer the flexibility in how an aircraft can be used, the fuel type will not change within a given category. Therefore, six scenarios are considered where the fuel type depends only on the aircraft type. The FUS evaluated are shown in Table 1.

Scenario #1 is the "no change" scenario used as a baseline. Scenario #2 introduces LH_2 for smaller aircraft. Given current research developments, this scenario could eventuate in the near future. Scenario #3 introduces LCH_4 as a second cryogenic aviation fuel. This scenario could eventuate if the energy storage density of LH_2 proves to be too great a hurdle. Scenario #4 is an all-cryogenic scenario, where SAF has been completely ousted from the market and smaller aircraft use LH_2 and larger ones LCH_4. Scenarios #5 and #6 are academic scenarios to show the effects of an all hydrogen and all methane aviation industry, respectively.

The second aspect is the change in specific energy demand when cryogenic fuels are used. For aircraft using LH_2, a distinction can be made between hydrogen used in fuel cells or turbines. For LCH_4, only combustion processes are considered. In literature, the change in specific energy demand is only available for a certain number of aircraft

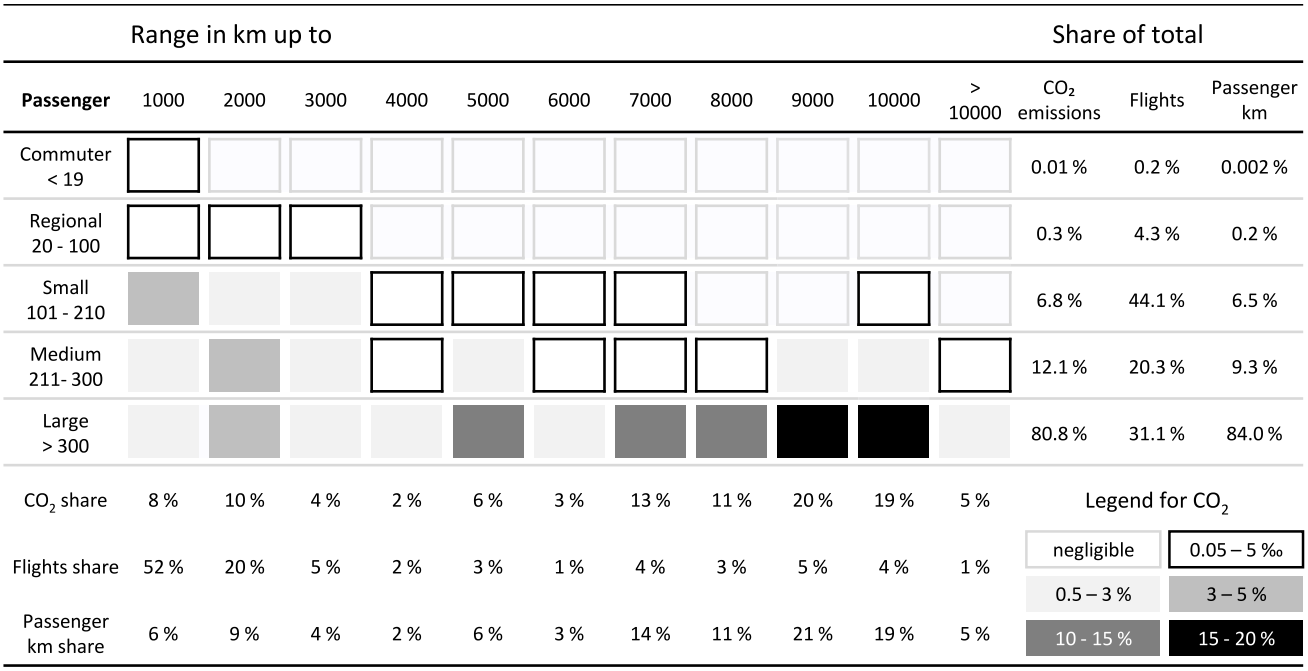

Fig. 4. Visualisation of the flight movement scenario of FRA, forecast year 2050.

types. The range and propulsion type are also given. Table 2 lists an excerpt of the currently available data.

Unfortunately, this data is not sufficient to give a value for every combination of aircraft type, flight range and fuel considered in this study. Furthermore, there is a great difference between the values given for large LH_2 powered aircraft. This study considers the value of +9 %, the implications of +42 % are given in detail in section S.3 of the SI. In addition, assumptions and simplifications have to be made where data is not available. The values used in this study are listed in Table 12.

Determining the specific costs of flying

By applying the methodology described in section 2.1, the fuel demand and supply costs are estimated in €/MWh_{LHV}, i.e. from a "well-to-tank" perspective. The following aspects are considered to determine the costs resulting from utilization and thus, to evaluate the whole chain depicted in Fig. 2 and obtain the costs in $\frac{€}{PAX\ 100\ km}$:

- Flight distance → total fuel consumption for a given flight ($OPEX_{Flight}$)
- Number of passengers on board for a given flight
- Share of depreciation costs per flight ($CAPEX_{Flight}$)

Table 2
Literature data how the specific energy demand changes compared to SAF/Jet A-1 aircraft when cryogenic fuels are utilized.

Fuel	Capacity (PAX)	Range (km)	Propulsion	Change in specific energy demand	Source
LH_2	80	1,000	Fuel cell	− 8 %	[2]
LH_2	165	2,000	Fuel cell/ turbines	− 4 %	[2]
LH_2	250	7,000	Turbines	+ 22 %	[2]
LH_2	325	10,000	Turbines	+ 42 %	[2]
LH_2	401	11,800	Turbines	+ 9 %	[34]
LCH_4	154	≈ 6,500	Turbine	+ 5.6 %	[35]
LCH_4	≈ 189*	3,700	Turbine	+ 10 %	[36]

* Exact number not given – Boeing 737–800 is considered with 189 PAX maximum.

Ten sample routes departing from FRA are selected to determine the different flight costs. The routes are listed in Table 3, with the corresponding IATA airport codes as destinations. The distances are obtained by using an online calculator, which is also used to determine the CO_2 emissions of the corresponding flights [37] (details are given in section 3.4).

$OPEX_{Flight}$ is determined by the fuel supply costs, the change in specific energy demand given in Table 12 and the kerosene demand from the FMS. The seat capacity of each aircraft type is given in section 3.3, for every flight a load factor (LF) of 80 % is considered. Labor costs for the aircraft crew are neglected, since they will not depend on the fuel type.

The share of the depreciation costs per flight is determined by the acquisition cost and the lifetime of the aircraft. The methodology to estimate the acquisition cost is described in section 2.3. The lifetime of an aircraft is determined by the number of flight cycles (FC) or the total flight hours (FH). In aviation this is known as the limit of validity (LOV). An aircraft can be used after its LOV has been exceeded. However, this is generally not economically viable. In general, smaller aircraft that are used on shorter routes have several FC a day and can reach the FC limit first. Large widebody aircraft flying intercontinental routes are more likely to be limited by the FH rather than the FC. For this study, a certain number of FC is assumed for each aircraft and thus, $CAPEX_{Flight}$ is estimated by dividing the costs of the aircraft by the number of assumed flight cycles FC_{calc}. Exemplary values for FC and FH are given in the SI. The values used in this study are given in Table 12.

Estimating future aircraft costs

This study estimates future aircraft acquisition costs for three different aircraft sizes (see Fig. 4). A regional aircraft with a capacity of 100 PAX, a small aircraft with a capacity of 180 PAX and a large aircraft with a capacity of 425 PAX. For each aircraft size, a conventional tube-and wing design is considered. Other forms are evaluated as sensitivities, these are a blended-wing body (BWB) and a truss-braced wing (TBW). The results for these sensitivities are given in the SI in section S.3. The methodology for estimating the costs of future aircraft requires two models, namely the "modified Raymer-Dapca IV model" [38] and the "Markish model" [39]. How these models are used and what input

Table 3
Exemplary flights and their distances from Frankfurt.

ID	1	2	3	4	5	6	7	8	9	10
Destination	MUC	CDG	MAD	IST	KEF	CAI	IKA	DOH	JFK	BKK
Distance [km]	300	447	1,419	1,863	2,399	2,921	3,774	4,632	6,184	8,995

parameters are required is depicted in Fig. 5.

The baseline research and development (R&D) costs and the costs for the theoretical first unit (TFU) are determined using the Raymer-Dapca IV model. The calibration factors for the Raymer-Dapca IV model are determined by matching published R&D costs (see Table S.4) with the default model empty mass, cruise speed, NASA inflation factor and composite percentage of the Airbus A220-300 for the 100 and 180 PAX aircraft and the A350–900 for the 425 PAX aircraft. The model is then calibrated. Baseline costs for the 100, 180 and 425 PAX tube-and-wing aircraft are estimated by using the empty masses and cruise speeds from the Embraer E-190, Boeing 737–800 Max and Boeing 777–9, respectively (see Table S.5). Manufacturer bias in the model is minimized by using aircraft from Airbus to determine the calibration factor and aircraft from Embraer and Boeing for the baseline empty masses and cruise speeds.

The Markish model is used to estimate the changes in R&D and production costs due to modifications of the aircraft form factor (e.g., from a tube and wing design to a BWB) and due to modifications resulting from the utilization of LH_2 or LCH_4. This is achieved by estimating complexity factors for each subsystem and then adjusting the manufacturing margin of the new R&D costs to the baseline R&D costs. In the Markish model, "subsystem complexity factors" are metrics that indicate how much more effort it would cost to develop and produce a subsystem compared to the original system. Simplified changes in the complexity factors are assumed for each subsystem, as they are not considered to be determined at this stage. The values are given in section 3.3 in Table 10 and Table 11.

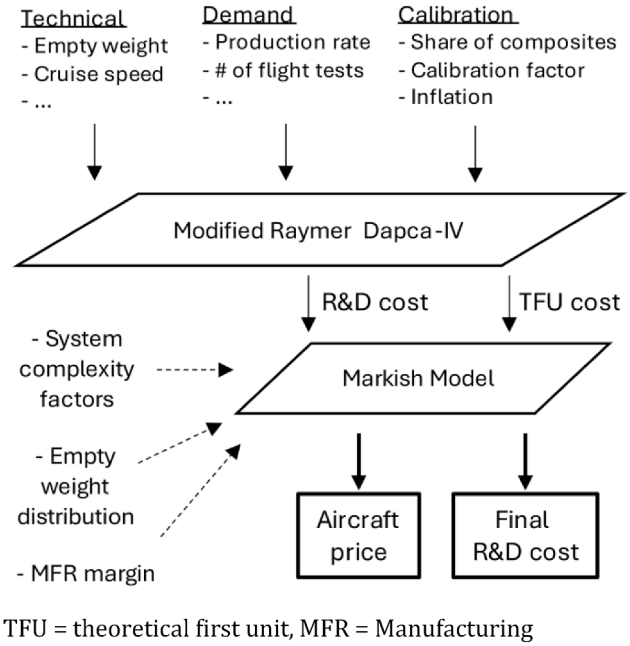

Fig. 5. Methodological approach to determine future aircraft costs TFU = theoretical first unit, MFR = Manufacturing.

Input data

Domestic distribution

Railway transport and inland waterway transport is considered for domestic distribution. The distance from Wilhelmshaven to MUC via railway transport is 840 km. The distance to FRA by waterway is 653 km. All distances are determined using an online tool [40].

Rail transport

The costs of transporting fuel by rail are based on a report by Panteia [41]. In that study, the costs are given on different specific bases e.g., € per km, € per hour or € per tonne-km. For this study "costs per km" is used. The values are listed in Table 4. "Fixed costs" result from leasing the locomotives and wagons. As different wagons are used for different types of fuel, it is not possible to give a single value. Instead, the costs are based on individual wagons which are depreciated over 20 years. The "General operating costs" are a 15 % surcharge on the remaining costs.

Rail transport of Jet A-1 and LNG is state of the art with volumetric capacities per railway car of 85 m^3 and 110 m^3 for Jet A-1 and LNG, respectively [42,43]. While the transport of LH_2 by rail dates back to the1960s [44], due to the lack of LH_2 demand the technology is not yet as commercialized. To determine the "fixed costs" for different fuel types i.e., the depreciation costs for the wagons, the investment for the rail undercarriage and the actual tanks are considered. Other railcar costs such as installation, delivery etc. are neglected. Costs for the undercarriage and the LH_2 tank are taken from Amos [45]. The costs of the undercarriage are $\$_{1995}$ 100,000, which translates to 137,000 $€_{2020}$. The costs of the LH_2 tank are $\$_{1995}$ 400,000. Costs for the Jet A-1 tank are based on a truck trailer tank system. Here, the cost of transporting liquid hydrocarbons is in the range of 100,000 – 150,000 € [46,47]. Assuming that the tank is one third of the cost of a truck trailer tank system and a scaling factor of 0.67, the costs for the Jet A-1 tank amount to 75,000 $€_{2020}$. Thus, the costs for the Jet A-1 rail car are 225,000 $€_{2020}$. The costs for a small scale LNG tank are taken from Mariani and Lebrato [48]. They reported costs for LNG tanks with a capacity from 20 – 60 m^3 in the range of 95,000 – 135,500 $€_{2016}$. Based on their data, the cost of a 126 m^3 tank is estimated to be around 171,000 $€_{2020}$. The input data for each rail tank car are listed in Table 5 where the total volumetric capacity is given. For cryogenic tanks a usable capacity of 4 – 98 % of the total capacity is assumed, while SAF can use 0–98 % of the total capacity. The number of cars per train is determined by a maximum length of all wagons of 600 m due to the handling at the airport or by the total maximum weight of 2,200 t [49]. Boil-off that occurs during transport is flared. The values for boil-off are given in the SI.

Inland waterway transport

Fuel transport costs via inland waterways are based on a report from Panteia [41]. As for rail transport, costs are retrieved in "costs per km".

Table 4
Literature cost data for railway transport.

Cost component	Liquid bulk | €/km (41)
Fixed costs	6.29
Variable (energy) costs	4.56
Staff costs	1.49
Mode-specific costs (track access and shunting)	3.59
General operating costs	2.39

Table 5
Technical and economic data for fuel transport via railway vehicles.

Fuel	Capacity [t]	Capacity [m^3]	Railway cars per train	Cost per railway car [$€_{2020}$]
LH_2	9.07	128	24	686,150
LCH_4	49.91	111	24	308,000
Jet A-1	70.4	88	22	225,000

The values are listed in Table 6 "Fixed costs" are depreciations, insurance and partly maintenance. Variable costs are fuel costs and other maintenance costs. General operating costs result from permits and other operating costs like administration, IT, communications etc. As for the railway transport, it is not possible to give a single value due to the different fuel types. Instead, the costs are based on individual ships which are depreciated over 20 years.

The transport of Jet A–1 by inland waterways is state of the art and is one of the fuel sources for Frankfurt Airport [50]. Vessels of up to 110 m in length deliver fuel to the airport with fuel via the port of Raunheim [51]. The reference vessel for the transport of Jet A-1 is the "Eline" (IMO: 9652727), with a length of 110 m and a volumetric capacity of 3,019 m^3 [52]. Since 2013, LNG has been transported on the Rhine by the vessel "Greenstream" (IMO: 9664990) [53]. It has the same external dimensions as the "Eline" and a volumetric capacity of 3,130 m^3. For LH_2, there is no direct reference inland vessel. Although the first LH_2 carrier, the "Suiso Frontier" was launched in 2019 [54], the shape of the ship is not suitable for inland waterways up to the port of Raunheim. The "Greenstream" is therefore used as a reference. The volumetric capacity is reduced by 5 % due to the higher insulation requirements. As for the railway cars, a usable capacity of 4 – 98 % of the total capacity is assumed for cryogenic vessels, while 0–98 % of the total capacity can be used for SAF. The costs for the Jet A-1 ship is taken from Hekkenberg, where the costs are divided into the costs for the hull, propulsion, other equipment and navigation [55]. A rough estimate of the costs for large LNG vessels is given in the IGU report [56]. It gives specific costs in the order of $ 1200/m^3. As these values are for large-scale vessels, the value for the inland waterway ship will be higher, i.e. the lower benchmark is $ 3.76 million. With the cost structure given in Hekkenberg the costs for a LCH_4 carrier are estimated at 5 million €. The costs for the LH_2 vessel are assumed to be 2 million € higher due to stricter safety regulations and higher insulation requirements that occur when using LH_2 instead of LCH_4. The values are summarized in Table 7. Boil-off that occurs during transport is flared. The values for boil-off are given in the SI.

Airport infrastructure

The introduction of cryogenic fuels in aviation will require significant investments in airport infrastructure. Fig. 6 shows the components required, with a reliquefication plant as an example of a boil-off management unit. However, depending on the of boil-off amount, other utilization approaches like burning, supplying fuel cells for electricity production etc. could be pursued.

A holistic evaluation of the changes in the airport infrastructure when LH_2 is introduced as aviation fuel has been published by Hoelzen et al. [13]. Their study shows, how the departures per month vary over the course of the year compared to the annual average. The range is

Table 6
Literature cost data for waterway transport with large ships.

Cost component	Liquid bulk | €/km (41)
Fixed costs	9.90
Variable costs (energy + maintenance)	3.51
Staff costs	8.80
Mode-specific costs (port fees)	0.43
General operating costs	0.40

Table 7
Technical and economic data for fuel transport via inland waterway vessels.

Fuel	Capacity [t]	Capacity [m^3]	Cost per ship [Mio. €]	Source
LH_2	210.6	2,974	7.0	Assumption
LCH_4	1,407.4	3,130	5.0	Based on [55,56]
Jet A-1	2,415.2	3,019	3.79	[55]

from + 10 % in the summer to −15 % in February. This range is relevant for assessing the storage capacity required at the airport. The current Jet A–1 storage capacity at Munich airport amounts to 44,000 m^3 (4 x 4,500 m^3 + 12,000 m^3 + 14,000 m^3) [57]. In 2019, the total demand for Jet A–1 was in the order of 2.2 billion litres [58]. The storage capacity is therefore able to supply the airport with Jet A-1 for approximately one week at peak demand. This timeframe of storage capacity is considered for each fuel type according to the fuel utilization scenarios evaluated. The equipment costs for the kerosene storage tank are taken from Woods [59]. To obtain the final costs of the installed tank so called "Lang-factors" are used, as described in a previous study [25]. The final costs of kerosene storage amount to 250 €/m^3. The costs for large-scale LNG storage vessels are given in a report by Baker [60]. Converting the costs to $€_{2020}$ result in specific costs of 2,660 €/m^3 for a fully installed LCH_4 storage tank with a capacity of 29,000 m^3. Using data from Hoelzen et al., specific costs for LH_2 storage are in the order of 2,025–2,422 €/m^3 for tanks in the size of 280–7,800 m^3. Since it is unlikely that LH_2 storage is cheaper than LCH_4 storage, specific LH_2 storage costs of 3,000 €/m^3 are assumed. Costs for cryopumps are taken from Hoelzen et al., the costs for kerosene pumps are taken from Peters et al. [61]. The LH_2 fuelling system was also evaluated by Hoelzen et al. They concluded that an underground fuelling system with hydrants could save 0.01 $\$_{2020}/kg_{LH_2}$ compared to a fuelling system with trucks, if the demand of the airport exceeds 125 kt $_{LH_2}$/a. As they further stated that the choice of design may not only be based on economics but also on safety issues, an underground fuelling system will be considered in this study. The techno-economic input data for an underground LH_2 fuelling system are taken from Hoelzen et al. The same input data for LH_2 is also considered for LCH_4. The techno-economic input data for an underground SAF fuelling system is taken from Hromádka and Cíger [62]. The current lengths of these underground pipeline systems are 17 and 60 km in Munich and Frankfurt, respectively [63,64]. To reduce the costs, it is assumed that the pipeline system is optimized and a total length of 15 km is assumed for Munich and 50 km for Frankfurt. This is a more conservative estimate than the 3 km considered by Hoelzen et al. If an underground fuelling system is used, so called "dispenser trucks" are required to fuel the aircraft. They act as a final filter system and are the interface between the hydrant of the pipeline and the aircraft. Average costs are 204,000 $€_{2013}$ for a Jet A–1 dispenser truck according to Hromádka and Cíger. In comparison, Hoelzen et al. quoted $\$_{2020}$ 90,000 for a LH_2 dispenser truck. It is unlikely, that the trucks for LH_2 will be cheaper than the trucks for (renewable) Jet A-1. As the costs in Hromádka and Cíger were obtained through a data collection questionnaire, their costs are considered. Therefore, costs for cryogenic dispenser trucks are assumed to be around 400,000 €. Back-up fuel trucks, as mentioned in Hromádka and Cíger, are neglected. The number of required dispenser trucks is determined with the number of flights, i.e. by the FMS. It is assumed that fuelling takes 10, 20, 30 or 40 min depending on the aircraft size. The time increases with the aircraft capacity, which is given in Table 12. Dispenser trucks have a utilization rate of 60 % during the considered 18 h of operation per day. A liquefaction unit is considered if reliquefication is more economical than flaring. The costs for the hydrogen liquefaction unit are taken from the "IdealHy" project, the cost curve is shown in a previous study [65,66]. For methane liquefaction a conservative estimate of 2000 $/tpa (tons per annum) is considered, based on a study from Songhurst [67]. The input data are summarized in Table 8. Costs for hydrants are neglected

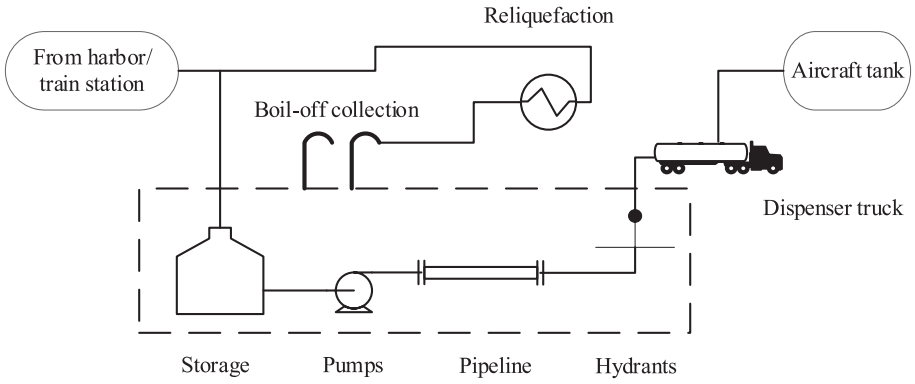

Fig. 6. Required airport infrastructure to provide cryogenic fuels to aircraft.

Table 8
Technical and economic input data for underground fuelling systems.

Fuel	Storage costs [€/m^3]	Pump costs [€/(kg/h)]	Pipeline costs in Mio $_{2020}	Dispenser truck [€]
LH_2	3,000	256.3	$\frac{5}{72} \bullet \dot{M}_{H_2} \bullet 2 \bullet d$	400,000
LCH_4	2,660	42.9	$\frac{5}{429.8} \bullet \dot{M}_{CH_4} \bullet 2 \bullet d$	400,000
Jet A-1	250	0.66	$0.679 \bullet d$	250,000

since they are low compared to the remaining costs.

Future aircraft

As stated in section 2.3 three different designs are being considered for future aircraft, each with unique implications for R&D costs, aircraft production costs and fuel demand.

- The conventional tube-and-wing design uses a stretched fuselage of varying lengths to accommodate the cylindrical storage of the cryogenic fuels.
- The blended-wing-body (BWB) maintains a constant aerodynamic shape with common cylindrical fuel storage for all fuel types.
- The truss braced wing (TBW) also uses fuselages of different lengths but with a longer wingspan supported by a truss.

The TWB is assumed to fly slower than the BWB and tube-and-wing but maintains block time with a twin–aisle configuration to speed up de/-boarding. The ONERA TBW concept includes a twin–aisle configuration with an elongated aft fuselage to store hydrogen source. A DLR study found that between 5 and 8 min of block time can be covered with a twin-aisle configuration featuring 180 seats [68]. This study uses the NASA N + 4 TBW which has a conventional single–aisle configuration [35].

The input parameters used to determine the future aircraft costs are listed in the following section. First, the empty weight distributions of the corresponding aircraft types are listed in Table 9. The empty weight distributions are taken directly from the Markish model. The truss-brace-wing configuration is assumed to have the same empty weight distribution as the tube and wing configuration.

The increases in the complexity factors of the aircraft subsystem due to the different designs are shown in Table 10. By default, each subsystem is assigned a complexity factor of 1, representing no additional development or production effort compared to a conventional aircraft of the same subsystem empty weight. Each entry corresponds to all aircraft sizes unless there are multiple entries, these are assigned to the 100, 180 and 425 PAX sizes respectively. The simplifying assumptions used to estimate the complexity factors are as follows: A 66 % factor is applied to the BWB centre body system to accommodate internal structural pressurization in addition to the supporting wing structure. A 25 % increase is applied to the BWB "systems" to account for the increase in the number flight control surfaces relative to a tube-and-wing aircraft. A 26 % increase in the swing complexity factor for the TBW wing subsystem was added to reflect the average difference between the span and the wing area between the NASA N + 4 TBW and the Boeing 737 Max 8 [35].

Increases in aircraft subsystem complexity factors due to the different fuel types are listed in Table 11. Each entry corresponds to all aircraft sizes for all alternative fuel types. In cells with multiple entries, each entry corresponds to LCH_4 and LH_2, respectively. The complexity factors for the fuel types are multiplied by the complexity factors for the aircraft form when both are present for the same subsystem. Simplifying assumptions for the fuel type complexity factors are as follows: The 14.8 % and 29.6 % increases for the fuselage subsystem in the tube-and-wing and TBW designs correspond to the ratio of the baseline length to the increased length required to store cryogenic fuel in the cargo bay under the forward cabin and directly behind the aft pressure bulkhead. For the payload subsystem, the 25 % increase results due to the strengthening of the aft-bulkhead to meet crash resistance requirements to store cryogenic fuel behind the cabin. For the installed engine, a 25 % increase is estimated for changing the combustor to either LCH_4 or LH_2 while the other 3 major engine subsystems, the fan, compressor and turbine are assumed to remain unchanged. Lastly, a 10 % increase in systems factor is estimated to cover changes to the fuel system and flight computers to handle the different fuel types. The BWB retains a common aerodynamic shape and therefore requires only installed engine and systems energy complexity factors.

The final aircraft costs, the change in fuel demand as well as the limits of validity are listed in Table 12. The R&D costs for all aircraft and the aircraft production prices for the remaining aircraft designs are listed in the SI in section S.2. Furthermore, a sensitivity analysis is conducted where the change in specific fuel demand of cryogenic fuels is varied from −20 % to + 50 %. These results are given in the SI as well.

Table 9
Empty weight distribution in the corresponding aircraft types.

Aircraft Shape	Wing	Empennage	Landing Gear	Fuselage/Centre Body	Installed Engine	Systems	Payloads
Tube-and-wing/ TBW	23 %	3 %	8 %	23 %	18 %	10 %	15 %
BWB	18.2 %	4 %	10.3 %	24.9 %	14.5 %	8.6 %	13 %

Table 10
Increase in complexity factors & composite percentage and manufacturing margin in the Markish model.

Aircraft Shape	Composite percentage	Wing	Empennage	Fuselage/Centre Body	Installed Engine	Systems	Payloads	Manufacturing Margin
Tube and Wing	30 % 30 % 50 %*							5.7 %
BWB	50 %			66 %		25 %		11.4 %
TBW	30 %	26 %						6.9 %

* Values are valid in the given order for aircraft with 100, 180 and 425 seats.

Table 11
Energy complexity factor difference by aircraft type.

Aircraft Shape	Wing	Empennage	Fuselage/Centre Body	Installed Engine	Systems	Payload
Tube and Wing			29.6/14.8 % *	25 %	10 %	25 %
BWB				25 %	10 %	
TBW			29.6/14.8 % *	25 %	10 %	25 %

* Values are valid in the given order for LH_2 and LCH_4.

Table 12
Input data to determine costs for flying with LH_2, LCH_4 and SAF.

Plane type Capacity	Aircraft cost [Mio. €]			Change in fuel demand		LOV [FC_{calc}]
	SAF	LH_2	LCH_4	LH_2	LCH_4	All fuels
Regional jet 100 PAX	48.8	53.5	52.3	−8 %	+5.6 %	50,000
Small narrowbody 180 PAX	83.2	91.1	89.1	−4 %	+10 %	50,000
Large widebody 425 PAX	255.9	280.3	274.1	+9%	+12 %	44,000

Current costs for air travel

The introduction of SAF is the current politically-endorsed pathway to decarbonize the aviation industry. Only the fuel source is different from fossil Jet A–1, the rest of the distribution chain is unaffected and the existing infrastructure can be used. Ticket prices are obtained using a common metasearch engine [69]. The tickets are economy class, return trip and for one person. The cheapest flights are selected with a time window from November 2023 to March 2024. The Jet A–1 demand is obtained from an online calculator that determines the personal carbon footprint of a given flight [37]. This methodology is independent of the other evaluations in this study. A typical modern aircraft is assumed. A ratio of 3.16 kg CO_2 emitted per burned kg of Jet A–1 is considered. Based on the kerosene demand, the fuel cost for fossil Jet A–1 as well as the costs for renewable SAF are estimated. The same flight routs as introduced in Table 3 are selected. The emissions, fuel demand, ticket prices and fuel costs are listed in Table 13. Fuel specific costs of 0.66 €/kg are assumed, which applied in July 2023 [70]. The implications how these costs might change SAF is utilized are given in section 4.3.

Results and discussion

This work focuses on aspects of how the future cost of air travel will change depending on the fuel used. In this section, first the fuel supply costs to the exemplary airports are given. Then based on the costs of future aircraft, the costs for flying excl. airport taxes, fees etc. will be evaluated. The introduction of sustainable aviation fuel (SAF) is the most likely scenario. From 2025, there will be quotas for the blending of SAF in the EU, starting at 2 % and to 70 % by 2050 [8]. The impact on current air travel costs with 100 % SAF share is assessed in section 4.3. As some of the properties of these fuels are relevant to the further discussion, the main physical properties are listed in Table 14.

Evaluation of the fuel supply chain

In the following, first the main results of the fuel supply chain are

Table 14
Physical properties of the evaluated aviation fuels. Liquefaction energy demand is taken from Cardella et al. [71] and Al-Breiki et al. [72].

Property	Unit	LH_2	LCH_4	SAF
Density (liq./ @ 1 bar)	kg/m^3	70.8	422.6	810*
Energy density – volumetric	MJ_{LHV}/m^3	8.50	21.13	34.83
Energy content – mass based	MJ_{LHV}/kg	120	50	43*
Energy demand for (re)-liquefaction	kWh_{El}/kg	6	0.34	–
Ratio energy content/ energy demand for (re)-liquefaction	kWh_{El}/kWh_{LHV}	0.18	0.025	–

* Average value.

Table 13
Exemplary flight paths and their kerosene demand per person – return trip.

ID	To	Plane	Distance [km]	CO_2 emitted [kg]	Kerosene demand [kg]	Ticket price [€$_{2023}$]	Fuel costs [€$_{2023}$]
1	MUC	A320 neo	300	57	18	186	12
2	CDG	A320 neo	447	72	23	134	15
3	MAD	A320 neo	1,419	166	53	125	35
4	IST	A321 neo	1,863	194	61	161	41
5	KEF	A321 neo	2,399	245	78	177	51
6	CAI	A321 neo	2,921	306	97	475	64
7	IKA	B787-900	3,774	480	152	421	100
8	DOH	B787-900	4,584	576	182	498	120
9	JFK	A350-1000	6,184	693	219	420	145
10	BKK	A350-1000	8,995	1,155	366	880	241
6*	CAI			347	110	311	73
10*	BKK			1,444	457	573	302

* The indirect flight was cheaper than a non-stop connection in the considered time period.

presented. Details are given in the supplementary information.

Total fuel demand

Based on the flight movement scenario (FMS), the fuel utilization scenarios (FUS) from Table 1 and the changes of the specific energetic fuel demand given in Table 12, the total annual fuel demand for the year 2050 is estimated for FRA and MUC. Due to the different physical properties the gravimetric, volumetric and energetic results are given in Fig. 7.

From an airport operator's point of the volumetric changes are the most relevant results as there may be spatial limitations at the airport. The required tank capacities are listed in Table 15 and Table 16. For comparison, the current fuel capacities in FRA and MUC are 186,000 m^3 and 44,000 m^3, respectively [57,63]. The capacity at FRA is therefore already higher than it should be based on the definition in section 3.2. This fact does not affect the general comparison of this paper. Any FUS with a cryogenic fuel increases the volumetric storage demand at the airport. In particular if no SAF is considered the demand increases by at least a factor of 2 compared to scenario #1.

Regarding the energetic fuel demand, it can be seen that there is little change between scenario #1 and #2. If the share of cryogenic fuels is increased, the energetic fuel demand increases and is highest in scenario #5. However, the energetic fuel demand at the airport is only one aspect. In order to evaluate the whole supply chain depicted in Fig. 2, it is also necessary to consider the fuel production efficiency, which was evaluated in a previous study [26]. The fuel supply efficiencies (defined as fuel output divided by electrical input at the sweet spot) are 52.8 % for LH_2, 43 % for LCH_4 and 18.5 % for SAF (34.7 % if the by-product of the FT-synthesis is included). The total annual electrical energy demand is depicted in Fig. 8. It can be seen that although the scenario #1 requires the least energy at the airport, it has the highest electrical energy

Table 15
Required tank capacity in m^3 in Frankfurt – depending on the scenario.

Fuel type \Scenario	#1	#2	#3	#4	#5	#6
LH_2	0	44,606	1,731	44,606	620,814	0
LCH_4	0	0	47,219	231,587	0	249,215
SAF	137,483	127,723	111,019	0	0	0
Sum	137,483	172,329	159,969	276,193	771,696	249,215

Table 16
Required tank capacity in m^3 in Munich – depending on the scenario.

Fuel type \Scenario	#1	#2	#3	#4	#5	#6
LH_2	0	46,295	2,376	46,295	266,810	0
LCH_4	0	0	37,441	88,124	0	106,423
SAF	58,746	48,601	37,518	0	0	0
Sum	58,746	94,896	77,335	134,419	318,318	106,423

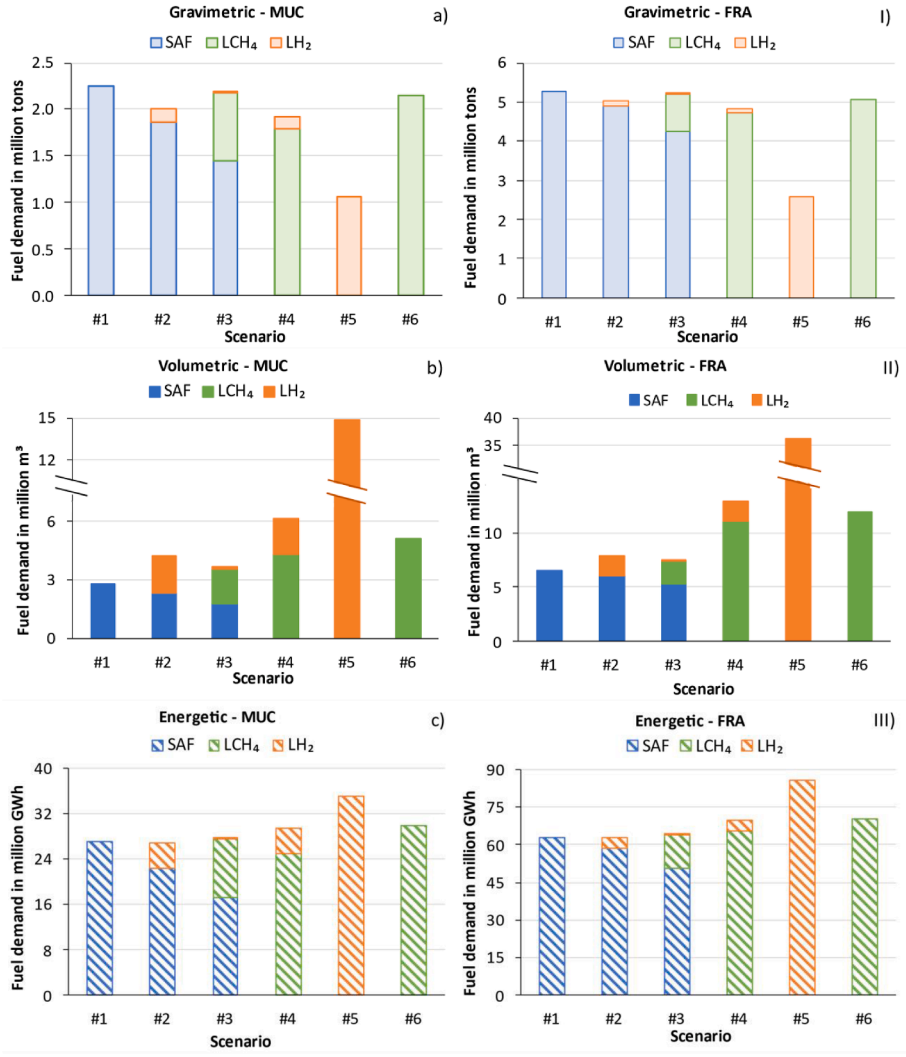

Fig. 7. Gravimetric (a, I), volumetric (b, II) and energetic (c, III) fuel demand for MUC (a, b, c) and FRA (I, II, III).

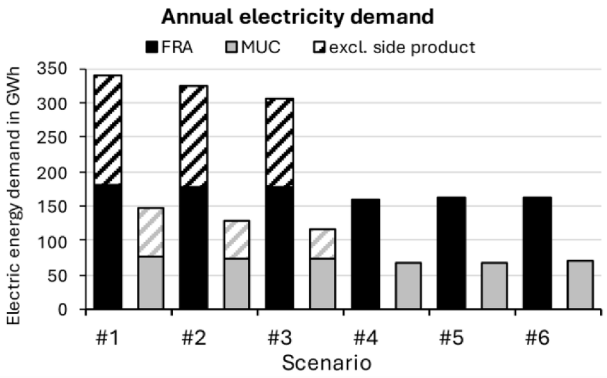

Fig. 8. Annual electrical energy demand at the sweet spot to produce the required aviation fuels.

demand at the fuel source. The hatched area indicates the influence of the two given efficiencies of the SAF supply (with and without the by-product). When the by-product is excluded, the efficiency is lower and thus, the electricity demand is higher.

In addition to the efficiencies, it is relevant to know how much of the corresponding fuel demand given in Fig. 7, could be met by the plants evaluated in Raab and Dietrich [26]. In this previous study a gaseous hydrogen mass flow of 25.74 t/h is converted to the different aviation fuels. In the supply chain considered, the amount of fuel arriving in Wilhelmshaven is either 217.7 kt/a of LH_2, 425.87 kt/a of LCH_4 or 218.5 kt/a of SAF. The percentages given in Table 17 therefore indicate how much of the corresponding fuel demand could be met by the individual supply chains based on 25.74 t/h hydrogen production abroad.

For example, to meet the fuel demand of scenario #1, a total of 10 of the plants considered in Raab and Dietrich are required to supply kerosene to MUC, while 25 are required for FRA. If the amount of cryogenic fuels is increased, the total number of plants required to meet the demand is reduced. This is an aspect to be considered in order to keep the overall investments low (fuel productions plants + airport infrastructure + aircraft research and development).

Total fuel supply costs

The fuel import costs are 157 €/MWh for LH_2, 220 €/MWh for LCH_4 and 279 €/MWh for SAF based on the previous study [26]. These costs are valid at the import terminal shown in Fig. 2. With the input data given in section 3, the costs for the domestic distribution and the airport infrastructure are estimated to obtain the final fuel supply costs. Fig. 9 shows the costs that are added to the import costs for MUC for the scenarios considered in Table 1. The pillars within a scenario represent LH_2, LCH_4 and SAF from left to right. If a certain fuel type is not considered in the given scenario, no pillar is shown. A logarithmic scale is used to better illustrate the different cost elements.

For SAF, it can be seen that the costs in addition to the import costs are of the order of 1.1 €/MWh for each scenario which equals to 1.3 ct/kg. The order of magnitude of this figure has been confirmed by personal communication with a person from Munich Airport. The costs for handling of cryogenic fuels are higher and depend on the total amount

Table 17
Share of fuel demand coverage depending on the analysed scenarios.

	MUC			FRA		
Scenario	LH_2	LCH_4	SAF	LH_2	LCH_4	SAF
#1	–	–	10 %	–	–	4 %
#2	163 %	–	12 %	169 %	–	4 %
#3	2,968 %	58 %	15 %	4,073 %	46 %	5 %
#4	163 %	24 %	–	169 %	9 %	–
#5	25 %	–	–	10 %	–	–
#6	–	20 %	–	–	8 %	–

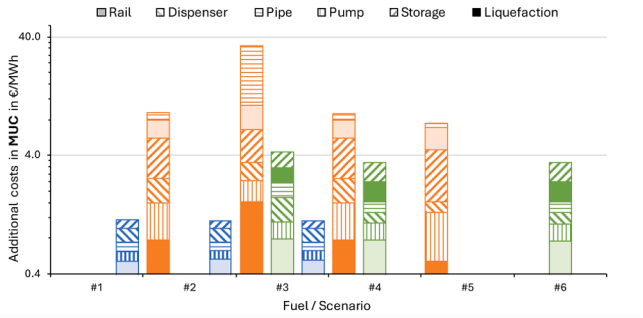

Fig. 9. Costs for domestic distribution and fuelling at Munich airport.

that is handled (the annual amount of fuel that is handled is shown in Fig. 7). For LH_2 and LCH_4 the costs for domestic distribution and airport infrastructure are highest in scenario #3. This is due to the fact, that in this scenario the smallest quantities are required for both fuels. In particular, the costs for the LH_2 pipeline system are very high in scenario #3. In this scenario, the amount of LH_2 handled would not justify a pipeline system and a truck delivery system might be the better choice to transport the fuel from the tank farm to the aircraft. In scenario #5 and #6 the fuel handling costs are lowest for LH_2 and LCH_4. It can be seen, that after a certain amount of fuel that is handled per year, the handling costs do not decrease any further. This lower limit is around 9 €/MWh for LH_2 (ignoring scenario #5 as it is only an academic scenario) and 3.5 €/MWh for LCH_4. This corresponds to 30 ct/kg and 4.9 ct/kg for LH_2 and LCH_4, respectively. Hoelzen et. al obtained costs of 0.19 $\$_{2020}$/kg for handling liquid hydrogen at the airport but also considered a shorter pipeline length. Fig. 10 shows the costs in addition the import costs for FRA for the scenarios considered in Table 1. A logarithmic scale is used to better illustrate the different cost elements.

The same aspects from the case of MUC can be concluded for FRA. The costs are slightly different due to the different transport pathway to the airport and the longer length of the pipeline system, resulting in a higher boil-off of the cryogenics. The costs for SAF amount to 1.5 €/MWh which equals to 1.8 ct/kg, the lower threshold for LH_2 handling costs is 14 €/MWh, equal to 47 ct/kg (neglecting scenario #5). For LCH_4, handling costs are 4.7 €/MWh, equal to 6.5 ct/kg. The fuel supply costs are summarized in Table 18. These are the "minimum fuel supply costs" mentioned in section 2. With these costs, the flight costs are evaluated in $\frac{€}{\text{PAX } 100\text{ km}}$.

Costs for fuel utilization

This section presents the results for the total costs of flying for the conventional tube-and-wing aircraft designs utilizing either LH_2, LCH_4 or SAF. The results for the BWB and TBW are depicted in the section S.2 of the SI. Ten exemplary routes are considered, starting from Frankfurt, and are listed in Table 3. Based on the fuel supply costs from Table 18, the specific fuel demand given in the FMS for future aircraft as well as

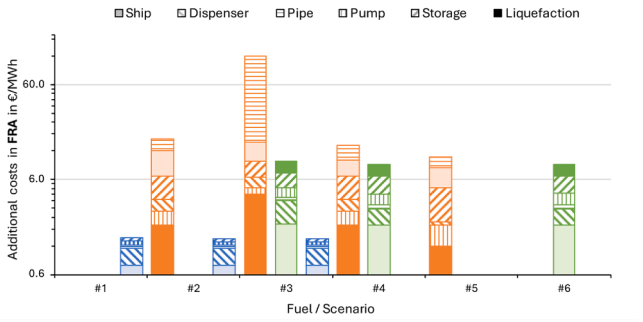

Fig. 10. Costs for domestic distribution and fuelling at Frankfurt airport.

Table 18
Summary of fuel supply costs in €/MWh_{LHV}.

Fuel type	Import costs	Fuelling in MUC	Fuelling in FRA
LH_2	157	9	14
LCH_4	220	3.5	4.7
SAF	279	1.1	1.5

the aircraft costs and number of flight cycles given in Table 12, the costs for flying are determined. Boil-off losses once the fuels are inside the aircraft are not considered. A load factor (LF) of 80 % is assumed for each aircraft, meaning that only 80 % of the available seats are occupied. The results for the regional jet sized aircraft with a total capacity of 100 passengers are shown in Fig. 11.

The values of the columns are represented by the left axis and indicate the specific costs in $\frac{€}{PAX\ 100\ km}$. The dashed part of the column corresponds to the fuel costs while the blank part represents the depreciation costs of the aircraft. The distances that are covered increase from left to right. It can be seen that the absolute share of depreciation costs decreases with increasing flight distance and almost negligible for flights to IKA (3774 km). For this distance the total corresponding values are 4.73, 7.01 and 8.14 $\frac{€}{PAX\ 100\ km}$ LH_2, LCH_4 or SAF, respectively. The total costs per passenger in $\frac{€}{PAX}$ for any given flight are shown by the pyramid, circle and diamond shaped dots. The values are given on the right axis. While the difference between the different fuel types is rather small for short distances, the cost advantage of LH_2 over LCH_4 over SAF becomes more pronounced as the flight distance increases. The results for the small aircraft with a total capacity of 180 passengers are shown in Fig. 12.

The same convention for both axes as in Fig. 11 is considered in Fig. 12. Comparing the total costs for the flight to IKA (Tehran, Iran) as example destination, it can be seen that the costs for the small aircraft are between 94 and 193 €/PAX for the corresponding fuel, while they are in the range of 180 and 309 €/PAX for the regional jet sized aircraft. The longer the distance, the greater is the cost advantage of LH_2 over LCH_4 and SAF. For the longest distance covered (6184 km to JFK), the total corresponding values are 3.08, 4.57 and 5.11 $\frac{€}{PAX\ 100\ km}$ for LH_2, LCH_4 and SAF, respectively. As aircraft depreciation is not a major factor over long distances, the ranking is hardly affected by higher acquisition costs for cryogenic aircraft. The results for the large aircraft with a total capacity of 425 passengers are shown in Fig. 13.

Fig. 13 uses the same convention for both axes as in Fig. 11. Comparing the total costs for the flight to JFK (New York, USA) as example destination, it can be seen that the costs for the small aircraft are between 190 and 316 €/PAX for the corresponding fuel, while they are in the range of 263 and 385 €/PAX for the large aircraft. Thus, the specific costs increase for the larger aircraft. The specific costs also increase, for the highest distance covered (8995 km to BKK) the corresponding values are 4.25, 5.72 and 6.09 $\frac{€}{PAX\ 100\ km}$ for LH_2, LCH_4 and SAF, respectively. The higher costs for the larger aircraft result from the specific higher fuel demand, given in Table S.6 and are provided by the FMS. The increase from a small aircraft to the larger aircraft can be explained with the equation for the hydraulic drag, the force acting on a body in the opposite direction of its motion. The force of the hydraulic drag is directly proportional to the cross-sectional area of the body, in this case the aircraft. Considering two exemplary aircraft, namely the A321 and the A350, the cross-sectional area of the fuselage per passenger is lower for an A321, than for an A350. The calculation is given in the SI. Therefore, the higher the fuel supply costs, the more prominent is the cost advantage of narrowbody aircraft over widebody aircraft. The results for LH_2 shown in Fig. 13 are valid for a 9 % increase in the specific energy demand compared to an aircraft using SAF. As a value of + 42 % is also reported in literature, the implications of the higher increase have also been considered and the results are shown as a sensitivity in Figure S.1.

Impact of 100 % SAF on current air travel costs

In section 3.4, current ticket prices are given for return trips from FRA to the destinations listed in Table 3. Using current Jet A–1 costs, the fuel cost share is estimated of these ticket prices. This is depicted with the columns in Fig. 14. To evaluate the impact if fossil Jet A–1 is completely substituted by SAF, the specific fuel demand is determined and multiplied by the SAF supply costs of this study. The results are indicated with the black dots in Fig. 14. The "error-bars" represent the share of the current ticket prices excl. the current fuel costs. Thus, the total height represents the total ticket prices if 100 % SAF had been used. An example: The current indirect return trip costs to CAI* are roughly 300 €, made up of 72 € for "fossil Jet A-1 share" and 235 € for "Ticket price excl. fuel". The costs for SAF for this return trip are 370 € (shown by the black dot), now adding 235 € for "Ticket price excl. fuel", the perspective total ticket price amounts to 605 € (higher end of the error bar). It can be seen, that for short-haul flights the absolute increase is rather small and in the order of expected price fluctuations. For long-distance flights the cost increase is very significant. As stated above,

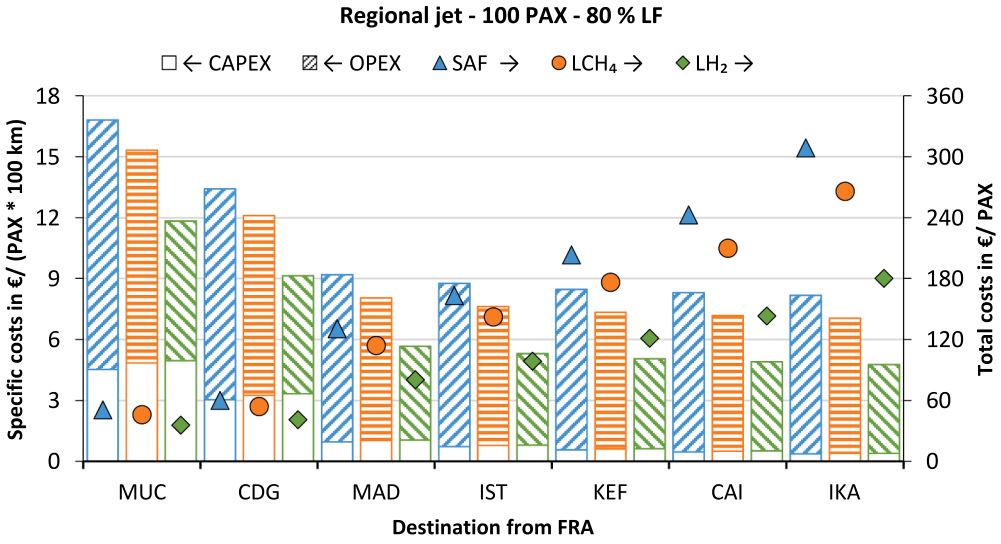

Fig. 11. Cost of flying with a conventional tube-and-wing design regional jet sized aircraft.

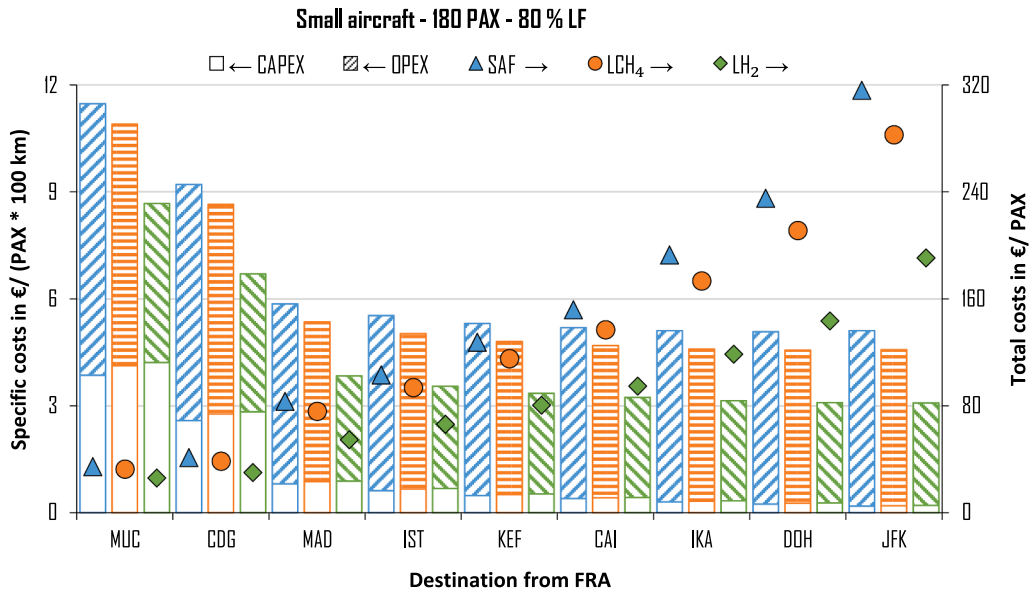

Fig. 12. Cost of flying with a conventional tube-and-wing design small sized aircraft.

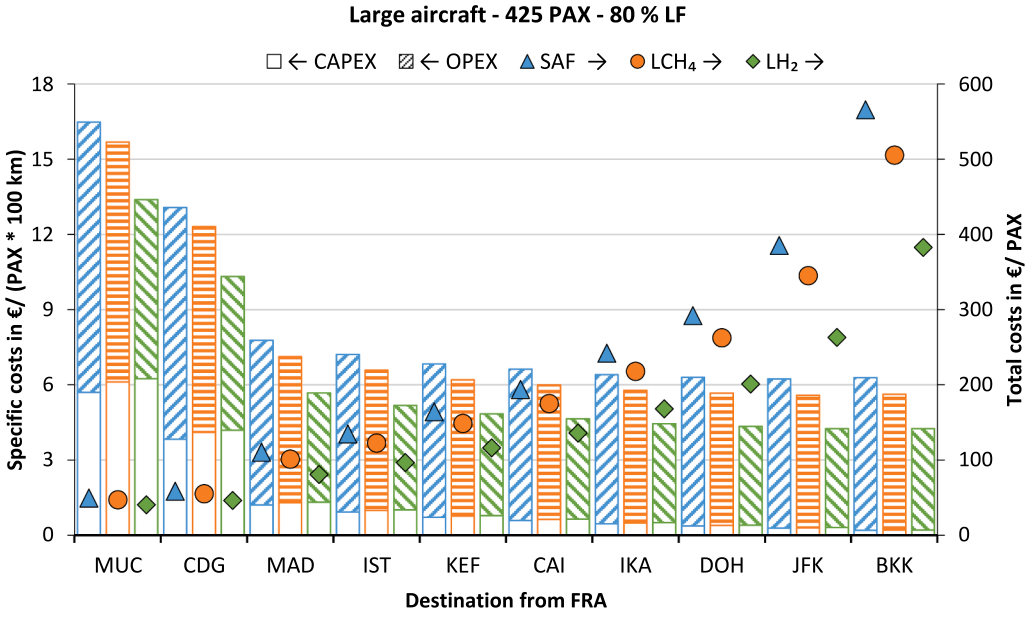

Fig. 13. Cost of flying with a conventional tube-and-wing design large sized aircraft.

all trips are non-stop routes except those marked with an asterisk (*).

Discussion

Two consecutive assessments have been carried out in this study to compare the implications of LH_2, LCH_4 and SAF as potential aviation fuels. The study was carried out with an exclusive focus on technical and economic aspects and did not consider regulatory issues related to certification, allowances or a life cycle assessment. Firstly, the fuel demand together with the fuel storage requirements were evaluated for several scenarios. Based on these results, the costs for domestic distribution and fuelling at the respective airport were assessed. It has been shown that the introduction of cryogenic fuels leads to a high increase in storage demand at the airports, mainly due to their lower volumetric energy density. Based on the scenario evaluations, a lower threshold for the fuel supply costs to the aircraft has been determined. It is shown that the overall fuel supply costs are dominated by the import costs and that the costs for domestic distribution and costs for the airport infrastructure have a less dominant role. The case where this cost share is highest, is the case of LH_2 supply to FRA. There, the costs account for 9 % of the overall supply costs (14 €/MWh out of 171 €/MWh). For SAF the additional costs are even lower. The accuracy of the cost estimation used in a previous study [26] to determine the fuel import costs for SAF is likely to be a source of greater uncertainty than the additional costs resulting from domestic distribution, storage and fuelling. Secondly, based on the fuel supply costs and the estimated aircraft acquisition costs, the costs for air travel were estimated in $\frac{€}{\text{PAX 100 km}}$ for different aircraft sizes and different fuel types. Furthermore, the total costs for the considered flights were determined in $\frac{€}{\text{PAX}}$. The lower threshold for the specific air travel costs for each aircraft type considered is listed in Table 19. The values are valid for the maximum distance that could be flown with the corresponding aircraft type. In addition, the values are listed for the case where new aircraft but fossil Jet A-1 are used (in

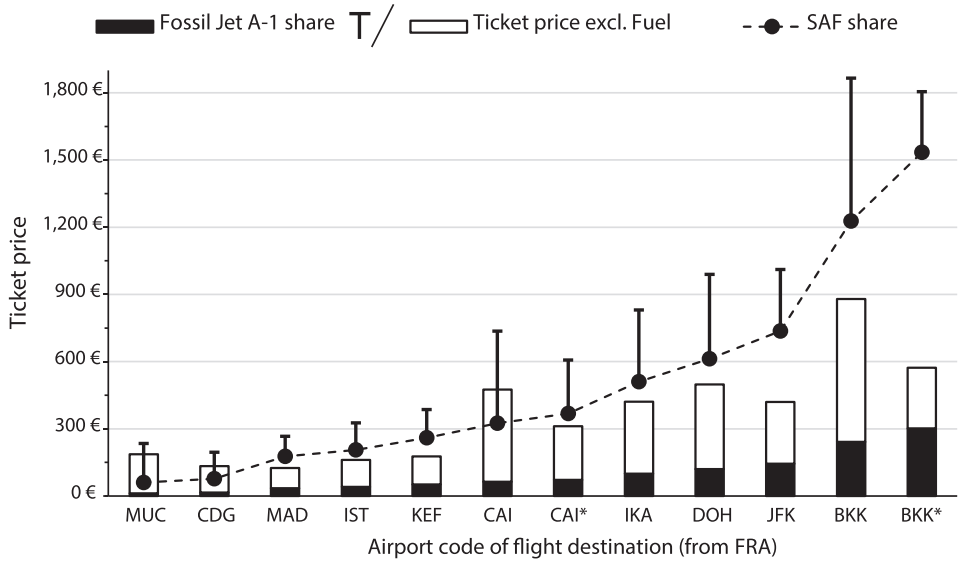

Fig. 14. Current return trip costs of air travel from FRA and the implication of SAF introduction. The share of fuel costs is determined by the individual CO_2 emissions.

Table 19

Lowest specific costs for flying in $\frac{€_{2020}}{\text{PAX}\,100\,\text{km}}$.

	LH_2	LCH_4	SAF	Fossil Jet A-1
Regional jet	4.73	7.01	8.14	1.53
Small aircraft	3.08	4.57	5.11	1.15
Large aircraft	4.25/ 5.48*	5.72	6.09	1.39

* This value is valid for an increase in energy demand of + 42 % compared to SAF.

contrast to section 4.3 where current aircraft data are considered). Specific costs of 0.66 €/kg are considered for fossil Jet A-1 which is equivalent to 55.3 €/MWh.

The values show, that for each aircraft type the costs are highest when SAF is utilized, followed by LCH_4 and LH_2 as the most economic option to replace fossil Jet A-1. These results are valid if the production of renewable hydrogen is the first step and both, SAF and LCH_4 are assumed to be converted from hydrogen as depicted in Fig. 2 and not from biogenic origins. Biofuels have been excluded from this study, as discussed in section 1.2. The costs given Table 19 depend mainly on the overall fuel supply costs, as shown in Fig. 11, Fig. 12 and Fig. 13. The fuel supply costs are dominated by the costs for importing these fuels to Wilhelmshaven. A thorough analysis and literature comparison for these costs was carried out in a previous study [26]. The values listed in Table 19 also show the huge cost increase between the use of fossil Jet A-1 and electricity-based renewable fuels. The socio-economic implications of this aspect must be taken into account in future research.

It has been shown that the aircraft acquisition costs given in Table 12 have a minor role and that the overall ranking is determined by the fuel supply costs and the specific fuel demand. These results are valid under the assumption that it is technically and economically feasible to manufacture the respective aircraft. Hydrogen and methane powered aircraft with a tube-and-wing design face the challenge, that cryogenic fuels cannot be stored in the wings in the conventional way. This challenge is compounded by the lower volumetric energy density of cryogenic fuels as shown in Table 14. Due to the additional isolation requirements of cryogenic fuels, there are hurdles that need to be overcome for the introduction of cryogenic fuels in aviation. For the purpose of this study, it has only been considered that the obstacles can be overcome to demonstrate the economic benefits of aircraft propelled with cryogenic fuels.

The lower fuel supply costs of LH_2 and LCH_4 allow a certain energy penalty i.e., a higher specific energy "consumption" for propulsion. Even if the increase amounts to + 42 %, as it is considered in a sensitivity for LH_2 (results are in Figure S.1), the utilization of LH_2 is still more economical than the utilization of LCH_4 or SAF. The fact that costs for air travel listed in Table 19 are higher for the large aircraft than for the small aircraft can be explained with the higher cross-sectional area of the aircraft. Moreover, no belly cargo has been assumed for the large aircraft, which typically contributes significantly to the capacity offered. As current ticket prices include fees, taxes etc. and considering that slots at airports are limited, the aspect of the specific higher fuel demand may not be too relevant for comparably low fuel costs. With rising fuel prices in the future, airlines might focus on using smaller (narrowbody or single-aisle) aircraft to decrease the fuel demand for their services. However, this must be offset by the generally shorter range and lower passenger capacity of smaller aircraft.

In this study the cost implications of phasing out fossil fuels from aviation industry are evaluated. Similar studies have been conducted by Proesmans et al. [73] and Dray et al. [27]. However, Proesmans et al. performed an optimisation approach where either the cost optimal or climate optimal solution was determined and thus, included a life cycle assessment in their study. While Dray et el. considered a feedback from increased costs of air travel on the demand for air travel. Both aspects have not been considered in this study. However, Proesmans et al and Dray et al. both state how the cost of air travel will be increased by reducing the climate impact. The results are given in Table 20 together with the cost increase of this study based on the values from Table 19. It has to be mentioned that the cost of air travel of this study considers the fuel costs and depreciation costs of the aircraft. Remaining aspects like salary of cabin crew, fees, taxes etc. are not considered. Therefore, the values from Table 20 do not indicate, that ticket prices will increase by the corresponding factor.

In Dray et el. a generic cost increase in the range of 10 – 16 % is

Table 20

Increase in air travel costs compared to fossil kerosene – comparison with literature data.

	LH_2	LCH_4	SAF	LH_2 [73]	SAF [73]
Regional jet	309 %	458 %	532 %	30 %	8 %
Small aircraft	268 %	397 %	444 %	42 %	14 %
Large aircraft	306 %	412 %	438 %	69 %	26 %

given. The vast difference between the results of this study and can to a certain extent be explained by different fuel cost assumptions. Proesmans et al. considers costs of 132 and165 $/MWh$_{LHV}$ for LH_2 and eSAF, respectively. Dray et al. considers an upper limit of 130 $/MWh$_{LHV}$ for SAF based on hydrogen and atmospheric CO_2 in the year 2050. In this manuscript, SAF costs of roughly 280 €/MWh$_{LHV}$ are considered. Also, different fossil kerosene baseline costs and fuel demand scenarios lead to different outcomes.

Another aspect that is an indirect result of this study is the fact, that if cryogenic fuels are introduced as aviation fuel in the future, enormous amounts of energy will be stored at airports in the state of a *meta*-stable cryogenic liquid. In scenario #2 (and #4) the LH_2 storage capacity in Munich amounts to 46,295 m^3, as given in Table 16. At the density given in Table 14, a fully loaded tank has the capacity to store 3,200 tons, the energy content of which is equivalent to 92 kT TNT (1 kt TNT = 4.184 $\cdot 10^{12}$ J). This potential hazard could lead to discussions with the local authorities and neighbourhoods who could be affected in the event of an incident. Spatial constraints on the installation of the required tank capacity at the airports have not been considered in this study. Other safety issues that could be caused from cryogenic fuels or potential GHG emissions from leakage, slip or utilization have also been excluded. Maintenance costs have been neglected in this study but might be different for planes with fuel cells and turbines. The engines of smaller planes have a lifetime of roughly 20,000 h [74]. Small aircraft usually have their engines replaced twice before they reach their end of life i.e. after 60,000 flight hours.

Conclusion

The research question of this paper is how the costs of air travel will be affected by a complete transition to electricity-based fuels and how the costs will differ if LH_2, LCH_4 or SAF are used for specific flight routes. Based on two previous studies the whole chain was evaluated including the hydrogen production based on renewable energy at a remote location [25], the subsequent synthesis and transport to Germany [26] as well as the domestic distribution and utilization. To the authors' knowledge, no study has yet compared the fuels including their entire supply chain to answer the following overarching question: If the aviation industry wants to reduce the use of fossil kerosene, is it more economical to simply change the fuel source or should the fuel itself be changed? Assuming that it is possible to manufacture aircraft utilising cryogenic fuels, it is concluded that the fuel supply costs dominate the overall costs and therefore LH_2 is the most economic option, followed by LCH_4 and SAF.

In view of the results of this study, future research should focus on the aspects with the highest leverage on the overall costs. These are the changes in the specific fuel demand for the different aircraft given in Table 12 and the fuel import costs. Only the former has been considered in this study, therefore future research suggestions focus on this matter. The change in specific fuel demand could improve from developments in fuel cells or by improvements in tank materials allowing better on-board storage of cryogenic liquids. Dual-fuel aircraft could also reduce cost of flying, as not all the energy would have to be supplied from SAF. If for example, SAF is stored in the wings and LCH_4 is stored in a fuselage tank the overall costs for a given flight could be reduced. Moreover, acceptance by operators could be improved with dual-fuel aircraft, as these types could also be operated from airfields not equipped with LCH_4 refuelling infrastructure.

Another field of research could be the utilization of the cryogenic temperature level in the power electronics i.e., superconductive electric engines. Since it is the overall target to reduce the GHG emissions of the aviation industry, the GHG emissions of the whole chain should also be considered to evaluate the environmental impact of cryogenic fuels in aviation. This aspect has been excluded from this study since estimating the emissions resulting from utilization alone is a very complex task with numerous variables like flight height, flight time, slip of unburned fuel (−components) etc. [75–78]. Assuming that SAF is equal to $C_{12}H_{26}$, it can be said that the water vapor emissions resulting from fuel combustion are roughly 2.3 times higher for LH_2 than for SAF for every energy unit provided. This, as well as the aspects mentioned above, has to be considered in order to find the most appropriate pathway to decarbonize the aviation industry.

CRediT authorship contribution statement

Moritz Raab: Writing – original draft, Investigation. **Ralph-Uwe Dietrich:** Writing – review & editing, Supervision. **Paula Philippi:** Software. **Jonathan Gibbs:** Writing – review & editing, Validation, Investigation. **Wolfgang Grimme:** Writing – review & editing, Validation, Investigation.

Declaration of competing interest

The authors declare the following financial interests/personal relationships which may be considered as potential competing interests: Jonathan Gibbs reports a relationship with Savion Aerospace Pty Ltd that includes: board membership. The corresponding author (MR) now works at HIF EMEA GmbH, a company aiming to build and operate plants that produce synthetic fuels. The work of this paper was done while he was still employed at the DLR. The work will also be published with his affiliation under the DLR. If there are other authors, they declare that they have no known competing financial interests or personal relationships that could have appeared to influence the work reported in this paper.

Data availability

Data will be made available on request.

Appendix A. Supplementary data

Supplementary data to this article can be found online at https://doi.org/10.1016/j.ecmx.2024.100611.

References

[1] ICAO. 2023 Long term global aspirational goal (LTAG) for international aviation [First accessed on: 17.12.2023 - Available from: https://www.icao.int/environmental-protection/Pages/LTAG.aspx.].
[2] Fuel Cells, Hydrogen 2 Joint Undertaking. Hydrogen-powered aviation – A fact-based study of hydrogen technology, economics, and climate impact by 20502020.
[3] Greg Hemighaus, Tracy Boval, John Bacha, Barnes F, Matt Franklin, Lew Gibbs, et al. Aviation Fuels - Technical Review. 2007.
[4] Tongpun P, Wang W-C, Srinophakun P. Techno-economic analysis of renewable aviation fuel production: From farming to refinery processes. J Clean Prod 2019; 226:6–17. https://doi.org/10.1016/j.jclepro.2019.04.014.
[5] Eswaran S, Subramaniam S, Geleynse S, Brandt K, Wolcott M, Zhang X. Techno-economic analysis of catalytic hydrothermolysis pathway for jet fuel production. Renew Sustain Energy Rev 2021;151:111516. https://doi.org/10.1016/j.rser.2021.111516.
[6] Weyand J, Habermeyer F, Dietrich R-U. Process design analysis of a hybrid power-and-biomass-to-liquid process – An approach combining life cycle and techno-economic assessment. Fuel 2023;342:127763. https://doi.org/10.1016/j.fuel.2023.127763.
[7] Su-ungkavatin P, Tiruta-Barna L, Hamelin L. Biofuels, electrofuels, electric or hydrogen?: A review of current and emerging sustainable aviation systems. Prog Energy Combust Sci 2023;96:101073. https://doi.org/10.1016/j.pecs.2023.101073.
[8] European Council. Initiative „ReFuelEU Aviation": Rat verabschiedet neuen Rechtsakt zur Dekarbonisierung des Luftfahrtsektors 2023. https://www.consilium.europa.eu/de/press/press-releases/2023/10/09/refueleu-aviation-initiative-council-adopts-new-law-to-decarbonise-the-aviation-sector/.
[9] IATA. Fact Sheet 2 - Sustainable Aviation Fuel: Technical Certification [First accessed on: 31.08.2023 - Available from: https://www.iata.org/contentassets/d13875e9ed784f75bac90f000760e998/saf-technical-certifications.pdf.].
[10] Atlantic V Virgin Atlantic flies world's first 100% Sustainable Aviation Fuel flight from London Heathrow to New York JFK [press release]. 2023.
[11] Brewer GD. Aviation usage of liquid hydrogen fuel—prospects and problems. Int J Hydrogen Energy 1976;1(1):65–88. https://doi.org/10.1016/0360-3199(76)90011-2.

[12] Korycinski PF. Air terminals and liquid hydrogen commercial air transports. Int J Hydrogen Energy 1978;3(2):231–50. https://doi.org/10.1016/0360-3199(78)90021-6.

[13] Hoelzen J, Flohr M, Silberhorn D, Mangold J, Bensmann A, Hanke-Rauschenbach R. H2-powered aviation at airports – Design and economics of LH2 refueling systems. Energy Conversion Manage: X. 2022;14:100206. https://doi.org/10.1016/j.ecmx.2022.100206.

[14] Mangold J, Silberhorn D, Moebs N, Dzikus N, Hoelzen J, Zill T, et al. Refueling of LH2 Aircraft— Assessment of Turnaround Procedures and Aircraft Design Implication. Energies 2022;15(7):2475. https://doi.org/10.3390/en15072475.

[15] CORDIS. 2000 Liquid hydrogen fuelled aircraft - system analysis (CRYOPLANE) [First accessed on: 13.07.2023 - Available from: https://cordis.europa.eu/project/id/G4RD-CT-2000-00192/de.].

[16] Westenberger A. Cryoplane–Hydrogen Aircraft. H2 Expo (11 October Hamburg 2003). 2003.http://www.h2hh.de/downloads/Westenberger.pdf.

[17] Airbus. 2022 The ZEROe demonstrator has arrived [First accessed on: 13.07.2023 - Available from: https://www.airbus.com/en/newsroom/stories/2022-02-the-zeroe-demonstrator-has-arrived.].

[18] Carson L, Davis G, Versaw E, Cunnington Jr G, Daniels E. Study of methane fuel for subsonic transport aircraft. 1980. https://ntrs.nasa.gov/citations/19800024025.

[19] Eurocontrol The challenge of long-haul flight decarbonisation: When can cutting-edge energies and technologies make a difference? [press release]. 2023.

[20] Marty K. Bradley, Droney CK. Subsonic Ultra Green Aircraft Research - Phase II: N+4 Advanced Concept Development. 2012. https://ntrs.nasa.gov/api/citations/20120009038/downloads/20120009038.pdf.

[21] Jane O'Malley NP, Stephanie Searle. Estimating sustainable aviation fuel feedstock availability to meet growing European Union demand2021.

[22] Jaramillo P, S. Kahn Ribeiro, P. Newman, S. Dhar, O.E. Diemuodeke, T. Kajino, D.S. Lee, S.B. Nugroho, X. Ou, A. Hammer Strømman, J. Whitehead. Transport. In IPCC, 2022: Climate Change 2022: Mitigation of Climate Change. Contribution of Working Group III to the Sixth Assessment Report of the Intergovernmental Panel on Climate Change. 2022.

[23] European Parliament. Renewable energy directive 2018/2001/EU. 2022.

[24] Pipitone G, Zoppi G, Pirone R, Bensaid S. Sustainable aviation fuel production using in-situ hydrogen supply via aqueous phase reforming: A techno-economic and life-cycle greenhouse gas emissions assessment. J Clean Prod 2023;418:138141. https://www.sciencedirect.com/science/article/pii/S0959652623022990.

[25] Raab M, Körner R, Dietrich R-U. Techno-economic assessment of renewable hydrogen production and the influence of grid participation. Int J Hydrogen Energy 2022;47(63):26798–811. https://doi.org/10.1016/j.ijhydene.2022.06.038.

[26] Raab M, Dietrich R-U. Techno-economic assessment of different aviation fuel supply pathways including LH2 and LCH4 and the influence of the carbon source. Energ Conver Manage 2023;293:117483. https://doi.org/10.1016/j.enconman.2023.117483.

[27] Dray L, Schäfer AW, Grobler C, Falter C, Allroggen F, Stettler MEJ, et al. Cost and emissions pathways towards net-zero climate impacts in aviation. Nat Clim Chang 2022;12(10):956–62. https://doi.org/10.1038/s41558-022-01485-4.

[28] Gelhausen MC, Berster P, Wilken D. Airport capacity constraints and strategies for mitigation: A global perspective. Academic Press; 2019.

[29] Cirium. FLEETS ANALYZER [First accessed on: 13.07.2023 - Available from: https://www.cirium.com/solutions/fleets-analyzer/.].

[30] OAG. GLOBAL AIRLINE SCHEDULES DATA [First accessed on: 13.07.2023 - Available from: https://www.oag.com/airline-schedules-data.].

[31] Schaefer M. Development of a Forecast Model for Global Air Traffic Emissions 2012.

[32] Commission E. Flightpath 2050 – Europe's vision for aviation – Maintaining global leadership and serving society's needs. Publications Office; 2011.

[33] Withers MR, Malina R, Gilmore CK, Gibbs JM, Trigg C, Wolfe PJ, et al. Economic and environmental assessment of liquefied natural gas as a supplemental aircraft fuel. Prog Aerosp Sci 2014;66:17–36. https://ui.adsabs.harvard.edu/abs/2014PrAeS.66...17W.

[34] Troeltsch FM, Engelmann M, Scholz AE, Peter F, Kaiser J, Hornung M. Hydrogen Powered Long Haul Aircraft with Minimized Climate Impact. AIAA AVIATION 2020 FORUM.

[35] Bradley MK, Droney CK. Subsonic ultra green aircraft research phase II: N+ 4 advanced concept development. 2012. https://ntrs.nasa.gov/citations/20120009038.

[36] Rompokos P, Kissoon S, Roumeliotis I, Nalianda D, Nikolaidis T, Rolt A. Liquefied Natural Gas for Civil Aviation. Energies 2020;13(22):5925. https://doi.org/10.3390/en13225925.

[37] Atmosfair. Ergebnisse Emissionsberechnung: atmosfair; [First accessed on: 24.01.2023 - Available from: https://www.atmosfair.de/de/kompensieren/flug/.].

[38] Raymer D. Aircraft design: a conceptual approach. American Institute of Aeronautics and Astronautics, Inc.; 2012.

[39] Markish J. Valuation techniques for commercial aircraft program design. Massachusetts Institute of Technology; 2002.

[40] Brenschede A. BRouter [First accessed on: 13.06.2023 - Available from: https://brouter.de/brouter-web/.].

[41] Van der Meulen S, Grijspaardt T, Mars W, Van der Geest W, Roest-Crollius A, Kiel J. Cost figures for freight transport–final report. Panteia. 2020:1–85.

[42] VTG. Flüssiggas-Kesselwagen für tiefkalte Gase - Datenblatt VTG-Typ G91.111D [First accessed on: 13.07.2023 - Available from: https://www.vtg.de/fluessiggas-kesselwagen-fuer-tiefkalte-gase-zagkks.].

[43] wascosa. Kesselwagen [First accessed on: 13.07.2023 - Available from: https://www.wascosa.ch/de/wagenpark/kesselwagen.].

[44] "Verfondern K. Safety consideration on liquid hydrogen. Germany: ; Forschungszentrum Juelich GmbH Institut fuer Energieforschung (IEF) Sicherheitsforschung und Reaktortechnik (IEF-6); 2008. Medium: ED; Size: 178 pages p.

[45] Amos WA. Costs of storing and transporting hydrogen. National Renewable Energy Lab.(NREL), Golden, CO (United States); 1999.

[46] mobile.de. Search for new tank trailers 2023 [First accessed on: 13.07.2023 - Available from: www.mobile.de.].

[47] Reuß M, Grube T, Robinius M, Preuster P, Wasserscheid P, Stolten D. Seasonal storage and alternative carriers: A flexible hydrogen supply chain model. Appl Energy 2017;200:290–302. https://doi.org/10.1016/j.apenergy.2017.05.050.

[48] Mariani F, Gonzalez D, Ribas X. Cost analysis of LNG refuelling stations. Studija Brussels: European Commision: FP7 LNG Blue Corridors, LNG BC D. 2016; 3.

[49] DIE GÜTERBAHNEN. 4 Promille - Empfohlene maximale Steigung für neu gebaute Schienenstrecken [First accessed on: 14.07.2023 - Available from: https://die-gueterbahnen.com/news/zahl-des-tages/4.html.].

[50] Luftfahrtmagazin. 2012 Neue Kerosin-Pipeline am Frankfurter Flughafen [First accessed on: 20.07.2023 - Available from: https://www.luftfahrtmagazin.de/aviation/zivile-luftfahrt/neue-kerosin-pipeline-am-frankfurter-flughafen-181567.html.].

[51] MarineTraffic. 2023 Global Ship Tracking Intelligence [First accessed on: 12.06.2023 - Available from: https://www.marinetraffic.com/en/ais/home/centerx:8.470/centery:50.024/zoom:14.].

[52] Streta. 2023 Inland tankbarge [First accessed on: 12.06.2023 - Available from: https://stetra.de/en/fleet/inland-tankbarge/.].

[53] Ship Technology. 2014 LNG Greenstream Tanker [First accessed on: 27.03.2024 - Available from: https://www.ship-technology.com/projects/lng-greenstream-tanker/.].

[54] Kawasaki. 2019 World's First Liquefied Hydrogen Carrier SUISO FRONTIER Launches Building an International Hydrogen Energy Supply Chain Aimed at Carbon-free Society [First accessed on: 21.07.2023 - Available from: https://global.kawasaki.com/en/corp/newsroom/news/detail/?f=20191211_3487.].

[55] Hekkenberg RG, editor A building cost estimation method for inland ships. European inland waterway navigation conference Budapest, Hungary; 2014.

[56] IGU. 2023 2022 WORLD LNG REPORT [First accessed on: 21.07.2023 - Available from: https://www.igu.org/resources/world-lng-report-2022/.].

[57] Skytanking. Verhalten bei Störfällen [First accessed on: 14.07.2023 - Available from: https://www.skytanking.com/fileadmin/user_upload/downloads/Skytanking_Munich_Oeffentl-Info-11-Verhalten-bei-Stoerfaellen_de_01.pdf.].

[58] Walter. D. 2021 Aiwanger wirbt für grünes Kerosin in Bayern - „dem Flugkunden das schlechte Gewissen nehmen" [First accessed on: 04.07.2023 - Available from: https://www.merkur.de/lokales/erding/flughafen-muenchen-ort60188/flughafen-muenchen-kerosingruen-oeko-aiwanger-passagiere-gewissen-91060762.html.].

[59] Woods DR. Rules of thumb in engineering practice. John Wiley & Sons; 2007.

[60] Baker. LNG Storage Tank Cost Analysis. Interiorgas. 2013. https://www.interiorgas.com/wpdm-package/lng-storage-tank-cost-analysis/.

[61] Peters MS, Timmerhaus KD, West RE. Plant design and economics for chemical engineers. McGraw-Hill New York; 2003.

[62] Hromadka M, Cíger A. Hydrant refueling system as an optimisation of aircraft refuelling. Transport Problems. 2015;10. https://yadda.icm.edu.pl/baztech/element/bwmeta1.element.baztech-0269da72-0918-4697-b410-a83b9532107e/c/Hromadka.pdf.

[63] Fraport. Facts and figures [First accessed on: 14.07.2023 - Available from: https://www.fraport.com/en/our-group/about-us/facts—figures.html.].

[64] International Airport Review. 2021 Sustainable aviation fuel to be used at Munich Airport from June 2021 [First accessed on: 02.08.2023 - Available from: https://www.internationalairportreview.com/news/158439/sustainable-aviation-fuel-munich-airport/.].

[65] Stolzenburg K, Berstad D, Decker L, Elliott A, Haberstroh C, Hatto C, et al., editors. Efficient liquefaction of hydrogen: results of the IDEALHY project. Proceedings of the XXth Energie—Symposium, Stralsund, Germany; 2013.

[66] Raab M, Maier S, Dietrich R-U. Comparative techno-economic assessment of a large-scale hydrogen transport via liquid transport media. Int J Hydrogen Energy 2021;46(21):11956–68. https://doi.org/10.1016/j.ijhydene.2020.12.213.

[67] Songhurst B. LNG plant cost reduction 2014–18. 2018. https://ora.ox.ac.uk/objects/uuid:f5bebe7f-1559-47ad-a80a-018ab9d78061.

[68] Fuchte J, Nagel B, Gollnick V. Twin Aisle for Short Range Operations - An Economically Attractive Alternative? 12th AIAA Aviation Technology, Integration, and Operations (ATIO) Conference and 14th AIAA/ISSMO Multidisciplinary Analysis and Optimization Conference.

[69] Swoodoo. Billige Flüge und Billigflüge suchen und buchen [First accessed on: 13.06.2023 - Available from: https://www.swoodoo.com/.].

[70] IATA. 2023 Jet Fuel Price Monitor [First accessed on: 26.01.2023 - Available from: https://www.iata.org/en/publications/economics/fuel-monitor/.].

[71] Cardella U, Decker L, Sundberg J, Klein H. Process optimization for large-scale hydrogen liquefaction. Int J Hydrogen Energy 2017;42(17):12339–54. http://www.sciencedirect.com/science/article/pii/S0360319917311746.

[72] Al-Breiki M, Bicer Y. Liquified hydrogen vs. liquified renewable methane: Evaluating energy consumption and infrastructure for sustainable fuels. Fuel 2023;350(128779). https://www.sciencedirect.com/science/article/pii/S0016236123013923.

[73] Proesmans P-J, Vos R, editors. Comparison of future aviation fuels to minimize the climate impact of commercial aircraft. AIAA Aviation 2022 Forum; 2022.

[74] Barke A, Thies C, Melo SP, Cerdas F, Herrmann C, Spengler TS. Maintenance, repair, and overhaul of aircraft with novel propulsion concepts – Analysis of environmental and economic impacts. Procedia CIRP. 2023;116:221–6. https://doi.org/10.1016/j.procir.2023.02.038.
[75] Svensson F, Hasselrot A, Moldanova J. Reduced environmental impact by lowered cruise altitude for liquid hydrogen-fuelled aircraft. Aerosp Sci Technol 2004;8(4):307–20. https://www.sciencedirect.com/science/article/pii/S1270963804000015X.
[76] Sand M, Skeie RB, Sandstad M, Krishnan S, Myhre G, Bryant H, et al. A multi-model assessment of the global warming potential of hydrogen. Commun Earth Environ 2023;4(1):203. https://doi.org/10.1038/s43247-023-00857-8.
[77] Nojoumi H, Dincer I, Naterer GF. Greenhouse gas emissions assessment of hydrogen and kerosene-fueled aircraft propulsion. Int J Hydrogen Energy 2009;34(3):1363–9. https://www.sciencedirect.com/science/article/pii/S0360319908015048.
[78] Yahyaoui M. The use of LNG as aviation fuel: combustion and emission. In: 13th International Energy Conversion Engineering Conference; 2015. p. 3730.

4 Results and discussion

The details of the comparative “well-to-wake” evaluation are discussed across the corresponding papers. In this chapter, the result of the analysis is placed in the context of the discussion on how modern society can be decarbonised. Then a detailed breakdown of the overall cost is given to indicate the most relevant contributors. Further, an analysis is conducted to evaluate the influence of the passenger capacity on the overall results.

4.1 Contextualization of the results

This thesis examines the question of how the decarbonisation of the aviation industry can be achieved in the most economical way. In Publication III, the costs are evaluated for three exemplary aircraft sizes. The lowest costs for the corresponding aircraft type are shown in Figure 11 together with a comparison if the SAF aircraft had been fuelled with fossil Jet A-1 at a fuel price of 0.66 €/kg.

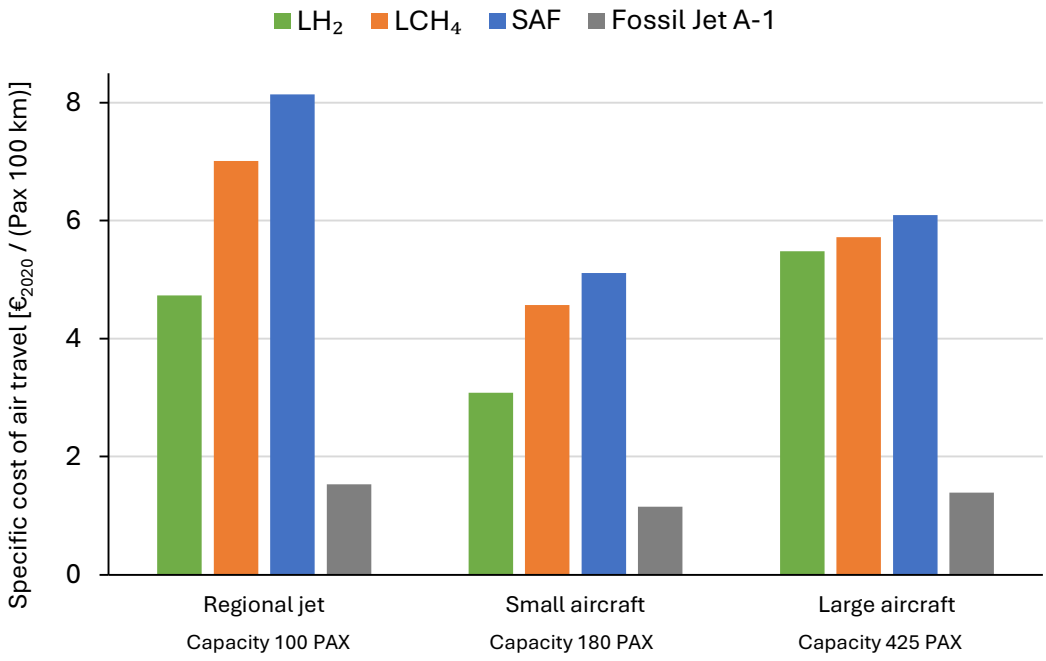

Figure 11: Lowest specific costs for flying in $\frac{€_{2020}}{PAX\ 100\ km}$

The most dominant aspect in Figure 11 is the vast cost increase from replacing fossil Jet A–1 with any of the considered fuels from this thesis. While the cost range of fossil Jet A–1 is between $1.15 - 1.50\ \frac{€_{2020}}{PAX\ 100\ km}$, the costs double at least for the case of LH_2 usage in small aircraft and increase by a factor of 7 for SAF usage in regional aircraft.

These factors alone do not give an indication of whether substituting fossil kerosene with electricity-based fuels is an economical or a costly way of reducing CO_2 emissions. This is addressed by determining the abatement costs for not emitting fossil CO_2. These are determined with Equation 7:

Equation 7: Determination of CO_2 abatement costs

$$C_{*\text{Renewable fuel}*}\left[\frac{€_{2020}}{t_{CO_2}}\right] = \frac{\text{Costs}_{*\text{Renewable fuel}*} - \text{Costs}_{Fossil\ Jet\ A-1}}{CO_2 \text{ emissions from fossil Jet A} - 1}$$

This is a simplified approach of determining CO_2 gas abatement costs. Since no life cycle assessment is conducted, the values only give a certain indication and do not consider the carbon footprint of the renewable fuels or other aspects like land use or water use. In Table 6, the corresponding CO2 abatement costs are given for every fuel type and every considered aircraft size.

Table 6: Estimated CO_2 abatement costs for the corresponding fuel and aircraft types

	Fuel demand	CO_2 emissions	C_{LH_2}	C_{LCH_4}	C_{SAF}
	$\frac{kg_{Jet\ A-1}}{PAX\ 100\ km}$	$\frac{kg_{CO_2}}{PAX\ 100\ km}$	$\frac{€_{2020}}{t_{CO_2}}$	$\frac{€_{2020}}{t_{CO_2}}$	$\frac{€_{2020}}{t_{CO_2}}$
Regional Jet	2.33	7.36	1,374	2,353	2,838
Small aircraft	1.47	4.63	1,316	2,332	2,700
Large aircraft	1.82	5.74	2,251	2,383	2,587

In the most economical way, the CO_2 abatement costs are slightly above 1300 $€_{2020}/t_{CO_2}$, though for SAF usage they do not fall below 2500 $€_{2020}/t_{CO_2}$. This means, that phasing out fossil-based fuels from the aviation industry is a cost intensive option for reducing global CO_2 emissions, as it is shown by comparing it with other processes were a fossil-based process is adapted that it does not emit CO_2 anymore. An example with renewable electricity production is made and the following exemplary values are considered:

- A wind turbine with levelized costs of electricity of 50 €/MWh and CO_2 emissions caused by the production the wind turbine of 50 kg_{CO_2}/MWh
- A coal fired power plant with levelized costs of electricity of 20 €/MWh and CO_2 emissions caused from burning coal of 750 kg_{CO_2}/MWh

In this case, the CO_2 abatement costs of changing the electricity source from a fossil to renewable source would be 43 €/t_{CO_2}. Since it is not only the aviation industry or the electricity sector that needs to reduce its CO_2 emissions, but every other aspect of the

society, an assessment like this is helpful to evaluate where CO_2 emissions can be reduced in the most economical way.

Another exemplary value is the price of CO_2 emission allowances handed out by the EU. They have reached values of 100 €/ t_{CO_2} during 2023 (102). It is the intention of the EU to introduce a CO_2 emission allowance system that includes the emissions from the traffic sector by the year 2027 (103). But even with a system in place, the emission allowances need to be more expensive than the values given in Table 6, i.e. at least a 29-fold increase from 45 to 1300 €/t_{CO_2} (103). Regarding the introductory question, how can the aviation industry reduce its CO_2 emissions while at the same time, demand for air travel is predicted to grow in the next decades. If these costs are directly transferred to the passengers, the demand for air travel will most likely not increase but there will be socio-economic and political challenges. It should be assessed if it is more economic to capture and sequestrate CO_2 instead of producing electricity-based fuels.

Before this harsh conclusion is drawn it is relevant to know how the overall costs are composed. Therefore, in the next section a detailed breakdown of the overall costs is given to indicate the most relevant contributors.

4.2 Breakdown of the overall costs

In the following figures, the cost breakdown is depicted for utilizing the respective fuels in small aircraft, thus with a capacity of 180 passengers. As in section 4.1, the lower threshold costs for the corresponding fuel types will be considered. The ordinate has the same range in every figure so that no false impression will be given. Every cost is assigned to a certain step (A-F) that has been introduced in section 1.3.2. The overall costs are sorted in ascending order of its overall contribution. The first ten cost contributors are also assigned a certain colour to indicate the step. Green for step A, dark blue for step B black for step C (only valid for LH_2) and red for step F.

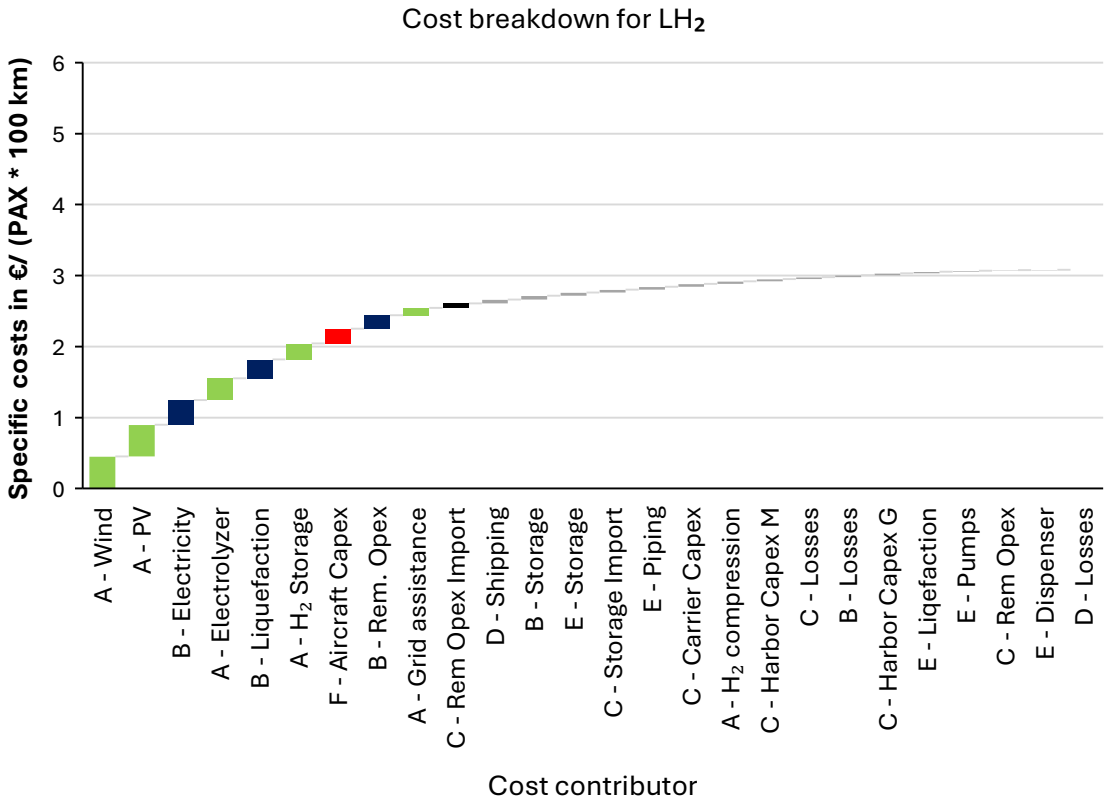

Figure 12: Detailed cost breakdown for utilizing LH_2 in small aircraft

In Figure 12 it is shown that the costs are mainly caused by step A in which hydrogen is produced from renewable energy and the subsequent liquefaction process in step B. The costs for aircraft usage plays only a minor role in the overall costs. Even if the costs for the aircraft procurement would increase by an exemplary factor of 3, the overall costs would hardly be affected. This issue is discussed in section 4.3 in more detail. The renewable electricity supply in step A and external electricity for the liquefaction process in step B account for more than a third of the overall costs. The term “Rem OPEX” is used to summarize the costs for labour, maintenance, administrative, plant overhead etc. The absolute and relative shares of every step are given in Figure 15.

In Figure 13 the cost breakdown is given for utilizing LCH_4 in small aircraft. Again, every cost is assigned to a certain step (A-F).

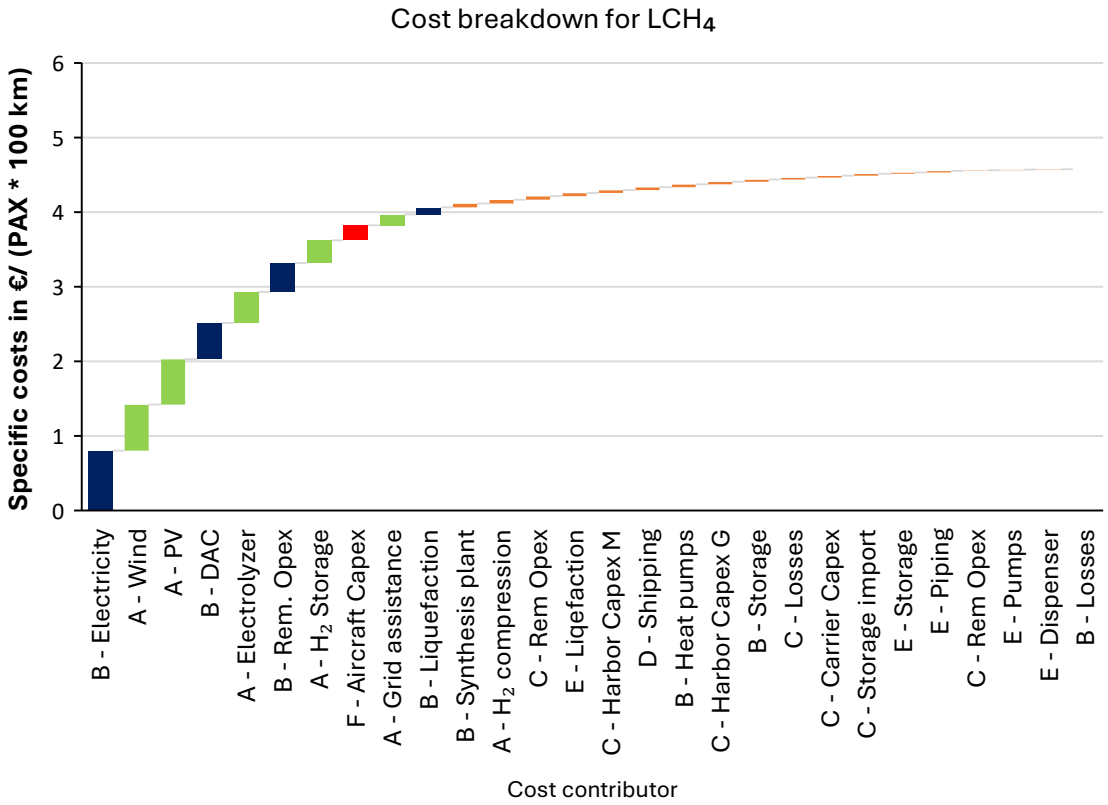

Figure 13: Detailed cost breakdown for utilizing LCH_4 in small aircraft

While the cost shares for renewable and external electricity account for 1.25 $\frac{€}{PAX\ 100\ km}$ in the case of LH_2 as aviation fuel, this value increases to 2.03 $\frac{€}{PAX\ 100\ km}$ in the case of LCH_4. This is an increase by more than 60 %. The reason for this increase has been described in Publication II. They are partially caused by energetic losses resulting from the methanation reaction. Another cause of the increase is the additional external electricity demand for the carbon capture unit. The cost increase resulting from the methanation reaction is also observed for the share of "A – Wind", which accounts for 0.45 $\frac{€}{PAX\ 100\ km}$ in the case of LH_2 and for 0.62 $\frac{€}{PAX\ 100\ km}$ in the case of LCH_4. Even though the amount of hydrogen fed to the conversion process is the same.

In Figure 14 the cost breakdown is given for utilizing SAF in small aircraft. Again, every cost is assigned to a certain step (A-F).

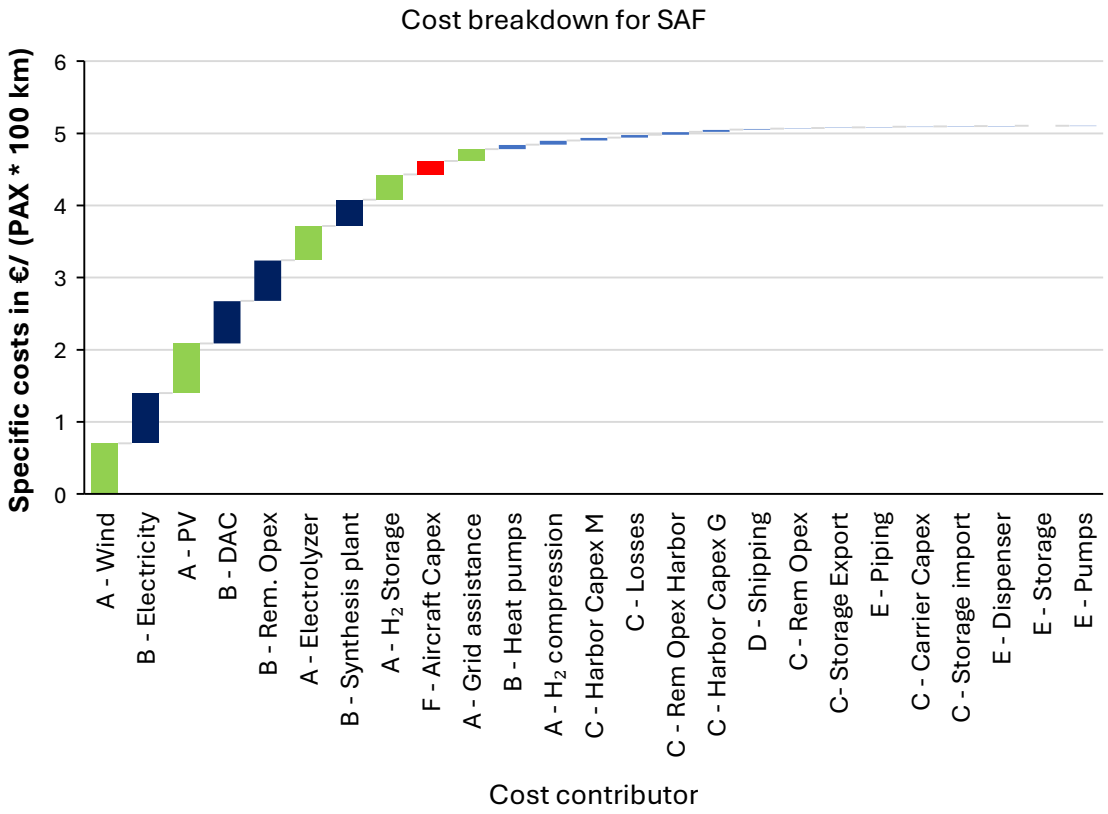

Figure 14: Detailed cost breakdown for utilizing SAF in small aircraft

The cost shares for renewable and external electricity account for 2.10 $\frac{€}{PAX\ 100\ km}$ when SAF is utilized in small aircraft. The share of "A – Wind" accounts for 0.70 $\frac{€}{PAX\ 100\ km}$, again a slight increase compared to LCH_4. The cost share for DAC is 0.48 $\frac{€}{PAX\ 100\ km}$ in the case of LCH_4 and 0.59 $\frac{€}{PAX\ 100\ km}$ in the case of SAF. This higher cost share can be explained by the fact, that in the case of SAF more carbon atoms are required for the same hydrogen feed.

To evaluate the influence of the different steps, the absolute and relative share for every step and every fuel type is given in Figure 15.

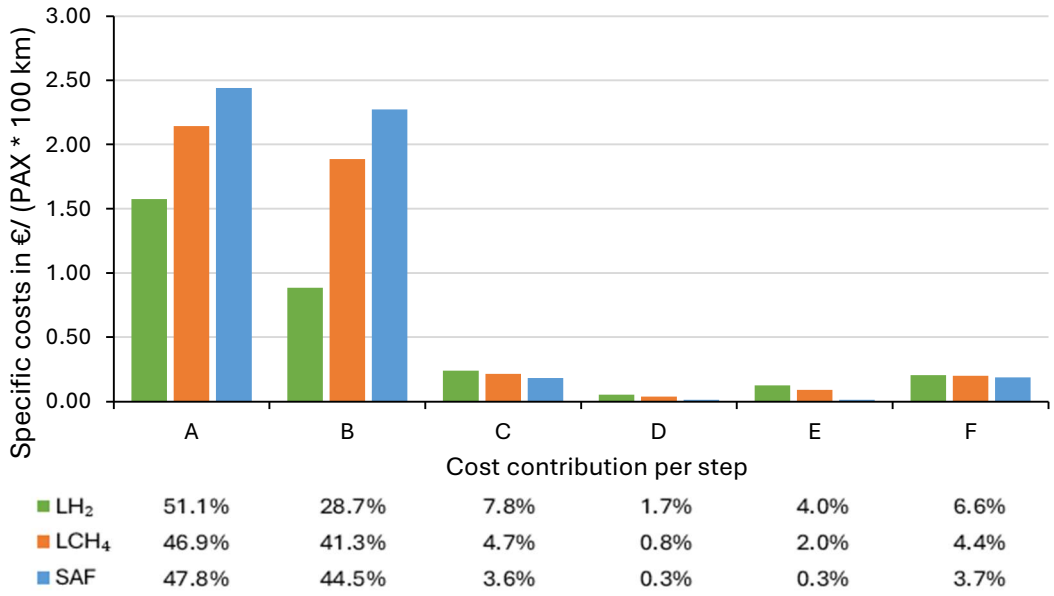

Figure 15: Absolute and relative cost share of the corresponding steps for small aircraft

It is shown that step A is the most expensive part of the chain for every fuel. Roughly 50 % of the costs of every fuel type account for this step. The high cost share of step B for carbon-based fuels can be substantiated by the necessity of a DAC unit instead of a liquefaction unit for LH_2. The costs for domestic distribution which are represented by step D as well as the costs for the required changes in airport infrastructure, represented by step E have a rather low influence on the overall costs.

In the previous section the question has been addressed, if it is more economic to capture and sequestrate CO_2 instead of producing electricity-based fuels. The cost breakdowns given in Figure 12 - Figure 15 show, that the most relevant cost driver are the costs of electricity. In step A and B, the electricity supply (including the share of Wind and PV) accounts for 44 %, 47 % and 44 % in the case LH_2, LCH_4 and SAF, respectively. While “electricity costs” might be a single value for the results of this thesis, they are also made up of numerous contributors like the procurement and installation costs of solar panels and wind turbines, inverters, copper, power lines etc. Future research needs to elaborate, how the costs of electricity can be reduced. This will be beneficial, not only for reducing the costs of renewable fuels, but also for every other aspect of the modern society that is effected by the energy transition. Current costs for carbon capture systems are projected to cost 226 – 835 \$/t $_{CO_2}$ as shown by Sievert et al. (104). With first carbon capture and sequestration projects on the way with the “northern lights” project as an example (105) and current discussion about carbon sequestration in Germany (106), this pathway might be a more economical solution to decarbonize the aviation industry. The introduction of electricity-based fuels, be it LH_2, LCH_4 or SAF, is

therefore an option to decarbonize the aviation industry that is not directly driven by economic incentives but other aspects. These could be technical limitations or a low social acceptance of carbon sequestration technologies, political reasons regarding energy dependencies, drying up of oil wells, different combustion behaviour of renewable fuels, reduction of local noise and particulate emissions etc.

4.3 Influence of passenger capacity

The analysis conducted in this thesis is based on numerous input variables with varying certainty levels. Many variables are not subject to uncertainties like the kinetics of a methanation process, while others are subject to many uncertainties. Especially the data of aircraft utilizing cryogenic fuels is highly uncertain since no reference aircraft exists today. The data involved is compromised by the costs, fuel consumption and the passenger capacity. Especially the last aspect is highly uncertain due to the low volumetric energy density of the fuels and its implications on the layout of the aircraft. Therefore, it has to be discussed how these variables influence the overall outcome of the comparison between the different fuels. Figure 15 shows, that the costs of aircraft utilizing the different fuels are not too significant. Even a threefold increase of the aircraft costs would not change the current ranking between the different fuels, though the difference between LCH_4 and SAF would be reduced to 0.10 $\frac{€}{PAX\ 100\ km}$.

The influence of the passenger capacity is discussed in the following. In Publication III, a passenger capacity of 180 PAX is assumed for small aircraft together with a loading factor of 80 %. Thus 144 passengers are on board. For the sake of simplicity, the loading factor is not changed in the further course. Table 7 states the passenger capacities of small aircraft, where for the maximum distance that can be covered (of the flight routes considered in Publication III), the specific costs are equal for every fuel type.

Table 7: Adaption of passenger capacities for a small aircraft

	LH_2	LCH_4	SAF
Passenger capacity	110	160	180
Capacity utilisation	88	128	144

Therefore, a small aircraft that utilizes LH_2 needs to have a capacity of 110 passenger or more in order to be as economic as an aircraft utilizing SAF. This statement is only valid for larger distances where the share of fuel costs plays a more dominant role than the depreciation costs of the aircraft. This is shown in Figure 16. For shorter distances covered, the seat capacity of LH_2 and LCH_4 aircraft must be higher than the values indicated in Table 7 in order to be as economic as SAF aircraft. Otherwise, the introduction of cryogenic fuels in the aviation sector cannot be economically justified.

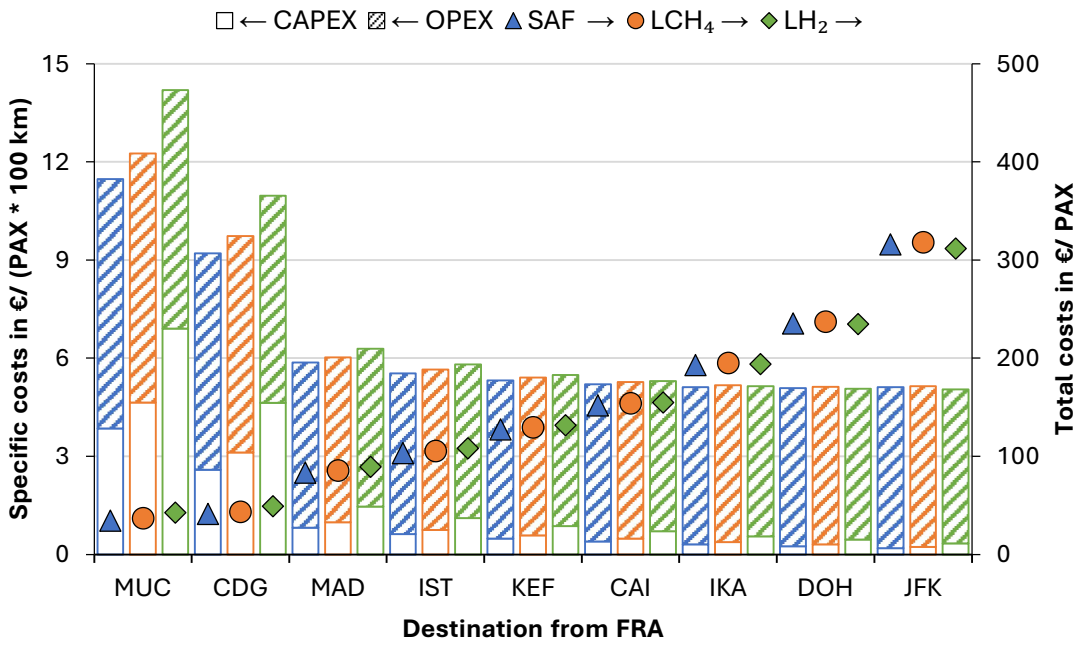

Figure 16: Cost of flying with a small sized aircraft – considering the capacity utilisation of Table 7

5 Summary and outlook

In the present thesis, a well-to-wake techno-economic evaluation is conducted on how the aviation industry can phase out fossil fuels by the introduction of SAF and cryogenic fuels. The entire chain, from the generation of renewable electricity in a remote location to the required modifications to airport infrastructure and the introduction of new aircraft, has been taken into account. Each step has been subjected to in-depth analysis and the findings have been published in the relevant academic literature. In light of the overarching objective of reducing CO_2 emissions, it is demonstrated that, given the high costs of electricity-based fuels, carbon sequestration could represent an alternative for reducing the net carbon emissions of the aviation industry, provided that the regulatory framework conditions permit it and credibility is achievable. However, this is not assessed in the present thesis.

If carbon sequestration is not a viable solution, utilizing SAF is the most expensive option to phase out fossil fuels. Consequently, a shift to cryogenic fuels will prove to be a more economically viable long-term strategy. Nevertheless, SAF permits the utilization of existing aircraft and infrastructure, and in certain instances, it will almost certainly remain a necessity, e.g. in the case of certain military applications or rescue helicopters.

A significant amount of research is currently being conducted with the aim of introducing LH_2 as an aviation fuel. This includes research into aircraft design and fuel cells, among other areas. Hydrogen has the advantage that no carbon is required and thus no CO_2 is released during utilization. However, its low volumetric energy density presents a challenge, especially when longer distances must be covered. Many research findings can be transferred to aircraft utilizing LCH_4. As LCH_4 would be burned in turbines and there is already a global supply chain in place for LNG, these aircraft could be realized in a faster fashion.

This thesis considered a fuel supply chain from a remote location to Germany. But in the real world there are several other options how fuels can be produced and the production potential of every fuel source has to be evaluated in the context of the global energy system. The production potential of biogenically produced methane needs to be evaluated and compared to the CO_2 abatement costs of this thesis. Moreover, methane is less hazardous from a safety perspective, exhibiting a lower explosive limit than hydrogen and being easier to handle.

Another aspect that needs to be studied is a thorough life cycle assessment that considers losses along the pathway as well as the fuel utilization (including non-CO_2 emissions). When cryogenics are handled boil-off losses are unavoidable. Both methane

and hydrogen have a global warming potential when emitted to the atmosphere. Also, water emissions during fuel utilization have to be taken into account. The amount of water vapor emitted for every energy unit that is utilized is highest for LH_2. These aspects will influence the net benefit of these fuels compared to fossil fuels and again raise the question whether it is worth the effort.

This thesis ends with a personal comment:

It should be the overarching target to reduce the effects from human behaviour on the climate. It is not the economies of the countries that must be “saved” but the livelihood of the human race in harmony with nature on planet earth. In order to achieve this, humanity must agree on the following statement: “After every interaction with the environment, the previously found state must be restored”. This is not only a personal opinion but also intergenerational justice. While this is of course not possible when a tree is cut down or during hunting or fishing, but it is applicable on longer time frames. This includes the CO_2 emissions. Every kg of CO_2 emitted from an individual action must be taken out of the atmosphere in a reasonable time frame and the person who caused this emission is responsible for that.

Aviation based on renewable fuels is possible, not at current costs but still affordable. Since it is a global market, politicians around the world must accept on global rules. The current European initiative “ReFuelEU Aviation” is disadvantageous towards european airlines since for a two leg flight (e.g: from Munich to Singapore) having a layover just outside the EU, not the same regulations apply as for a directly connected flight. Without adjustments, this initiative is doomed to failure.

References

1. IATA Resolution on the industry's commitment to reach net zero carbon emissions by 2050 [press release]. IATA2021.
2. UNFCCC. 2015 The Paris Agreement [First accessed on: 20.06.2024 - Available from: https://unfccc.int/process-and-meetings/the-paris-agreement.]
3. Gössling S, Humpe A. The global scale, distribution and growth of aviation: Implications for climate change. Global Environmental Change. 2020;65:102194.https://www.sciencedirect.com/science/article/pii/S0959378020307779
4. FCH-JU. Fuel Cells and Hydrogen 2 Joint Undertaking, Hydrogen-powered aviation : a fact-based study of hydrogen technology, economics, and climate impact by 2050: Publications Office; 2020.
5. European Council. Initiative „ReFuelEU Aviation“: Rat verabschiedet neuen Rechtsakt zur Dekarbonisierung des Luftfahrtsektors 2023.https://www.consilium.europa.eu/de/press/press-releases/2023/10/09/refueleu-aviation-initiative-council-adopts-new-law-to-decarbonise-the-aviation-sector/
6. Sacchi R, Becattini V, Gabrielli P, Cox B, Dirnaichner A, Bauer C, Mazzotti M. How to make climate-neutral aviation fly. Nature Communications. 2023;14(1):3989.https://doi.org/10.1038/s41467-023-39749-y
7. Graver B, Rutherford D, Zheng S. CO_2 Emissions from Commercial Aviation: 2013, 2018, and 2019. ICCT; 2020.
8. IRENA. Biofuels for aviation: Technology brief 2017.
9. IATA. 2021 Net zero 2050: new aircraft technology [First accessed on: 31.08.2023 - Available from: https://www.iata.org/en/iata-repository/pressroom/fact-sheets/fact-sheet-new-aircraft-technology/.]
10. Eurocontrol The challenge of long-haul flight decarbonisation: When can cutting-edge energies and technologies make a difference? [press release]. 2023.
11. Greg Hemighaus, Tracy Boval, John Bacha, Barnes F, Matt Franklin, Lew Gibbs, et al. Aviation Fuels - Technical Review. 2007.
12. ASTM. D7566-22a. Standard Specification for Aviation Turbine Fuel Containing Synthesized Hydrocarbons 2022.
13. IATA. Fact Sheet 2 - Sustainable Aviation Fuel: Technical Certification [First accessed on: 31.08.2023 - Available from: https://www.iata.org/contentassets/d13875e9ed784f75bac90f000760e998/saf-technical-certifications.pdf.]
14. ATAG. Powering global, economic growth, employment, trade links, tourism and support for sustainable development through air transport. 2018.
15. DLR 100 Prozent nachhaltiges Kerosin im Emissions-Check [press release]. DLR, 06.09.2023 2023.
16. Rosegrant MW, Msangi S. Consensus and Contention in the Food-Versus-Fuel Debate. Annual Review of Environment and Resources. 2014;39(1):271-94.https://www.annualreviews.org/doi/abs/10.1146/annurev-environ-031813-132233

17. Tomei J, Helliwell R. Food versus fuel? Going beyond biofuels. Land Use Policy. 2016;56:320-6.https://www.sciencedirect.com/science/article/pii/S0264837715003579
18. Jane O'Malley NP, Stephanie Searle. Estimating sustainable aviation fuel feedstock availability to meet growing European Union demand2021.
19. Habermeyer F, Weyand J, Maier S, Kurkela E, Dietrich R-U. Power Biomass to Liquid — an option for Europe's sustainable and independent aviation fuel production. Biomass Conversion and Biorefinery. 2023.https://doi.org/10.1007/s13399-022-03671-y
20. Eurostat Oil import dependency down to 91.7% in 2021 [press release]. 2023.
21. König D. Techno-ökonomische Prozessbewertung der Herstellung synthetischen Flugturbinentreibstoffes aus CO2 und H2: University of Stuttgart; 2016.
22. Lilium. Introducing the first electric vertical take-off and landing jet [First accessed on: 31.08.2023 - Available from: https://lilium.com/.]
23. Barzkar A, Ghassemi M. Electric Power Systems in More and All Electric Aircraft: A Review. IEEE Access. 2020;8:169314-32
24. Schäfer AW, Barrett SRH, Doyme K, Dray LM, Gnadt AR, Self R, et al. Technological, economic and environmental prospects of all-electric aircraft. Nature Energy. 2019;4(2):160-6.https://doi.org/10.1038/s41560-018-0294-x
25. Winter CJ. Hydrogen in high-speed air transportation. International Journal of Hydrogen Energy. 1990;15(8):579-95.https://doi.org/10.1016/0360-3199(80)90006-3
26. Airbus The ZEROe demonstrator has arrived [press release]. Airbus2022.
27. Zeroavia. Truly Clean Aviation: Hydrogen-electric engines for zero-emission flight [First accessed on: 31.08.2023 - Available from: https://zeroavia.com/.]
28. DLR Ein Flugzeug wird zum fliegenden Wasserstofflabor [press release]. DLR, 06.09.2023 2023.
29. H2Fly. Breaking the hydrogen barrier. [First accessed on: 31.08.2023 - Available from: https://www.h2fly.de/.]
30. Lufthansa. 2023 Airbus A380-800 [First accessed on: 16,10.2023 - Available from: https://www.lufthansagroup.com/de/unternehmen/flotte/lufthansa-und-regionalpartner/airbus-a380-800.html.]
31. Carson L, Davis G, Versaw E, Cunnington Jr G, Daniels E. Study of methane fuel for subsonic transport aircraft. 1980.https://ntrs.nasa.gov/citations/19800024025
32. Yahyaoui M, editor The Use of LNG as Aviation Fuel: Combustion and Emission. 13th International Energy Conversion Engineering Conference; 2015.
33. IGU. WORLD LNG REPORT. 2023.
34. Derwent RG. Global Warming Potential (GWP) for Methane: Monte Carlo Analysis of the Uncertainties in Global Tropospheric Model Predictions. Atmosphere. 2020;11(5):486.https://www.mdpi.com/2073-4433/11/5/486
35. Enzmann F, Mayer F, Rother M, Holtmann D. Methanogens: biochemical background and biotechnological applications. AMB Express. 2018;8(1):1.https://doi.org/10.1186/s13568-017-0531-x
36. Shiva Kumar S, Lim H. An overview of water electrolysis technologies for green hydrogen production. Energy Reports. 2022;8:13793-813.https://www.sciencedirect.com/science/article/pii/S2352484722020625
37. Adelung S. Fischer-Tropsch based Power-to-Liquid process – Technical, economic, uncertainty and sensitivity analysis 2023.

38. de Klerk A. Fischer–Tropsch refining: technology selection to match molecules. Green Chemistry. 2008;10(12):1249-79
39. Albrecht FG, König DH, Baucks N, Dietrich R-U. A standardized methodology for the techno-economic evaluation of alternative fuels – A case study. Fuel. 2017;194:511-26.https://www.sciencedirect.com/science/article/pii/S0016236116312248
40. HIF. 2023 Haru Oni - Demonstration Plant [First accessed on: 05.11.2023 - Available from: https://hifglobal.com/location/haru-oni/.]
41. Engie ENGIE and POSCO Led Consortium to develop a Green Ammonia Project of up to a 1.2 mtpa in Oman [press release]. 2023.
42. BMBF Karliczek: Germany and Namibia form partnership for green hydrogen [press release]. 2021.
43. Hoffmann H. 2023 Hier soll grüner Wasserstoff in gigantischem Ausmaß produziert werden: Spiegel; [First accessed on: 05.11.2023 - Available from: https://www.spiegel.de/ausland/luederitz-namibia-hier-soll-gruener-wasserstoff-in-gigantischem-ausmass-produziert-werden-a-a160205b-2215-4c98-8300-969eba4d3a5e.]
44. Stölzel T. Aus diesen Kraftwerken wird Strom nur 1 Cent pro Kilowattstunde kosten. WirtschaftsWoche. 2023 11.03.2023.
45. Mallapragada DS, Gençer E, Insinger P, Keith DW, O'Sullivan FM. Can Industrial-Scale Solar Hydrogen Supplied from Commodity Technologies Be Cost Competitive by 2030? Cell Reports Physical Science. 2020;1(9):100174. https://www.sciencedirect.com/science/article/pii/S2666386420301855
46. Vartiainen E, Breyer C, Moser D, Román Medina E, Busto C, Masson G, et al. True Cost of Solar Hydrogen. Solar RRL. 2022;6(5):2100487. https://onlinelibrary.wiley.com/doi/abs/10.1002/solr.202100487
47. Schnuelle C, Wassermann T, Fuhrlaender D, Zondervan E. Dynamic hydrogen production from PV & wind direct electricity supply – Modeling and techno-economic assessment. International Journal of Hydrogen Energy. 2020;45(55):29938-52.https://www.sciencedirect.com/science/article/pii/S0360319920330391
48. Szyszka A. Ten years of solar hydrogen demonstration project at Neunburg vorm Wald, Germany. International Journal of Hydrogen Energy. 1998;23(10):849-60.https://www.sciencedirect.com/science/article/pii/S0360319997001729
49. H2orizon. H2ORIZON – ein Meilenstein in der Energiewende [First accessed on: 23.11.2023 - Available from: https://www.h2orizon.de/.]
50. Process. 2024 BASF installiert Stacks für die Wasserstoff-Elektrolyse [08.09.2024]. First accessed on: - Available from: https://www.process.vogel.de/produktion-von-erneuerbarem-wasserstoff-bei-basf-in-ludwigshafen-a-cd3bad49e3f182440244ec05941b96ad/?cmp=nl-98&uuid=9f5dc2e20489bc6f89da51a68ab5ac9b).]
51. Brewer GD. Aviation usage of liquid hydrogen fuel—prospects and problems. International Journal of Hydrogen Energy. 1976;1(1):65-88.https://www.sciencedirect.com/science/article/pii/0360319976900112
52. Korycinski PF. Air terminals and liquid hydrogen commercial air transports. International Journal of Hydrogen Energy. 1978;3(2):231-50. https://doi.org/10.1016/0360-3199(78)90021-6

53. Ramachandran R, Menon RK. An overview of industrial uses of hydrogen. International Journal of Hydrogen Energy. 1998;23(7):593-8. https://www.sciencedirect.com/science/article/pii/S0360319997001122
54. Krasae-in S, Stang JH, Neksa P. Development of large-scale hydrogen liquefaction processes from 1898 to 2009. International Journal of Hydrogen Energy. 2010;35(10):4524-33. https://www.sciencedirect.com/science/article/pii/S0360319910004118
55. Air Liquide Air Liquide inaugurates in the U.S. its largest liquid hydrogen production facility in the world [press release]. 2022.
56. The Korean Economic Daily Korea's SK E&S to produce 30,000 tons of liquid hydrogen per year [press release]. Seo-Woo Jang2022.
57. Berstad DO, Stang JH, Nekså P. Large-scale hydrogen liquefier utilising mixed-refrigerant pre-cooling. International Journal of Hydrogen Energy. 2010;35(10):4512-23. https://www.sciencedirect.com/science/article/pii/S0360319910002363
58. Eckroll J, editor Concepts for Large Scale Hydrogen Liquefaction Plants2017.
59. Cardella U, Decker L, Sundberg J, Klein H. Process optimization for large-scale hydrogen liquefaction. International Journal of Hydrogen Energy. 2017;42(17):12339-54. http://www.sciencedirect.com/science/article/pii/S0360319917311746
60. Al Ghafri SZS, Munro S, Cardella U, Funke T, Notardonato W, Trusler JPM, et al. Hydrogen liquefaction: a review of the fundamental physics, engineering practice and future opportunities. Energy & Environmental Science. 2022;15(7):2690-731. http://dx.doi.org/10.1039/D2EE00099G
61. Drolet B, Gretz J, Kluyskens D, Sandmann F, Wurster R. The euro-québec hydro-hydrogen pilot project [EQHHPP]: demonstration phase. International Journal of Hydrogen Energy. 1996;21(4):305-16. https://www.sciencedirect.com/science/article/pii/0360319995000836
62. Yoshino Y, Harada E, Inoue K, Yoshimura K, Yamashita S, Hakamada K. Feasibility Study of “CO2 Free Hydrogen Chain” Utilizing Australian Brown Coal Linked with CCS. Energy Procedia. 2012;29:701-9. https://www.sciencedirect.com/science/article/pii/S1876610212015020
63. Snyder J World’s first LH2 carrier completes historic voyage [press release]. 2022.
64. Cryolor. Liquid hydrogen transport [First accessed on: - Available from: https://www.cryolor.com/cryogenic-transport/liquid-hydrogen-transport.]
65. Verfondern K. Safety consideration on liquid hydrogen2008.
66. Hoelzen J, Flohr M, Silberhorn D, Mangold J, Bensmann A, Hanke-Rauschenbach R. H2-powered aviation at airports – Design and economics of LH2 refueling systems. Energy Conversion and Management: X. 2022;14:100206. https://www.sciencedirect.com/science/article/pii/S2590174522000290
67. Mangold J, Silberhorn D, Moebs N, Dzikus N, Hoelzen J, Zill T, Strohmayer A. Refueling of LH2 Aircraft—Assessment of Turnaround Procedures and Aircraft Design Implication. Energies. 2022;15(7):2475. https://doi.org/10.3390/en15072475
68. GmbH AD. Liquid Hydrogen Fuelled Aircraft – System Analysis. 2003 24.9.2003.
69. Vietze M, Weiland S. System analysis and requirements derivation of a hydrogen-electric aircraft powertrain. International Journal of Hydrogen Energy. 2022;47(91):38793-810. https://www.sciencedirect.com/science/article/pii/S0360319922041313
70. DLR Brennstoffzellenbasierter Antriebsstrang für Luftfahrzeuge 1,5+ MW [press release]. 2023.

71. Svensson F, Hasselrot A, Moldanova J. Reduced environmental impact by lowered cruise altitude for liquid hydrogen-fuelled aircraft. Aerospace Science and Technology. 2004;8(4):307-20. https://www.sciencedirect.com/science/article/pii/S127096380400015X
72. Sand M, Skeie RB, Sandstad M, Krishnan S, Myhre G, Bryant H, et al. A multi-model assessment of the Global Warming Potential of hydrogen. Communications Earth & Environment. 2023;4(1):203. https://doi.org/10.1038/s43247-023-00857-8
73. MAN ES Storengy rüstet gemeinsam mit MAN Energy Solutions eine französische Kläranlage mit einem Methanisierungsreaktor aus [press release]. 2022.
74. Store and Go. 2016 - 2022 Results and publications of the project [First accessed on: - Available from: https://www.storeandgo.info/index.html.]
75. Li L, Zeng W, Song M, Wu X, Li G, Hu C. Research Progress and Reaction Mechanism of CO2 Methanation over Ni-Based Catalysts at Low Temperature: A Review. Catalysts. 2022;12(2):244. https://www.mdpi.com/2073-4344/12/2/244
76. Omar MNB. Thermodynamic and Economic Evaluation of Existing and Perspective Processes for Liquefaction of Natural Gas in Malaysia: Technische Universitaet Berlin (Germany); 2016.
77. Wikipedia. 2023 Greenstream_(Schiff) [First accessed on: 12.06.2023 - Available from: https://de.wikipedia.org/wiki/Greenstream_(Schiff).]
78. VTG. Flüssiggas-Kesselwagen für tiefkalte Gase - Datenblatt VTG-Typ G91.111D [First accessed on: 13.07.2023 - Available from: https://www.vtg.de/fluessiggas-kesselwagen-fuer-tiefkalte-gase-zagkks.]
79. Volvo. Volvo FH mit Gasantrieb [First accessed on: - Available from: https://www.volvotrucks.de/de-de/trucks/gas-powered/volvo-fh-gas-powered.html.]
80. Marty K. Bradley, Droney CK. Subsonic Ultra Green Aircraft Research - Phase II: N+4 Advanced Concept Development. 2012. https://ntrs.nasa.gov/api/citations/20120009038/downloads/20120009038.pdf
81. Reichert L. Design of an LNG Powered Wide-Body Aircraft and Assessment of CO2 Emissions and Fuel Efficiency Benefits: Technische Universität Hamburg-Harburg; 2015.
82. Gibbs J, Siegel D, Donaldson A. A Natural Gas Supplementary Fuel System to Improve Air Quality and Energy Security. 50th AIAA Aerospace Sciences Meeting including the New Horizons Forum and Aerospace Exposition.
83. DLR Neues Verfahren für nachhaltiges Kerosin aus Methanol [press release]. 05.11.2023 2022.
84. KEROSyN100. Die Defossilisierung der Luftfahrt [First accessed on: 10.11.2023 - Available from: https://www.kerosyn100.de/.]
85. Davis BH. Fischer–Tropsch synthesis: Overview of reactor development and future potentialities. Topics in Catalysis. 2005;32(3):143-68. https://doi.org/10.1007/s11244-005-2886-5
86. Martinelli M, Gnanamani MK, LeViness S, Jacobs G, Shafer WD. An overview of Fischer-Tropsch Synthesis: XtL processes, catalysts and reactors. Applied Catalysis A: General. 2020;608:117740. https://www.sciencedirect.com/science/article/pii/S0926860X20303331
87. Daza YA, Kuhn JN. CO2 conversion by reverse water gas shift catalysis: comparison of catalysts, mechanisms and their consequences for CO2 conversion to liquid fuels. RSC Advances. 2016;6(55):49675-91. http://dx.doi.org/10.1039/C6RA05414E
88. Adelung S, Maier S, Dietrich R-U. Impact of the reverse water-gas shift operating conditions on the Power-to-Liquid process efficiency. Sustainable Energy Technologies and

Assessments. 2021;43:100897. https://www.sciencedirect.com/science/article/pii/S2213138820313242
89. Jin S, Hao Z, Zhang K, Yan Z, Chen J. Advances and challenges for the electrochemical reduction of CO2 to CO: from fundamentals to industrialization. Angewandte Chemie. 2021;133(38):20795-816
90. Suppiah DD, Daud WMAW, Johan MR. Supported Metal Oxide Catalysts for CO2 Fischer–Tropsch Conversion to Liquid Fuels–A Review. Energy & Fuels. 2021;35(21):17261-78. https://doi.org/10.1021/acs.energyfuels.1c02406
91. Pöhlmann F, Jess A. Interplay of reaction and pore diffusion during cobalt-catalyzed Fischer–Tropsch synthesis with CO2-rich syngas. Catalysis Today. 2016;275:172-82. https://www.sciencedirect.com/science/article/pii/S0920586115006355
92. Barrera JL, Hartvigsen JJ, Hollist M, Pike J, Yarosh A, Fullilove NP, Beck VA. Design optimization of integrated cooling inserts in modular Fischer-Tropsch reactors. Chemical Engineering Science. 2023;268:118423. https://www.sciencedirect.com/science/article/pii/S0009250922010089
93. Ineratec Spatenstich für E-Fuel Produktionsanlage in Frankfurt am Main [press release]. 2023.
94. Lufthansa Lufthansa unterstützt die weltweit erste Produktionsanlage für CO2-neutrale, synthetische Flugtreibstoffe [press release]. 2021.
95. Markosyan M DHL, Sasol, HH2E team up for eSAF production in Germany [press release]. 2023.
96. DLR Technologieplattform PtL – Blick in die Zukunft [press release]. 2023.
97. IATA. Jet Fuel Price Monitor [First accessed on: 10.11.2023 - Available from: https://www.iata.org/en/publications/economics/fuel-monitor/.]
98. Adelung S. Global sensitivity and uncertainty analysis of a Fischer-Tropsch based Power-to-Liquid process. Journal of CO2 Utilization. 2022;65:102171. https://www.sciencedirect.com/science/article/pii/S2212982022002906
99. Brynolf S, Taljegard M, Grahn M, Hansson J. Electrofuels for the transport sector: A review of production costs. Renewable and Sustainable Energy Reviews. 2018;81:1887-905. https://www.sciencedirect.com/science/article/pii/S1364032117309358
100. Schemme S, Breuer JL, Köller M, Meschede S, Walman F, Samsun RC, et al. H2-based synthetic fuels: A techno-economic comparison of alcohol, ether and hydrocarbon production. International Journal of Hydrogen Energy. 2020;45(8):5395-414. https://www.sciencedirect.com/science/article/pii/S0360319919318580
101. Detsios N, Theodoraki S, Maragoudaki L, Atsonios K, Grammelis P, Orfanoudakis NG. Recent Advances on Alternative Aviation Fuels/Pathways: A Critical Review. Energies. 2023;16(4):1904. https://www.mdpi.com/1996-1073/16/4/1904
102. Umweltbundesamt. 2023 Der Europäische Emissionshandel [09.05.2024]. First accessed on: - Available from: https://www.umweltbundesamt.de/daten/klima/der-europaeische-emissionshandel#teilnehmer-prinzip-und-umsetzung-des-europaischen-emissionshandels.]
103. Bundesregierung. CO2-Preis steigt auf 45 Euro pro Tonne. 2024.https://www.bundesregierung.de/breg-de/aktuelles/co2-preis-kohle-abfallbrennstoffe-2061622
104. Sievert K, Schmidt TS, Steffen B. Considering technology characteristics to project future costs of direct air capture. resource. 2024.https://doi.org/10.1016/j.joule.2024.02.005

105. equinor. 2024 The Northern Lights project [01.06.2024]. First accessed on: - Available from: https://www.equinor.com/energy/northern-lights.]
106. Tagesschau. 2024 Regierung stimmt für umstrittene CO2-Speicherung [01.06.2024]. First accessed on: - Available from: https://www.tagesschau.de/wirtschaft/abstimmung-co2-speicherung-100.html.]

Appendix

In the following pages, the appendices of the three publications are given in the corresponding order.

Techno-economic assessment of renewable hydrogen production and the influence of grid participation

Supplementary information

S.1. Mathematical model

Table S.1: Variables and subscripts used in the mathematical model (except decision variables)

Variable	***Description***	***Subscript***	***Description***
C	Costs	h	Referring to the individual hour of the year (as a function of time)
η	Efficiency	PV	PV farm
E	Energy	Wind	Wind farm
q	Specific energy demand	Grid	Electric grid
k	Charging factor	Bat	Referring to the battery system (Li-ion, Pb or VRF)
φ	Leakage ratio	ES	Electricity storage
σ	Self-discharge factor	Elec	Electrolyzer
		Comp	Compressor
		CHS	Compressed hydrogen storage
		RTE	Round trip efficiency
		Level	Referring to the level of a storage system

Table S.2: Decision variables

Variable	Unit	Description
x_1	m²	Total area of PV farm
x_2	-	Number of wind turbines
$x_{3,bat}$	kWh	Capacity of a battery storage
x_4	kW	Capacity of electrolyzer
x_5	kW	Power demand for H_2 compression
x_6	kg	Size of H_2 storage

Equation S.1: Objective function of the mathematical model

$$C_{Total} = C_{PV} \cdot x_1 + C_{Wind} \cdot x_2 + \sum_{Bat} C_{Battery} \cdot x_{3,bat} + C_{Elec} \cdot x_4 + C_{Comp} \cdot x_5 + C_{C-St} \cdot x_6 + C(h)_{Grid} \sum_{h=1}^{8760} E_{Grid,h}$$

S.1.1. Constraints

Every hour, the PV energy that is used in the system, $vE_{PV,used}(h)$, is smaller than or equal to the energy provided from the PV farm, $vE_{PV}(h)$, which is obtained by multiplying x_1 with the total solar irradiation $E_{PV,irr}(h)$ and the efficiency of the PV panels η_{PV}. The v is introduced to mark the variable as a *slack variable* (1).

$$vE_{PV}(h) = x_1 \cdot \eta_{PV} \cdot E_{PV,irr}(h)$$
$$vE_{PV,used}(h) \leq vE_{PV}(h)$$

Every hour, the wind energy that is used in the system, $vE_{Wind,used}(h)$, is smaller than or equal to the energy provided from the wind farm,$vE_{Wind}(h)$, which is obtained by multiplying x_2 with the calculated energy generated by one turbine, $E_{Wind,Turbine}(h)$.

$$vE_{Wind}(h) = x_2 \cdot E_{Wind,Turbine}(h)$$
$$vE_{Wind,used}(h) \leq vE_{Wind}(h)$$

Every hour, the energy drawn from the grid, $vE_{Grid,used}(h)$ must be smaller than the maximum allowed quantity set for the simulated case, MAX_{Grid}:

$$vE_{Grid,used}(h) \leq MAX_{Grid}$$

Every hour, the total used energy, $vE_{Total,used}(h)$, is equal to the used energy from PV, wind turbines and the grid.

$$vE_{Total,used}(h) = vE_{PV,used}(h) + vE_{Wind,used}(h) + vE_{Grid,used}(h)$$

Every hour, the total energy used, $vE_{Total,used}(h)$ will be distributed either to an electricity storage medium, $E_{ES-in,bat}(h)$, or towards hydrogen production and processing, $vE_{Dir}(h)$:

$$vE_{Total,used}(h) = vE_{ES-in,bat}(h) + vE_{Dir}(h)$$

Every hour, the electricity storage level for each type, $vE_{ES-level,bat}(h)$, is equal to the electricity storage level of the last hour, $vE_{ES-level,bat}(h-1)$, times the self-discharge coefficient σ_{bat}, minus the outflow of electric energy at that hour, $vE_{ES-out,bat}(h)$, plus the inflow of electricity that hour, $vE_{ES-in,bat}(h)$:

$$vE_{ES-level,bat}(h) = vE_{ES-level,bat}(h-1) \cdot \sigma_{bat} + vE_{ES-in,bat}(h) - vE_{ES-out,bat}(h)$$

Every hour, the useful outflow of electricity from the electricity storage medium, $vE_{ES-useful,bat}(h)$, is the outflow $vE_{ES-out,bat}(h)$ times the round-trip efficiency, $\eta_{ES-RTE,bat}$ of the electricity storage system:

$$vE_{ES-useful,bat}(h) = vE_{ES-out,bat}(h) \cdot \eta_{ES-RTE,bat}$$

Every hour, the electricity storage level, $vE_{ES-level,bat}(h)$, is smaller than or equal to the third decision variable $x_{3,bat}$, which is the size of each respective electricity storage system.

$$vE_{ES-level,bat}(h) \leq x_{3,bat}$$

Every hour, for each electricity storage type, the inflow $vE_{ES-in,bat}(h)$ and outflow $vE_{ES-out,bat}(h)$ of electricity into the electricity storage systems, is smaller than or equal

to the upper limit for charging and discharging, which is calculated by multiplying the third decision variable $x_{3,bat}$ with the charging factor $k_{ES-charge,bat}$ and discharging factor $k_{ES-discharge,bat}$ (which relates storage size to discharging capacity in kW/kWh), respectively:

$$vE_{ES-in,bat}(h) \leq x_{3,bat} \cdot k_{ES-charge,bat}$$
$$vE_{ES-out,bat}(h) \leq x_{3,bat} \cdot k_{ES-discharge,bat}$$

Every hour, the energy distributed towards the hydrogen production directly from the RE sources and the grid, $vE_{Dir}(h)$, as well as the useful outflow from the electricity storage systems, $vE_{ES-useful,bat}(h)$, is equal to the energy consumption by the electrolyzer, $vE_{Elec}(h)$ and the hydrogen storage compressor, $vE_{Comp}(h)$

$$vE_{Dir}(h) + vE_{ES-useful,bat}(h) = vE_{Elec}(h) + vE_{Comp}(h)$$

Every hour, the electrolyzer energy consumption is smaller than or equal to the fourth decision variable x_4, the installed electrolyzer capacity:

$$vE_{Elec}(h) \leq x_4$$

Every hour, the total mass of hydrogen produced, $vM_{H_2}(h)$ is equal to the energy required from the electrolyzer, $vE_{Elec}(h)$ multiplied by the amount of energy required to produce one kilogram of hydrogen, q_{Elec}.

$$vM_{H_2}(h) = vE_{Elec}(h) \cdot q_{Elec}$$

Every hour, the mass of hydrogen produced, $vM_{H_2}(h)$, gets distributed to supply the downstream plant, $vM_{H_2,Dir}(h)$, or towards the hydrogen storage system, $vM_{CHS-in}(h)$.

$$vM_{H_2}(h) = vM_{H_2,Dir}(h) + vM_{CHS-in}(h)$$

Every hour, the actual amount of hydrogen being stored, $vM_{CHS-in-useful}(h)$, is equal to the amount directed towards it, $vM_{CHS-in}(h)$ times a factor which considers hydrogen leakage during compression, φ_{comp}.

$$vM_{CHS-in-useful}(h) = vM_{CHS-in}(h) \cdot \varphi_{comp}$$

Every hour, the energy required by the compressor, $vE_{Comp}(h)$ is equal to the amount of hydrogen being compressed and stored in the hydrogen storage system, $vM_{CHS-in}(h)$ multiplied by the energy demand to compress one kg of hydrogen to the final storage pressure, q_{Comp}.

$$vE_{Comp}(h) =, vM_{CHS-in}(h) \cdot q_{Comp}$$

Every hour, the energy required by the compressor to compress and store hydrogen, $vE_{Comp}(h)$, must be smaller than the fifth decision variable x_5, the size of the compressor:

$$vE_{Comp}(h) \leq x_5$$

Every hour, the hydrogen storage level, $vM_{CHS-level}(h)$, is equal to the hydrogen storage level of the previous hour, $vM_{CHS-level}(h-1)$, minus the outflow of hydrogen from that hour, $vM_{CHS-out}(h)$, plus the inflow of hydrogen that hour, $vM_{CHS-in-useful}(h)$.

$$vM_{CHS-level}(h) = vM_{CHS-level}(h-1) + vM_{CHS-in-useful}(h) - vM_{CHS-out}(h)$$

Every hour, the hydrogen storage level, $vM_{CHS-level}(h)$, must be smaller than or equal to the sixth decision variable x_6 , the size of the hydrogen storage system:

$$vM_{CHS-level}(h) \leq x_6$$

Every hour, the hydrogen demanded, $vM_{H_2-Demand}(h)$, is equal to the flow of hydrogen from the electrolyzer, $vM_{H_2,Dir}(h)$ and the hydrogen flow from the hydrogen storage system, $vM_{CHS-out}(h)$.

$$vM_{H_2-Demand}(h) = vM_{H_2,Dir}(h) + vM_{CHS-out}(h)$$

S.1.2. Exemplary results

The diagrams in Figure S.*1* - Figure S.*3* show exemplary results of the modelled temporal course for **Pampa Anita in the G-25 case** (no sensitivity). The starting point (t = 0 d) is at 3006 hours into the evaluated year.

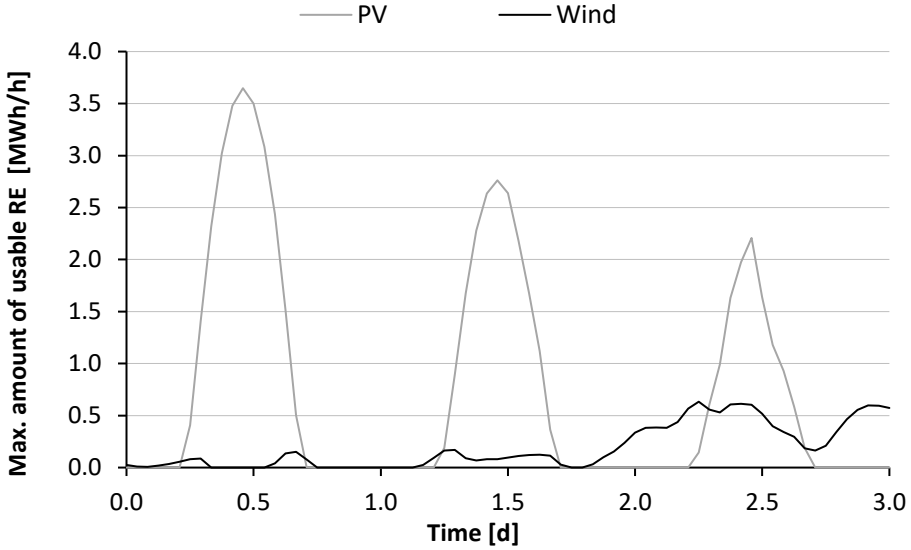

Figure S.1: Temporal course of RE availability

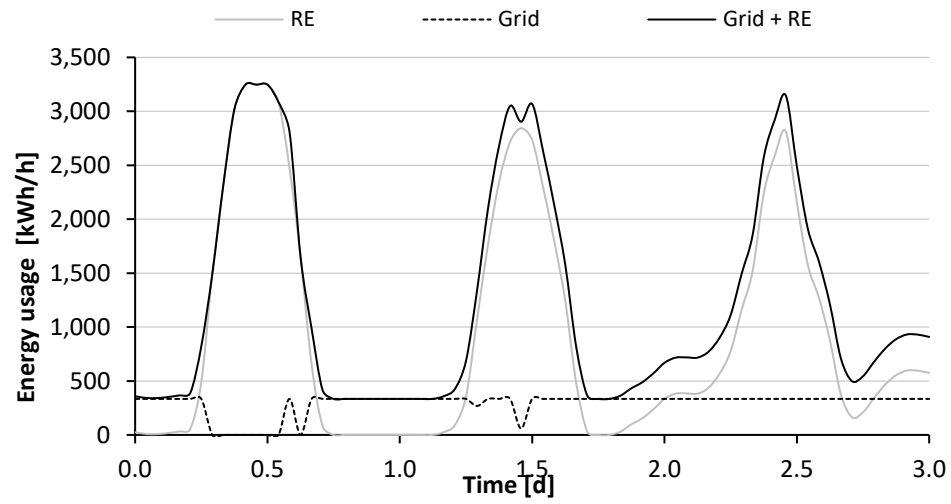

Figure S.2: Temporal course of energy usage

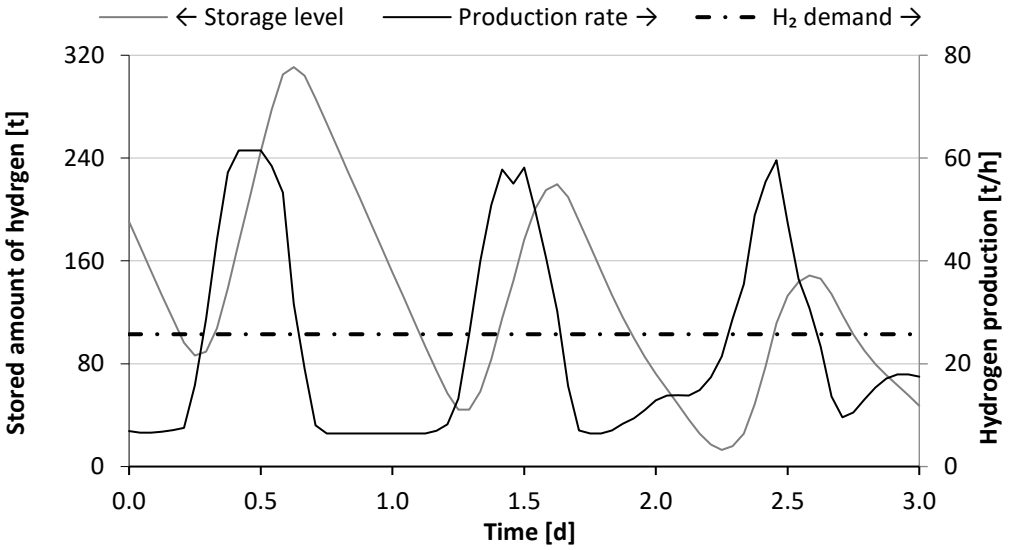

Figure S.3: Temporal course of hydrogen storage and production rate

The data in Table S.*1* correspond to the timeslot t = 2.5 d from the Figure S.*1* - Figure S.*3* (t = 3066 h of the evaluated year).

Table 3: Snapshot of the model at t = 3066 h

Variable	Value	Unit	Variable	Value	Unit
Total irradiance	0.477	kW/m²	PV Energy produced	1’638’421	kWh
Wind speed (ref. height)	7.51	m/s	Wind Energy produced	518’839	kWh
Wind speed (Hub height)	8.13	m/s	Grid Energy used	333’977	kWh
Hydrogen produced	47’350	kg	Hydrogen stored	21’610	kg
Energy used for storing	33’755	kWh	Hydrogen storage level	132’956	kg

S.2. General input data

Table S.4: General input data

Input	Value	Unit	Source
Labor costs - Chile	5'616.60	2019 CLP/h	(2)
Labor costs - Saudi Arabia	164.10	2020 SAR/h	Assumption based on (3)
Labor costs - Spain	24.90	2020 €/h	(4)
Labor costs - Australia	44.89	2020 AUD/h	(5, 6)
Exchange rate - Chile	787.65	CLP/€	(7)
Exchange rate - Saudi Arabia	4.29	SAR/€	(8)
Exchange rate - Australia	1.66	AUD/€	(9)
Exchange rate - USA	1.142	US-$/€	(10)
Resulting labor costs - Chile	7.13	2020 €/h	
Resulting labor costs - SA	38.25	2020 €/h	
Resulting labor costs - AUS	27.04	2020 €/h	
FTE	2080	h/a	(11)

Table S.5: Grid electricity cost data

Input	Value	Unit	Source
Chile	73.145	CLP/kWh	(12)
Saudi Arabia	18	Halalah/kWh	(13)
Spain	7.05	€-ct/kWh	(14)
Australia	32.8605	AUD-ct/kWh	(15)

S.3. Specific input data of unit operations

S.3.1. Input data for solar energy

Table S.6: Total installed costs for utility scale PV

Country	Value	Unit	Source
Chile	1'047	2020 US-$/kW	(16)
Saudi Arabia	1'008	2020 US-$/kW	(16)
Spain	761	2020 US-$/kW	(16)
Australia	1'061	2020 US-$/kW	(16)
Chile – S1	513	2020 US-$/kW	Assumption
Saudi Arabia – S1	477	2020 US-$/kW	Assumption
Spain – S1	558	2020 US-$/kW	Assumption
Australia– S1	510	2020 US-$/kW	Assumption

Equation S.*2* is used to determine the optimum tilt angle β (17):

Equation S.2: Tilt angle adaptation

$$\beta = A \cdot L^3 + B \cdot L^2 + C \cdot L + D$$

With *L* as the absolute value of the latitude of the location and

- A = $2.904 \cdot 10^{-5}$
- B = -0.008437
- C = 1.074
- D = 1.819

Table S.7: Further input data for PV

Input	Value	Unit	Source
Required labor force	46.33	FTE/GWp	(18)
Efficiency	20.3 %		(19)
O&M costs – OECD country	17.8	2020 US-$/kW a	(16)
O&M costs – non-OECD country	9	2020 US-$/kW a	(16)

S.3.2. Input data for wind energy

Table S.8: Installed costs for onshore wind projects

Country	Value	Unit	Source
Chile	1'607	2020 US-$/kW	(16)
Saudi Arabia	1'446	2020 US-$/kW	(16)
Spain	1'515	2020 US-$/kW	(16)
Australia	1'731	2020 US-$/kW	(16)

Table S.9: Further input data for wind turbines

Input	Value	Unit	Source
Required labor force	87	FTE/GW	(18)
O&M costs	50	2020 US-$/ (kW a)	Assumption based on(16)
Hub height – WT I	94	m	(20)
Hub height – WT II	110 / 139	m	(21)

Equation used to adapt the wind speed from the reference height to hub height (22).

$$v_i = v_{ref} \cdot \left(\frac{h_i}{h_{ref}}\right)^{\frac{1}{7}}$$

- with v as the wind speed at hub height and at reference height, respectively.
- With h as the hub height of the wind turbine and the reference height, respectively

S.3.3. Input data for electricity storage

Table S.10:Battery storage systems –technical input data

Input	Value	Unit	Source
Overall efficiency Li-ion battery	95%	-	(23)
Overall efficiency Pb battery	77%	-	(23)
Overall efficiency VRF battery	80%	-	(23)
Self-discharge rate – Li-ion	1	[%/month]	(23)
Self-discharge rate – Pb	2	[%/month]	(23)
Self-discharge rate – VRF	0.83	[%/month]	(23)

Table S.11:Battery storage systems –economic input data

Input	Value	Unit	Source
Li – ion battery	660	€$_{2015}$/kWh	(23)
Pb battery	240	€$_{2015}$/kWh	(23)
VRF battery	930	€$_{2015}$/kWh	(23)
Lang factor for every battery system	1.62	-	Assumption based on (29)

S.3.4. Input data for electrolysis

Table S.12: Hydrogen production – technic input data

Input	Value	Unit	Source
Efficiency (LHV) – alkaline	51.9	kWh/kg$_{H_2}$	(24)
Efficiency (LHV) – PEM	54.2	kWh/kg$_{H_2}$	(24)
Efficiency (LHV) – S2	48	kWh/kg$_{H_2}$	2030 target from (25)
H_2 exit pressure - alkaline	20	bar	(24)
H_2 exit pressure - PEM	30	bar	(24)
H_2 exit pressure – S2	50	bar	Assumption based on (26)
Stack overhaul period – alkaline	7	a	(24)
Stack overhaul period – PEM	5	a	(24)
Stack overhaul period – S2	10	a	Assumption based on (26)

Table S.13: Hydrogen production – economic input data

Input	Value	Unit	Source
Alkaline electrolysis – 100 MW$_{el}$	400	2020 US-$/kW	(27)
PEM electrolysis – 100 MW$_{el}$	500	2020 US-$/kW	(27)
Alkaline electrolysis S2 – 100 MW$_{el}$	160	€$_{2020}$/kW	Assumption based on (28)
Share - stack costs / system costs	45%	-	(24)
Lang factor	1.62	-	(29)
Service and maintenance – alkaline	19	€$_{2020}$ / kW a	(30)
Service and maintenance – PEM	13	€$_{2020}$ / kW a	(30)
Service and maintenance – S2	6	€$_{2020}$ / kW a	(28)
Insurance and taxes	0.02	1/a – FCI basis	(30)
Labor demand – workers per shift	2	1/100 MW$_{el}$	Assumption

S.3.5. Input data for hydrogen compression and storage

Table S.14: Input data for hydrogen compression

Input	Value	Unit	Source
Max. pressure ratio per step	3	-	(31)
Isentropic efficiency	70 %	-	
H_2 leakage	0.8 %	-	(32)
Specific costs	1'083	€/kW	(31)
Lang factor	3.78	-	(31)
Labor demand - workers per shift	0.2	1 / Compressor	(33)
O&M costs	0.05	1/a - FCI basis	(33)

Table S.15: Input data for hydrogen storage

Input	Value	Unit	Source
Max. pressure in storage tank	250	bar	Assumption based on (34)
Specific costs	700	2020 US-$/$kg_{H_2}$	(35)
Lang factor	2	-	Personal correspondence
Labor demand	1	person / 5 t capacity	Assumption
O&M costs	0.05	1/a - FCI basis	(33)

S.4. Detailed results

S.4.1. Detailed Results of Pampa Anita

S.4.1.1. Technical results

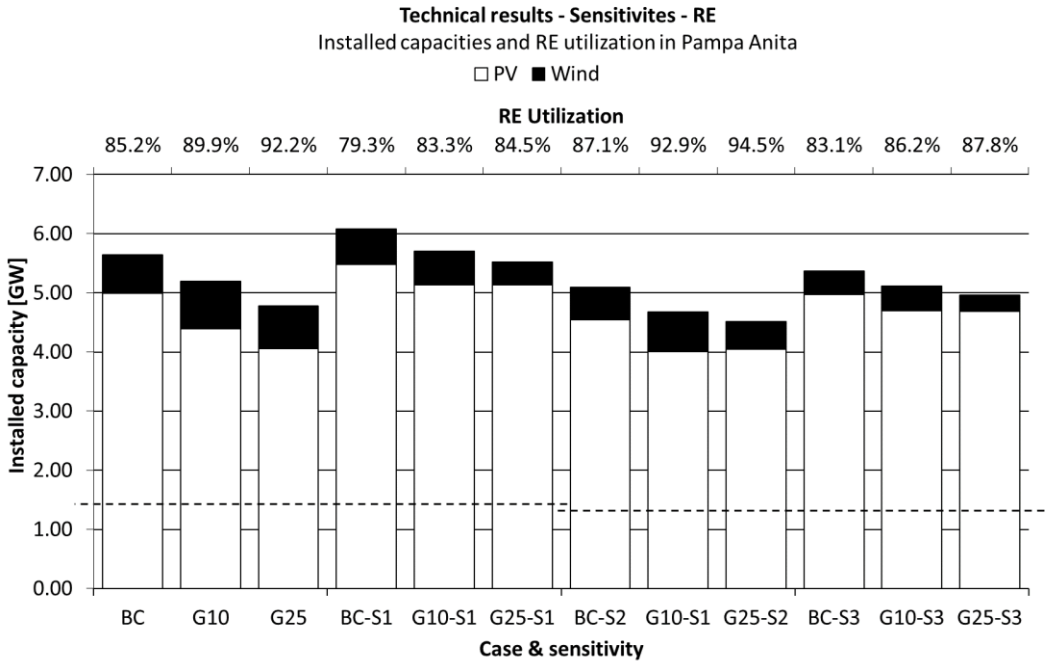

Figure S.4: Installed RE capacity and utilization rate in Pampa Anita - Current scenario and sensitivities

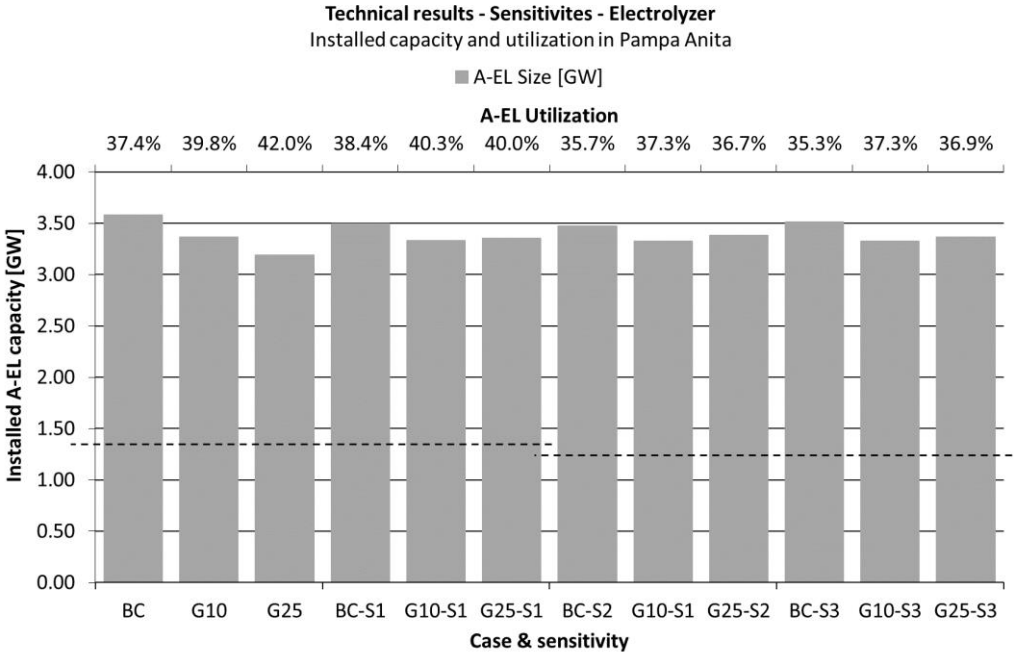

Figure S.5: Installed electrolyzer capacity and utilization rate in Pampa Anita - Current scenario and sensitivities

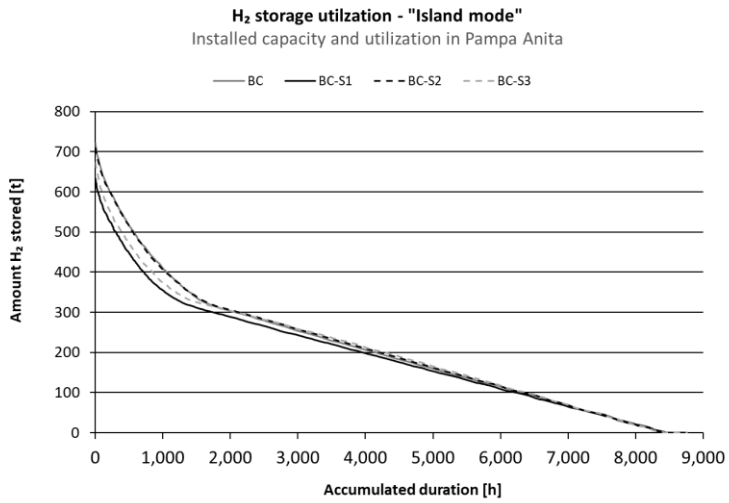

Figure S.6: "Frequency distribution" of stored H_2 mass in descending order – Pampa Anita in Island mode

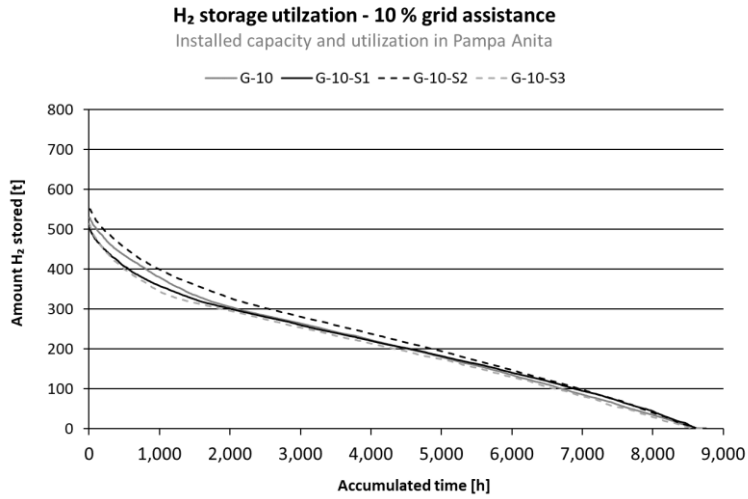

Figure S.7: "Frequency distribution" of stored H_2 mass in descending order – Pampa Anita with 10 % grid assistance

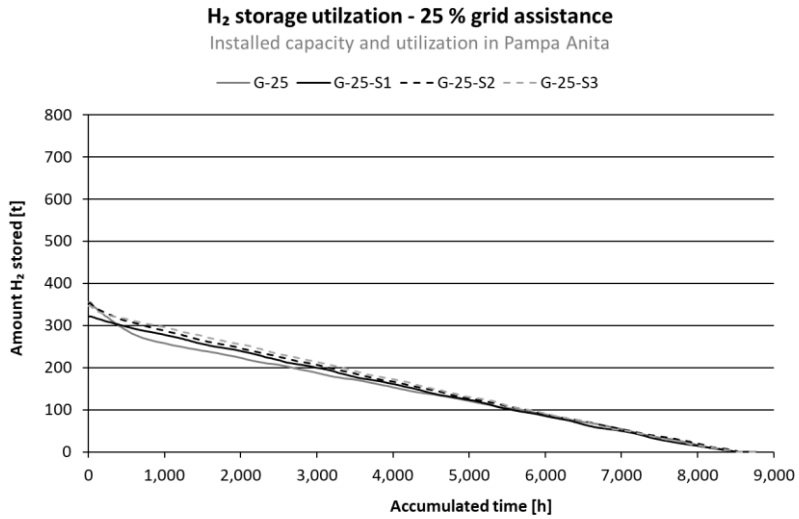

Figure S.8: "Frequency distribution" of stored H_2 mass in descending order – Pampa Anita with 10 % grid assistance

S.4.1.2. Economic results

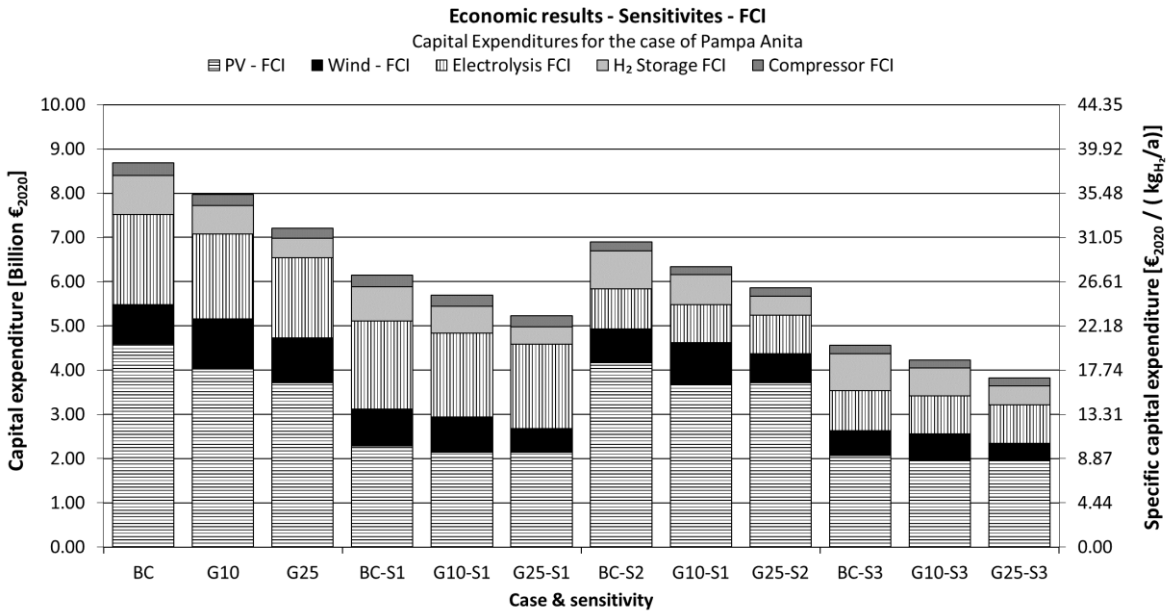

Figure S.9: CapEx in Pampa Anita - Current costs and sensitivities

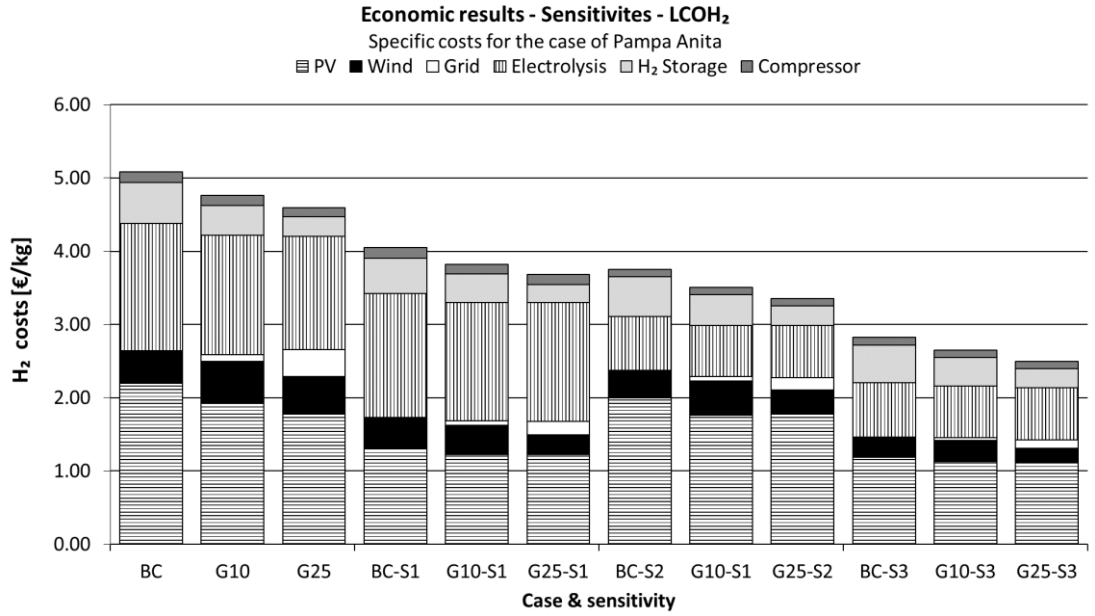

Figure S.10 $LCOH_2$ in Pampa Anita - Current costs and sensitivities

S.4.2. Detailed Results of Punta Arenas

S.4.2.1. Technical results

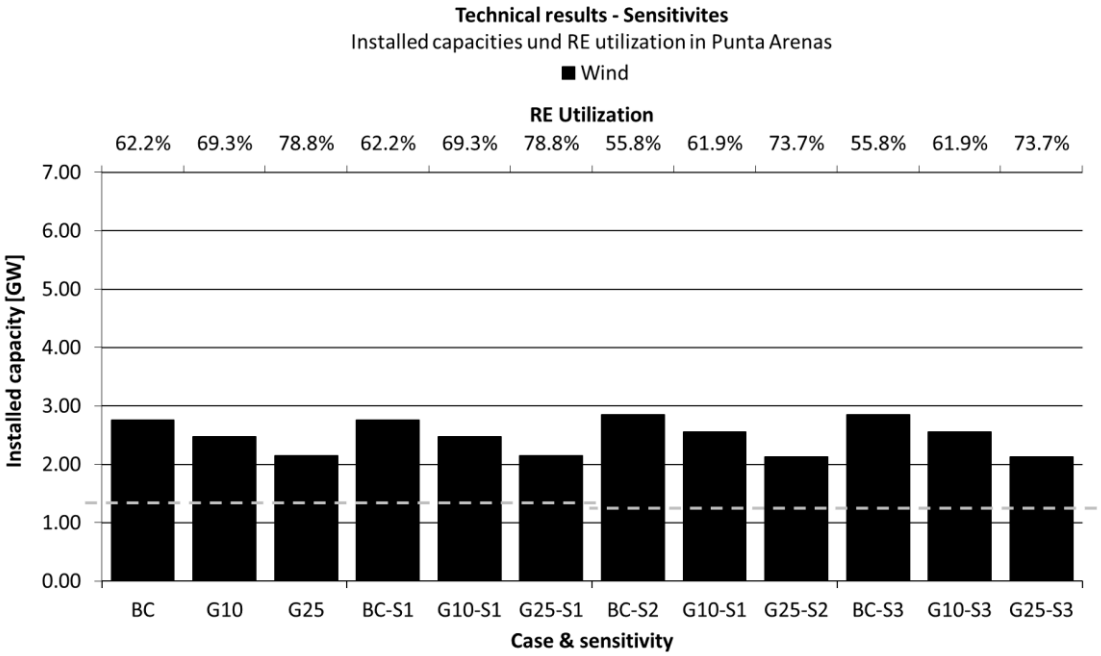

Figure S.11: Installed RE capacity and utilization rate in Punta Arenas - Current scenario and sensitivities

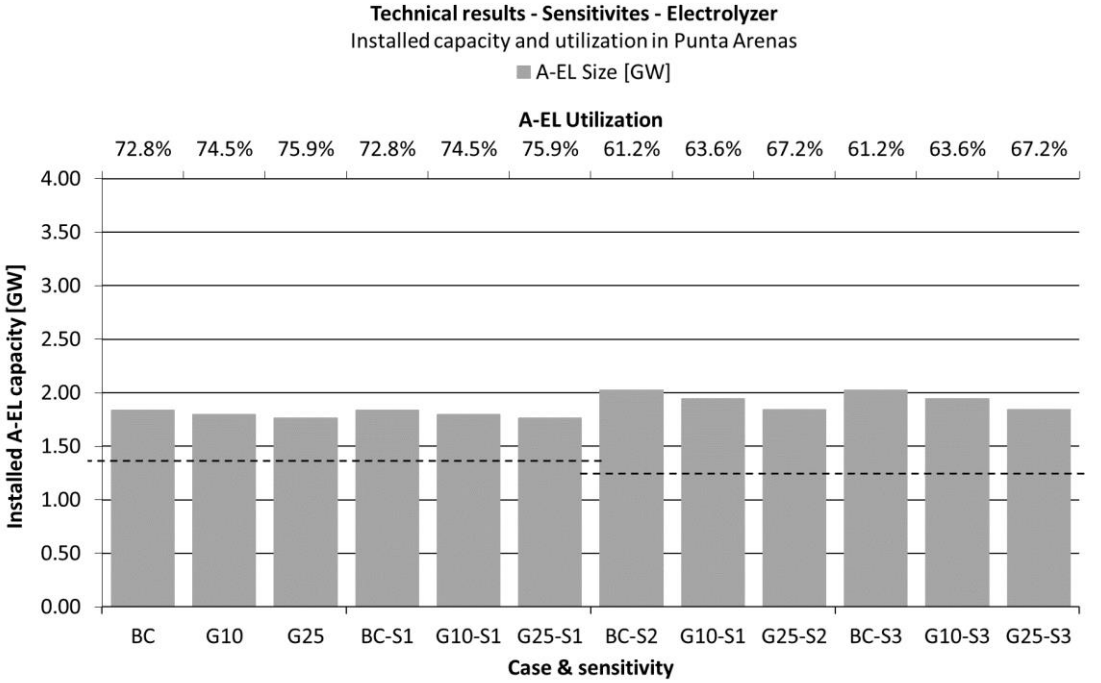

Figure S.12: Installed electrolyzer capacity and utilization rate in Punta Arenas - Current scenario and sensitivities

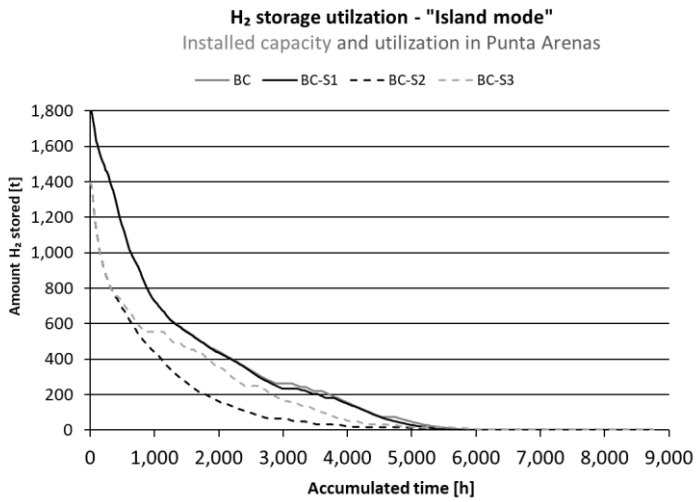

Figure S.13: "Frequency distribution" of stored H_2 mass in descending order – Punta Arenas in Island mode

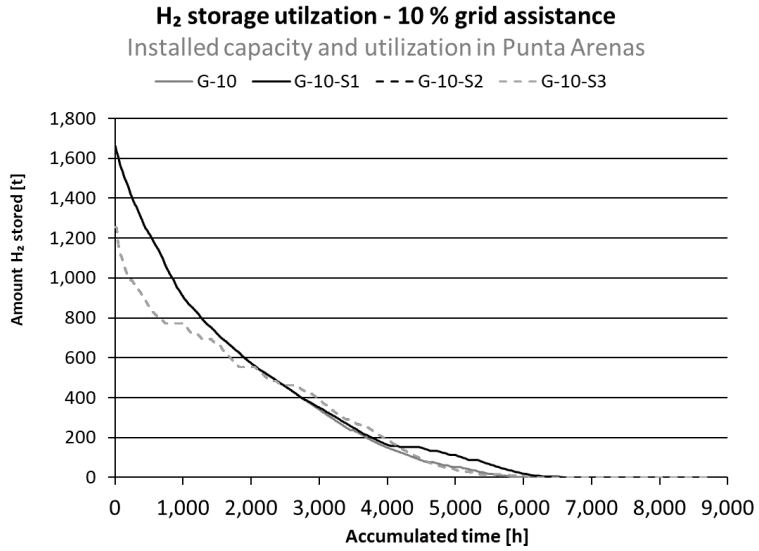

Figure S.14:Frequency distribution" of stored H_2 mass in descending order – Punta Arenas with 10 % grid assistance

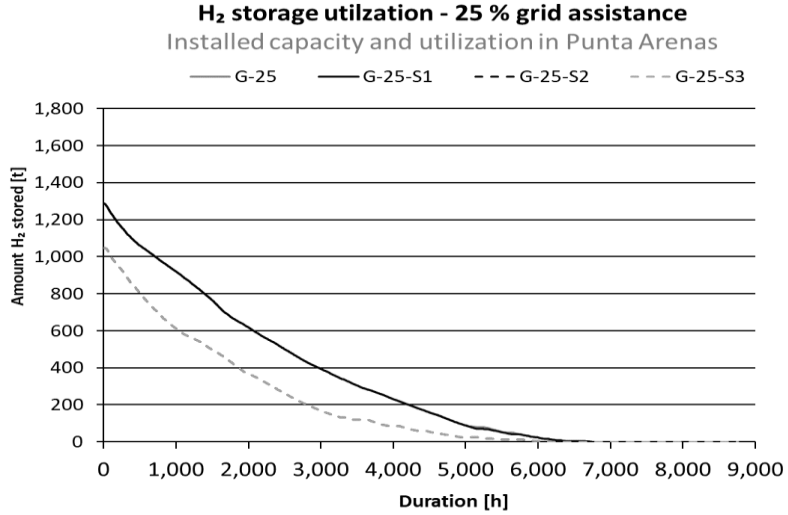

Figure S.15: Frequency distribution" of stored H_2 mass in descending order – Punta Arenas with 25 % grid assistance

S.4.2.2. Economic results

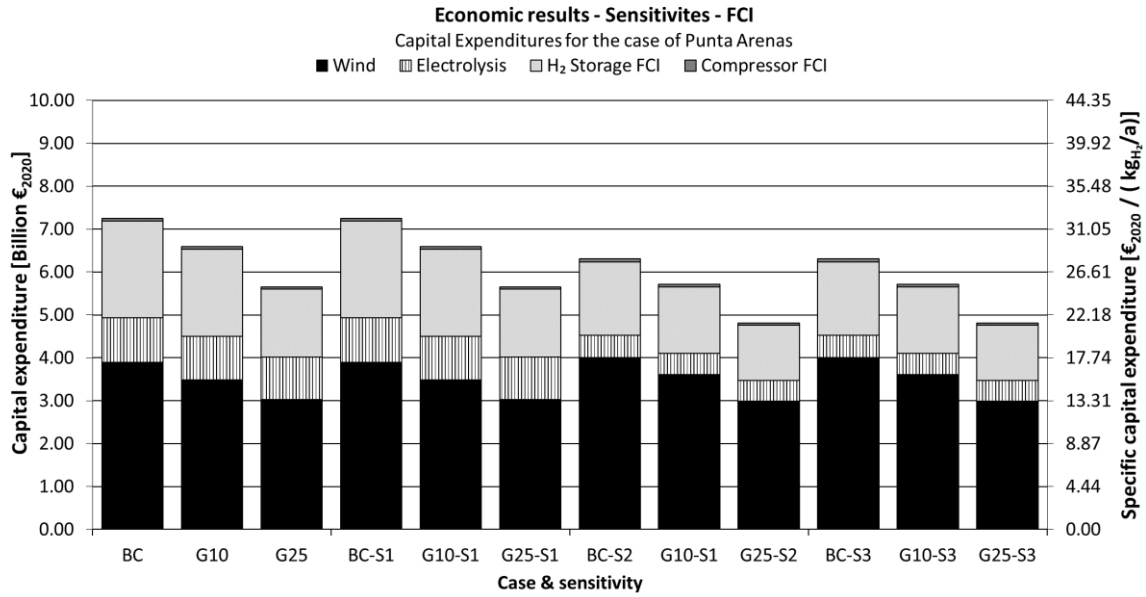

Figure S.16: CapEx in Punta Arenas - Current costs and sensitivities

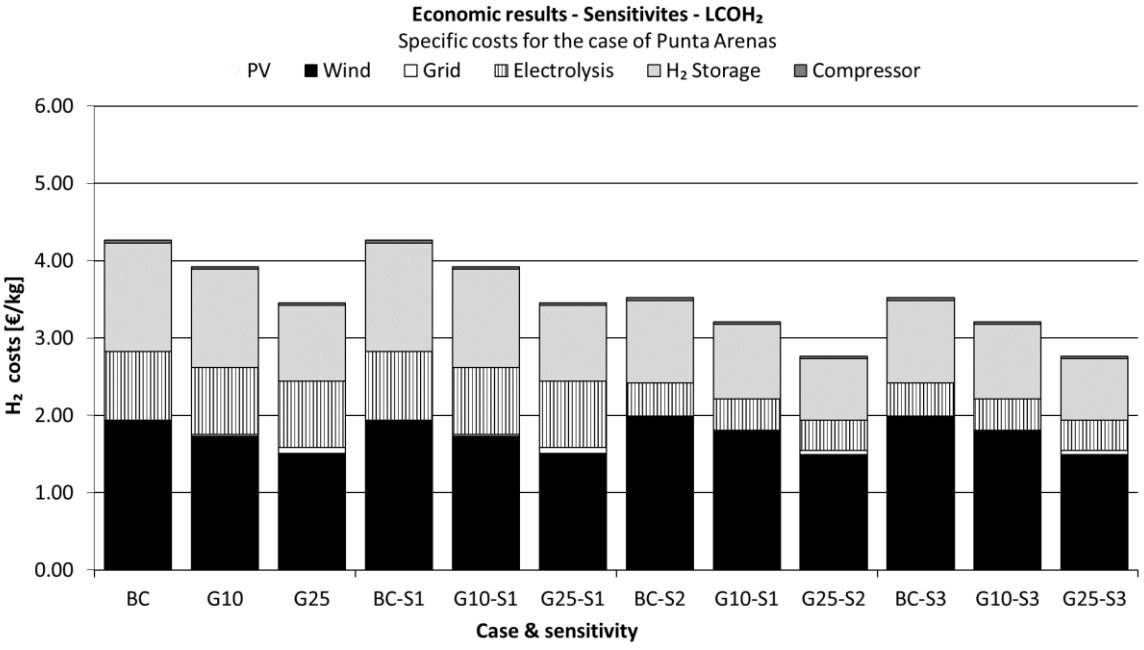

Figure S.17: $LCOH_2$ in Punta Arenas - Current costs and sensitivities

S.4.3. Detailed Results of Sakaka

S.4.3.1. Technical results

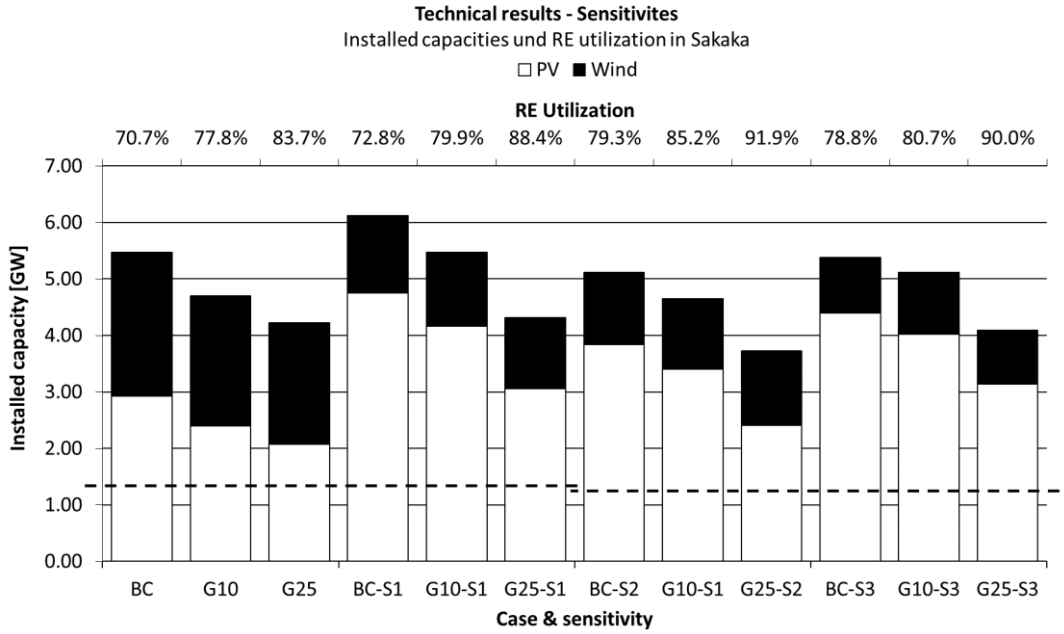

Figure S.18: Installed RE capacity and utilization rate in Sakaka - Current scenario and sensitivities

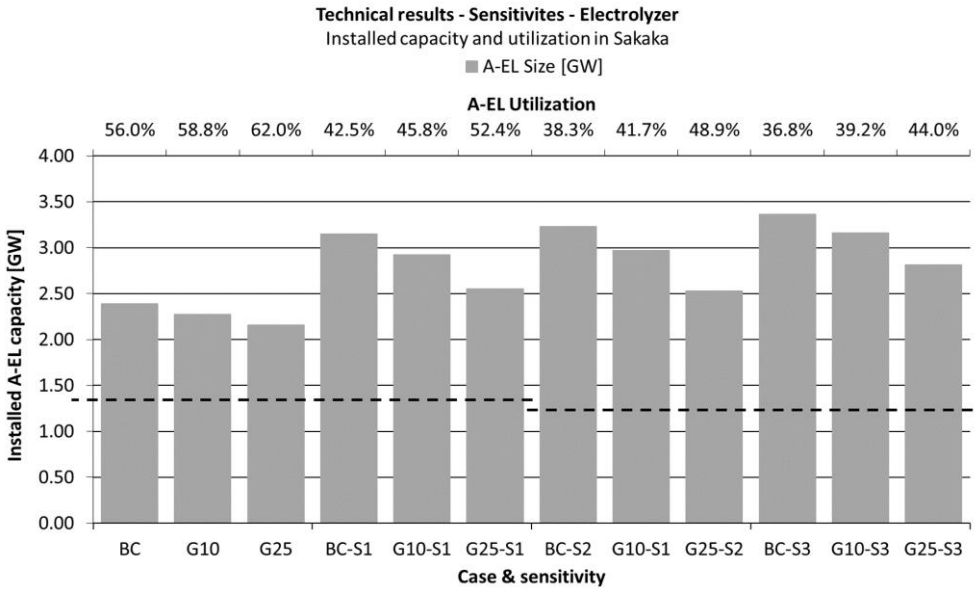

Figure S.19: Installed electrolyzer capacity and utilization rate in Sakaka - Current scenario and sensitivities

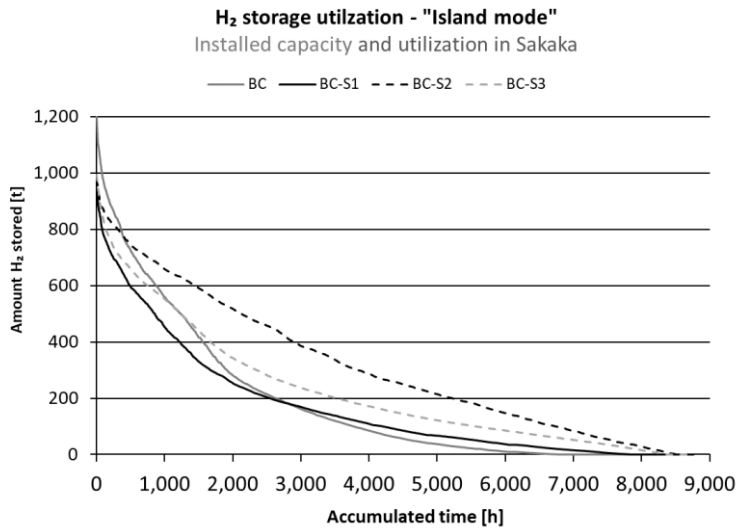

Figure S.20: "Frequency distribution" of stored H_2 mass in descending order – Sakaka in Island mode

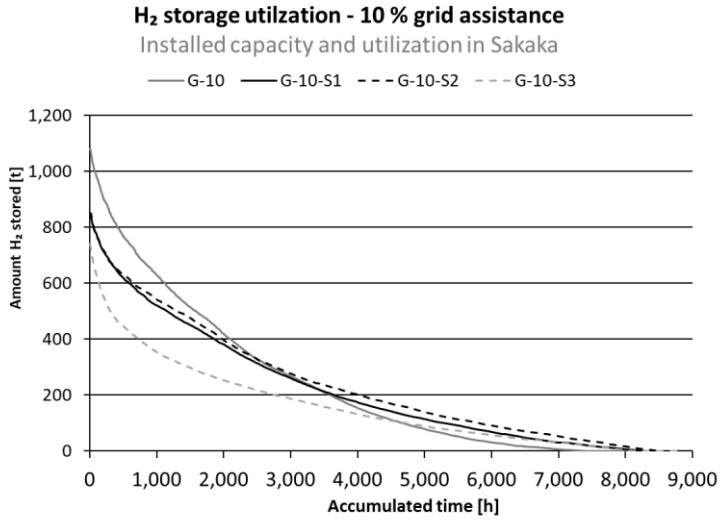

Figure S.21: "Frequency distribution" of stored H_2 mass in descending order – Sakaka with 10 % grid assistance

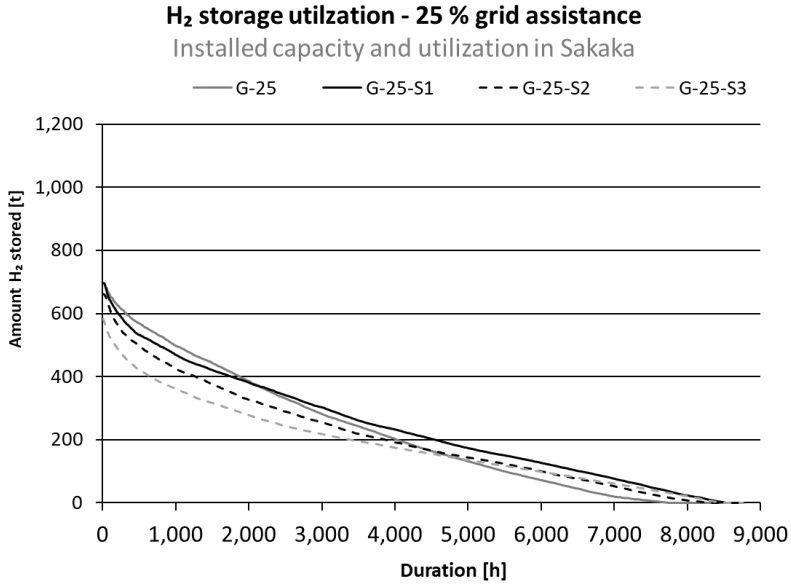

Figure S.22: "Frequency distribution" of stored H_2 mass in descending order – Sakaka with 25 % grid assistance

S.4.3.2. Economic results

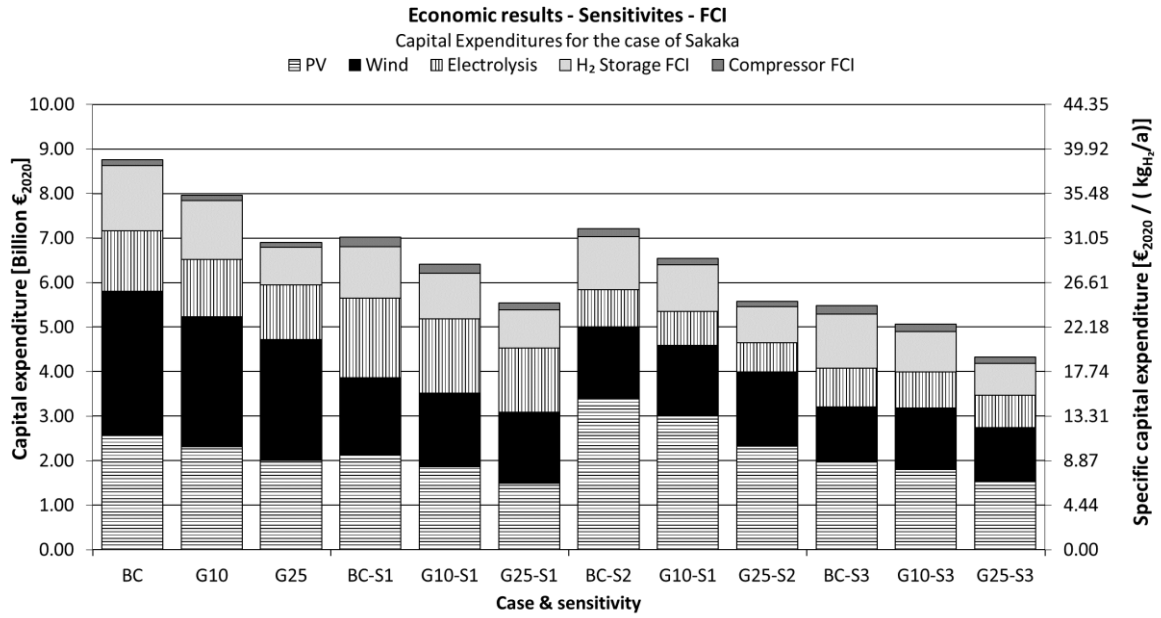

Figure S.23: CapEx in Sakaka - Current costs and sensitivities

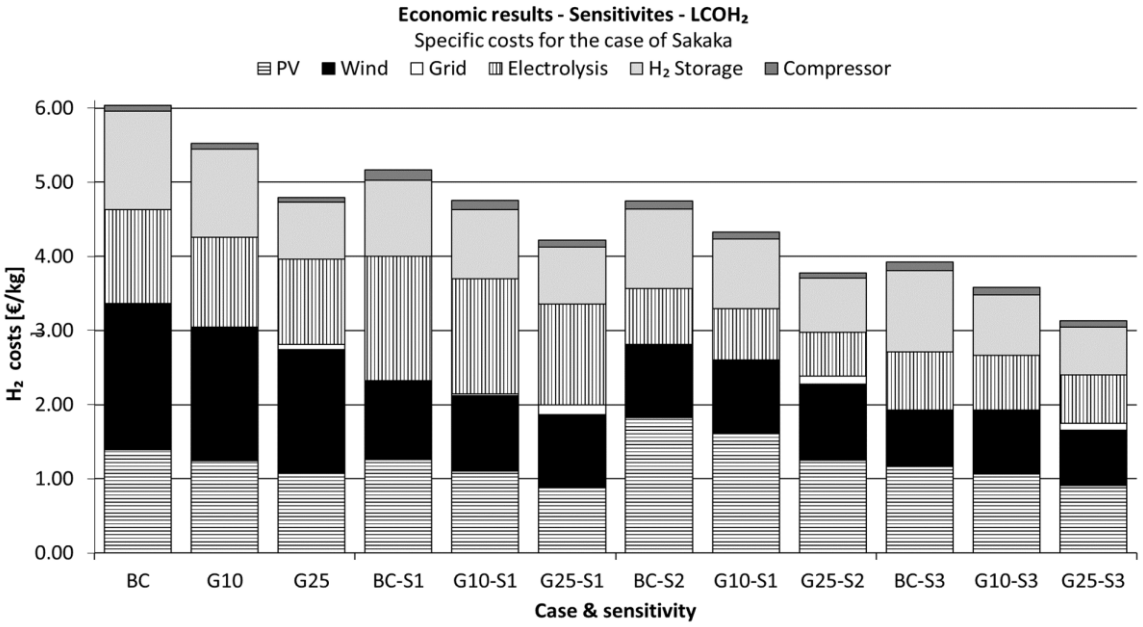

Figure S.24 $LCOH_2$ in Sakaka - Current costs and sensitivities

S.4.4. Detailed Results of for Almeria

S.4.4.1. Technical results

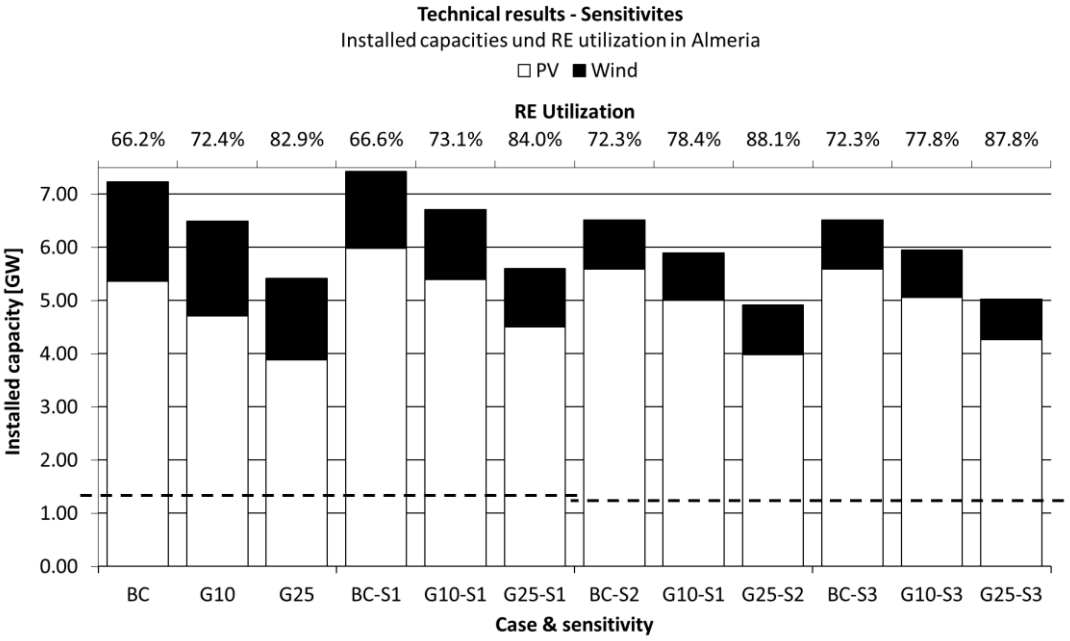

Figure S.25: Installed RE capacity and utilization rate in Almeria - Current scenario and sensitivities

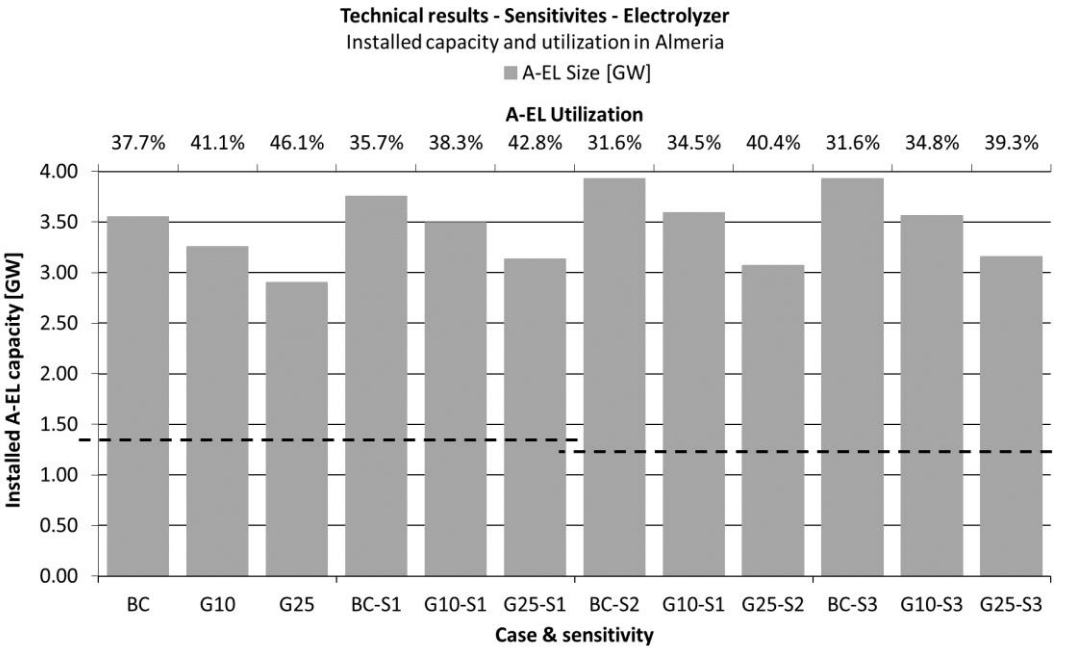

Figure S.26: Installed electrolyzer capacity and utilization rate in Almeria - Current scenario and sensitivities

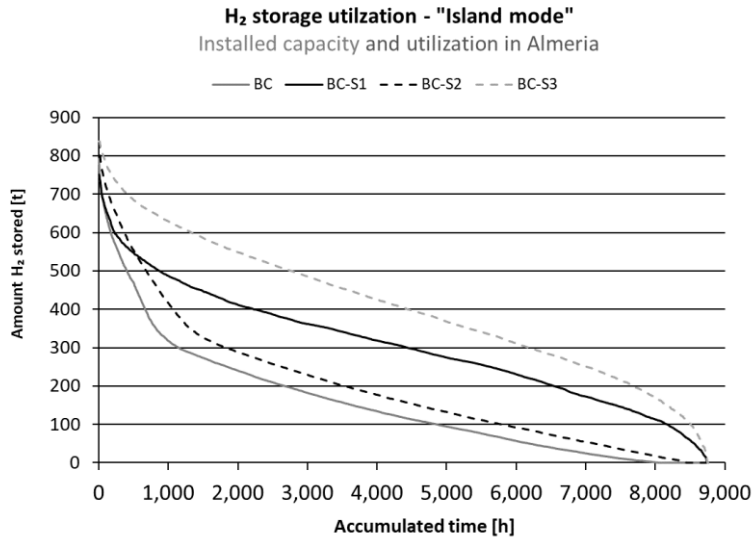

Figure S.27: "Frequency distribution" of stored H_2 mass in descending order – Almeria in Island mode

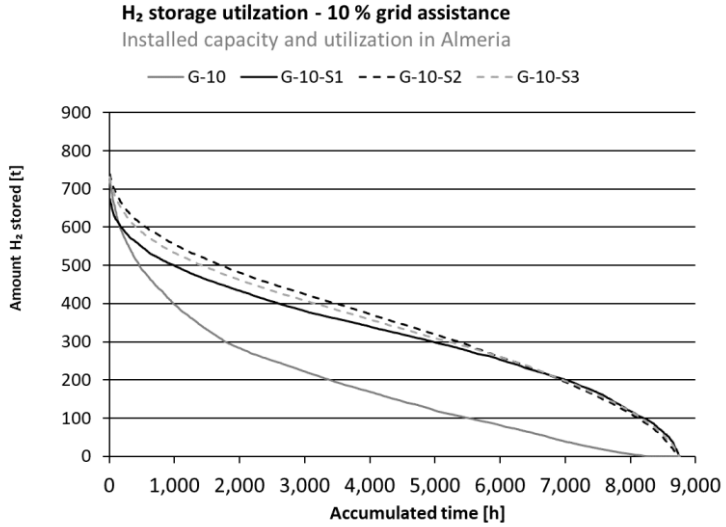

Figure S.28: "Frequency distribution" of stored H_2 mass in descending order – Almeria with 10 % grid assistance

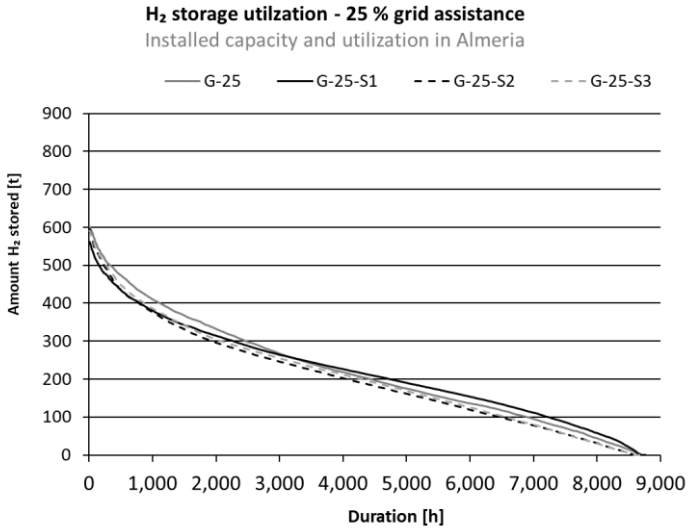

Figure S.29: "Frequency distribution" of stored H_2 mass in descending order – Almeria with 25 % grid assistance

S.4.4.2. Economic results

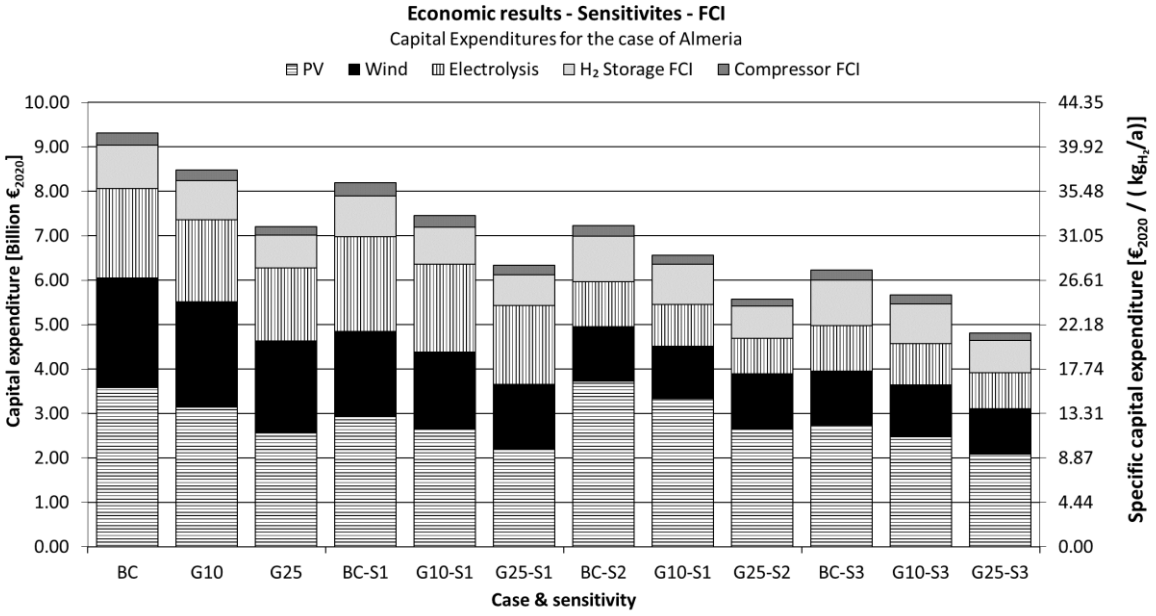

Figure S.30: CapEx in Almeria - Current costs and sensitivities

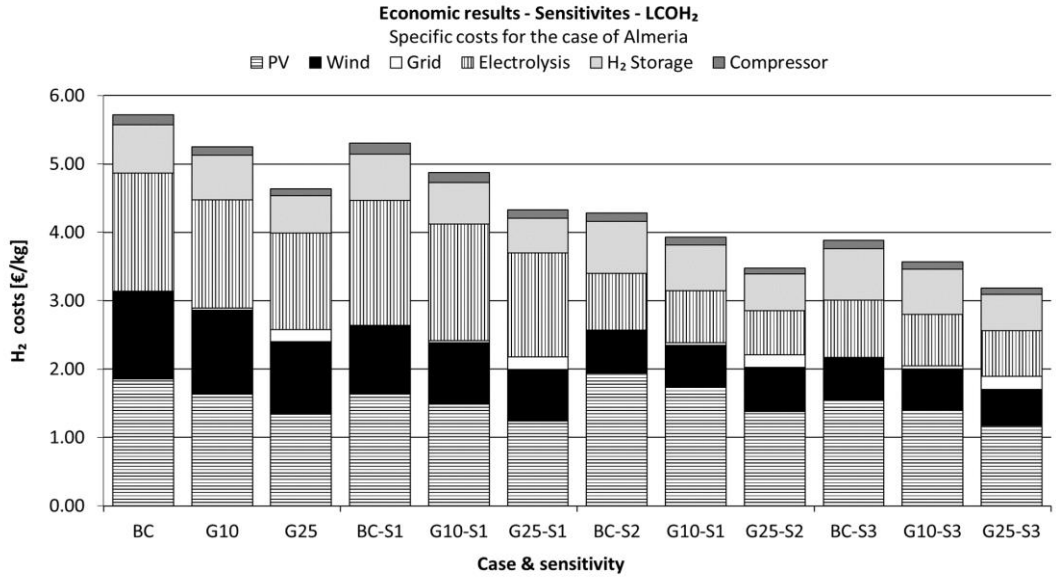

Figure S.31: $LCOH_2$ in Almeria- Current costs and sensitivities

S.4.5. Detailed Results of Northampton

S.4.5.1. Technical results

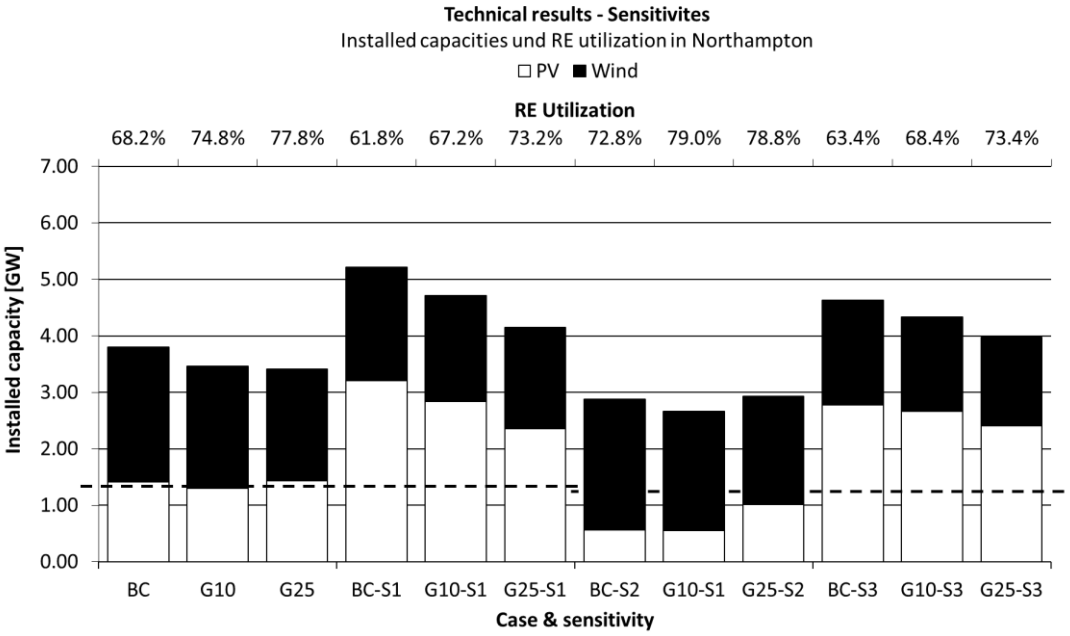

Figure S.32: Installed RE capacity and utilization rate in Northampton - Current scenario and sensitivities

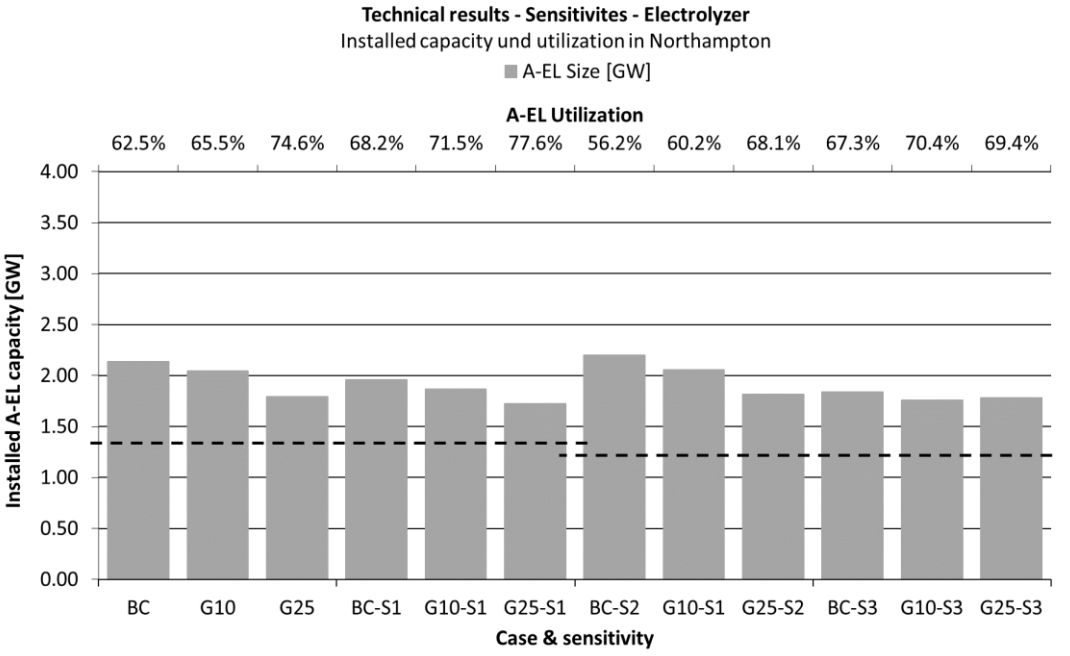

Figure S.33: Installed electrolyzer capacity and utilization rate in Northampton - Current scenario and sensitivities

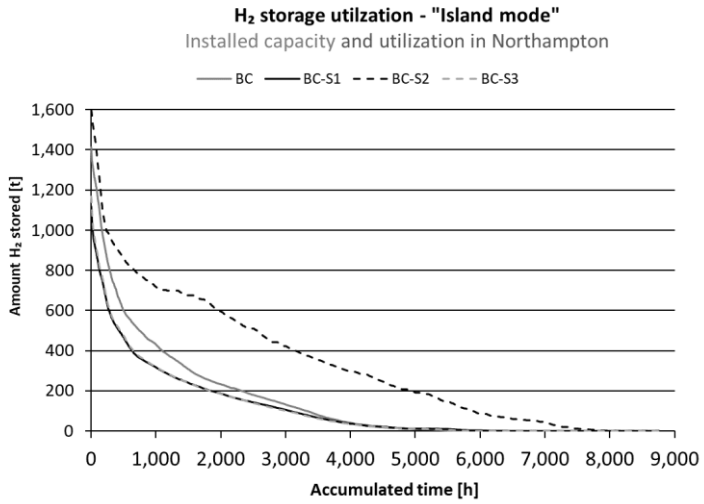

Figure S.34: "Frequency distribution" of stored H_2 mass in descending order – Northampton in Island mode

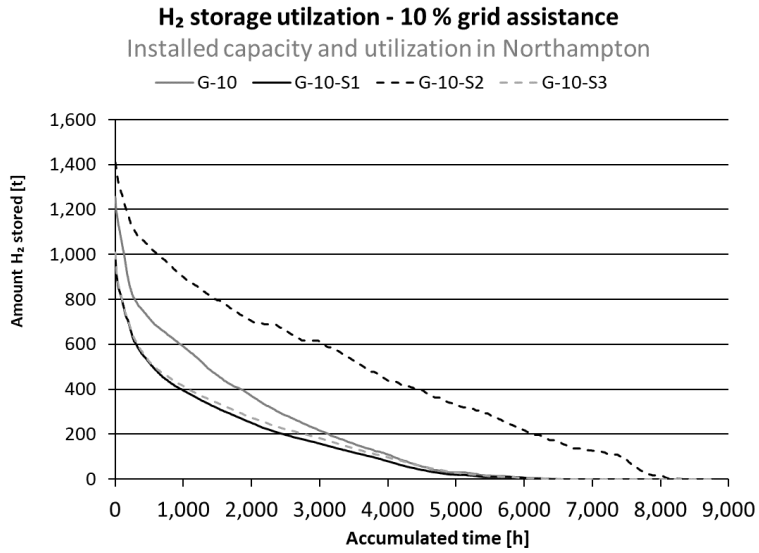

Figure S.35: "Frequency distribution" of stored H_2 mass in descending order – Northampton with 10 % grid assistance

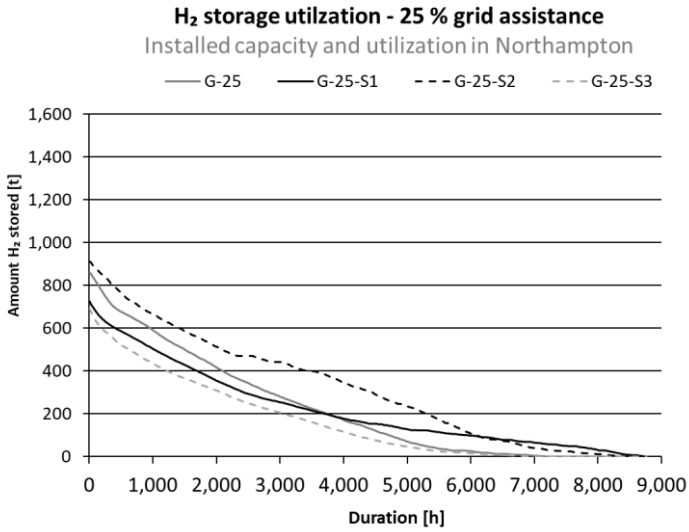

Figure S.36: "Frequency distribution" of stored H_2 mass in descending order – Northampton with 25 % grid assistance

S.4.5.2. Economic results

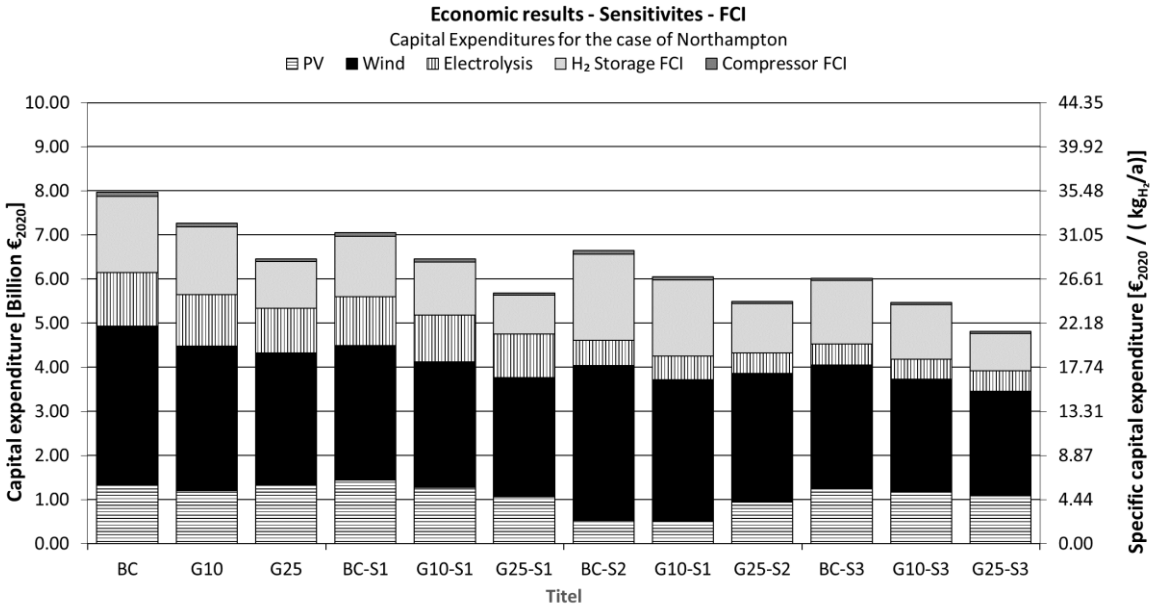

Figure S.37: CapEx in Northampton - Current costs and sensitivities

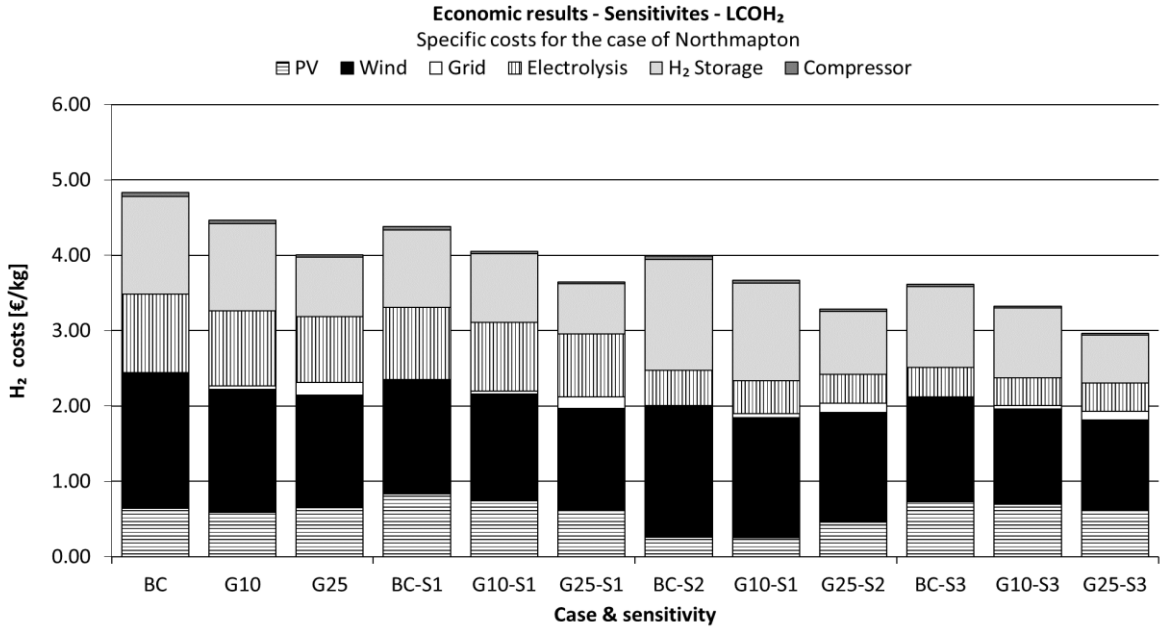

Figure S.38: $LCOH_2$ in Northampton- Current costs and sensitivities

List of figures

References

1. Stephen Boys LV. Convex Optimization 2009.
2. ILOSTAT. Average hourly labour cost per employee, local currency | Chile 2019 2021 [15.12.2021]. Available from: https://ilostat.ilo.org/data/country-profiles/.
3. ILOSTAT. Country profiles - Average monthly earnings of employees, local currency | Saudi Arabia 2020 2021 [Available from: https://ilostat.ilo.org/data/country-profiles/.
4. eurostat. Hourly labour costs 2021 [Available from: https://ec.europa.eu/eurostat/statistics-explained/index.php?title=Hourly_labour_costs#Hourly_labour_costs_ranged_between_.E2.82.AC6.5_and_.E2.82.AC45.8_in_2020.
5. Economics T. Australia Average Weekly Wages 2021 [Available from: https://tradingeconomics.com/australia/wages.
6. ANU. 2020 Salary on-costs 2021 [Available from: https://services.anu.edu.au/human-resources/salaries-benefits/salary-on-costs/2020-salary-on-costs.
7. ExchangeRates. Euro to Chilean Peso Spot Exchange Rates for 2019 2021 [Available from: https://www.exchangerates.org.uk/EUR-CLP-spot-exchange-rates-history-2019.html.
8. ExchangeRates. Euro to Saudi Riyal Spot Exchange Rates for 2020 2021 [Available from: https://www.exchangerates.org.uk/EUR-SAR-spot-exchange-rates-history-2020.html.
9. ExchangeRates. Euro to Australian Dollar Spot Exchange Rates for 2020 2021 [Available from: https://www.exchangerates.org.uk/EUR-AUD-spot-exchange-rates-history-2020.html.
10. ExchangeRates. Euro to US Dollar Spot Exchange Rates for 2020 2021 [Available from: https://www.exchangerates.org.uk/EUR-USD-spot-exchange-rates-history-2020.html.
11. Accountingtools. How to calculate FTEs 2021 [Available from: https://www.accountingtools.com/articles/how-to-calculate-ftes.html.
12. Statista. Average market price of electricity in Chile from January 2019 to October 2021 2021 [Available from: https://www.statista.com/statistics/1029737/chile-electricity-average-m/.
13. SaudiElectricityCompany. Tariffs & Connection Fees 2022 [Available from: https://www.se.com.sa/en-us/customers/Pages/TariffRates.aspx.
14. Statista. Prices of electricity for industry in Spain from 2008 to 2020 2022 [Available from: https://www.statista.com/statistics/595813/electricity-industry-price-spain/.
15. HorizonPower. Electricity prices 2022 [Available from: https://www.horizonpower.com.au/manage-my-account/pricing/#for-business.
16. IRENA. Renewable Power Generation Costs in 2020. 2021.
17. Chinchilla M, Santos-Martín D, Carpintero-Rentería M, Lemon S. Worldwide annual optimum tilt angle model for solar collectors and photovoltaic systems in the absence of site meteorological data. Applied Energy. 2021;281:116056.
18. Chapman AJ, Fraser T, Itaoka K. Hydrogen import pathway comparison framework incorporating cost and social preference: Case studies from Australia to Japan. Int J Energ Res. 2017;41(14):2374-91.
19. Xu Z, Xu X, Cui C, Huang H. A new uniformity coefficient parameter for the quantitative characterization of a textured wafer surface and its relationship with the photovoltaic conversion efficiency of monocrystalline silicon cells. Solar Energy. 2019;191:210-8.
20. Vestas. V112-3.45 MW® 2021 [Available from: https://www.vestas.com/en/products/4-mw-platform/V112-3-45-MW.
21. models Wt. GE General Electric GE 2.5 - 120 2021 [Available from: https://www.wind-turbine-models.com/turbines/310-ge-general-electric-ge-2.5-120.
22. Hsu SA, Meindl EA, Gilhousen DB. Determining the Power-Law Wind-Profile Exponent under Near-Neutral Stability Conditions at Sea %J Journal of Applied Meteorology and Climatology. 1994;33(6):757-65.
23. Jülch V. Comparison of electricity storage options using levelized cost of storage (LCOS) method. Applied Energy. 2016;183:1594-606.
24. Smolinka T, Wiebe N, Sterchele P, Palzer A, Lehner F, Jansen M, et al. Studie IndWEDe Industrialisierung der Wasser-elektrolyse in-Deutschland. 2018;1.

25. FCH. Fuel Cells and Hydrogen Joint Undertaking (FCH 2 JU). 2018.
26. Smolinka T, Wiebke N, Sterchele P, Lehner F, Jansen M. Sudie_IndWEDe-Industrialisierung der Wasserelektrolyse in Deutschland: Chancen und Herausforderungen für nachhaltigen Wasserstoff für Verkehr, Strom und Wärme: NOW GmbH; 2018.
27. IRENA. Green hydrogen cost reduction. 2020.
28. Vartiainen E, Breyer C, Moser D, Román Medina E, Busto C, Masson G, et al. True Cost of Solar Hydrogen. 2021;n/a(n/a):2100487.
29. Zauner A, Böhm H, Rosenfeld DC, Tichler RJDAofto, Ares ot-eoR. Innovative large-scale energy storage technologies and Power-to-Gas concepts after optimization. 2019:4315303.
30. Schnuelle C, Wassermann T, Fuhrlaender D, Zondervan E. Dynamic hydrogen production from PV & wind direct electricity supply – Modeling and techno-economic assessment. International Journal of Hydrogen Energy. 2020;45(55):29938-52.
31. Woods DR. Rules of thumb in engineering practice: John Wiley & Sons; 2007.
32. Stolzenburg K, Mubbala RJIdfdoeloh, FCH JU. Hydrogen Liquefaction Report. 2013.
33. Peters MS, Timmerhaus KD, West RE. Plant design and economics for chemical engineers: McGraw-Hill New York; 2003.
34. Baldwin D, editor Proceedings of DOE Hydrogen Compression, Storage, and Dispensing Cost Reduction Workshop2013: Hexagon Lincoln.
35. Abdin Z, Tang C, Liu Y, Catchpole K. Large-scale stationary hydrogen storage via liquid organic hydrogen carriers. iScience. 2021;24(9):102966.

Techno-economic assessment of different aviation fuel supply pathways including LH2 and LCH4 and the influence of the carbon source

Supplementary information

S.1. General input data

Table S.1: General input data

Input	Value	Unit	Source
Labor costs - Morocco	20	€/h	Based on (1)
Labor costs - Germany	120	€/h	Based* on (2)
Electricity purchase costs - Morocco -	150	€/MWh	Assumption**
Electricity selling revenue - Morocco -	100	€/MWh	Assumption***
Electricity purchase costs - Germany	100	€/MWh	Assumption***
Interest rate - Morocco (non-OECD)	7.5	%	(3)
Interest rate - Germany (OECD)	5.0	%	(3)
Sea distance	2000	NM	(4)
Exchange rate - USA	1.142	US-$$_{2020}$/€$_{2020}$	(5)
$CEPCI_{2020}$	596.2	-	
Oxygen - Morocco	0	€/t	Taken from HPP
Oxygen - Germany	25	€/t	(6)
Waste water treatment	3.8	€/m³	(7)

* Internal costs are higher than paid salaries - Average value assumed
** PV and wind turbines are included in the HPP and excess electricity can be used. Therefore, the grid electricity costs in Morocco are high because grid electricity is used in times when the PV farm and wind turbines have a low power output
*** Generalized average value over the course of a year

Table S.2: Factors used to determine the FCI based on the equipment costs | taken from Albrecht et al- (8)

Component	Factor	Component	Factor
Equipment installation	0.47	Service facilities	0.55
Instrumentation and control	0.36	Engineering and supervision	0.33
Piping	0.68	Construction	0.41
Electrical installation	0.11	Legal expenses	0.04
Buildings including services	0.18	Contractor's fee	0.22
Yard improvements	0.10	Contingencies	0.44

Table S.3: Factors used to determine the indirect OPEX | taken from Albrecht et al- (8)

ID	OPEX item	Basis	Factor
1	Operating supervision	Labor costs	0.15
2	Maintenance labor	FCI	0.01
3	Maintenance material	FCI	0.01
4	Operating supplies	2 + 3	0.15
5	Laboratory charges	Labor costs	0.20
6	Insurance and taxes	FCI	0.02
7	Plant overhead costs	Labor costs + 1 + 5	0.55
8	Administrative costs	7	0.33
9	Distribution and selling	Final fuel costs	0*
10	Research and development	Final fuel costs	0*

* Deviating from the cited literate this value is set to 0. Distribution are included in the assessment and no research costs are considered

Table S.4: Harbor cost data

Input	Value	Unit	Source
FCI jetty	2 x 54.1	Mio. $€_{2020}$	(9)
FCI for hydrocarbon loading/unloading lines	47,500	€/m	(10)
FCI for cryogenic loading/unloading lines	47,500	€/m	(10)
Length of loading/unloading lines	2 x 1,200	m	(10)
EQP costs flare (cryo fuels)	462.000	€	(10)

S.2. Specific input data of unit operations

S.2.1. LH_2 pathway

S.2.1.1. LH_2 - Input data

Table S.5: Input data for the LH_2 pathway

Input	Value	Unit	Source
Energy demand liquefaction	7	kWh/kg_{H_2}	Assumption as in (10)
H_2 losses during liquefaction	1.65 %	-	(11)
LH_2 losses per un/loading	5	m³	Assumption as in (10)
FCI per liquefaction unit	330.3	Mio. $€_{2020}$	(10)
Liquefaction capacity	3 x 225.5	tpd	Calculation results
LH_2 storage capacity - Morocco	3 x 60,000	m³	Calculation results
LH_2 storage capacity - Germany	3 x 60,000	m³	Calculation results
Labor demand - Morocco	40	People / shift	Assumption
Labor demand - Germany	4	People / shift	Assumption

Table S.6: Input data for LH_2 oversea transport

Input	Value	Unit	Source
Reference ship	ENERGY NAVIGATOR		(12)
Volumetric capacity	160,400	m³	Calculation result
Costs of carrier	211.2	Mio. US-$	Assumption based on (13)
Power demand of sailing ship	26.9	MW	(14)
Crew size	27	-	(15)
Labor costs	822,378	$€_{2020}$ / a	(16)
Supply costs	269,100	$€_{2020}$ / a	(17)
Maintenance main machine	931,300	$€_{2020}$ / a	(17)
Maintenance rest of ship	822,000	$€_{2020}$ / a	Assumption based on (17)
Insurance	10 % of OPEX		Assumption
Return trips per year	20.8		Calculation results
Ship utilization	70 %		Assumption

S.2.1.1. LH_2 - Block flow diagrams (BFDs)

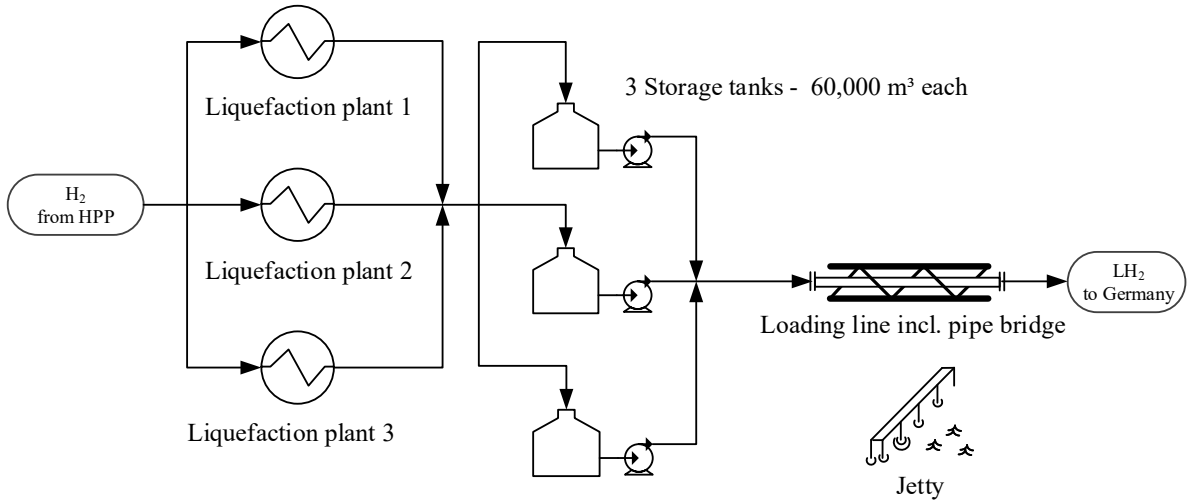

Figure S:1: BFD of LH_2 exporting site

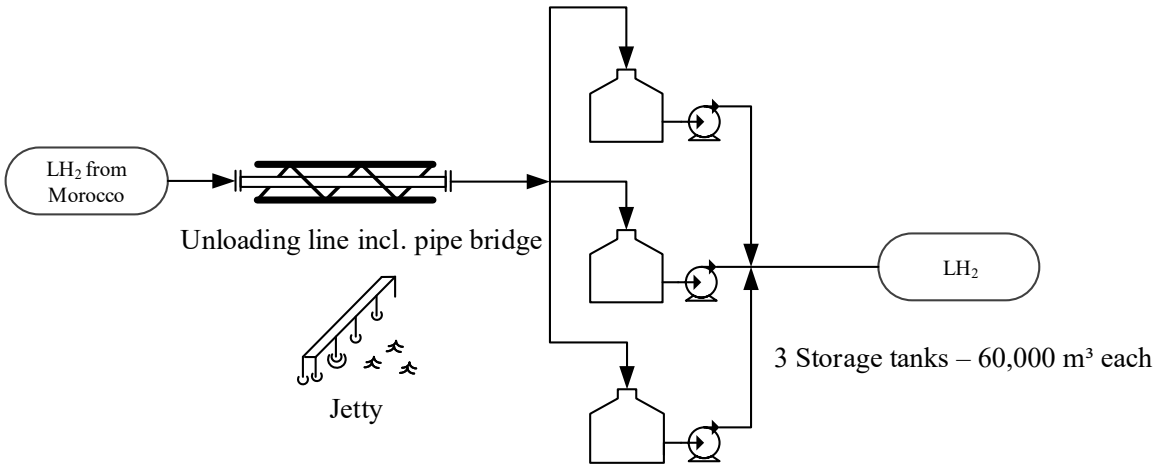

Figure S.2: BFD of LH_2 importing site

S.2.2. LOHC Transport

S.2.2.1. LOHC - Input data

Table S.7: Input data for H_2 shipping via LOHC

Input	Value	Unit	Source
Hydrogenation temperature	250	°C	(18)
Hydrogenation pressure	30	bar	Assumption
Dehydrogenation temperature	300	°C	(18)
Dehydrogenation pressure	2.5	bar	Assumption based on (19)
LOHC storage capacity - Morocco	2 x 110,000	m³	Calculation result
LOHC storage capacity - Germany	2 x 110,000	m³	Calculation result
Initial LOHC demand	400,000	m³	Calculation result
Degree of dehydrogenation	90	%	Assumption based on (19)
Labor demand - Morocco	15	People / shift	Assumption
Labor demand - Germany | LCH_4	6	People / shift	Assumption*
Labor demand - Germany | SAF	12	People / shift	Assumption

* The dehydrogenation reactors are in the system boundary of the methanation

Table S.8: Input data for LOHC oversea transport

Input	Value	Unit	Source
Reference ship	ALASKAN LEGEND		(20)
Volumetric capacity	205,100	m³	Calculation result
Costs of carrier	75	Mio. US-$	Assumption based on (13)
Power demand of ships sailing	18	MW	(20)
Crew size	21		(15)
Labor costs	758,186	€/a	(16)
Supply costs	246,400	€/a	(17)
Maintenance main machine	959,449	€/a	(17)
Maintenance rest of ship	846,845	€/a	Assumption based on (17)
Insurance	10 % of OPEX		Assumption
Return trips per year	20.1		Calculation results
Ship utilization	80 %		Assumption

S.2.2.2. LOHC - Block flow diagrams

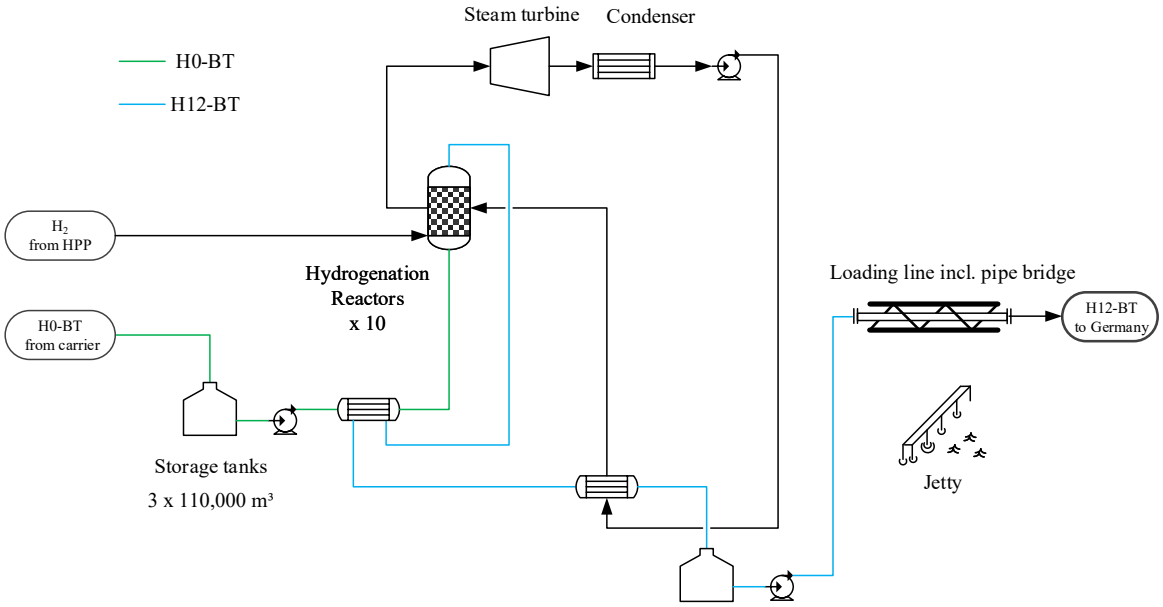

Figure S.3: Simplified BFD of LOHC hydrogenation

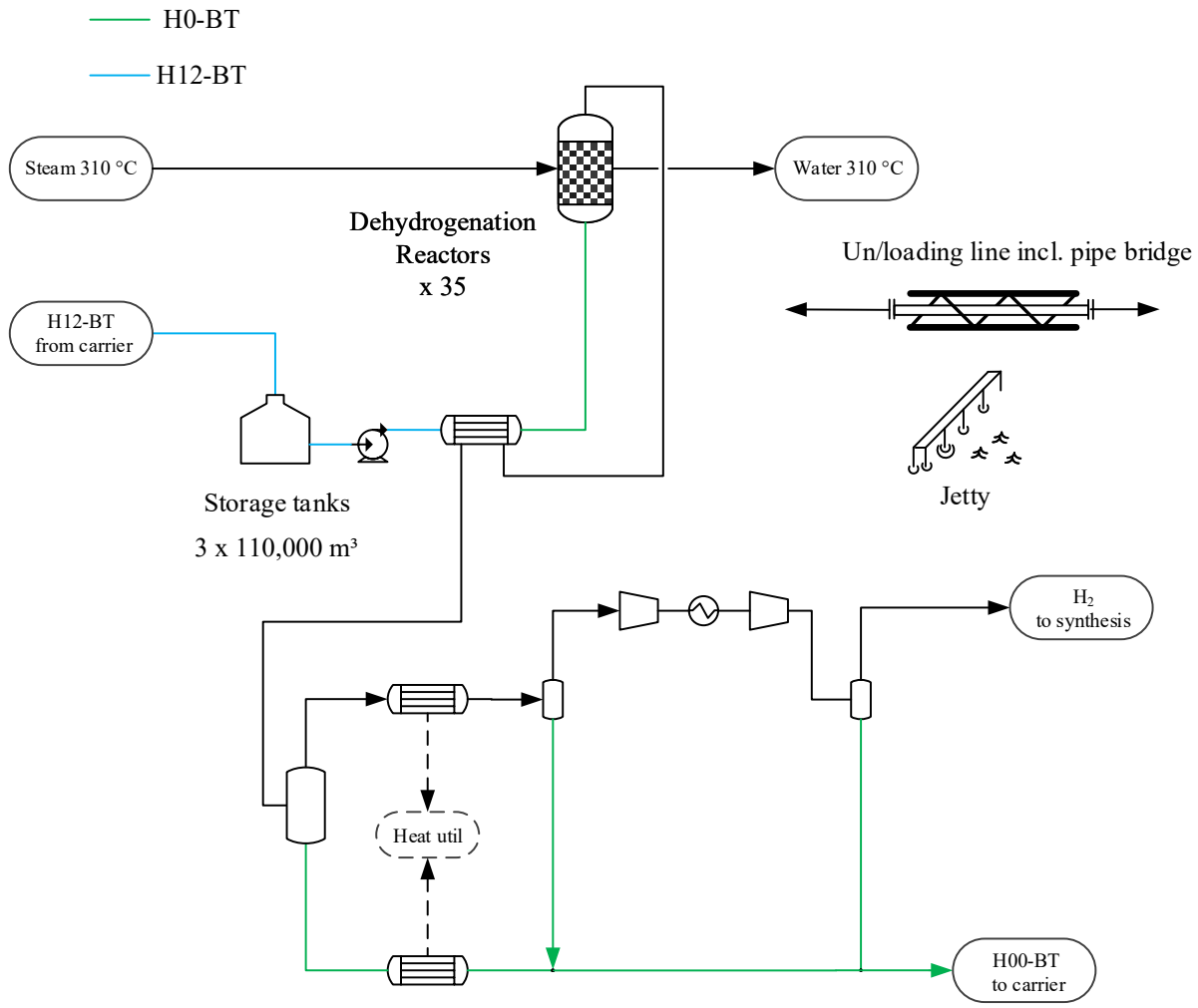

Figure S.4: Simplified BFD of LOHC Dehydrogenation | (valid for SAF - Number of reactors is reduced in LCH_4 synthesis)

S.2.3. DAC

S.2.3.1. DAC - Input data

Table S.9: Input data for DAC units

Input	Value	Unit	Source
Specific electricity demand - DAC	501.7	kWh_{el}/t	Technical SI from (18)
Specific heat demand @ 120 °C	3,478	kWh_{th}/t	Technical SI from (18)
Specific electricity demand - CO_2 liquefaction	216.7	kWh_{el}/t	Technical SI from (18)
FCI DAC	1048	€/ (t/a)	Technical SI from (18)
DAC resin demand	0.6	kg/t_{CO_2}	Technical SI from (18)
Co adsorption of water	2	mole H_2O / mole CO_2	Assumption

S.2.3.2. DAC - Block flow diagram

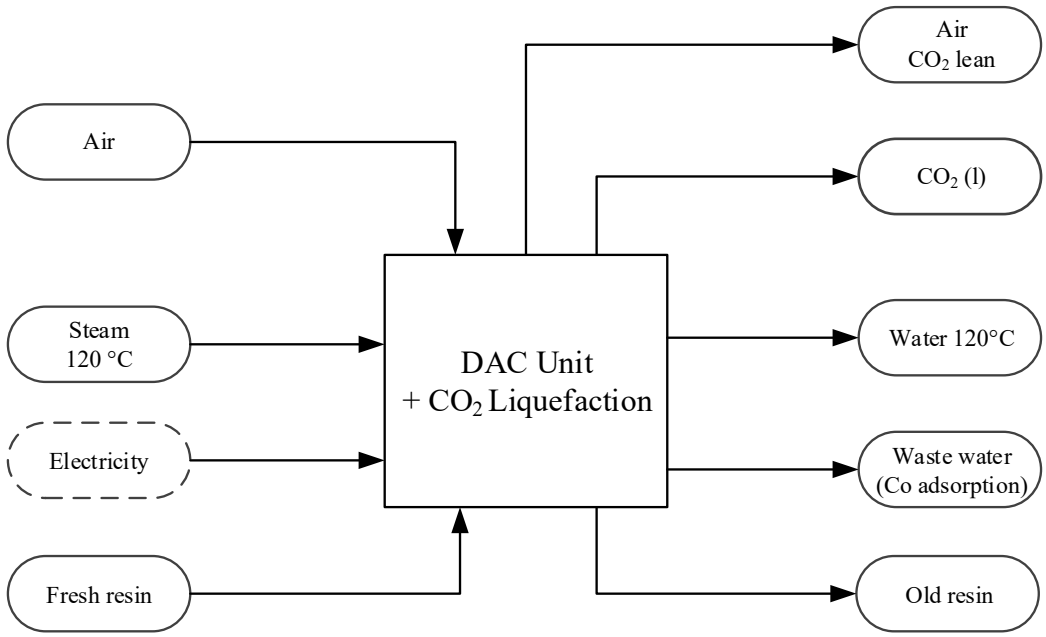

Figure S.5: DAC as black box system

S.2.4. MEA washing unit

S.2.4.1. MEA - Input data

Table S.10: Composition of exhaust gas from waste incineration plant

Component	Value [% Vol]
H_2O	15
CO_2	10
O_2	7
N_2	68
Ar	neglected

Table S.11: Input data for MEA scrubber units

Input	Value	Unit	Source
Capacity per train	30	t/h	Assumption
Specific electric energy demand	150.6	kWh_{el}/t_{CO_2}	Calculation result
Specific thermal energy demand	3.71	MJ_{th}/kg_{CO_2}	Calculation result
CO_2 delivery pressure to synthesis	3	bar	Assumption
Cost of MEA	3.50	€/kg	(21)
Labor demand	1	People / shift / train	
Degradation of MEA	0.5	kg_{MEA}/t_{CO_2}	(22)

S.2.4.2. MEA - Block flow diagram

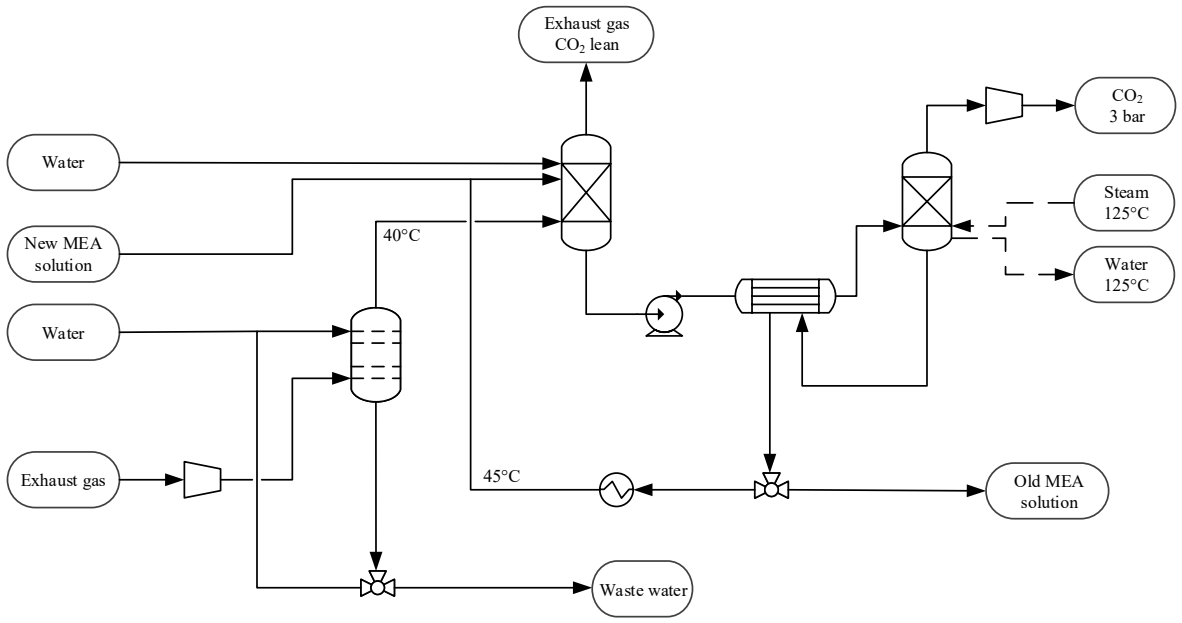

Figure S.6: Simplified BFD of amine scrubber with prewasher, absorber and desorber column

S.2.5. LCH_4 pathway

S.2.5.1. LCH_4 - Input data

Table S.12: Installed costs for onshore wind projects

Input	Value	Unit	Source
Labor demand - Morocco - Case A	30	People/shift	Assumption
Labor demand - Germany - Case A	2	People/shift	Assumption
Labor demand - Germany - Case B	25	People/shift	Assumption
Labor demand - Germany - Case C	20	People/shift	Assumption
Storage capacity - case A | Morocco	2 x 30,000	m³	Calculation results
Storage capacity - case A | Germany	2 x 30,000		Calculation results
Storage capacity - case B and C	2 x 10,000	m³	Calculation results

Table S.13: Input data for LCH_4 oversea transport

Input	Value	Unit	Source
Reference ship	LNG JIA XING (SAGA DAWN)		(23)
Volumetric capacity	53,550	m³	Calculation result
Costs of carrier	104	Mio. US-$	Assumption based on (13)
Power demand sailing ship	11.7	MW	(24)
Crew size	27		(15)
Labor costs	846,360	€/a	(16)
Supply costs	269,100	€/a	(17)
Maintenance main machine	453,957	€/a	(17)
Maintenance rest of ship	400,679	€/a	Assumption based on (17)
Insurance	10 % of OPEX		Assumption
Return trips per year	20.1		Calculation results
Ship utilization	75 %		Assumption

S.2.5.2. LCH_4- Block flow diagram

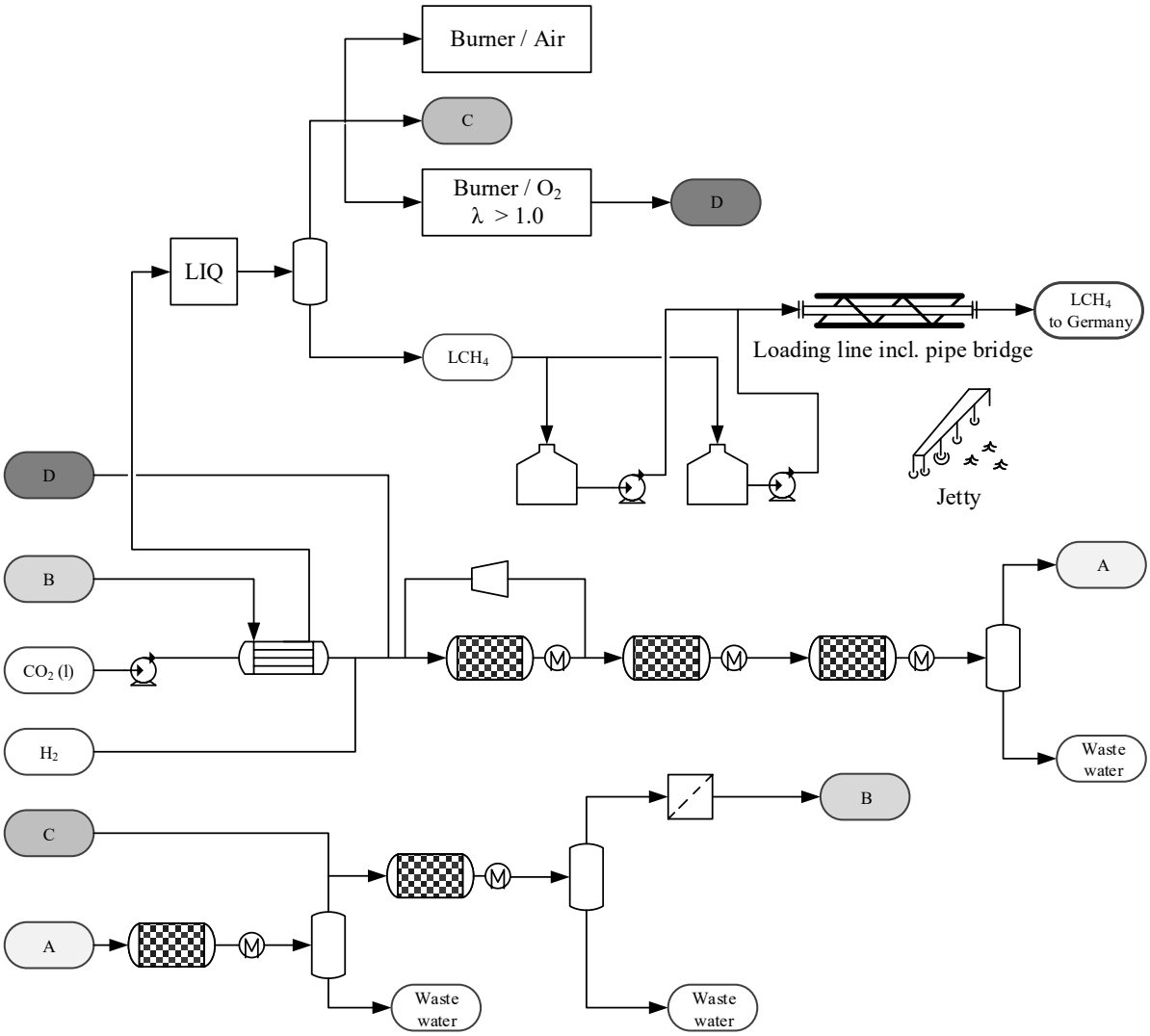

Figure S.7: Simplified BFD of methanation process for case A

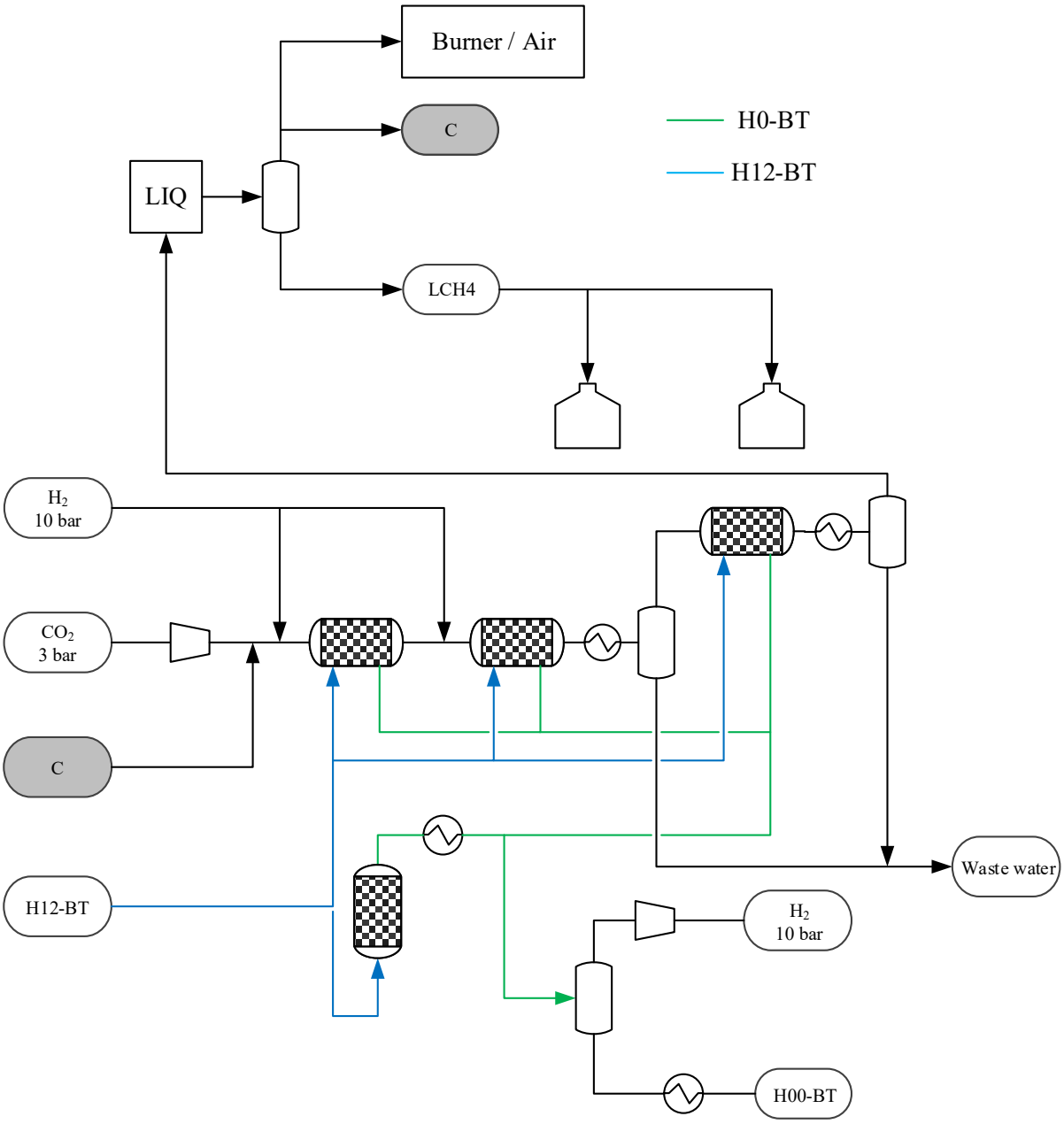

Figure S.8: Simplified BFD of methanation process for case B

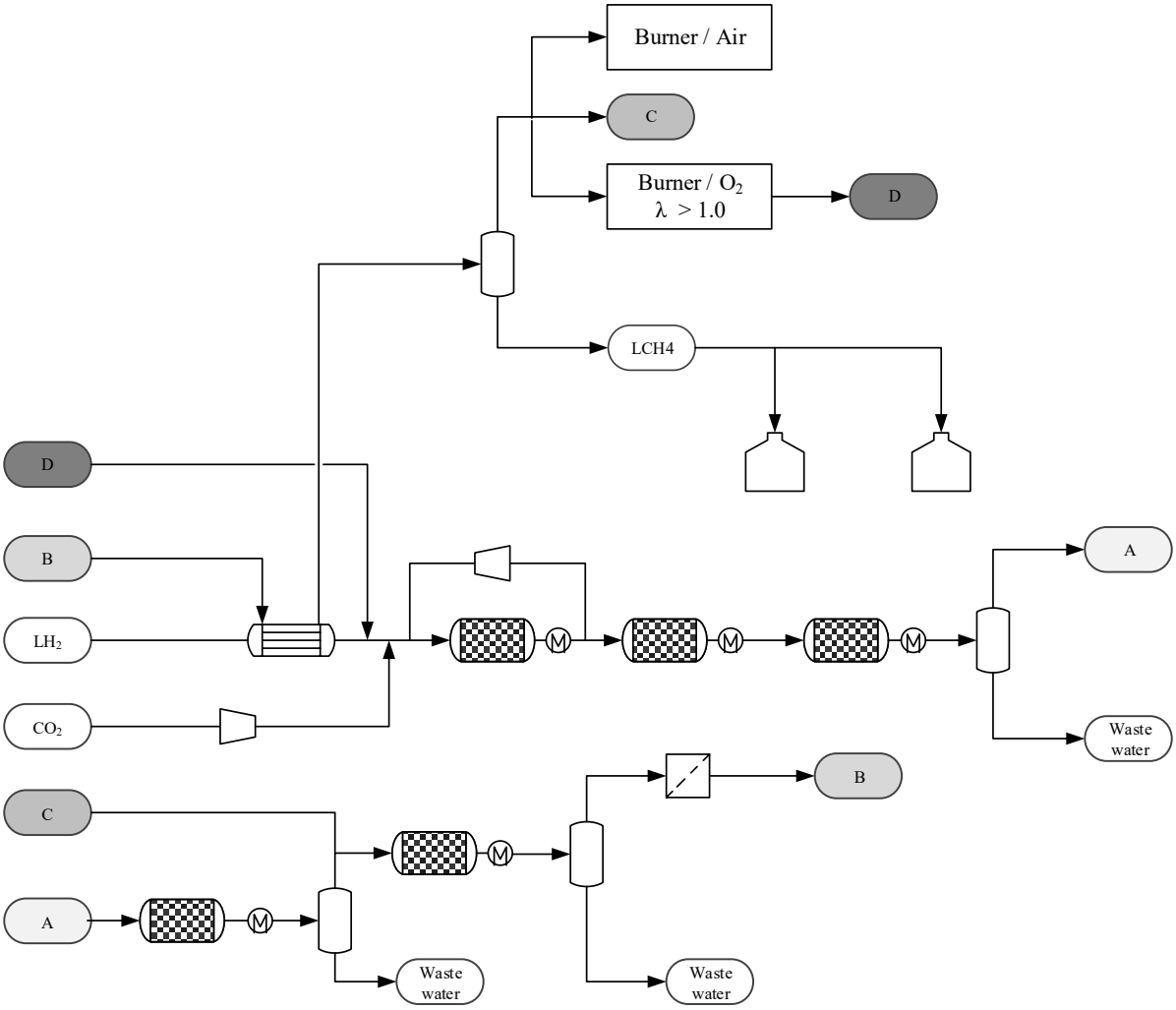

Figure S.9: Simplified BFD of methanation process for case C

S.2.6. SAF pathway

S.2.6.1. SAF - Input data

Table S.14: Input data for the SAF pathway

Input	Value	Unit	Source
FT reactor inlet temperature	220	°C	(8)
FT reactor 1 pressure	21	bar	(8)
FT reactor 2 pressure	20	bar	(8)
Per-pass CO conversion	40	%	(8)
H_2 / CO ratio entering reactor 1	2.05	mol/mol	(8)
H_2 + CO mole fraction entering reactor 1	≈ 0.6	mol/mol	(8)
Labor demand - Morocco - Case A	50	People / shift	Assumption
Labor demand - Germany - Case A	2	People / shift	Assumption
Labor demand - Germany - Case B	45	People / shift	Assumption
Labor demand - Germany - Case C	40	People / shift	Assumption
Storage capacity - Morocco - SAF	18,000	m³	Calculation results
Storage capacity - Morocco - Naphtha	17,000	m³	Calculation results
Storage capacity - Germany (Case A)	18,000	m³	Calculation results
Storage capacity - Germany (Case B/C)	10,000	m³	Calculation results
Power demand of ships in harbor	Neglected		Assumption

Table S.15: Input data for shipping in the FT pathway

Input	Value	Unit	Source
Reference ship	APATURA		(25)
Volumetric capacity	23,700	m³	
Costs of carrier	25	Mio. US-$	Assumption based on (13)
Power demand of ships sailing	6.6	MW	(25)
Crew size	20		(15)
Labor costs	758,186	€/a	(16)
Supply costs	246,400	€/a	(17)
Maintenance main machine	500,000	€/a	(17)
Maintenance rest of ship	205,500	€/a	Assumption based on (17)
Insurance	10 % of OPEX		Assumption

Return trips per year	19.7	Calculation results
Ship utilization	80 %	Assumption

S.2.6.2. SAF - Block flow diagram

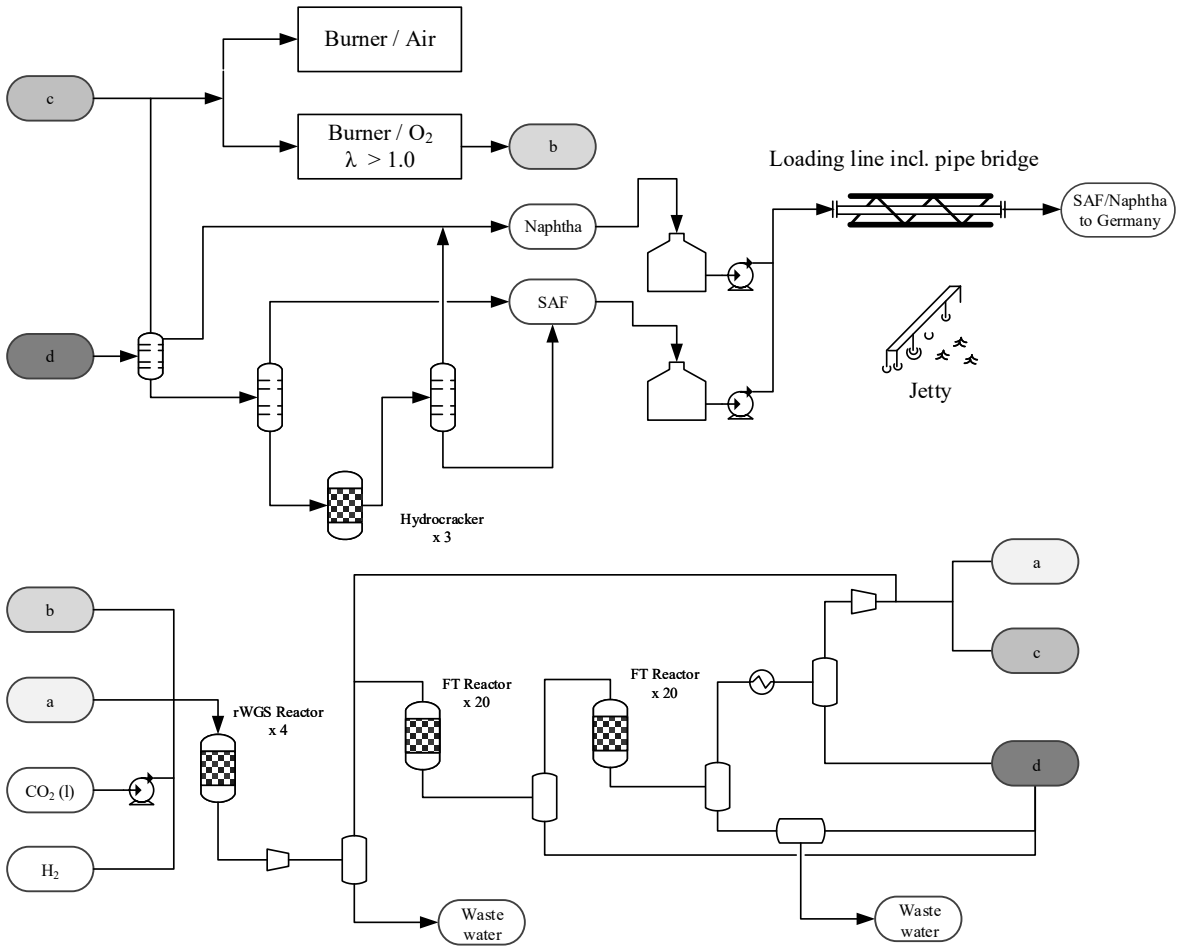

Figure S.10. Simplified BFD of FT-synthesis for case A

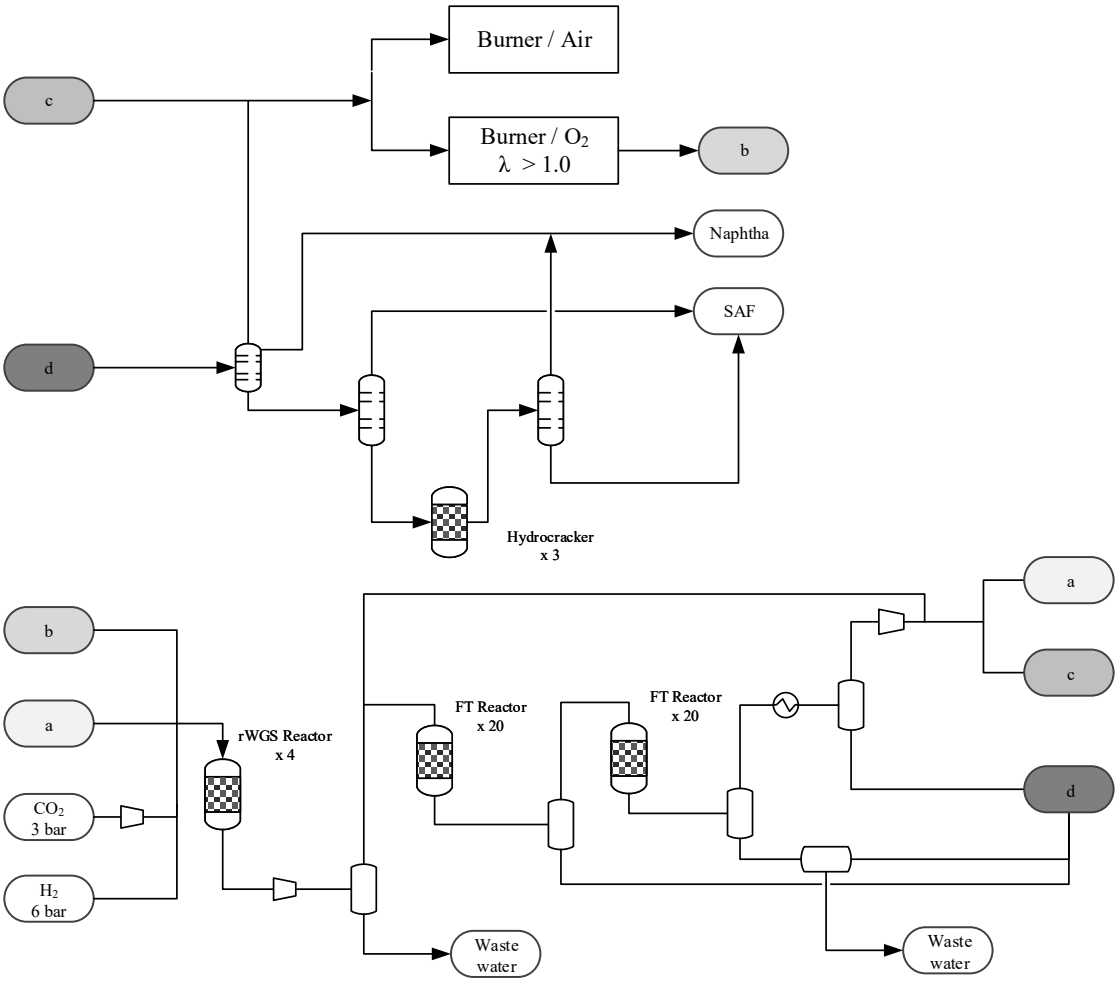

Figure S.11: Simplified BFD of FT-synthesis for case A

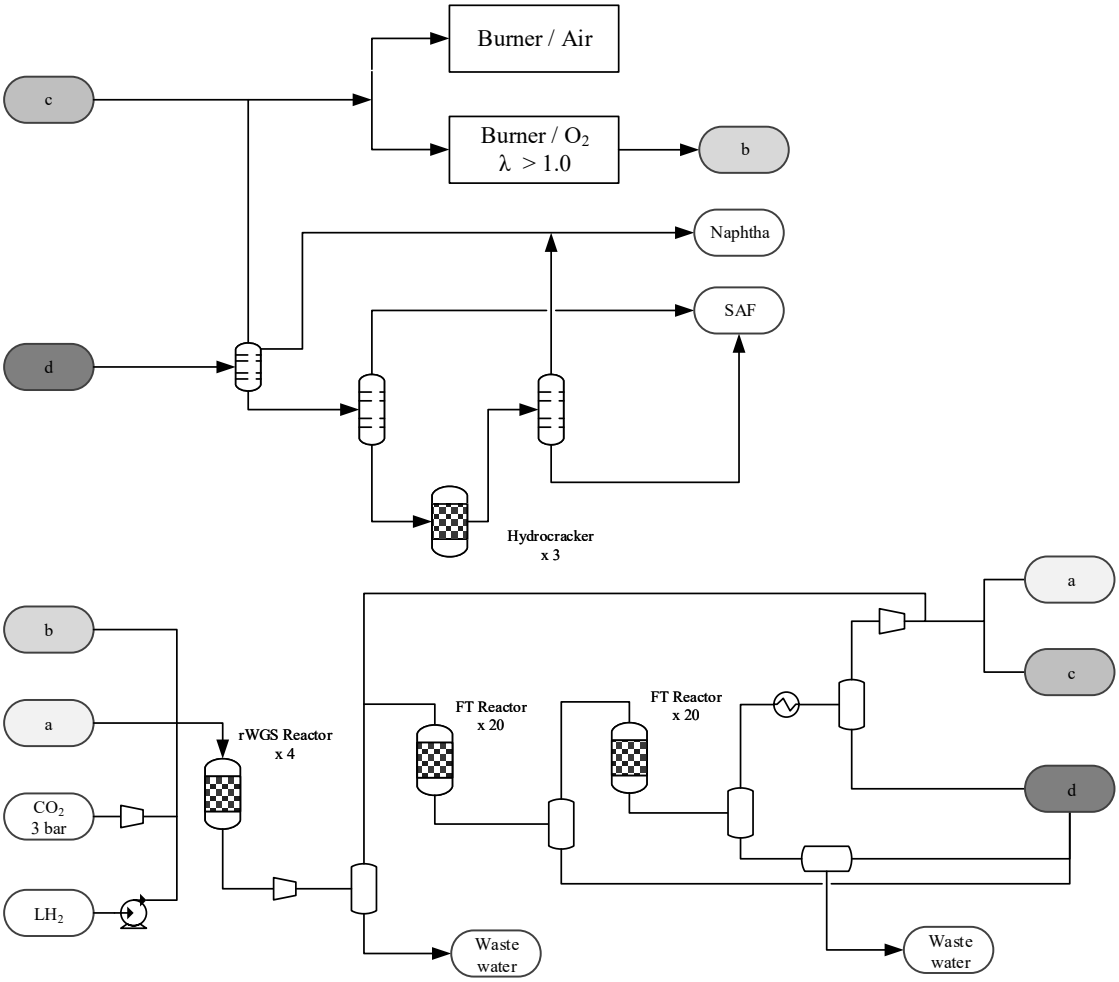

Figure S.12: Simplified BFD of FT-synthesis for case C

S.2.6.3. Detailed results

To show how carbon is recycled in the process, a carbon-Sankey diagram is shown in Figure S.13.

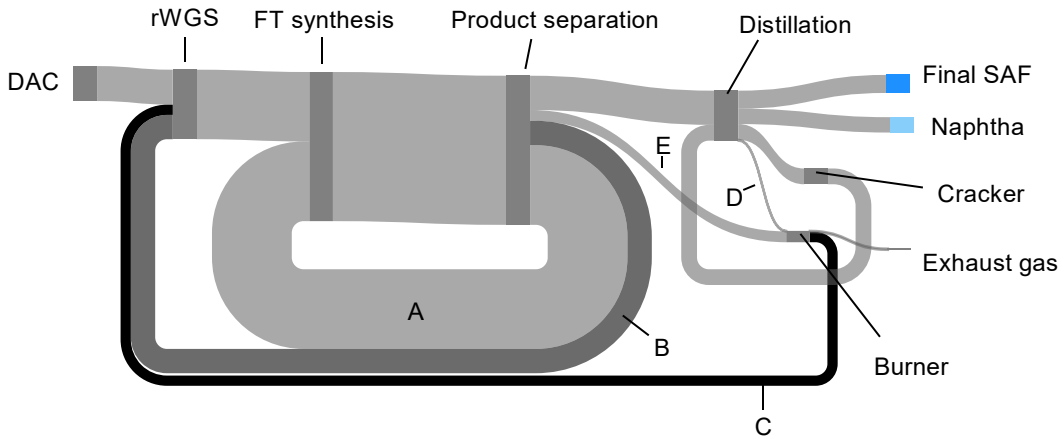

A = recycle gas after synthesis to FT reactor (short recycle)
B = recycle gas after synthesis to rWGS unit (long recycle)
C = exhaust gas after burner to rWGS unit
D = light products after distillation to burner
E = gases to burner (required to cover heat demand of rWGS unit)

Figure S.13: Carbon Sankey diagram of the FT synthesis - Case A

The high temperature heat pump with water as refrigerant requires intermediate cooling. The compression and cooling steps are shown in Figure S.*14*

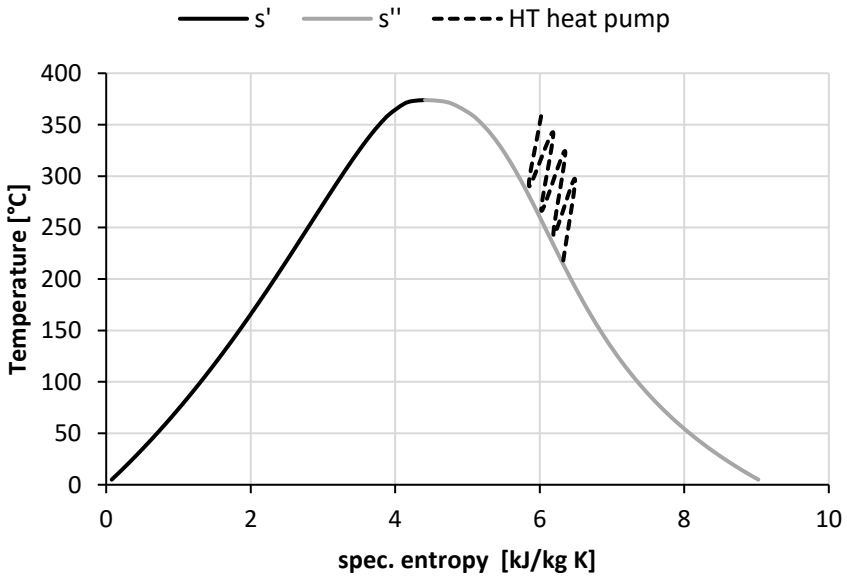

Figure S.14: T,s diagram of water with states of water vapor from HT heat pump

S.3. Input and results of H_2 production plant (HPP)

Weather data is retrieved from renewables.ninja for the location:
Lat": "28.476", "Lon": "-11.256

Table S.16: Relevant input parameter for HPP

Input	Value	Unit	Source
FCI PV today	754	€/kW_{peak}	Based on (26)
FCI PV perspective	492	€/kW_{peak}	(27)
FCI wind today	1.873	2020 US-$/kW	Based on (26)
EQP costs AEL today	400	2020 US-$/kW	(27)
EQP costs AEL perspective	160	$€_{2020}$/kW	(27)
Efficiency today	51,9	kWh_{el}/kg_{H_2}	(27)
Efficiency perspective	48	kWh_{el}/kg_{H_2}	(27)
Lang factor - AEL	1,62	-	(27)
Insurance and taxes	0,02	1/a – FCI basis	(27)
EQP storage costs	613	$€_{2020}$/kg	(27)
Lang factor - Storage	2	-	(27)
EQP compressor costs	1.083	$€_{2020}$/kW	(27)
Lang factor - compressor	3,78	-	(27)

Definition of grid assistance:
"If the grid assistance amounts to xy %, then the power that can be drawn from the electric grid is proportionate to xy % of the total hydrogen flow"

Example:

- In the study the hydrogen feed is 25.74 t_{H_2}/h.
- Costs of 25 % grid assistance with perspective data are considered
- 25 % of 25.74 t_{H_2}/h are 6.435 t_{H_2}/h
- With the perspective efficiency of 48 kWh_{el}/kg_{H_2} and 6.435 t_{H_2}/h the maximum power that can be drawn from the grid amounts to 308.88 MW

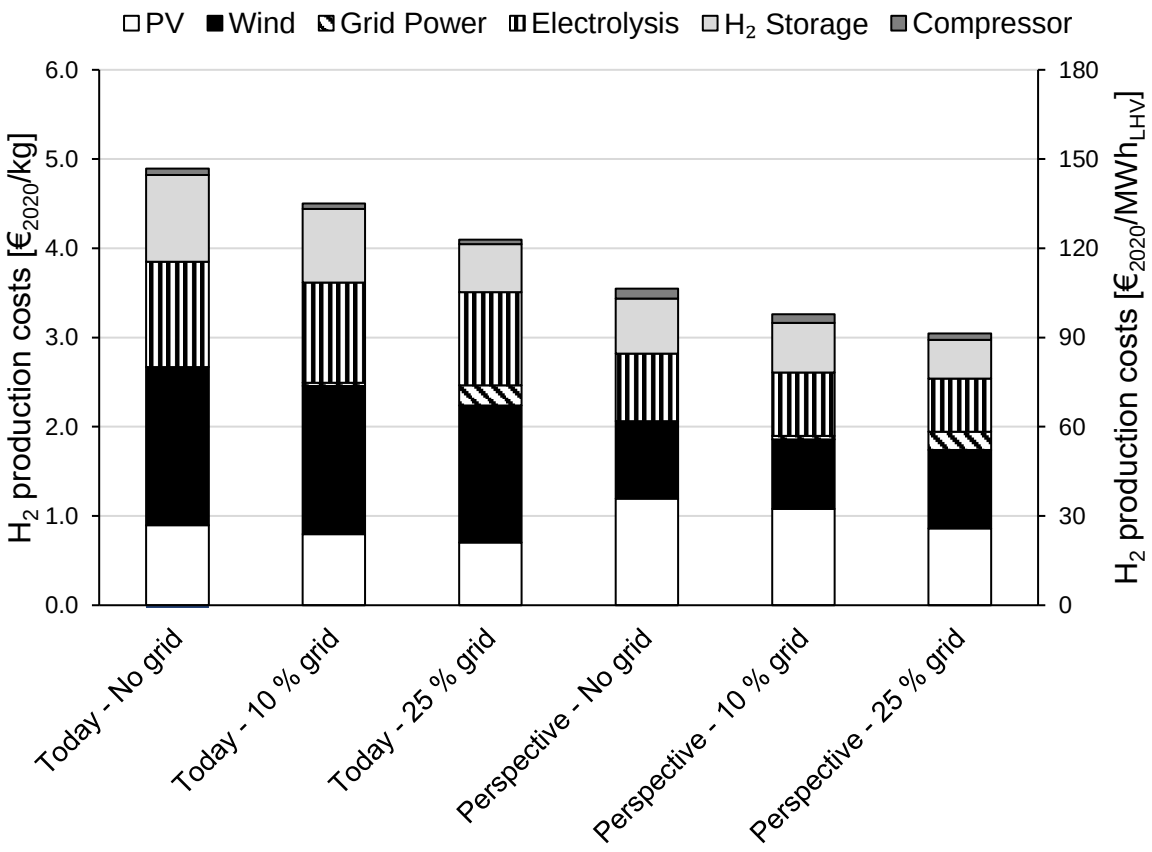

Figure S.15: Hydrogen production costs in El Ouatia, Morocco based on methodology from (27)

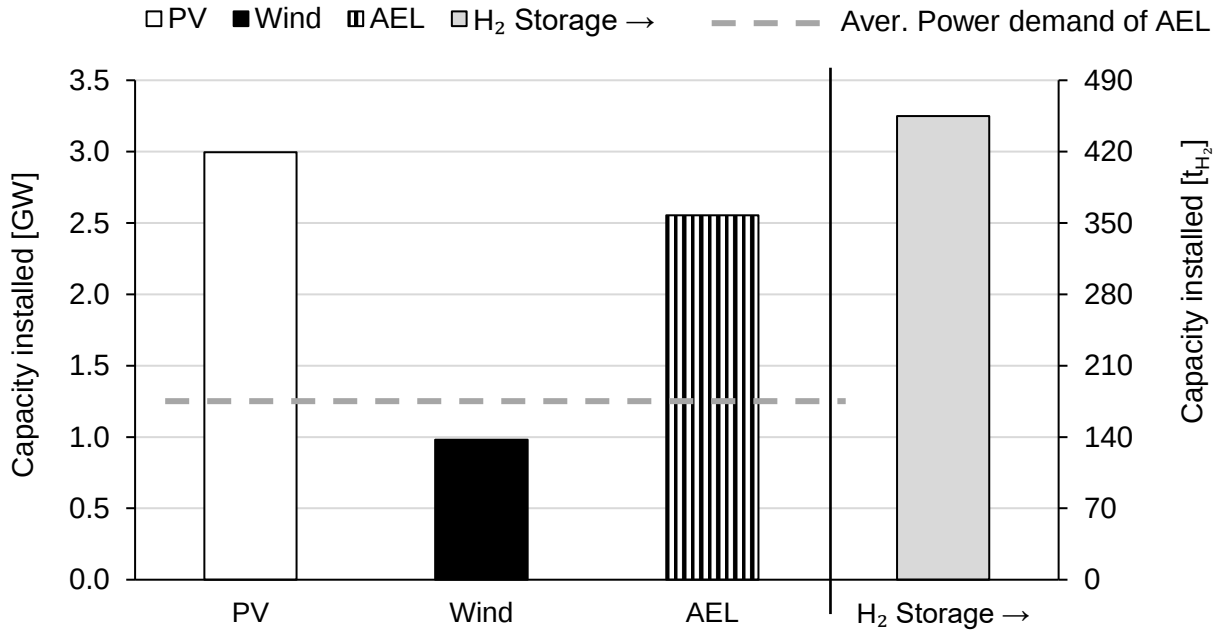

Figure S.16: Installed equipment sizes for the perspective - 25 % grid case

"Aver. Power demand of AEL" is power demand to produce 25.74 t_{H_2}/h with 48 kWh_{el}/kg_{H_2}

For **Case A** it is considered that the electricity demand of the fuel production units is partially supplied from excess renewable energy from the hydrogen production plant (HPP). This is shown in Figure S.17.

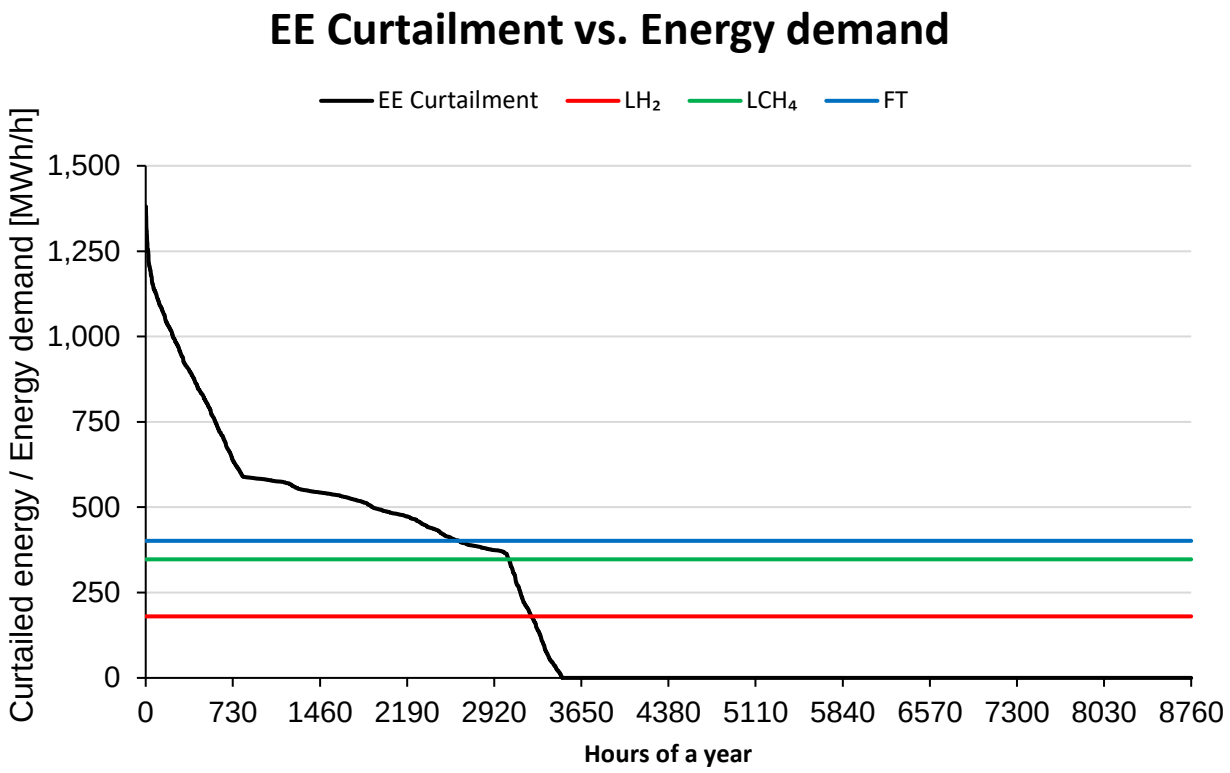

Figure S.17: Sorted values of EE curtailment for the perspective - 25 % grid case vs. electricity demand of fuel production processes

List of figures

List of tables

References

1. Nationmaster. Morocco Labor Stats [Available from: https://www.nationmaster.com/country-info/profiles/Morocco/Labor.
2. DESTATIS. Arbeitskosten im Jahr 2020: Nach wie vor starke regionale Unterschiede 2023 [Available from: https://www.destatis.de/DE/Presse/Pressemitteilungen/2022/07/PD22_280_624.html.
3. IRENA. Renewable Power Generation Costs in 20202021. Available from: https://www.irena.org/publications/2021/Jun/Renewable-Power-Costs-in-2020.
4. Sea-Distances. 2020 [Available from: https://sea-distances.org/.
5. ExchangeRates. Euro to US Dollar Spot Exchange Rates for 2020 2021 [Available from: https://www.exchangerates.org.uk/EUR-USD-spot-exchange-rates-history-2020.html.
6. Heimann N, Raab M, Pichlmaier S, Haas S, Wulff N, Dietrich R-U. Beitrag zur einheitlichen ökonomischen und ökologischen Analyse von strombasierten Prozessen zur Kraftstoffherstellung in Deutschland to be published.
7. ChemieparkWulfen. Preisblatt gemäß § 10 der AGB-E der Chemiepark BitterfeldWolfen GmbH Gültigkeit: ab 01.01.2020 2020 [Available from: https://www.chemiepark.de/fileadmin/chemiepark_de/content/dokumente/preisblatt_agb-e_ab_2020.pdf.
8. Albrecht FG, König DH, Baucks N, Dietrich R-U. A standardized methodology for the techno-economic evaluation of alternative fuels – A case study. Fuel. 2017;194:511-26.
9. Smith R. Comparatice research on LNG receiving terminals and FSRU. The University of Western Australia; 2017.
10. Raab M, Maier S, Dietrich R-U. Comparative techno-economic assessment of a large-scale hydrogen transport via liquid transport media. International Journal of Hydrogen Energy. 2021;46(21):11956-68.
11. Stolzenburg KRM. Hydrogen Liquefaction Report - Integrated Design for Demonstration of Efficient Liquefaction of Hydrogen (IDEALHY). 2013.
12. MarineTraffic. ENERGY NAVIGATOR [Available from: https://www.marinetraffic.com/en/ais/details/ships/shipid:665282/mmsi:432634000/imo:9355264/vessel:ENERGY_NAVIGATOR.
13. Compass maritime weekly report. https://compassmar.com/; 2019. Report No.: March 8th 2019 / Week 10.
14. ENERGY NAVIGATOR, IMO 9355264 [Available from: https://ships.jobmarineman.com/energy-navigator-9355264/.
15. Brodosplit. Tankers: Brodosplit; 2020 [Available from: http://hb.hr/wp-content/uploads/2014/12/tankers.pdf.
16. Cambanis DG. Challenge to the Industry Securing skilled crews in today's market place. 2011:20.
17. Spar Associates I, editor Naval Ship Life Cycle Cost (LCC) Model2018: Spar Associates, INC.
18. Ausfelder F, Tran DD. 4. Roadmap des Kopernikus-Projektes „P2X ": Phase II2022.
19. Rüde T, Dürr S, Preuster P, Wolf M, Wasserscheid P. Benzyltoluene/perhydro benzyltoluene – pushing the performance limits of pure hydrocarbon liquid organic hydrogen carrier (LOHC) systems. Sustainable Energy & Fuels. 2022;6(6):1541-53.
20. MarineLink. ALASKAN LEGEND [Available from: https://intelligence.marinelink.com/vessels/vessel/alaskan-legend-309224.
21. Jokora. Monoethanolamin 99% (2-Aminoethanol) (Kombinations-IBC a. 1000 kg) 2022 [Available from: https://www.jokora.de/organik/monoethanolamin/monoethanolamin-99-2-aminoethanol-kombinations-ibc-a.-1000-kg.
22. Goff GS, Rochelle GT. Monoethanolamine Degradation: O2 Mass Transfer Effects under CO2 Capture Conditions. Industrial & Engineering Chemistry Research. 2004;43(20):6400-8.

23. MarineTraffic. LNG JIA XING [Available from: https://www.marinetraffic.com/en/ais/details/ships/shipid:5902890/mmsi:477732500/imo:9769855/vessel:LNG_JIA_XING.
24. Marine L. SAGA DAWN: LNG Carrier [Available from: https://lntmarine.com/wp-content/uploads/2020/06/saga-dawn.pdf.
25. Hamburg H. Apatura [Available from: https://www.hafen-hamburg.de/en/vessels/apatura-23233/.
26. IRENA. Renewable Power Generation Costs in 2020. 2021.
27. Raab M, Körner R, Dietrich R-U. Techno-economic assessment of renewable hydrogen production and the influence of grid participation. International Journal of Hydrogen Energy. 2022;47(63):26798-811.

Aviation fuels of the future - A techno-economic assessment of distribution, fueling and utilizing LH_2, LCH_4 and e-kerosene (SAF)

Supplementary information

S.1. Input data

Table S.1: General input data for the evaluations

Input	Value	Unit	Source
Interest rate	5 %	-	Assumption
Depreciation time	20	a	Assumption
Exchange rate	0.95	€/US-$	Assumption
Electricity costs at the airport	100	€/MWh	Assumption
Boil-off in transport vessels with a volume of:			
< 100 m^3	0.4%	m^3/d	(1)
> 100 m^3 & < 20,000 m^3	0.2%	m^3/d	(1)
> 20,000 m^3	0.03 %	m^3/d	(1)
Boil-off in aircraft is neglected			

S.1.1. Input for domestic distribution

Table S.2: General input data for domestic distribution

Input	Value	Unit	Source
Waterway distance Wilhelmshaven to FRA	528	km	(2)
Rail distance Wilhelmshaven to MUC	840	km	(2)
Average train speed	40	km/h	(3)
Costs for undercarriage	100,000	$\$_{1995}$	(3)
Average inland waterway vessel speed	30	km/h	(4)

S.1.2. Input data for airport infrastructure

Table S.3: General input data for airport infrastructure

Input	Value / Equation	Unit	Source
Cost for H_2 liquefaction	$7.5887 \cdot \left(24 \cdot \frac{\dot{M}}{\left[\frac{t}{h}\right]} \right)^{0.7043}$	Mio $	(5, 6).
Cost for CH_4 liquefaction	$2000 \cdot \frac{\dot{M}}{\left[\frac{t}{a}\right]}$	$	(7)
Energy demand H_2 liquefaction	6	kWh/kg	(8)
Energy demand CH_4 liquefaction	0.34	kWh/kg	(9)

S.1.3. Input data to determine future aircraft costs

Table S.4: Research and development (R&D) cost data for reference aircraft

Aircraft	R&D costs	Source
A220	$ 5.4 billion	(10)
A350	$15.2 billion	(11)

Table S.5: Sources for empty mass for each aircraft size

Aircraft size	Reference aircraft	Source
100 PAX	Embraer E-190 E2	(12)
180 PAX	Boeing 737-8	(13) Rev-H, Section 2.1.2
425 PAX	Boeing 777-9	(14) Section 2.1.1

Table S.6: Limits of validity for exemplary aircraft

Model	LOV - FC / FC_{calc}	LOV - FH	Source
Dash 8-100	80,000		(15)
A321 series	48,000	60,000	(16)
A340–500, –600 Series	16,600	100,000	(16)
737 (NG)	75,000		(16)
777 (-200LR, -300ER)	40,000		(16)
787	44,000	140,000	(17)

Table S.7: Specific Jet A-1/SAF demand for tube-and-wing aircraft in kg/(PAX 100 km) – Departure from FRA

Destination	Regional jet	Small aircraft	Large aircraft
MUC	3.66	2.27	3.21
CDG	3.09	1.97	2.76
MAD	2.45	1.50	1.96
IST	2.39	1.46	1.88
KEF	2.36	1.44	1.82
CAI	2.34	1.43	1.80
IKA	2.33	1.43	1.78
DOH	-	1.44	1.77
JFK	-	1.47	1.77
BKK	-	-	1.82

Table S.8: Change in fuel demand for different aircraft designs

Aircraft design	Fuel burn improvement	Source
BWB	+ 12.8 %	(18)
TBW	+ 9.7 %	(19)

S.2. Detailed results of the fuel supply chain

S.2.1. Supply chain to Munich

Table S.9: Detailed values for boil-off losses in t/a during railway transport and liquefaction capacity at the airport

	Boil-off [t/a]		Reliquefication capacity [t/d]	
Scenario	**LH_2**	**LCH_4**	**LH_2**	**LCH_4**
2	274	-	5.25	-
3	14	1,326	0.27	30.1
4	274	3,121	5.25	70.9
5	1,884	-	36	-
6	-	3,769	-	85.6

S.2.2. Supply chain to Frankfurt

Table S.10: Detailed values for boil-off losses in t/a during inland waterway transport and liquefaction capacity at the airport

	Boil-off [t/a]		Reliquefication capacity [t/d]	
Scenario	**LH_2**	**LCH_4**	**LH_2**	**LCH_4**
2	280.4	-	16.66	-
3	10.9	1,776	0.65	111
4	280.4	8,710	16.66	545
5	4,850	-	288	-
6	-	9,373	-	587

S.3. Detailed results of future aircraft costs

S.3.1. Tube and Wing

S.3.1.1. R&D and procurement costs

Table S.11: Results for the 100 PAX aircraft – Composite content 30 %, manufacturing margin 5.7 %,

Fuel type	R&D costs [$]	Aircraft price [$]
LH_2	5,117,166,026	53,485,679
LCH_4	4,617,787,312	52,309,741
Jet A-1	3,709,679,751	48,822,933

Table S.12: Results for the 180 PAX aircraft – Composite content 30 %, manufacturing margin 5.7 %,

Fuel type	R&D costs [$]	Aircraft price [$]
LH_2	9,831,163,539	91,113,479
LCH_4	8,871,750,892	89,119,837
Jet A-1	7,127,083,257	83,199,934

Table S.13: Results for the 425 PAX aircraft – Composite content 50 %, manufacturing margin 5.7 %,

Fuel type	R&D costs [$]	Aircraft price [$]
LH_2	41,847,720,197	295,052,971
LCH_4	37,763,846,316	288,576,205
Jet A-1	30,337,424,942	269,362,645

S.3.1.2. Schematic drawings of the tube and wing aircraft

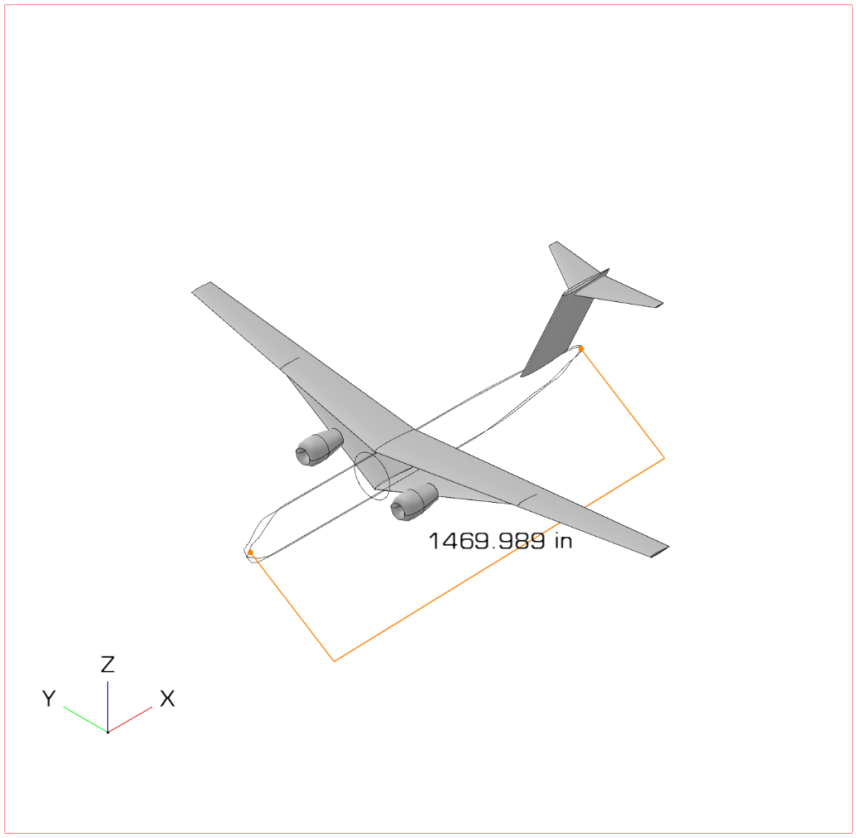

Figure S.1: Schematic representation of the 180 PAX tube-and-wing aircraft utilizing SAF

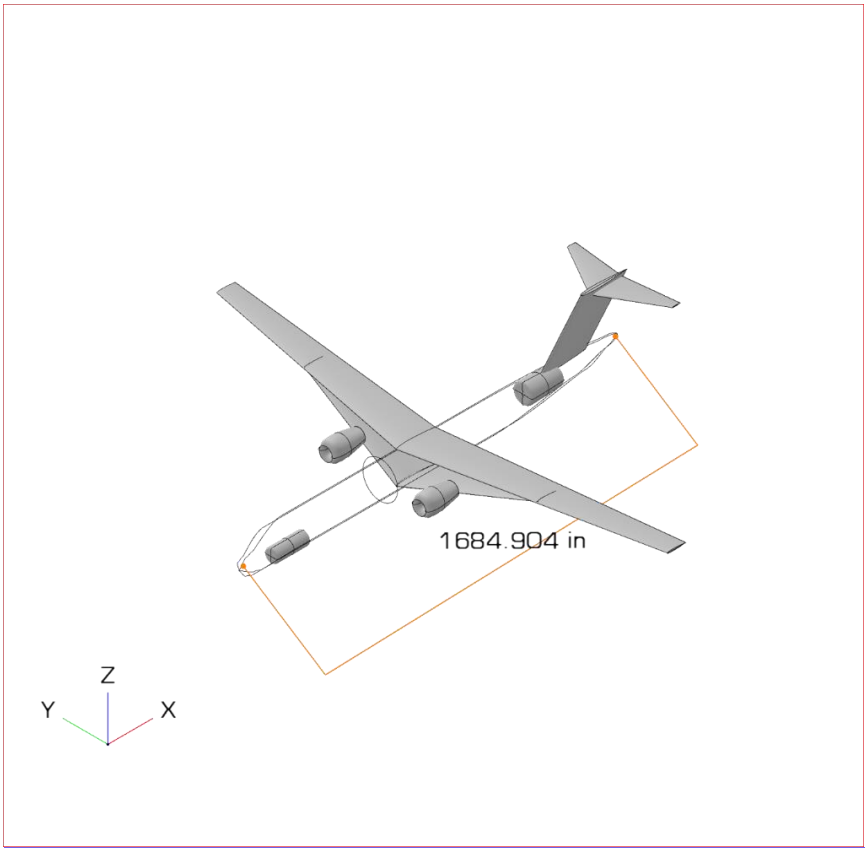

Figure S.2: Schematic representation of the 180 PAX tube-and-wing aircraft utilizing LCH_4 incl. the location of the tanks

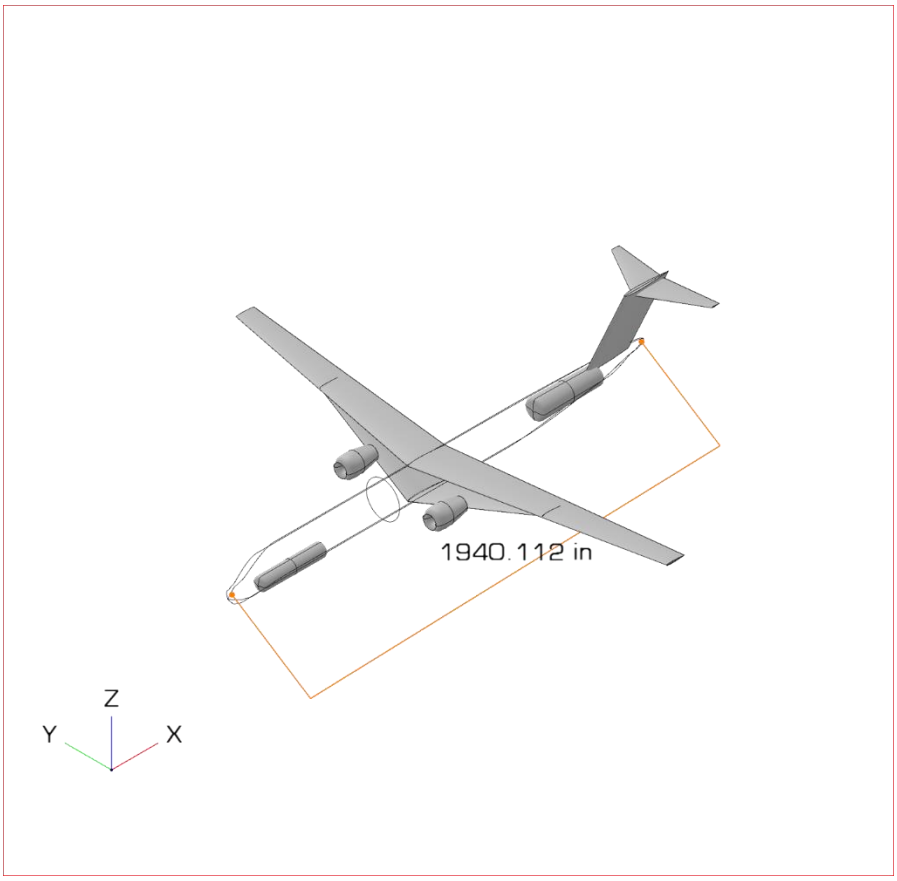

Figure S.3: Schematic representation of the 180 PAX tube-and-wing aircraft utilizing LH_2 incl. the location of the tanks

S.3.2. Blended wing body

S.3.2.1. R&D and procurement costs

Table S.14: Results for the 100 PAX aircraft – Composite content 50 %, manufacturing margin 11.4 %,

Fuel type	R&D costs [$]	Aircraft price [$]
LH_2	11,324,904,202	56,942,013
LCH_4	11,324,904,202	56,942,013
Jet A-1	10,577,014,421	54,562,850

Table S.15: Results for the 180 PAX aircraft – Composite content 50 %, manufacturing margin 11.4 %,

Fuel type	R&D costs [$]	Aircraft price [$]
LH_2	14,896,549,300	81,527,703
LCH_4	14,896,549,300	81,527,703
Jet A-1	13,912,790,251	78,121,295

Table S.16: Results for the 425 PAX aircraft – Composite content 50 %, manufacturing margin 11.4 %,

Fuel type	R&D costs [$]	Aircraft price [$]
LH_2	57,120,334,606	264,063,467
LCH_4	57,120,334,606	264,063,467
Jet A-1	53,348,142,472	253,012,958

S.3.2.2. Costs for flying

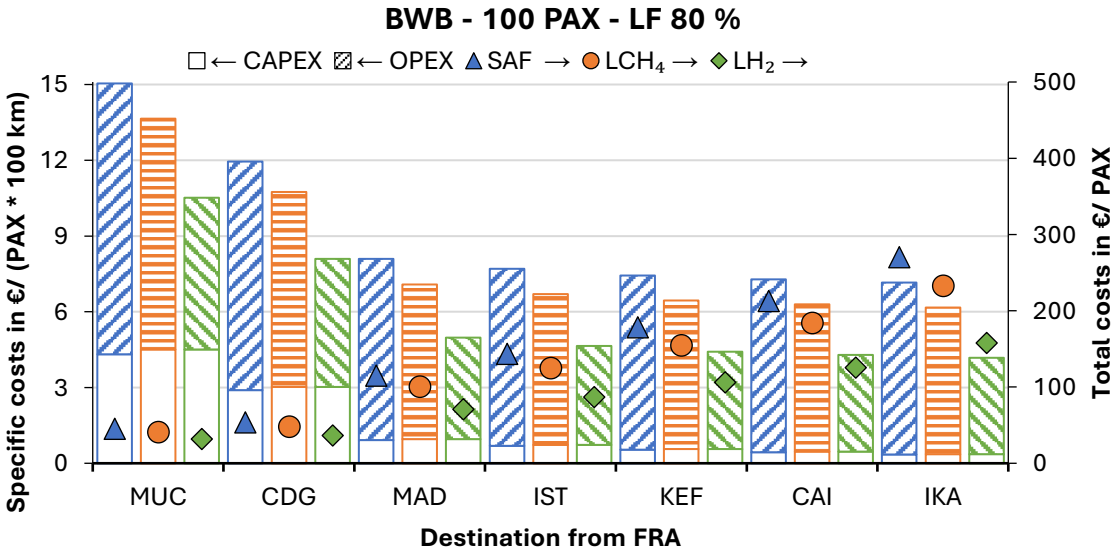

Figure S.4: Cost of flying with a blended wing body design regional jet sized aircraft

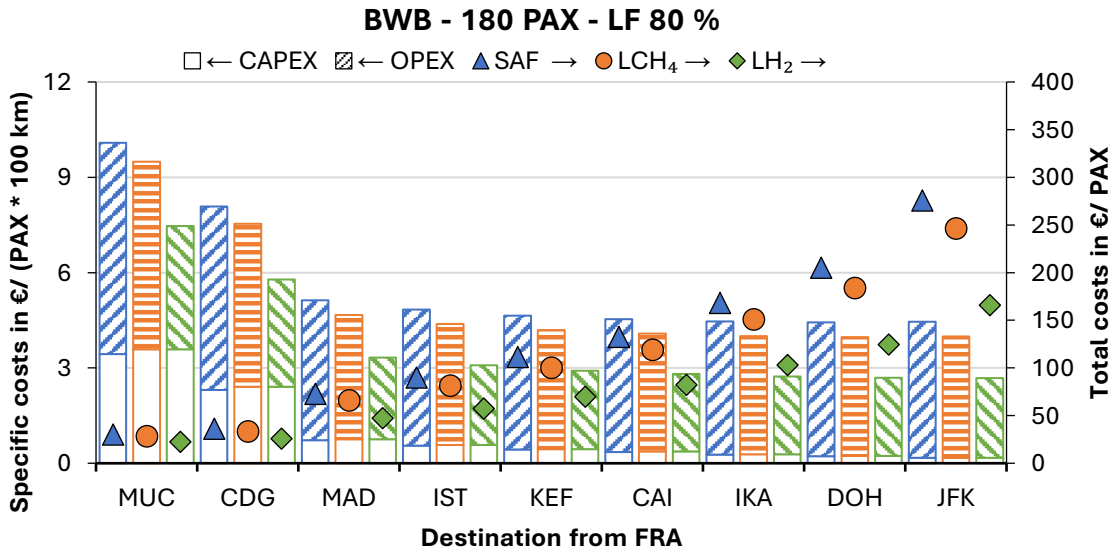

Figure S.5: Cost of flying with a blended wing body design small sized aircraft

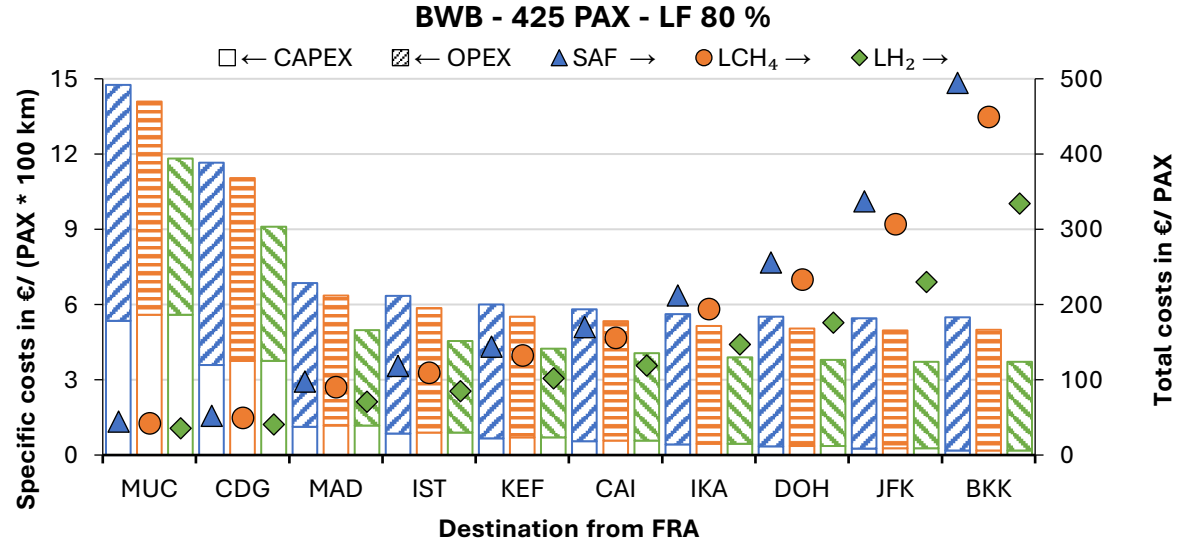

Figure S:6: Cost of flying with a blended wing body design large sized aircraft

S.3.3. Truss Braced Wing

S.3.3.1. R&D and procurement costs

Table S.17: Results for the 180 PAX aircraft – Composite content 30 %, manufacturing margin 6.9 %,

Fuel type	R&D costs [$]	Aircraft price [$]
LH_2	10,692,299,480	95,538,612
LCH_4	9,732,886,833	93,522,336
Jet A-1	7,988,219,198	86,552,603

S.3.3.2. Costs for flying

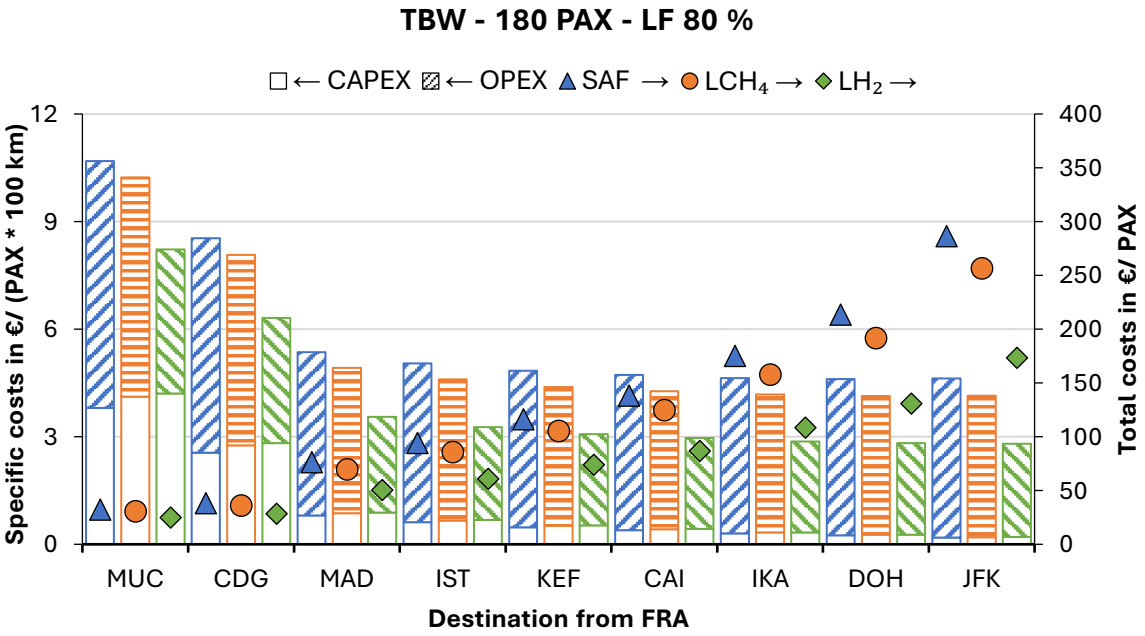

Figure S.7: Cost of flying with a truss braced wing design small sized aircraft

S.3.4. Calculation regarding the drag

The equation for the calculation of the hydraulic drag is the following.

$$F_D = \frac{1}{2}\rho v^2 C_D A$$

F_D is the force acting on the object due to the drag (Index D) in [N]
ρ is the density of the fluid in [kg/m^3]
v is the speed of the object relative to the fluid in [m/s]
C_D is a dimensionless number representing the drag coefficient
A is the cross-sectional area of the object [m^2]

Table S.18: Data regarding the fuselage diameter

	Unit	A321	A350
Fuselage diameter	m	3.95	≈ 6
Fuselage cross sectional area	m^2	12.25	28.27

Max. Passenger capacity	-	244	450
Area per passenger	m^2/PAX	0.05	0.062

S.4. Further analysis

S.4.1. Sensitivity regarding change of specific fuel demand based

Table S.19: Lowest specific costs for flying in $\frac{€_{2020}}{\text{PAX } 100 \text{ km}}$ depending on the fuel demand change

		Change in specific fuel demand compared to kerosene							
Fuel type	Aircraft type	-20%	-10%	±0%	+10%	+20%	+30%	+40%	+50%
LH_2	Regional jet	4.16	4.64	5.11	5.59	6.06	6.54	7.01	7.49
	Small aircraft	2.60	2.90	3.20	3.50	3.80	4.10	4.40	4.70
	Large aircraft	3.18	3.55	3.92	4.29	4.66	5.03	5.40	5.78
LCH_4	Regional jet	5.40	6.03	6.66	7.29	7.92	8.55	9.18	9.81
	Small aircraft	3.38	3.78	4.17	4.57	4.97	5.37	5.76	6.16
	Large aircraft	4.14	4.64	5.13	5.62	6.11	6.60	7.10	7.59

S.4.2. Detailed breakdown of the results for the whole costs of air travel

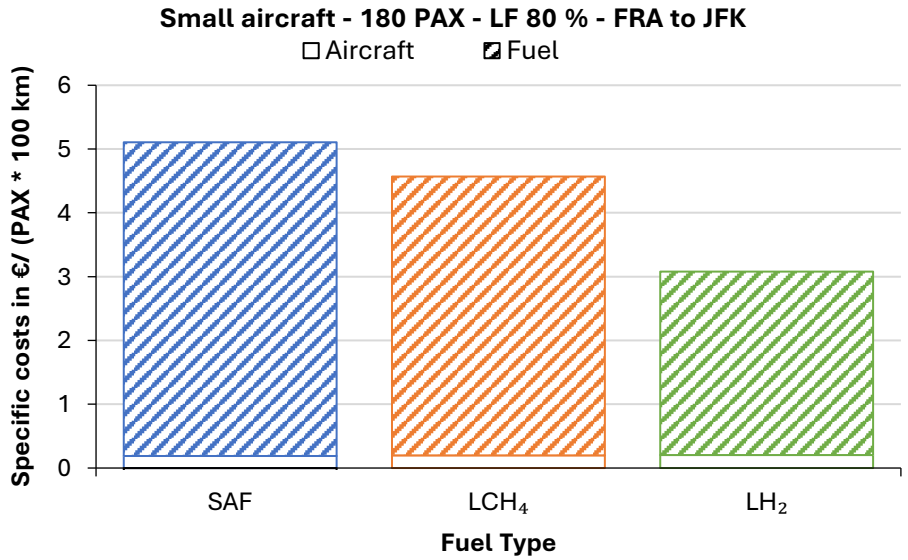

Figure S.8: Specific air travel costs for a flight from Frankfurt to New York depending on fuel type (same values as in the main manuscript)

The following figures show waterfall charts in ascending order of the corresponding cost contributors. The following coding is used to separate between the different steps:

A. Hydrogen production based on renewable energy – Methodology based on (20)
B. Fuel synthesis and if applicable, liquefaction – Details see (21)
C. Fuel transport to Germany - Methodology based on (6) – Details see (21)
D. Domestic fuel transport
E. Changes at the airport infrastructure
F. Aircraft depreciation

Furthermore, the following abbreviations are used:

- REM = remaining
- DAC = Direct air capture

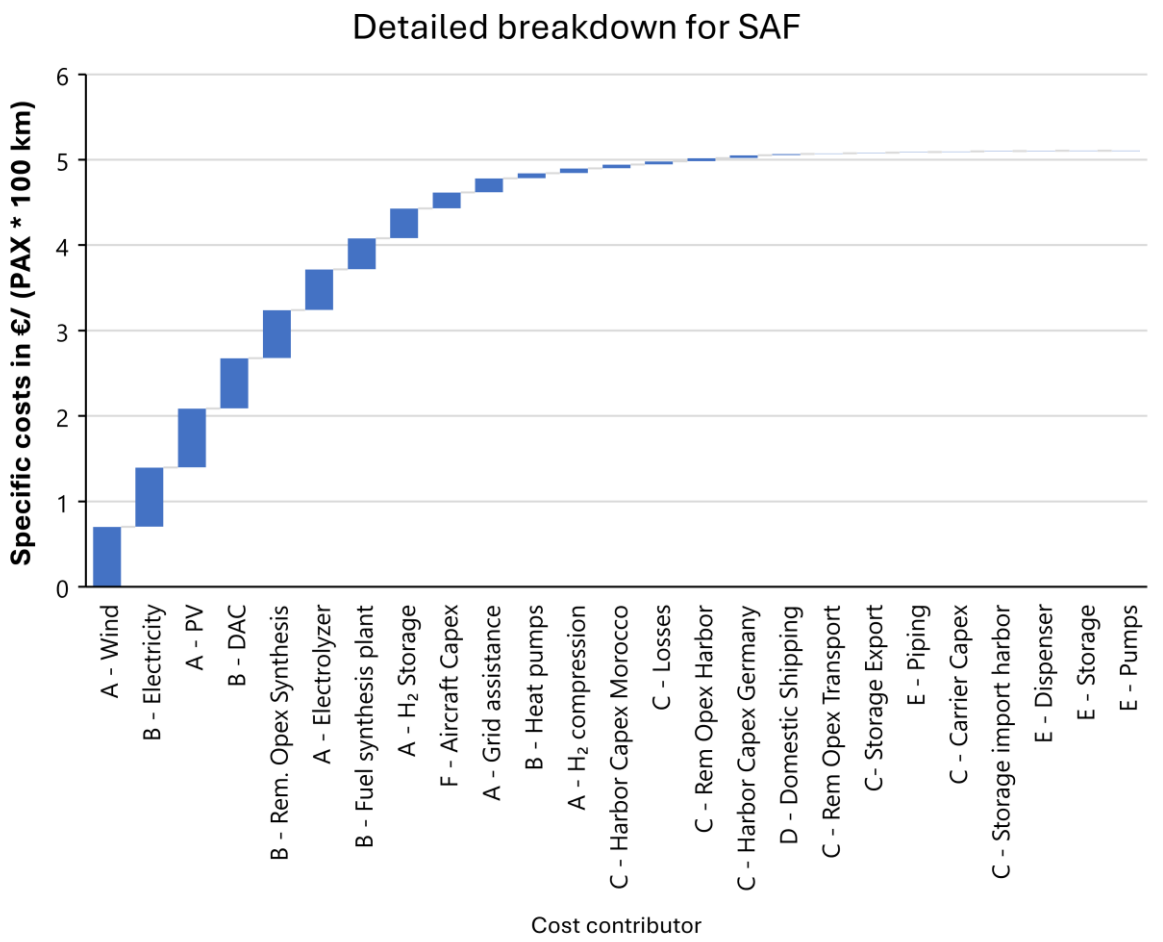

Figure S.9: Detailed cost breakdown for specific air travel costs for a flight from Frankfurt to New York with SAF

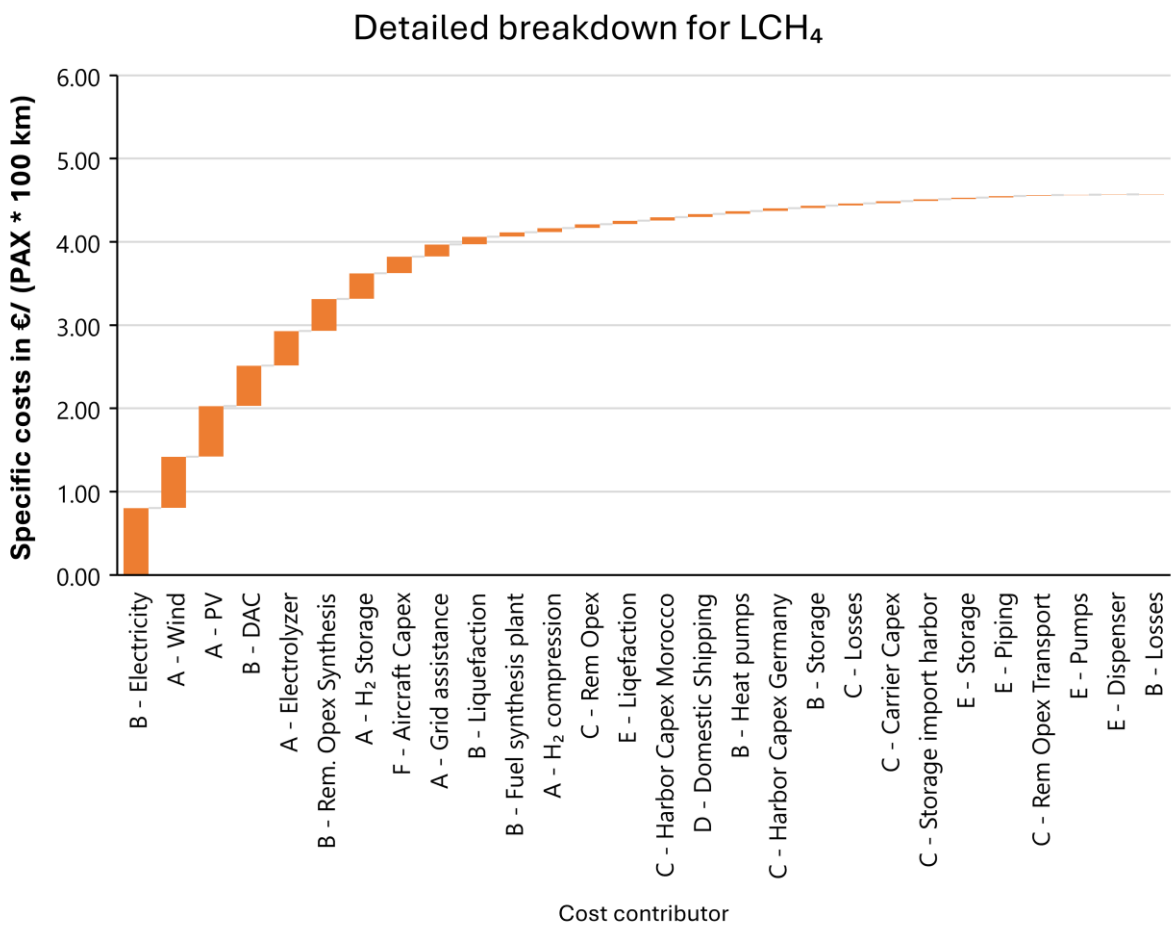

Figure S.10: Detailed cost breakdown for specific air travel costs for a flight from Frankfurt to New York with LCH_4

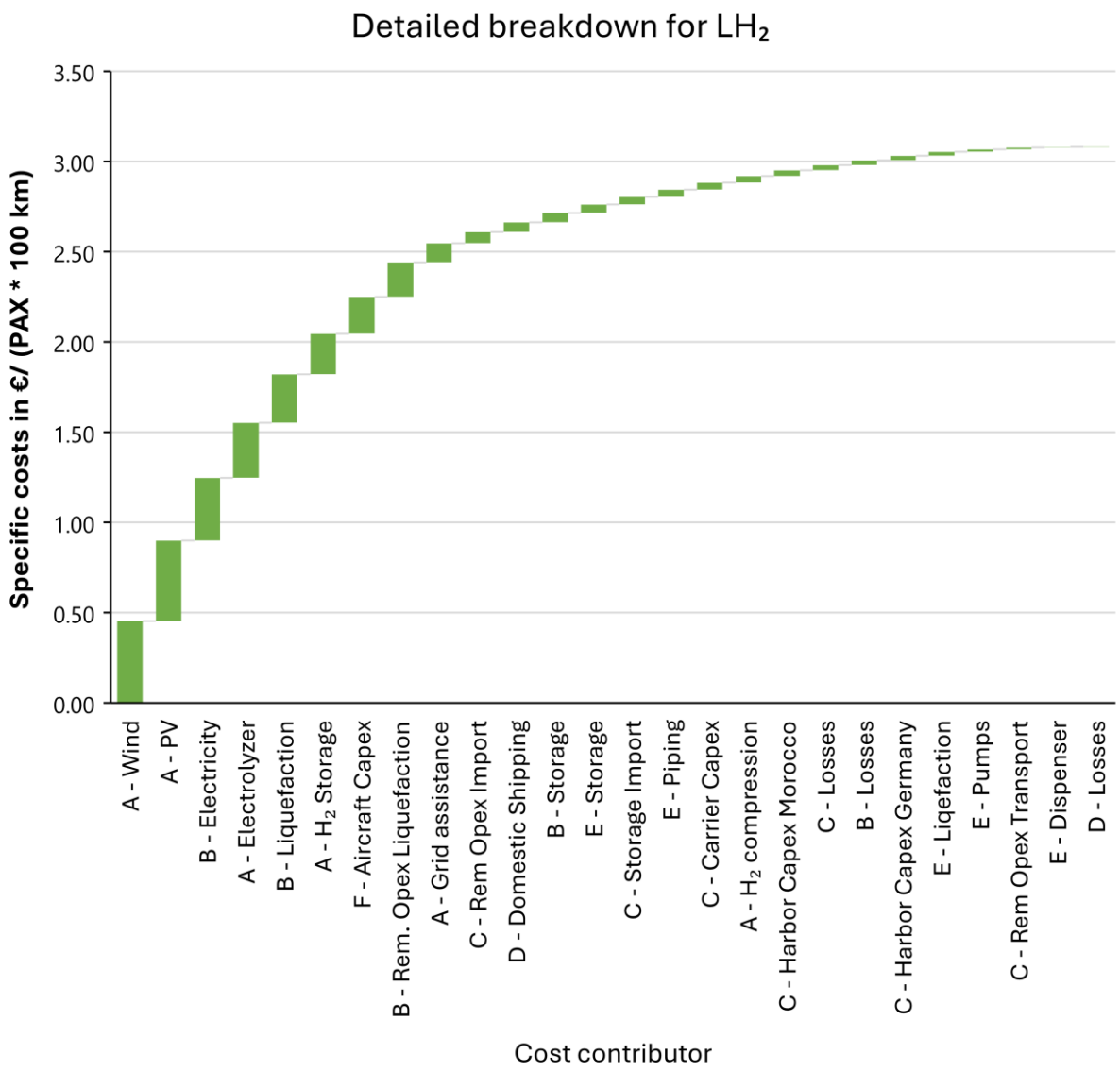

Figure S.11: Detailed cost breakdown for specific air travel costs for a flight from Frankfurt to New York with LCH_2

List of figures

List of tables

References

1. Simnick EJ, Sutherland E, Barckholtz T, Burgunder A, Casey D, Dillich S, et al. Hydrogen delivery technical team roadmap. Technical Report June; 2013.
2. Brenschede A. BRouter-Web [First accessed on: 31.05.2023 - Available from: https://brouter.de/brouter-web.]
3. Amos WA. Costs of storing and transporting hydrogen. National Renewable Energy Lab.(NREL), Golden, CO (United States); 1999.
4. Busch T, Gillessen B, Linßen J, Stolten D. Analyse von Transport-Optionen für flüssigen Wasserstoff in Deutschland. 2021
5. Stolzenburg K, Berstad D, Decker L, Elliott A, Haberstroh C, Hatto C, et al., editors. Efficient liquefaction of hydrogen: results of the IDEALHY project. Proceedings of the XXth Energie—Symposium, Stralsund, Germany; 2013.
6. Raab M, Maier S, Dietrich R-U. Comparative techno-economic assessment of a large-scale hydrogen transport via liquid transport media. International Journal of Hydrogen Energy. 2021;46(21):11956-68.https://doi.org/10.1016/j.ijhydene.2020.12.213
7. Songhurst B. LNG plant cost reduction 2014–18. 2018.https://ora.ox.ac.uk/objects/uuid:f5bebe7f-1559-47ad-a80a-018ab9d78061
8. Cardella U, Decker L, Sundberg J, Klein H. Process optimization for large-scale hydrogen liquefaction. International Journal of Hydrogen Energy. 2017;42(17):12339-54.http://www.sciencedirect.com/science/article/pii/S0360319917311746
9. Al-Breiki M, Bicer Y. Liquified hydrogen vs. liquified renewable methane: Evaluating energy consumption and infrastructure for sustainable fuels. Fuel. 2023;350:128779.https://www.sciencedirect.com/science/article/pii/S0016236123013923
10. Star T. 2015 Bombardier's CSeries jet certified for commercial service [First accessed on: 15.08.2023 - Available from: https://www.thestar.com/business/bombardier-s-cseries-jet-certified-for-commercial-service/article_dad0d7a3-118b-58d9-bb8c-b0e9adddbb5f.html.]
11. Reuters. 2009 Airbus says A350 project to cost 11 billion euro [First accessed on: 15.08.2023 - Available from: https://www.reuters.com/article/us-airshow-airbus-sb/airbus-says-a350-project-to-cost-11-billion-euro-idUSTRE55F1Y720090616/.]
12. Embraer. E190-E2 [First accessed on: 15.08.2023 - Available from: https://www.embraercommercialaviation.com/commercial-jets/e190-e2-commercial-jet/.]
13. Boeing. 2023 737 MAX - Airplane Characteristics for Airport Planning [First accessed on: 15.08.2023 - Available from: https://www.boeing.com/resources/boeingdotcom/commercial/airports/acaps/737MAX_RevH.pdf.]
14. Boeing. 2023 777-9 - Airplane Characteristics for Airport Planning [First accessed on: 15.08.2023 - Available from: https://www.boeing.com/resources/boeingdotcom/commercial/airports/acaps/777X_RevE.pdf.]
15. Agustin M. 2022 The De Havilland Canada Dash 8-100 will have an extended service life: Aviacionline; [First accessed on: 20.07.2023 - Available from: https://www.aviacionline.com/2022/04/the-de-havilland-canada-dash-8-100-will-have-an-extended-service-life/.]
16. Code of Federal Regulations. 2023 Title 14 Chapter I Subchapter G Part 121 Subpart AA §121.1115 [First accessed on: 20.07.2023 - Available from: https://www.ecfr.gov/current/title-14/chapter-I/subchapter-G/part-121/subpart-AA/section-121.1115.]
17. Boeing. 2019 787 AIRWORTHINESS LIMITATIONS [First accessed on: 20.07.2023 - Available from: https://de.scribd.com/document/477308129/2019-Jan-787-AWL.]
18. Nickol C, Mccullers L, editors. Hybrid wing body configuration system studies. 47th AIAA aerospace sciences meeting including the new horizons forum and aerospace exposition; 2009.
19. Marty K. Bradley, Droney CK. Subsonic Ultra Green Aircraft Research - Phase II: N+4 Advanced Concept Development. 2012.https://ntrs.nasa.gov/api/citations/20120009038/downloads/20120009038.pdf
20. Raab M, Körner R, Dietrich R-U. Techno-economic assessment of renewable hydrogen production and the influence of grid participation. International Journal of Hydrogen Energy. 2022;47(63):26798-811.https://doi.org/10.1016/j.ijhydene.2022.06.038

21. Raab M, Dietrich R-U. Techno-economic assessment of different aviation fuel supply pathways including LH2 and LCH4 and the influence of the carbon source. Energy Conversion and Management. 2023;293:117483.https://doi.org/10.1016/j.enconman.2023.117483